Advancing the atmospheric Cherenkov-method to detect gamma-rays with one Giga electron Volt

Sebastian Achim Mueller
Max-Planck-Institute for Nuclear Physics
sebastian-achim.mueller@mpi-hd.mpg.de

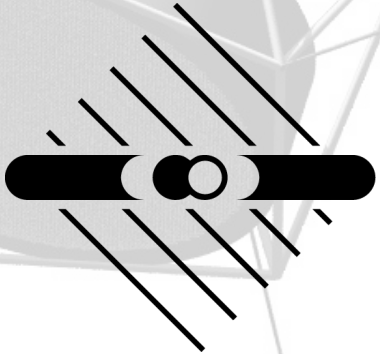

γ 2022
7th Heidelberg International Symposium on
High Energy Gamma-Ray Astronomy
Barcelona, July 4-8 2022

Explore Timing

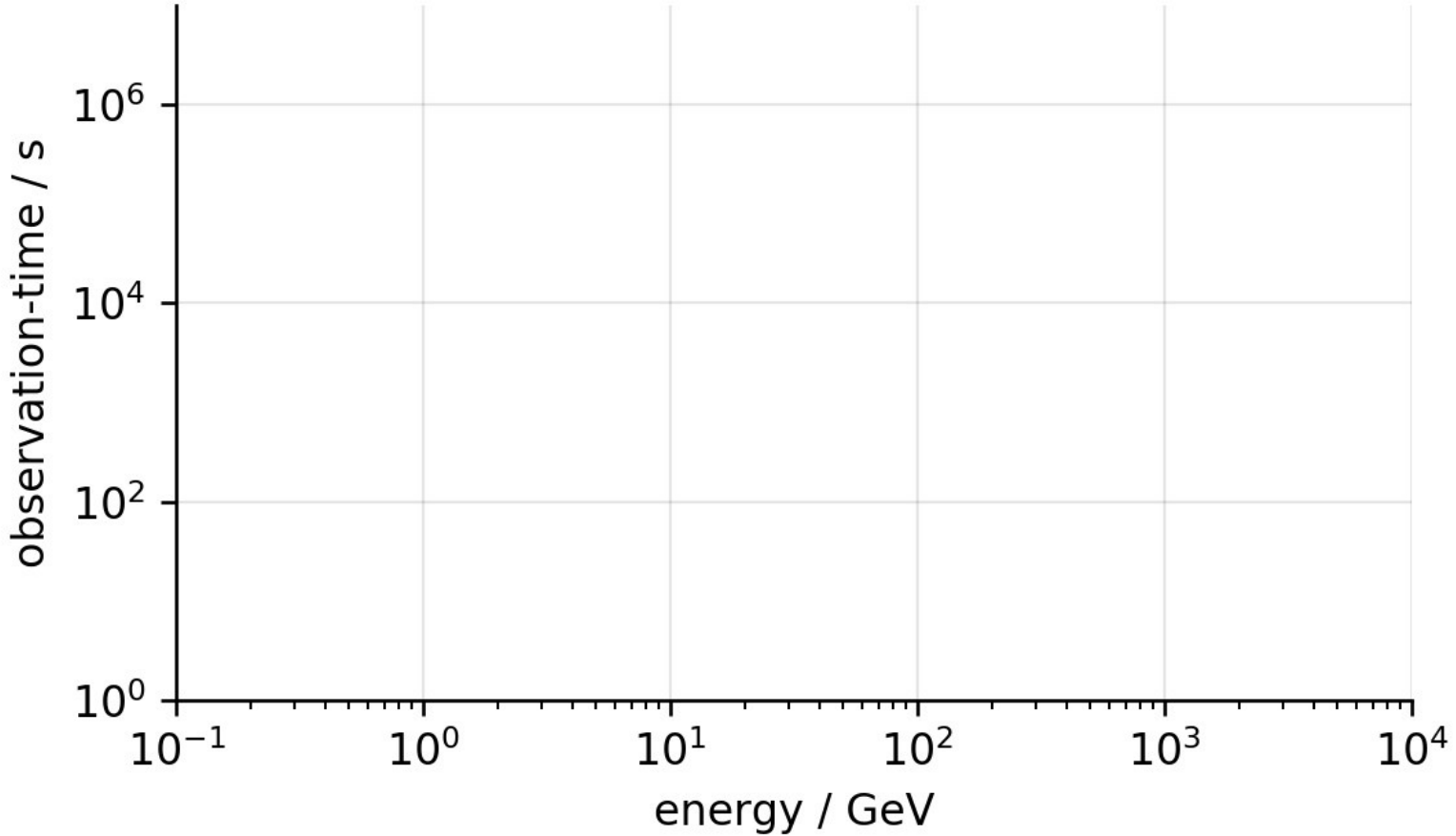

Explore Timing

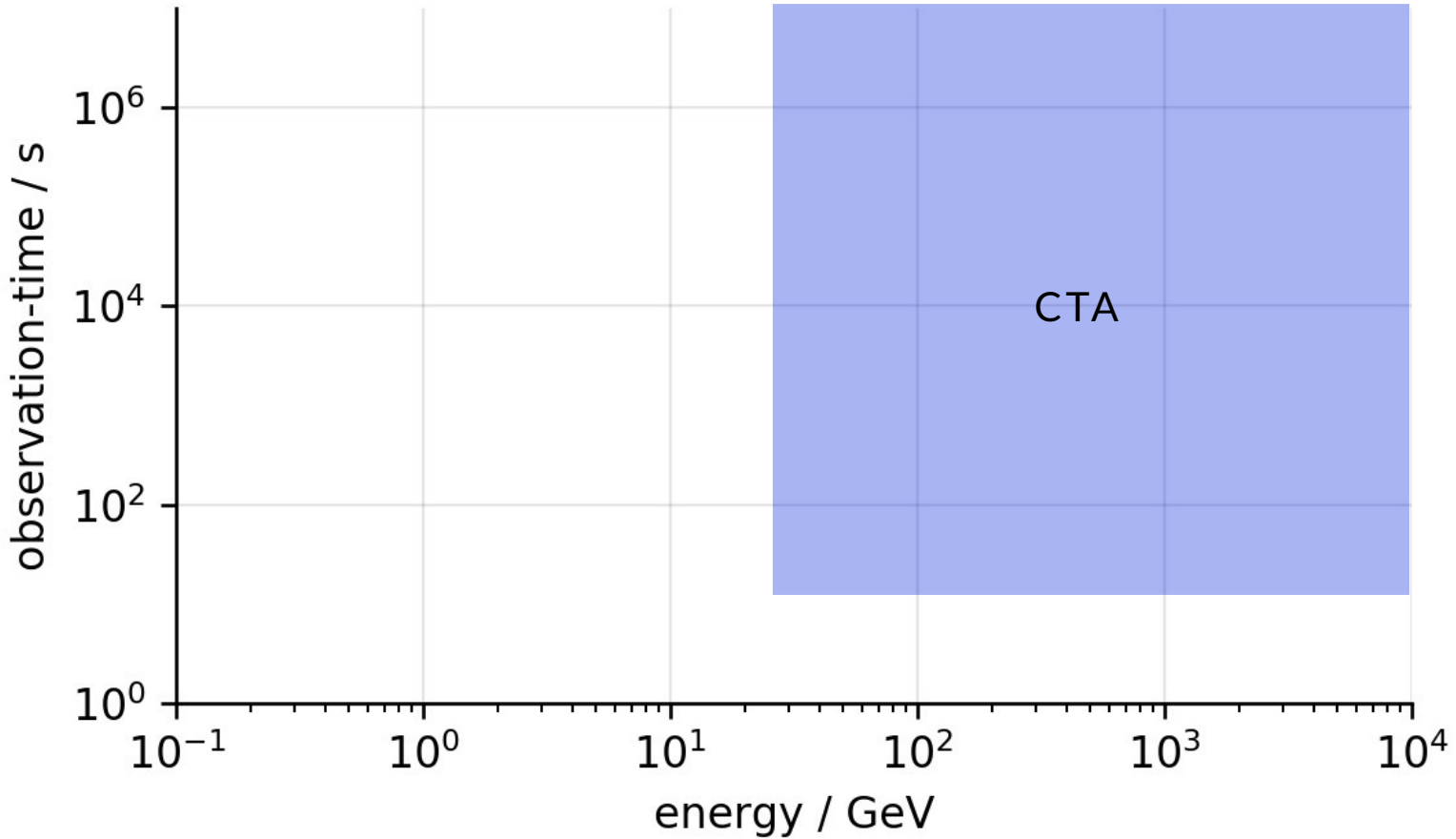

Explore Timing

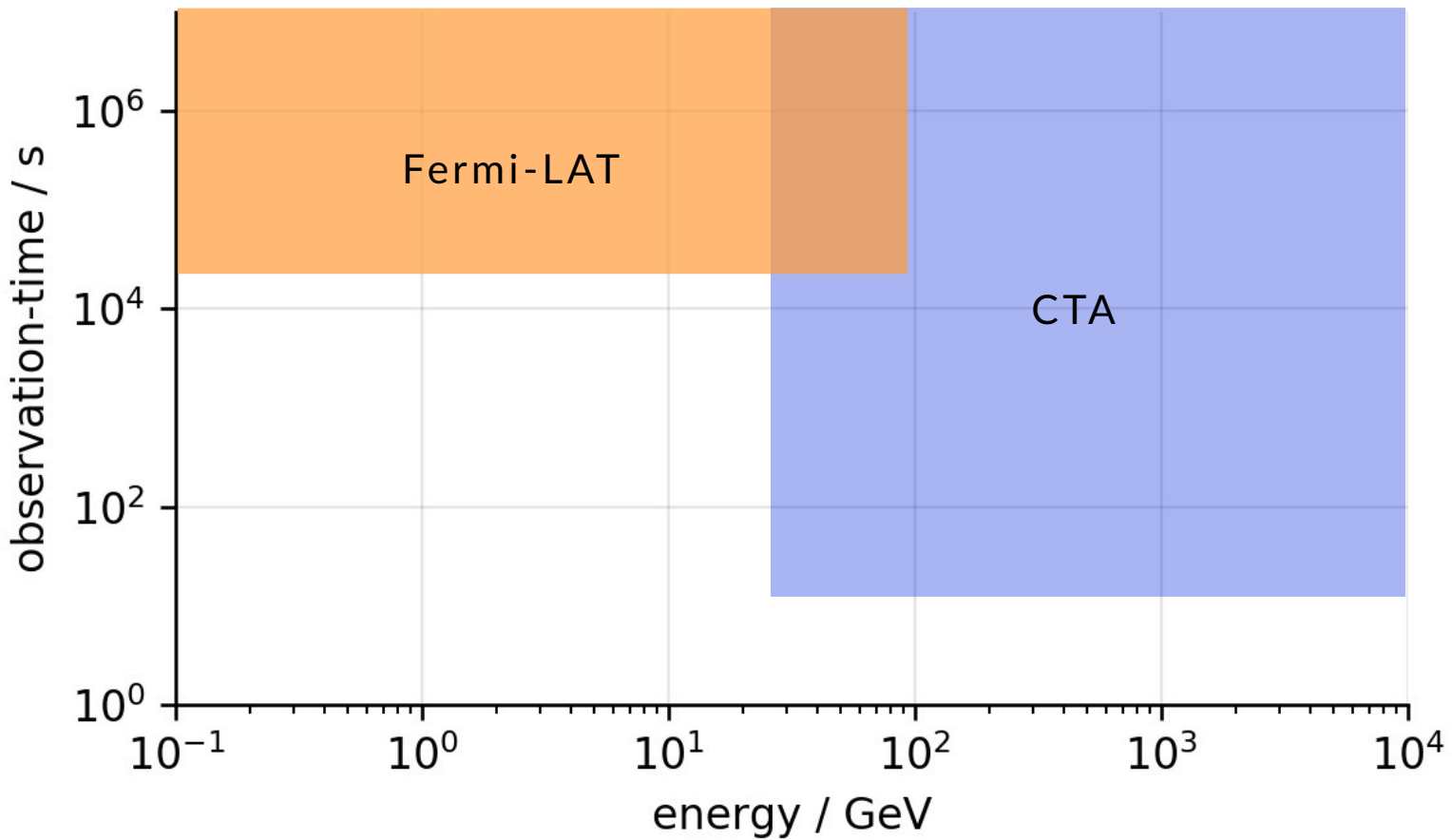

Explore Timing

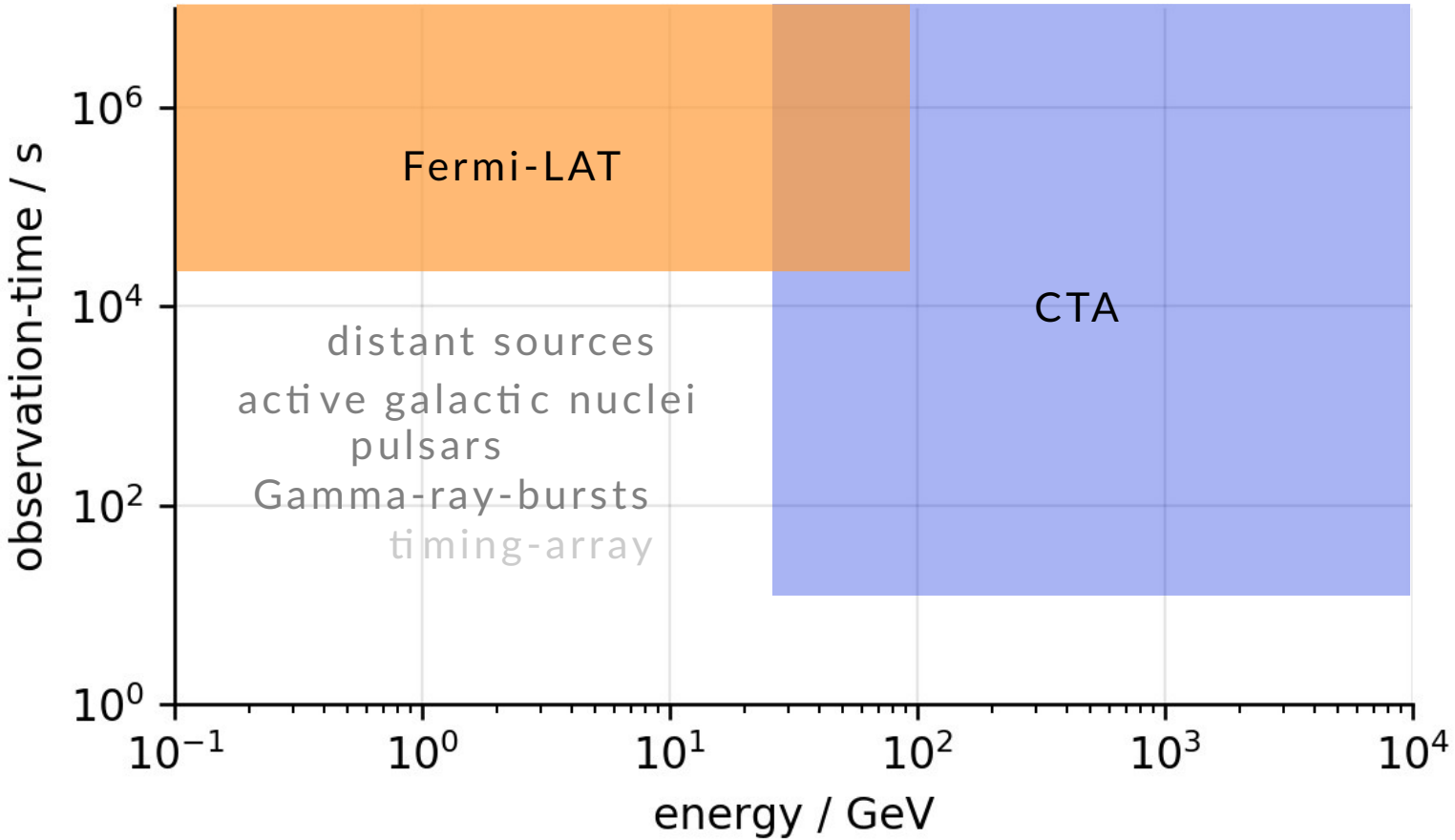

Explore Timing

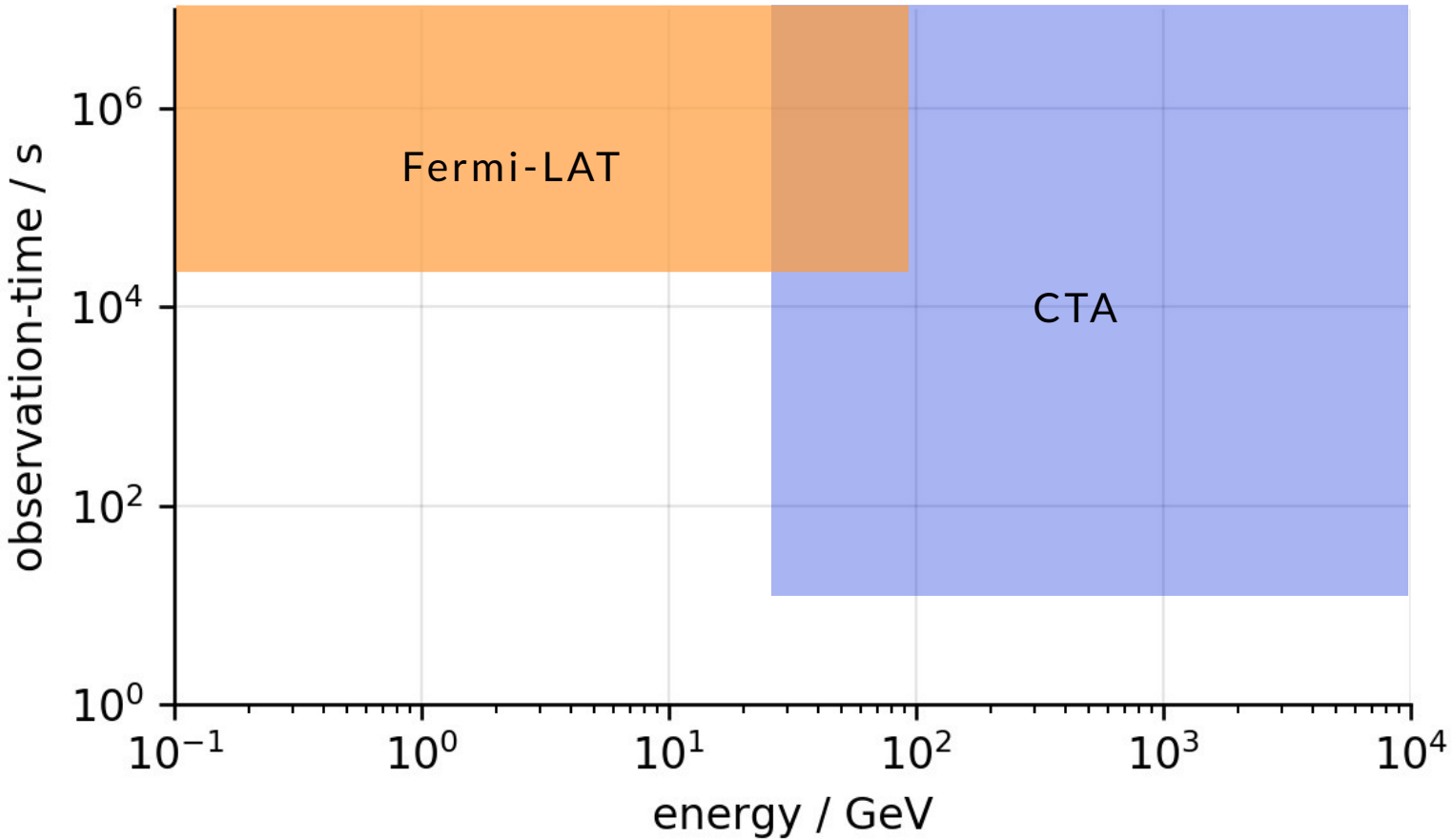

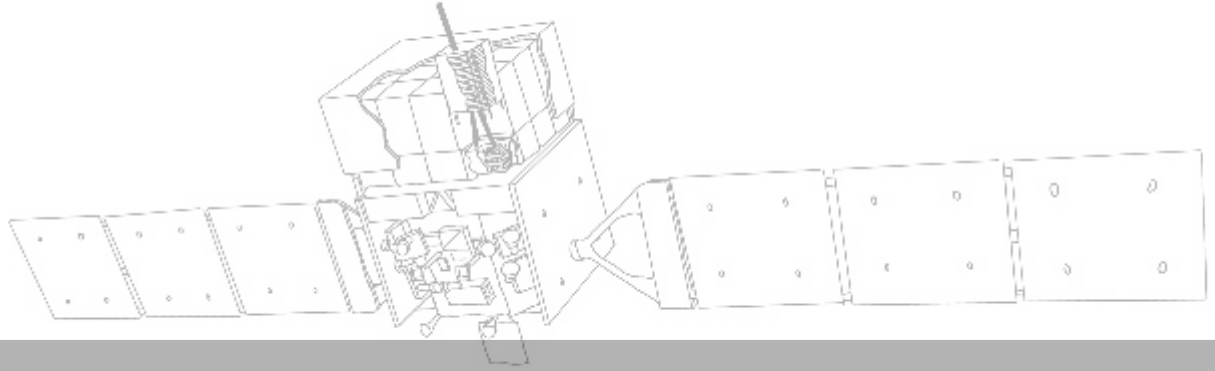

Today

Credit: https://www.mpi-hd.mpg.de/hfm/HESS/

Directly in Space

Credit: https://fermi.gsfc.nasa.gov/

Directly in Space

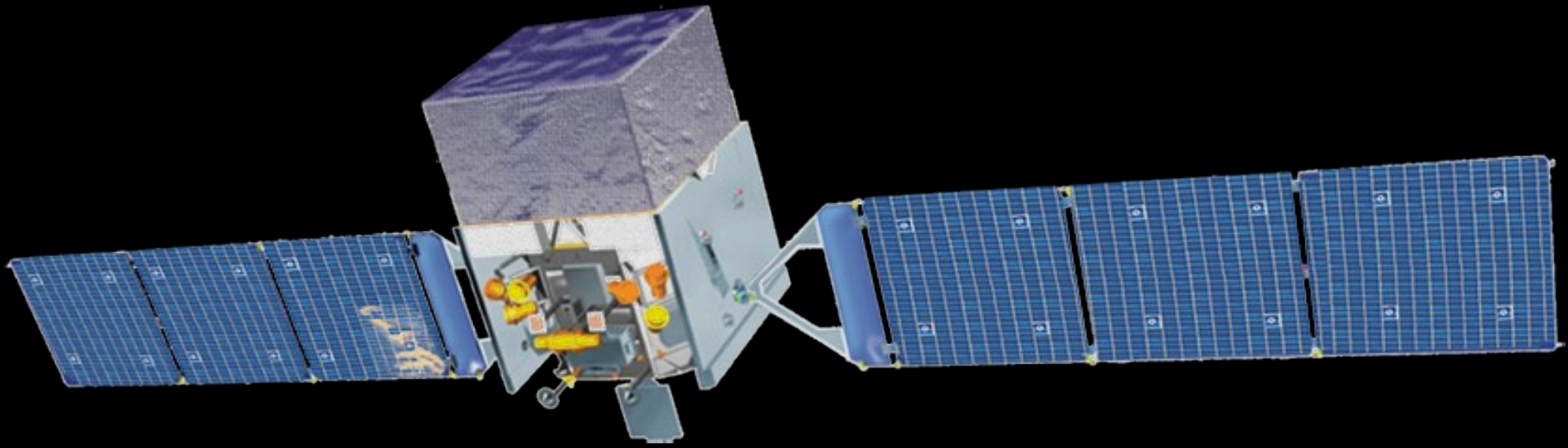

Credit: https://fermi.gsfc.nasa.gov/

Directly in Space

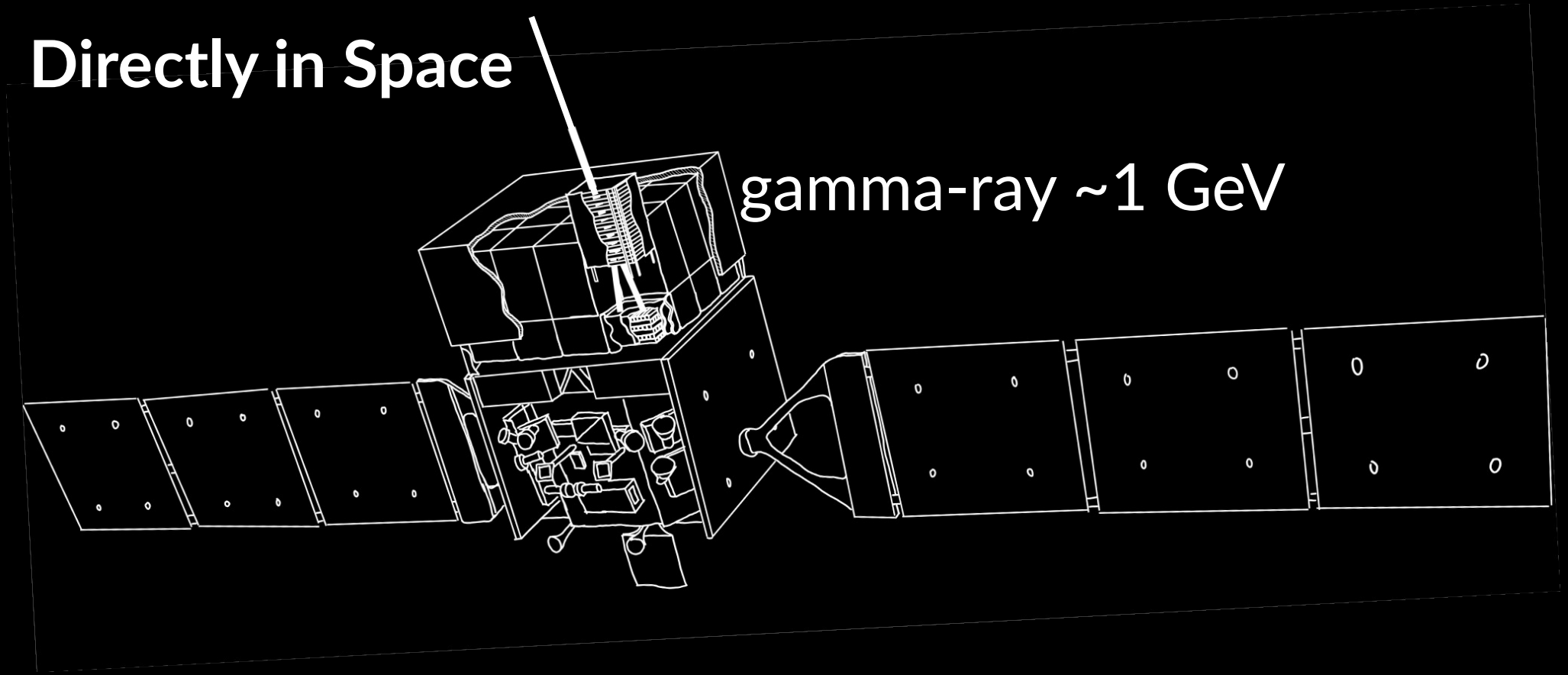

Directly in Space

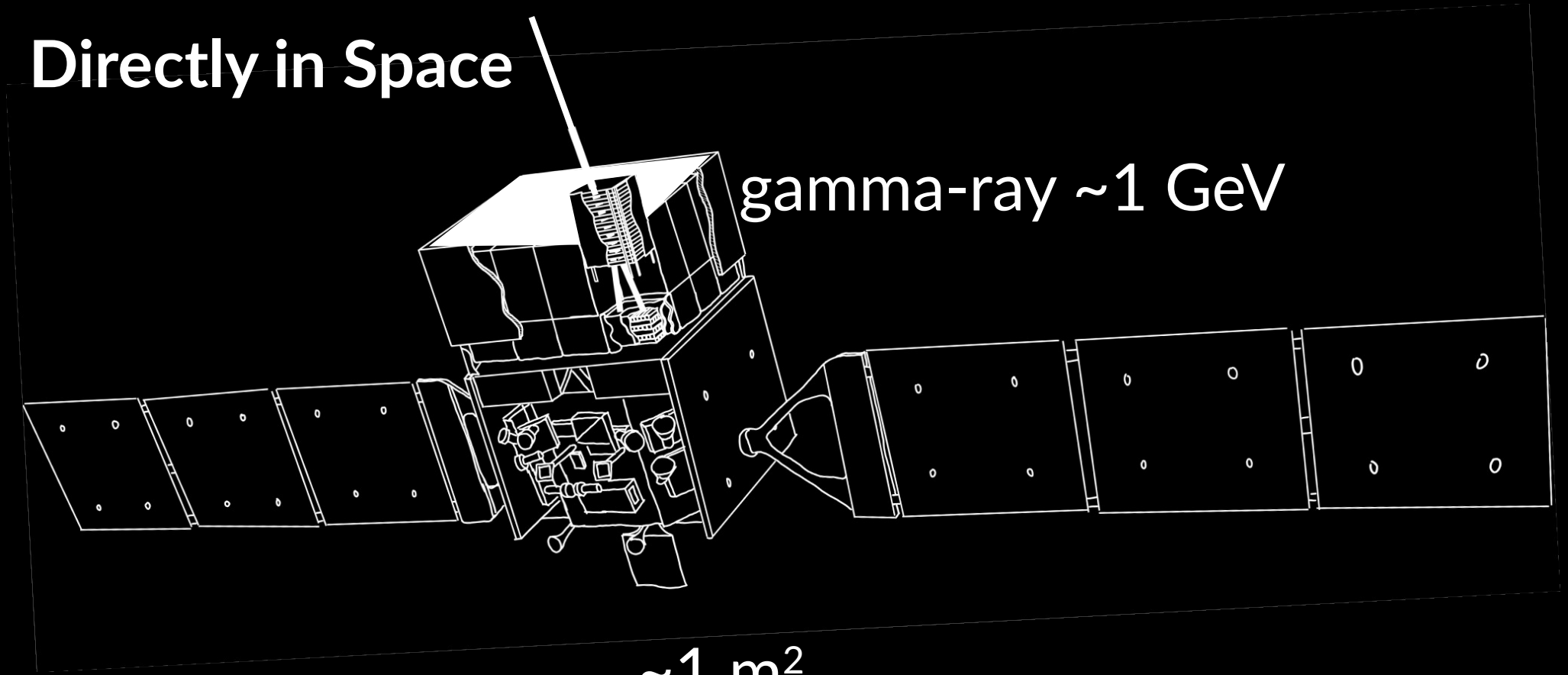

~1 m^2

Indirectly in Atmosphere

Credit: https://www.mpi-hd.mpg.de/hfm/HESS/

Indirectly in Atmosphere

gamma-ray ~100 GeV

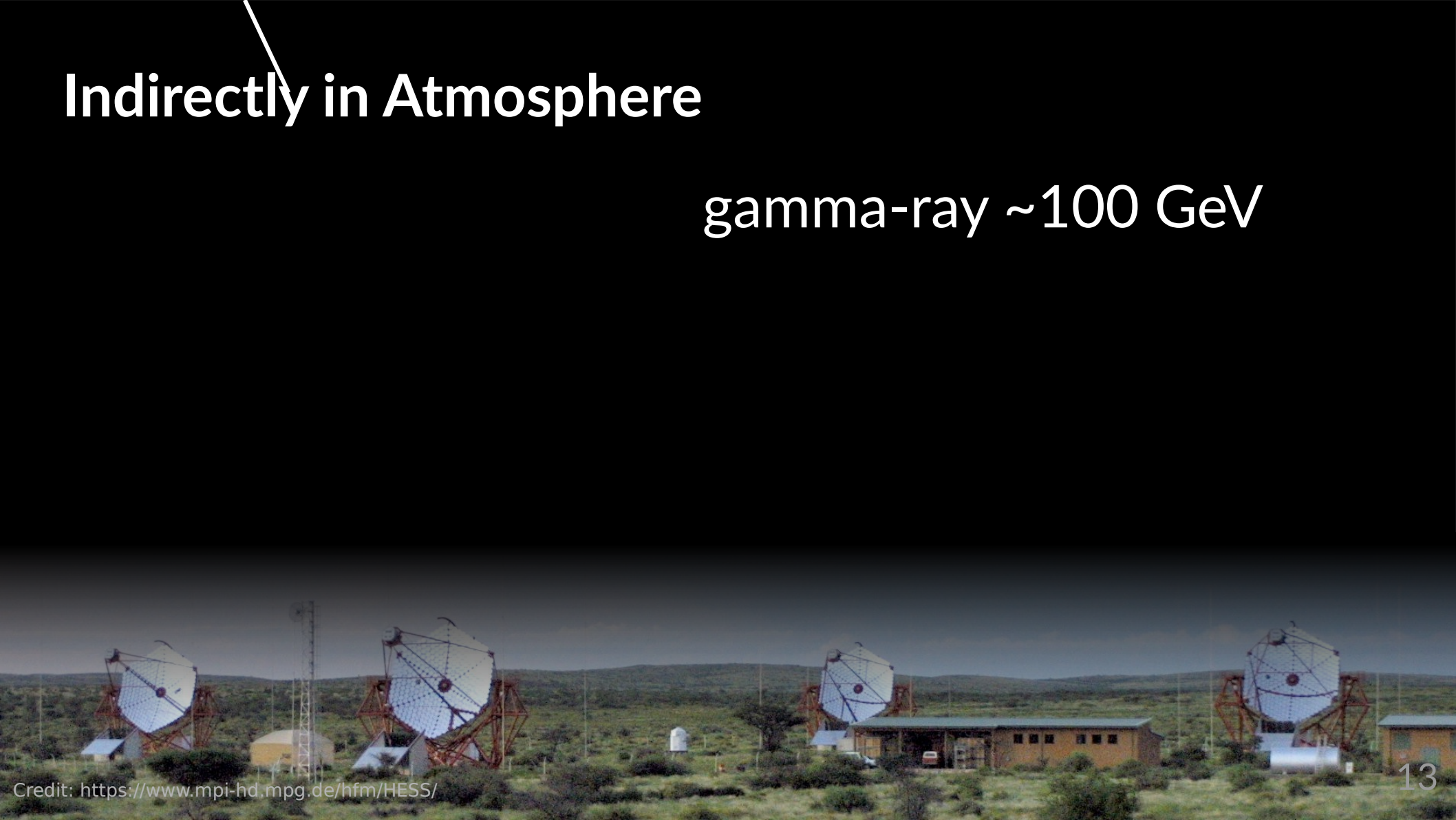

Credit: https://www.mpi-hd.mpg.de/hfm/HESS/

Indirectly in Atmosphere

gamma-ray ~100 GeV

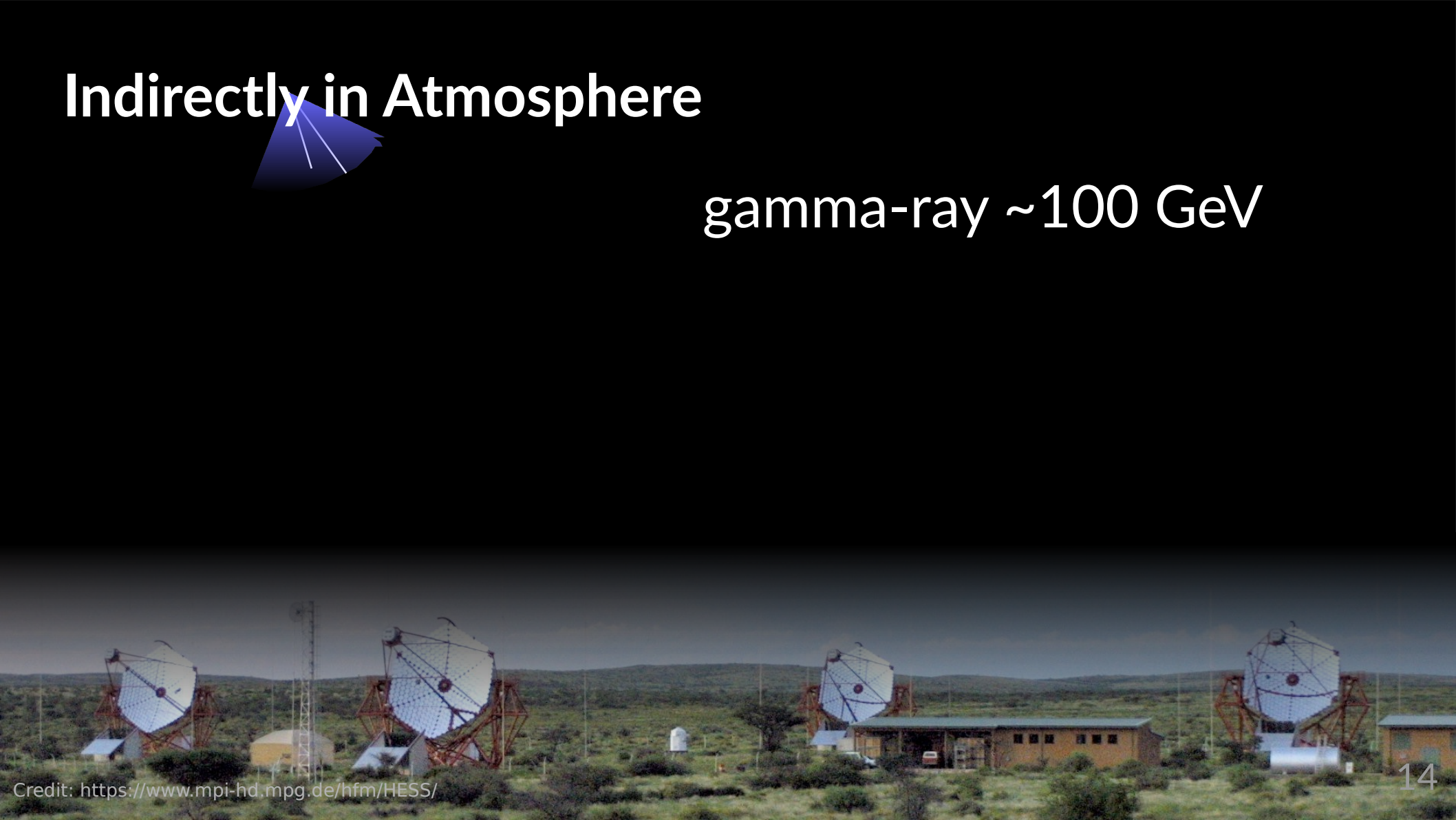

Credit: https://www.mpi-hd.mpg.de/hfm/HESS/

Indirectly in Atmosphere

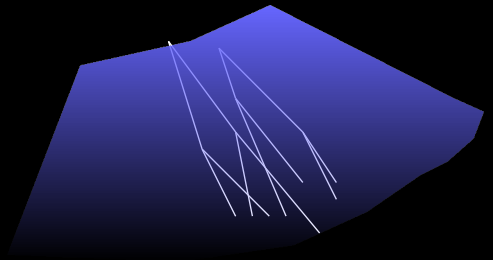

gamma-ray ~100 GeV

Credit: https://www.mpi-hd.mpg.de/hfm/HESS/

Indirectly in Atmosphere

gamma-ray ~100 GeV

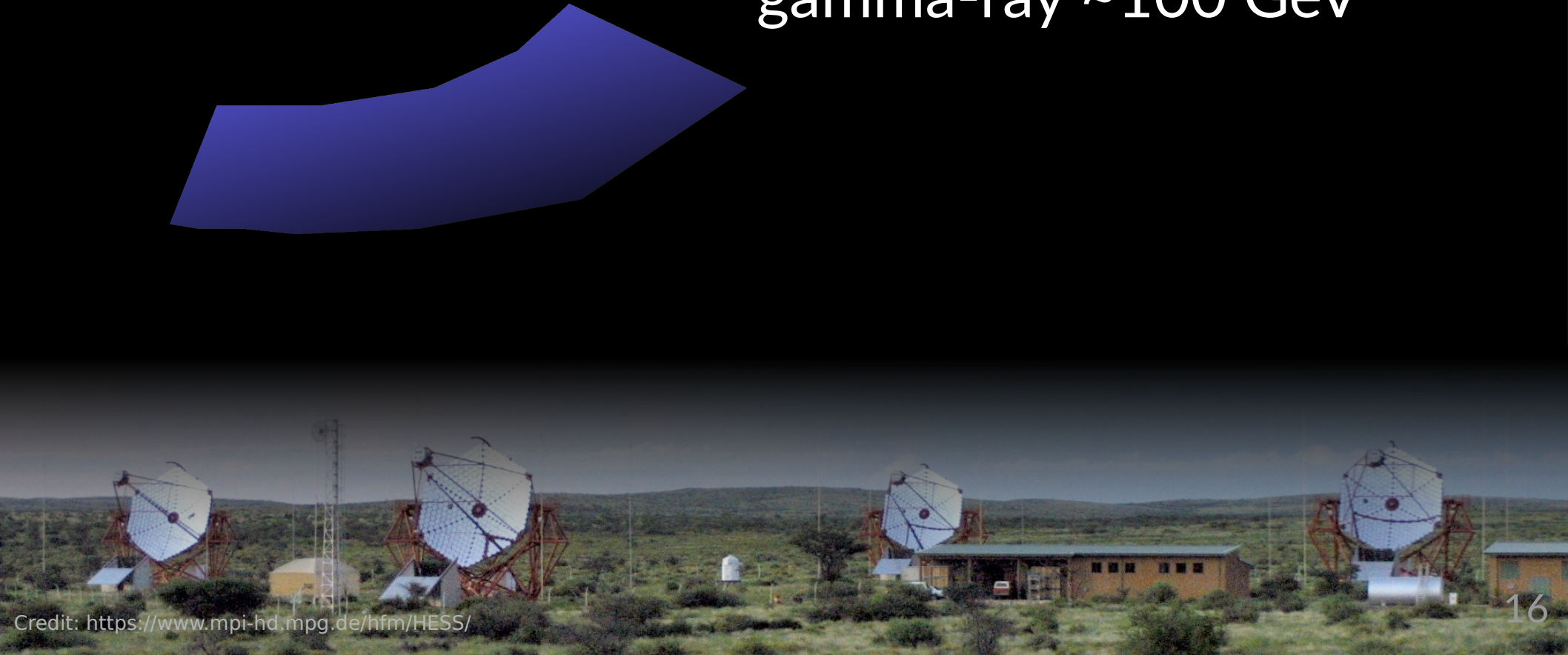

Credit: https://www.mpi-hd.mpg.de/hfm/HESS/

Indirectly in Atmosphere

gamma-ray ~100 GeV

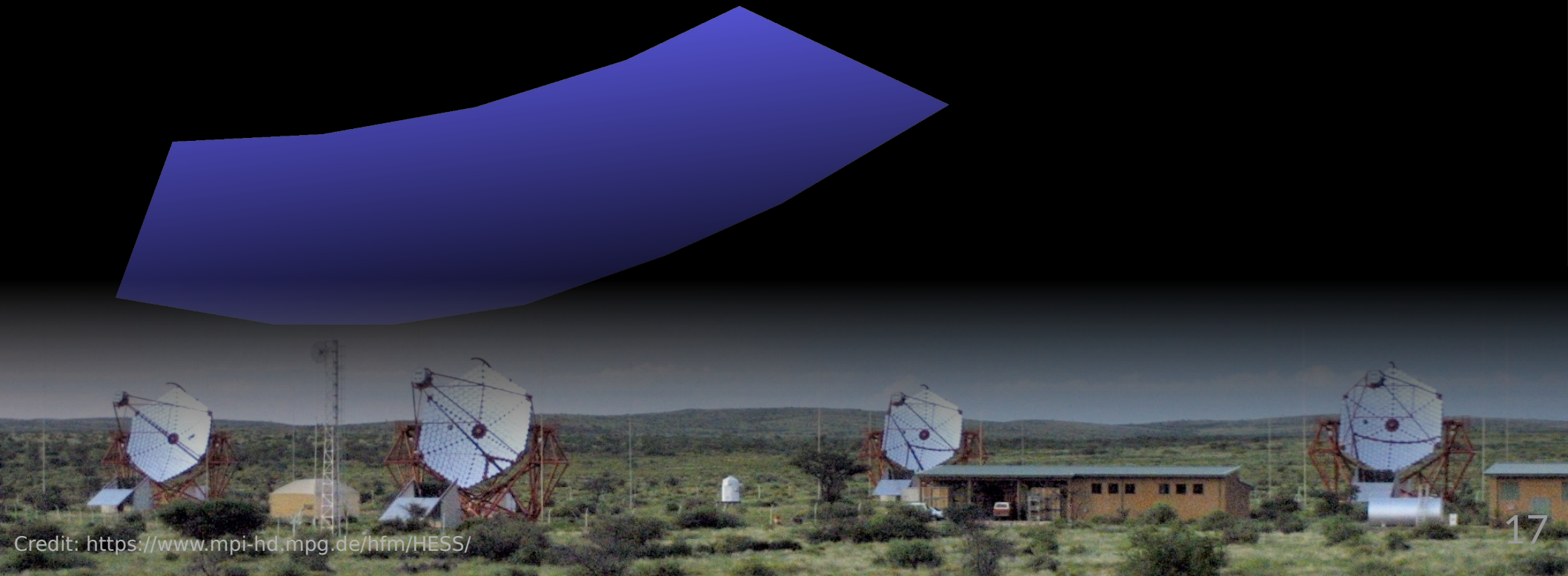

Credit: https://www.mpi-hd.mpg.de/hfm/HESS/

Indirectly in Atmosphere

gamma-ray ~100 GeV

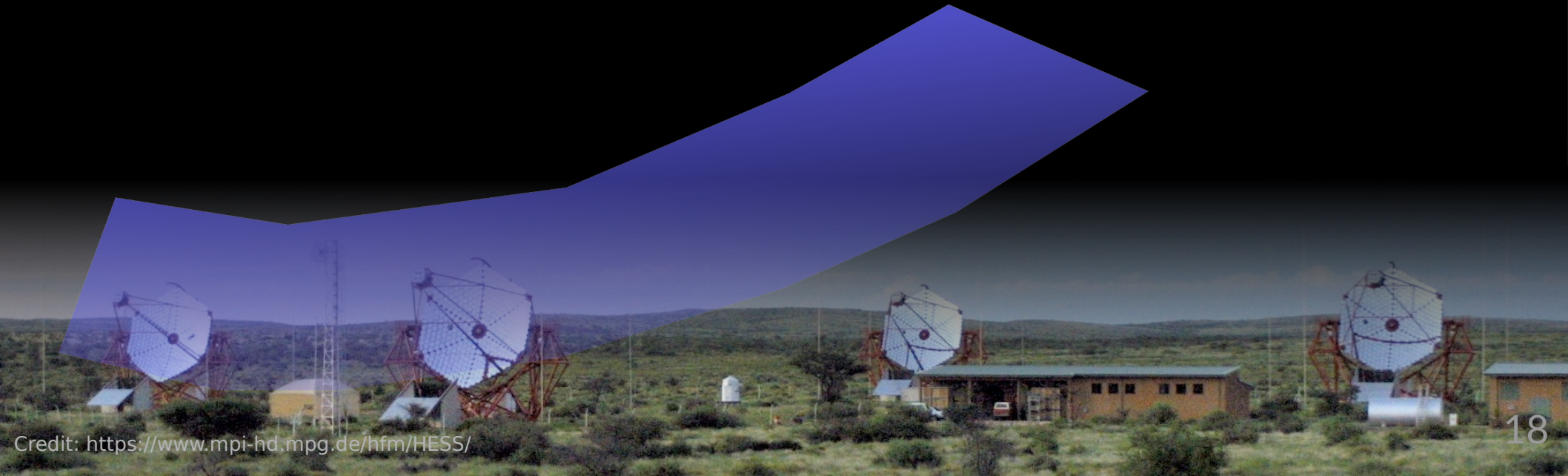

Credit: https://www.mpi-hd.mpg.de/hfm/HESS/

Indirectly in Atmosphere

gamma-ray ~100 GeV

Credit: https://www.mpi-hd.mpg.de/hfm/HESS/

Indirectly in Atmosphere

gamma-ray ~100 GeV

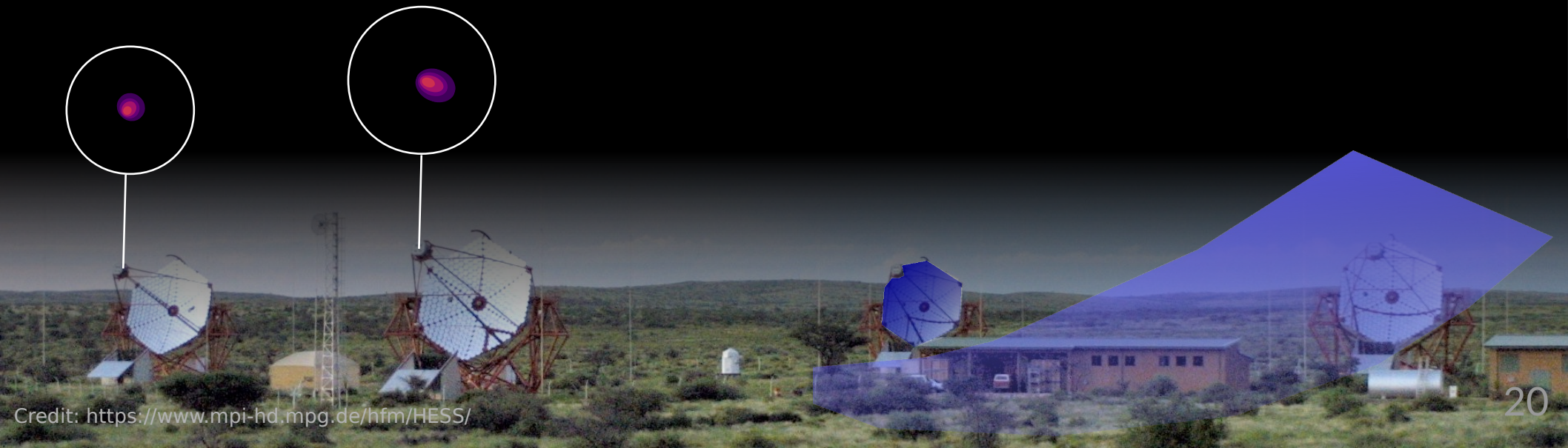

Credit: https://www.mpi-hd.mpg.de/hfm/HESS/

Indirectly in Atmosphere

gamma-ray ~100 GeV

Credit: https://www.mpi-hd.mpg.de/hfm/HESS/

Indirectly in Atmosphere

gamma-ray ~100 GeV

Credit: https://www.mpi-hd.mpg.de/hfm/HESS/

Indirectly in Atmosphere

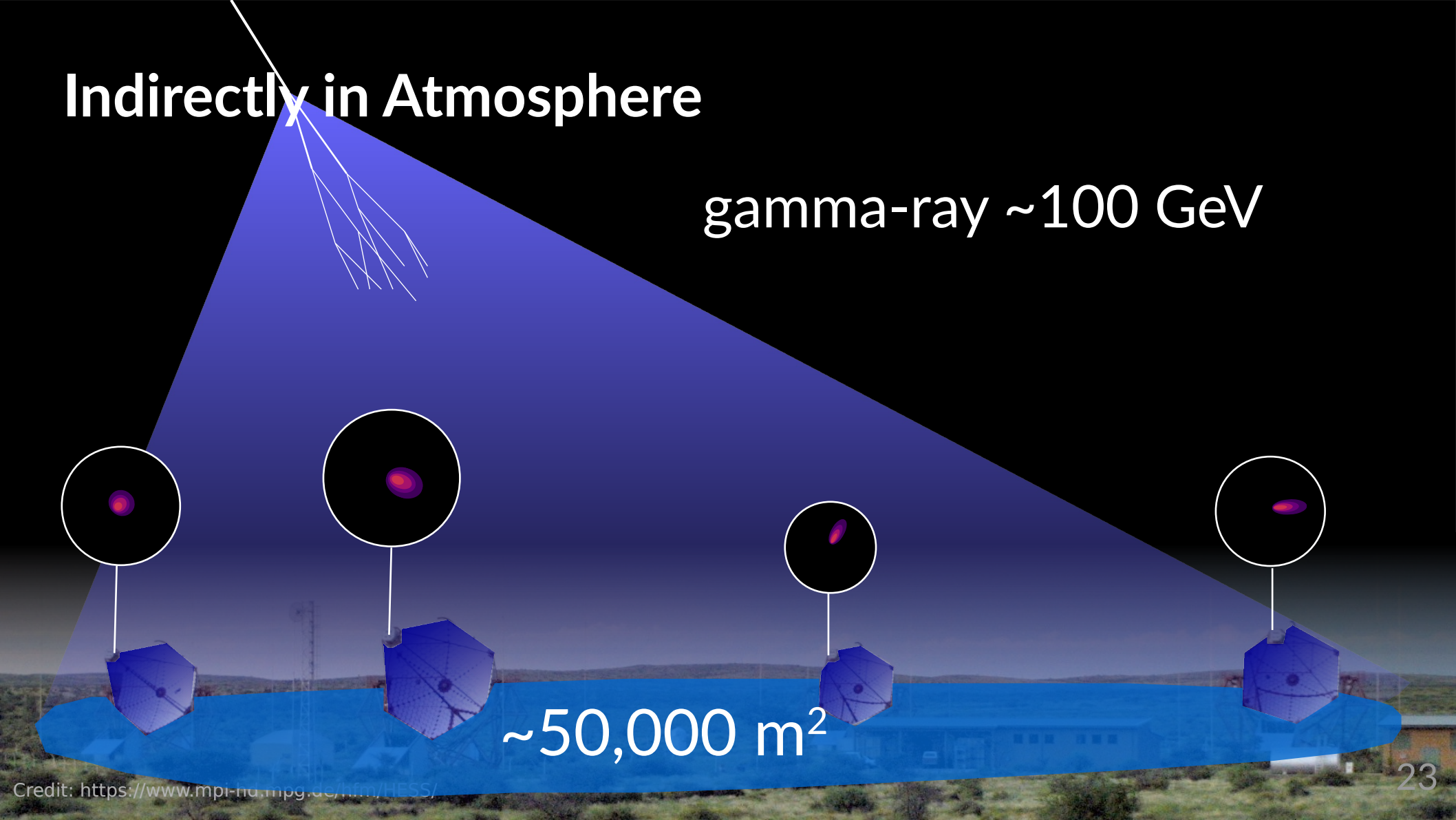

Credit: https://www.mpi-hd.mpg.de/hfm/HESS/

Indirectly in Atmosphere

gamma-ray ~10 GeV

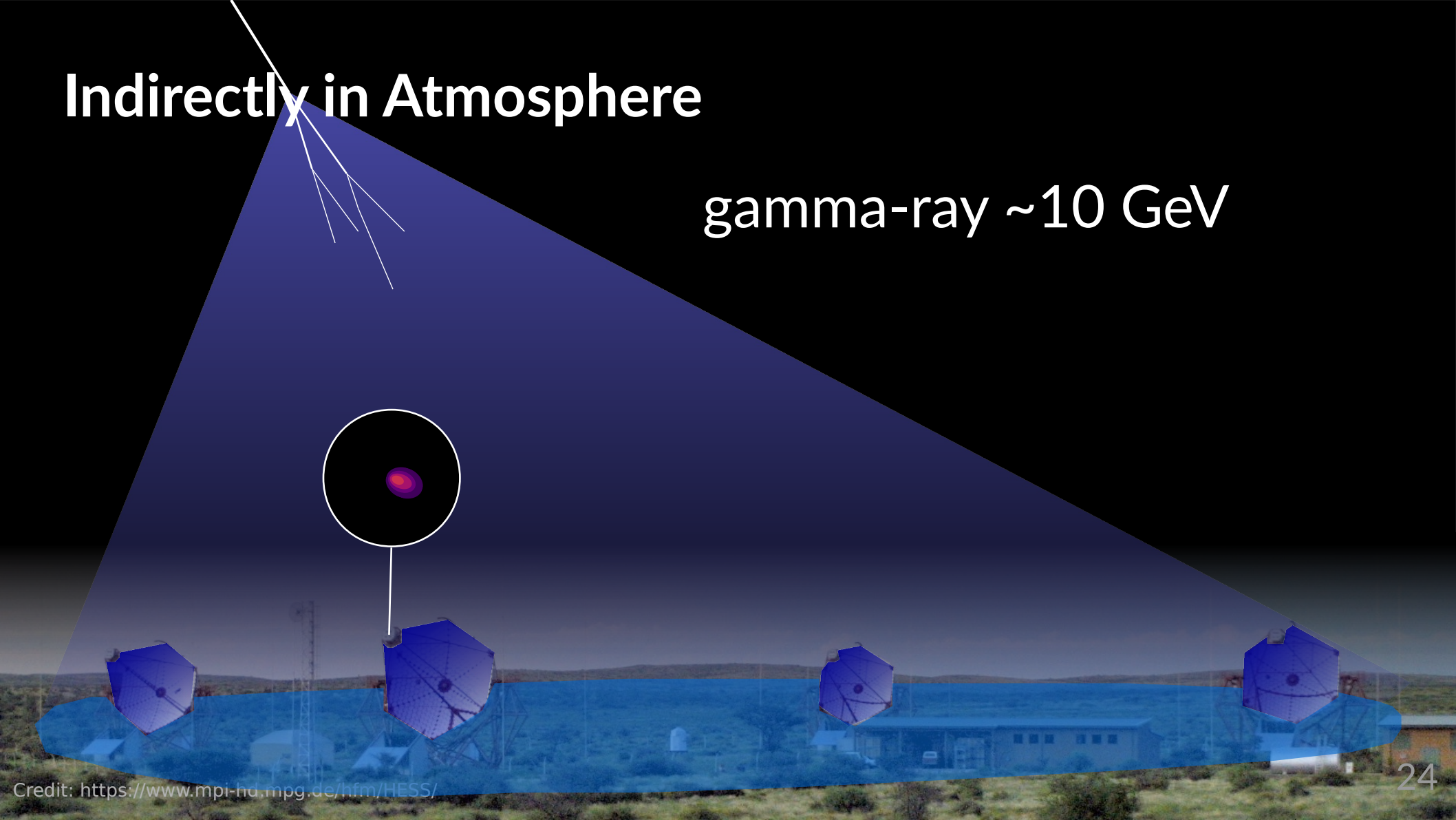

Credit: https://www.mpi-hd.mpg.de/hfm/HESS/

Indirectly in Atmosphere

gamma-ray ~1 GeV

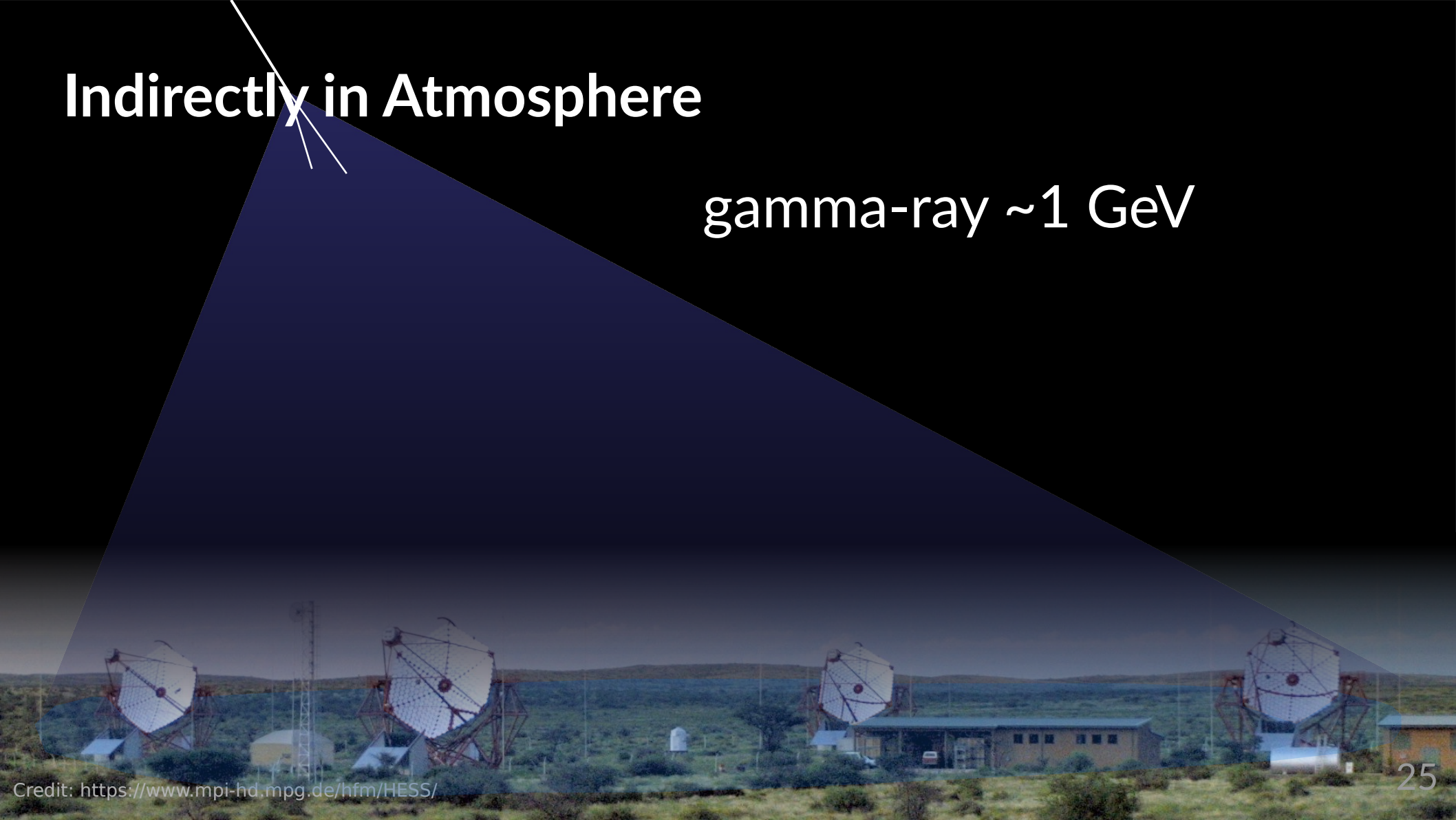

Credit: https://www.mpi-hd.mpg.de/hfm/HESS/

Centralized Trigger

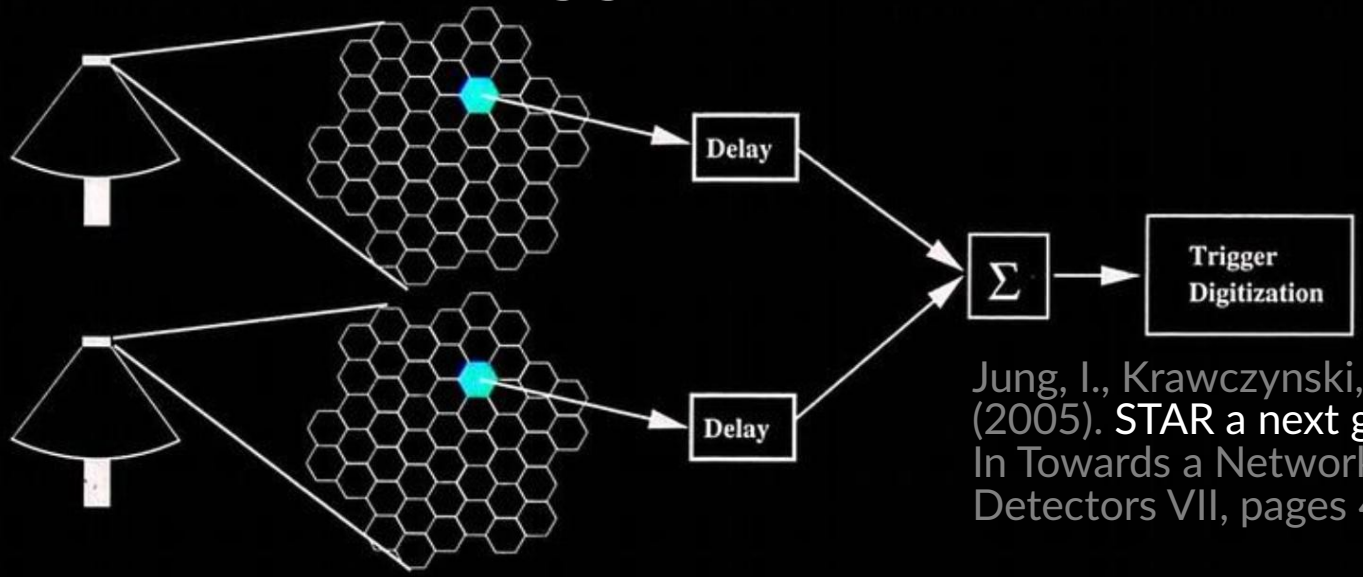

Jung, I., Krawczynski, H., Buckley, J., and Falcone, A. (2005). STAR a next generation Cherenkov telescope. In Towards a Network of Atmospheric Cherenkov Detectors VII, pages 463–6.

Credit: https://www.mpi-hd.mpg.de/hfm/HESS/

Centralized Trigger

López-Coto, R., Mazin, D., Paoletti, R., Bigas, O. B., and Cortina, J. (2016).
The Topo-Trigger: A new concept of stereo trigger system for imaging atmospheric Cherenkov telescopes.
Journal of Instrumentation, 11(04):P04005.

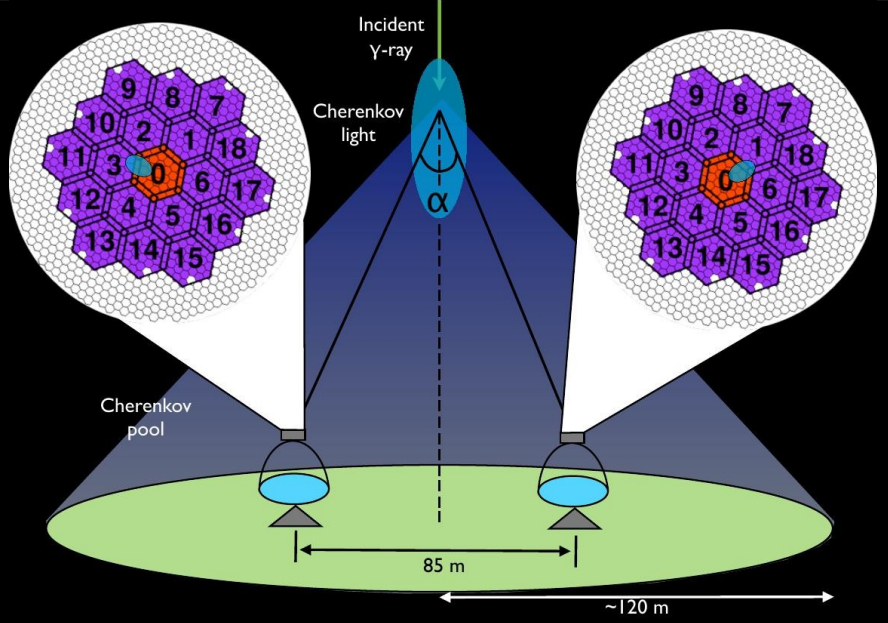

Credit: Thomas Kraehenbuehl

Large Telescope

Credit: Tomohiro Inada

Large Telescope

"... a problem with large telescopes ... is the very limited depth-of-field [Hofmann, W. 2001] ... . (Thus,) The useful size of large Cherenkov-telescopes is ... limited"

Bernlohr, K. et al. (2013).
Monte Carlo design studies for the Cherenkov Telescope Array.
Astroparticle Physics, 43:171–188.

Hofmann, W. (2001).
How to focus a Cherenkov telescope.
Journal of Physics G: Nuclear and Particle Physics,
27(4):933–939.

Credit: Tomohiro Inada

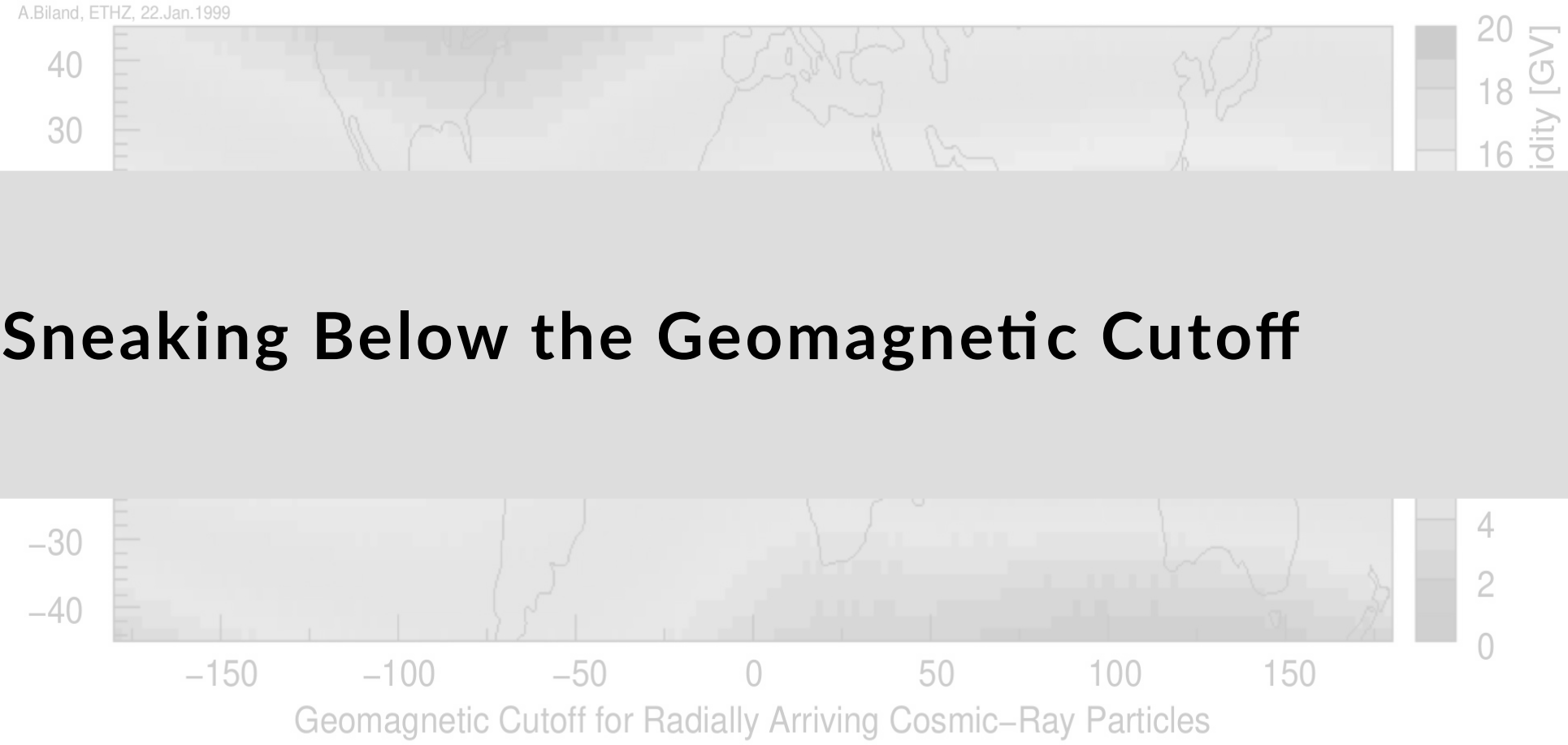

Sneaking Below the Geomagnetic Cutoff

Geomagnetic Cutoff

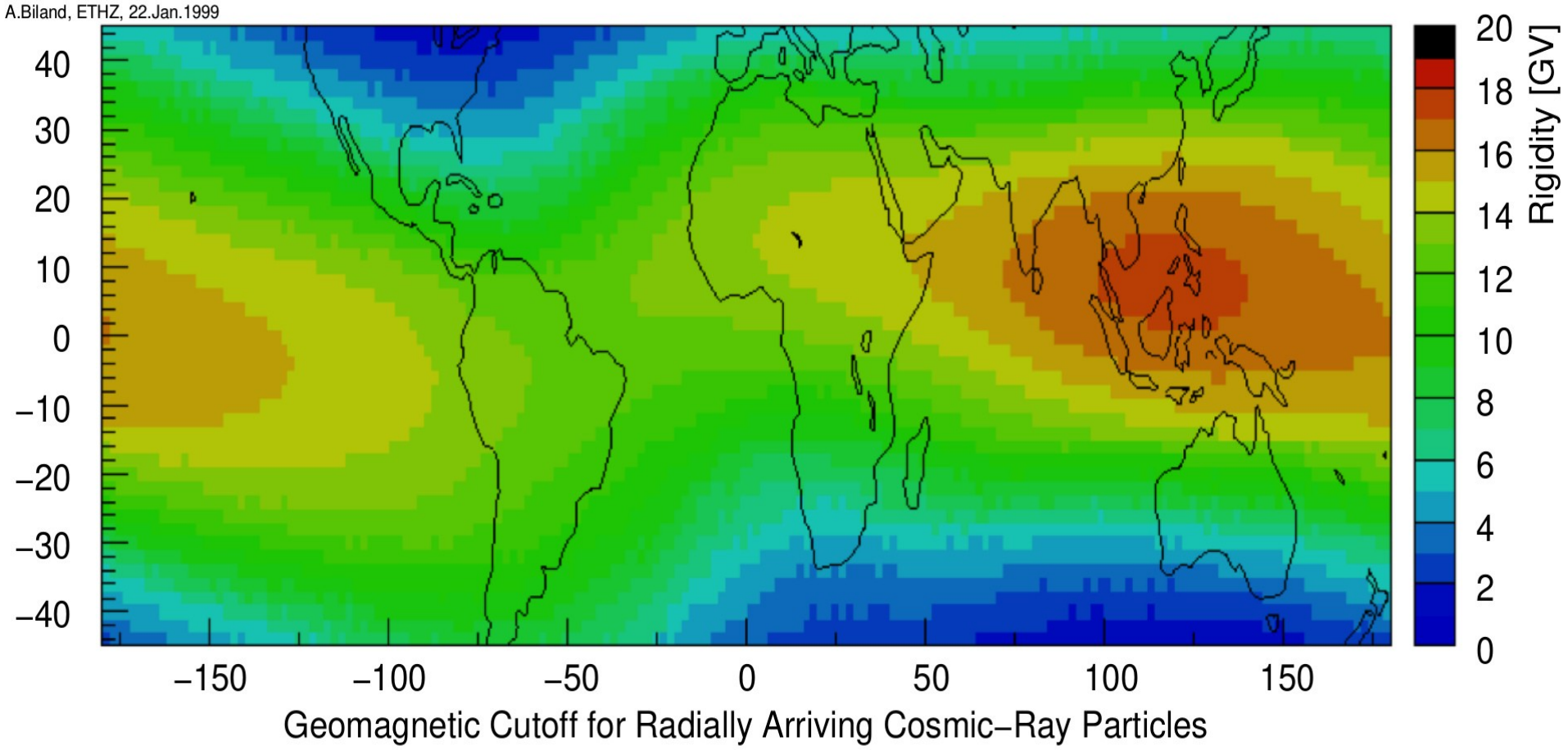

Adrian Biland, ETH Zurich, 1999

Geomagnetic Cutoff

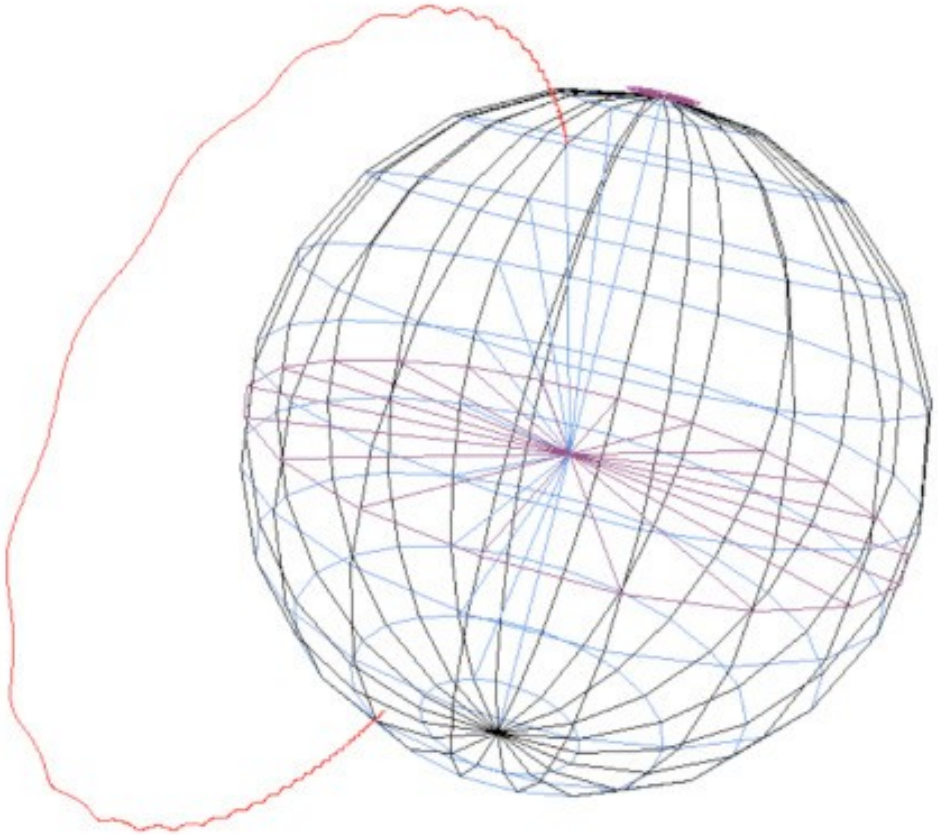

no-bounce

Geomagnetic Cutoff

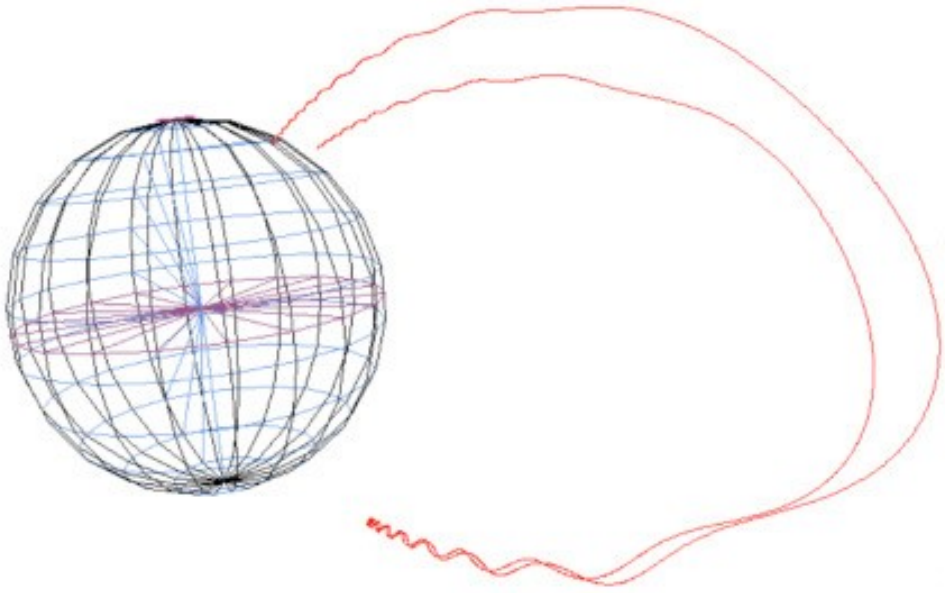

one-bounce

Geomagnetic Cutoff

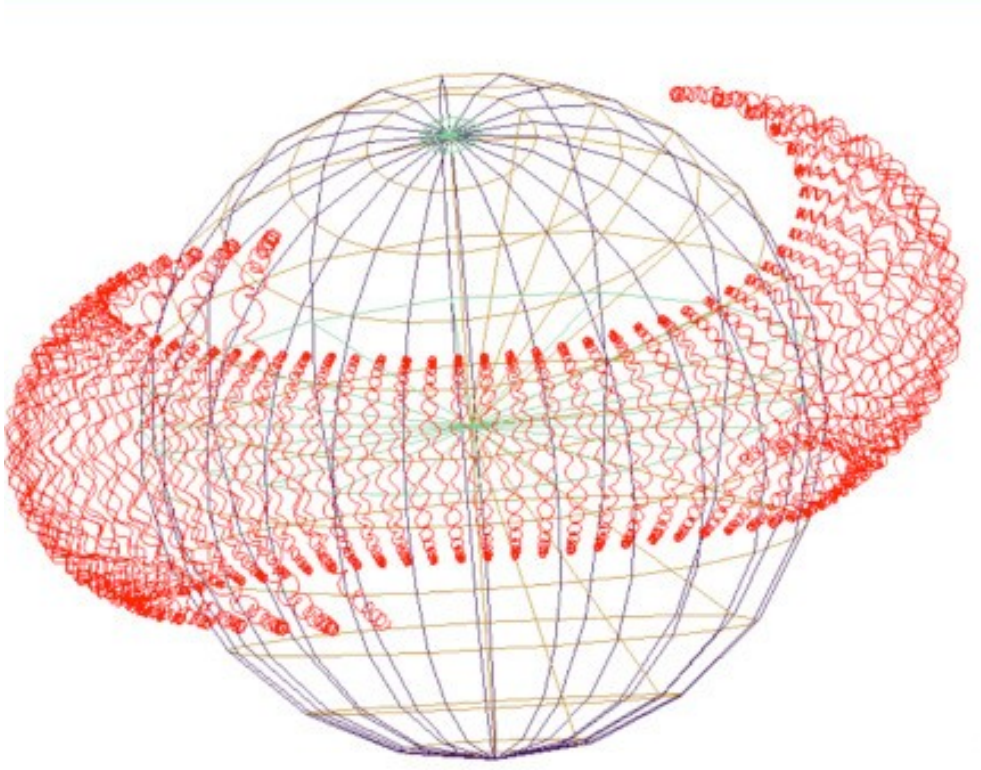

multi-bounce

Deflection of shower

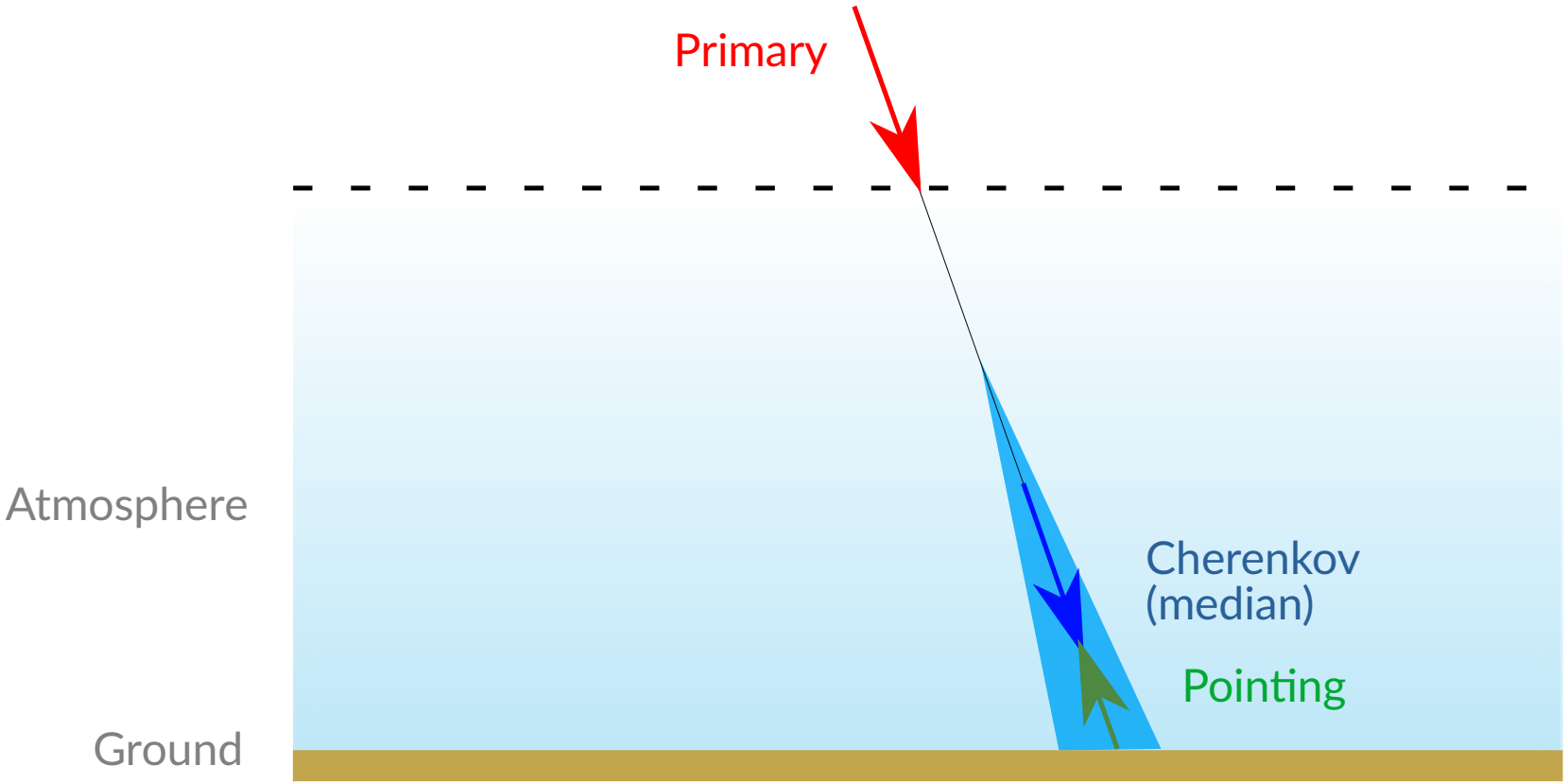

Deflection of shower

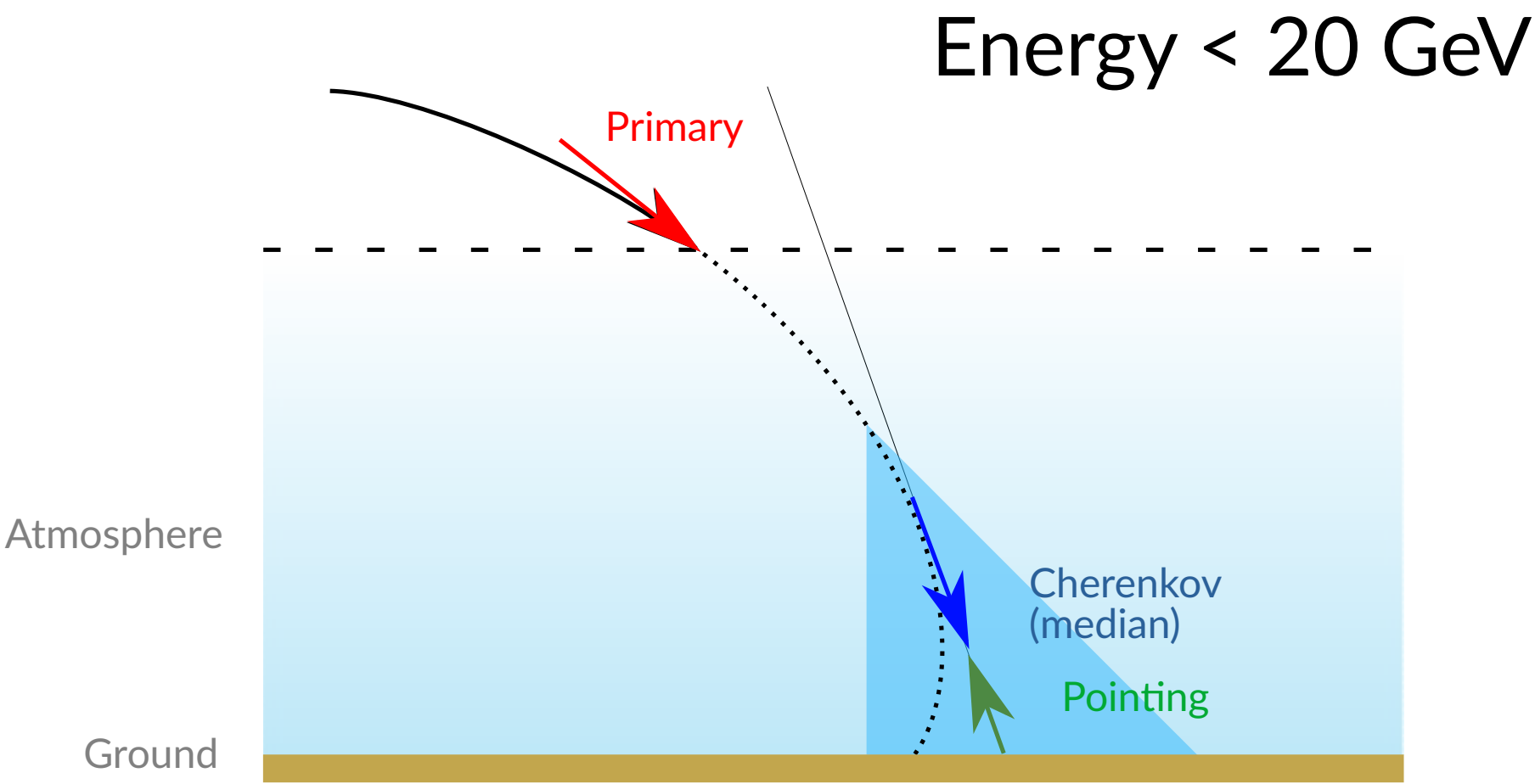

Deflection of shower

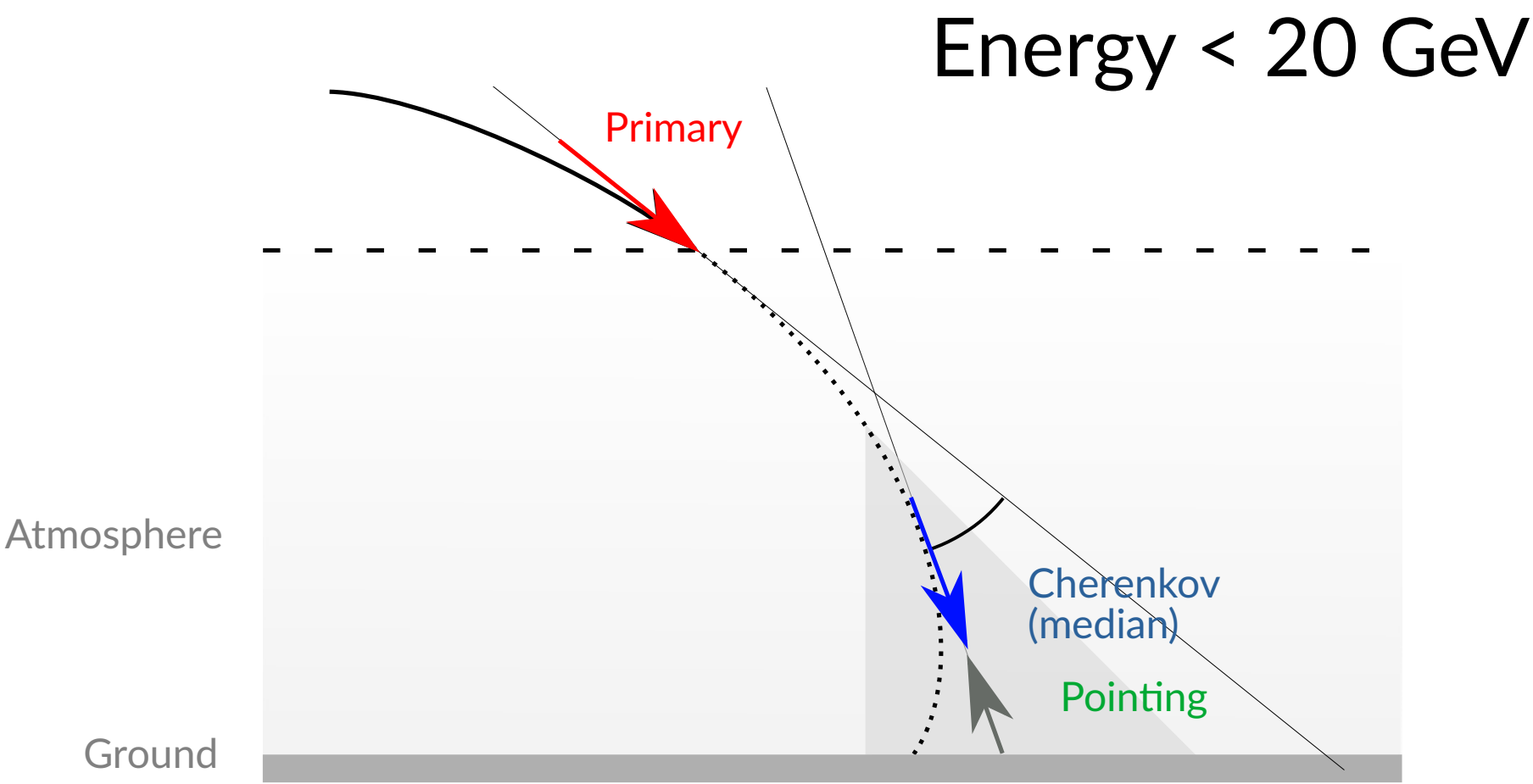

Deflection of shower

Helium

Gamsberg, Namibia

horizontal: 12.5uT
vertical: -25.9uT
2300m a.s.l.

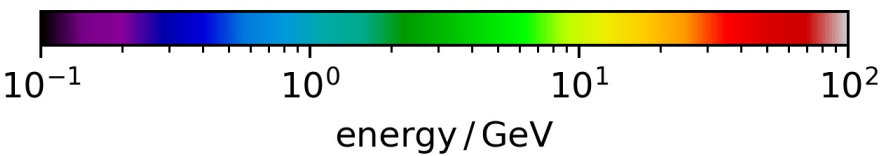

Direction of primary to get Cherenkov-light from zenith.

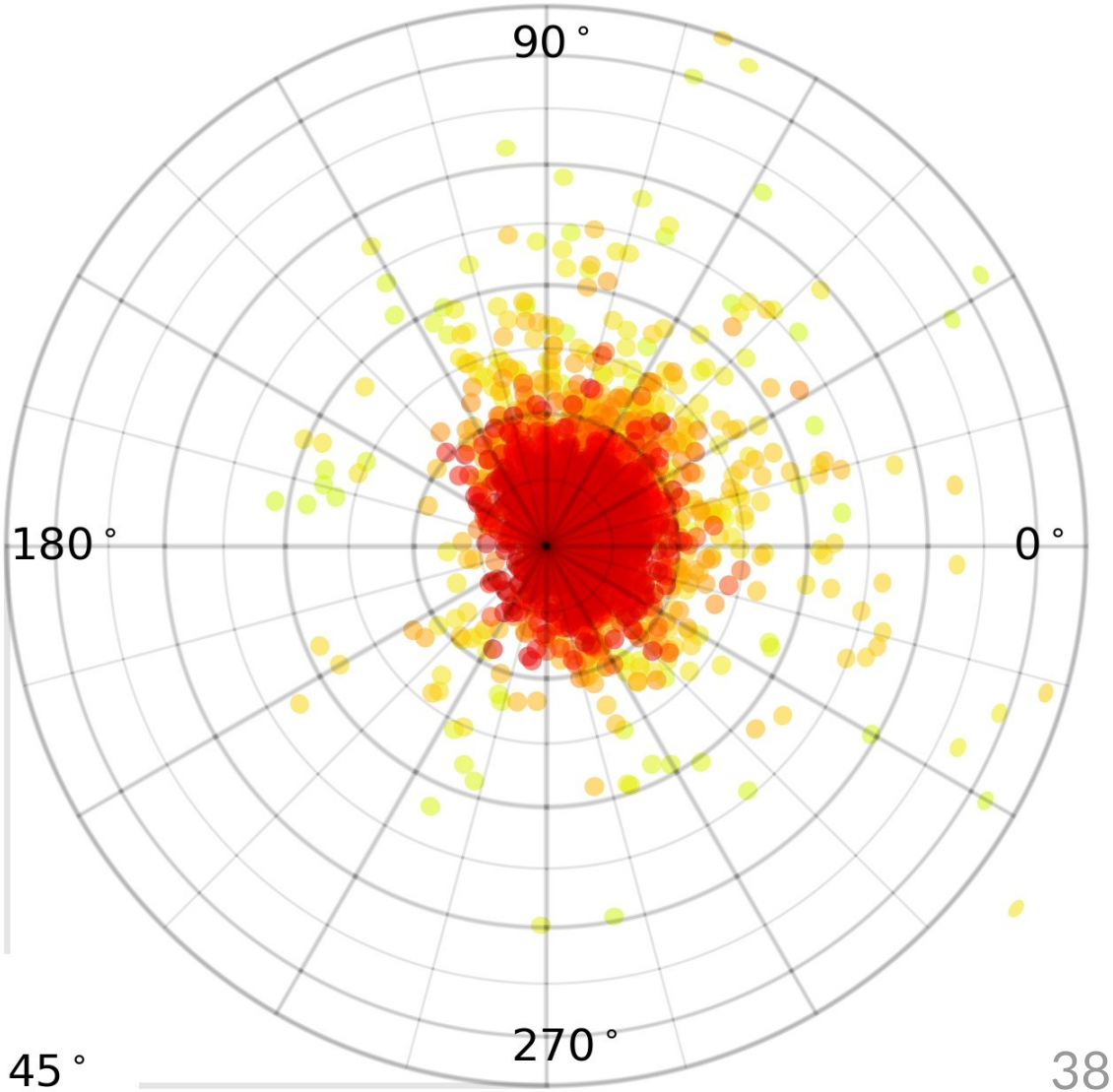

Deflection of shower

Proton

Gamsberg, Namibia

horizontal: 12.5uT
vertical: -25.9uT
2300m a.s.l.

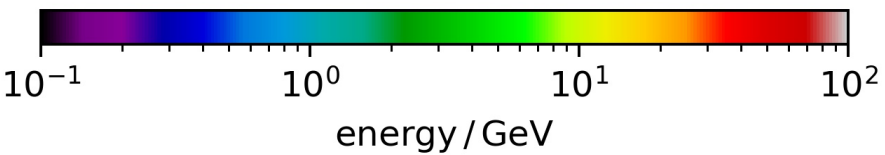

Direction of primary to get Cherenkov-light from zenith.

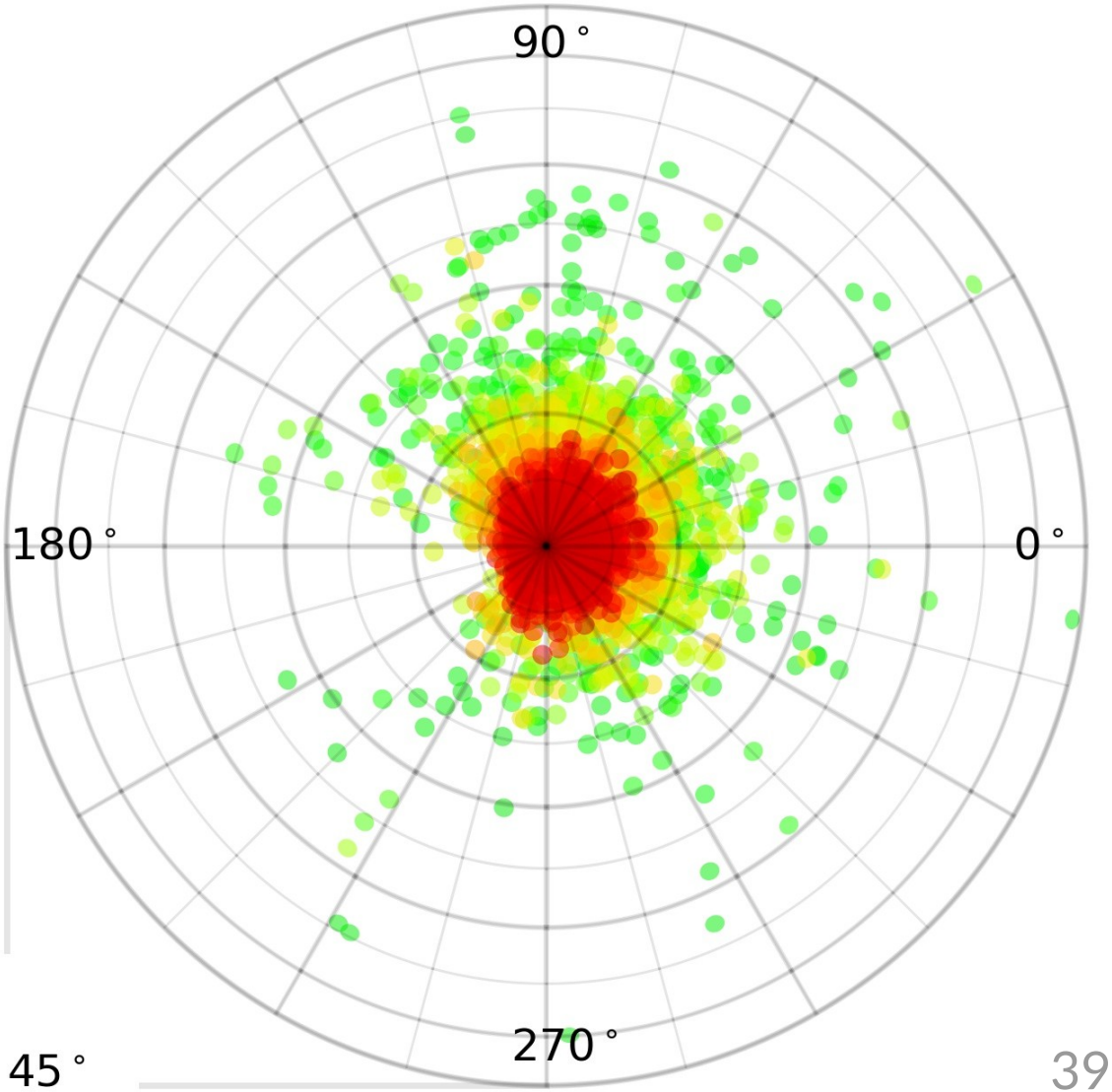

Deflection of shower

Electron

Gamsberg, Namibia

horizontal: 12.5uT
vertical: -25.9uT
2300m a.s.l.

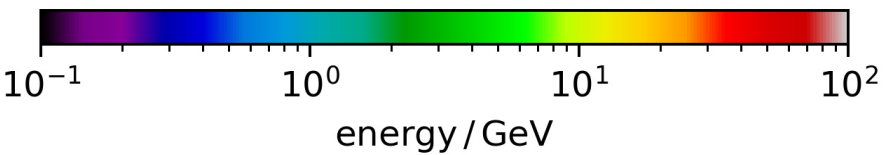

Direction of primary to get Cherenkov-light from zenith.

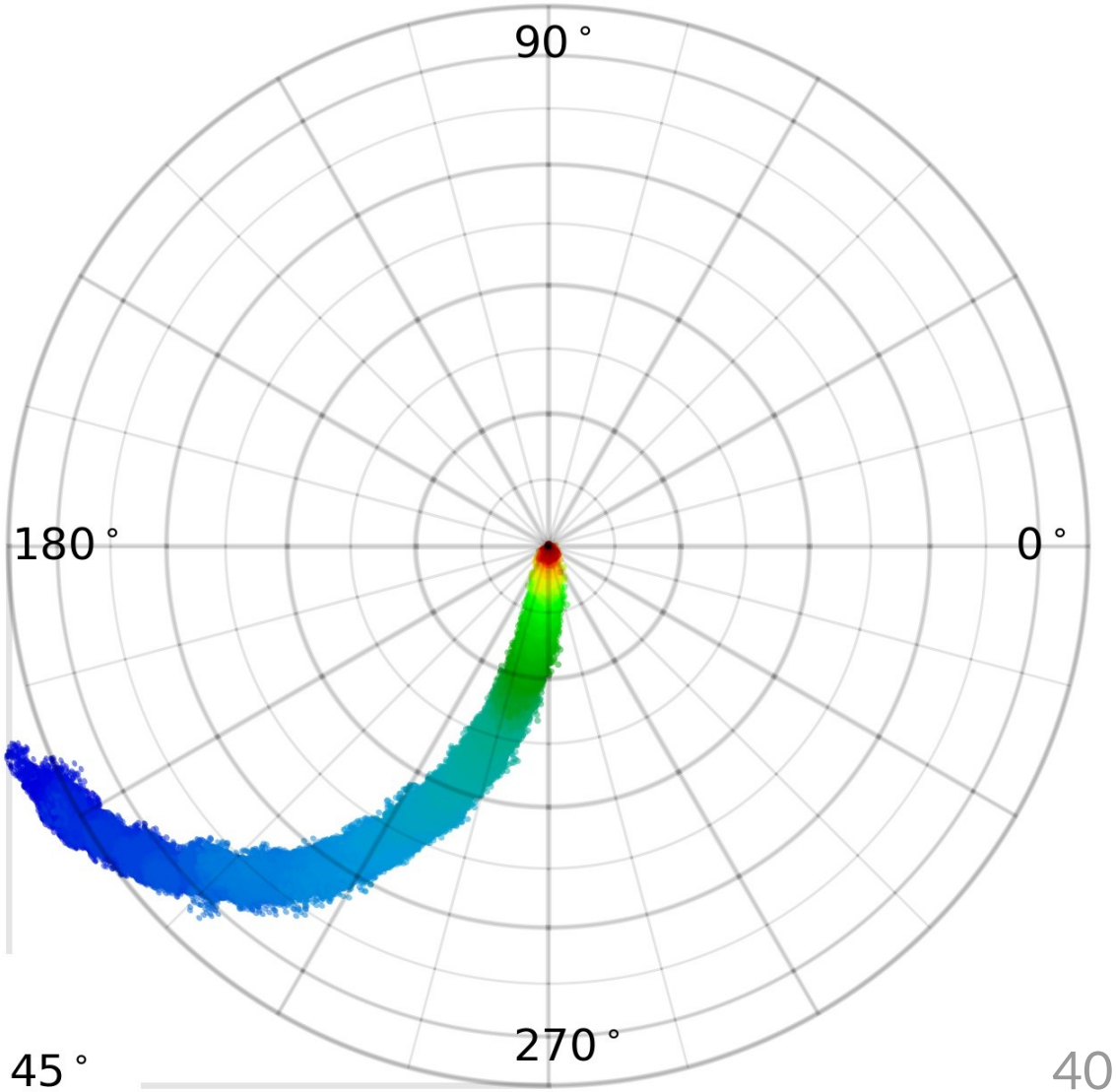

Deflection of shower

Gamma-ray

Gamsberg, Namibia

horizontal: 12.5uT
vertical: -25.9uT
2300m a.s.l.

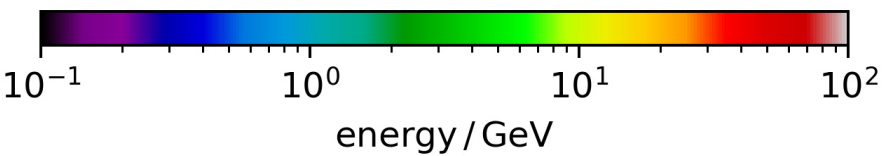

Direction of primary to get Cherenkov-light from zenith.

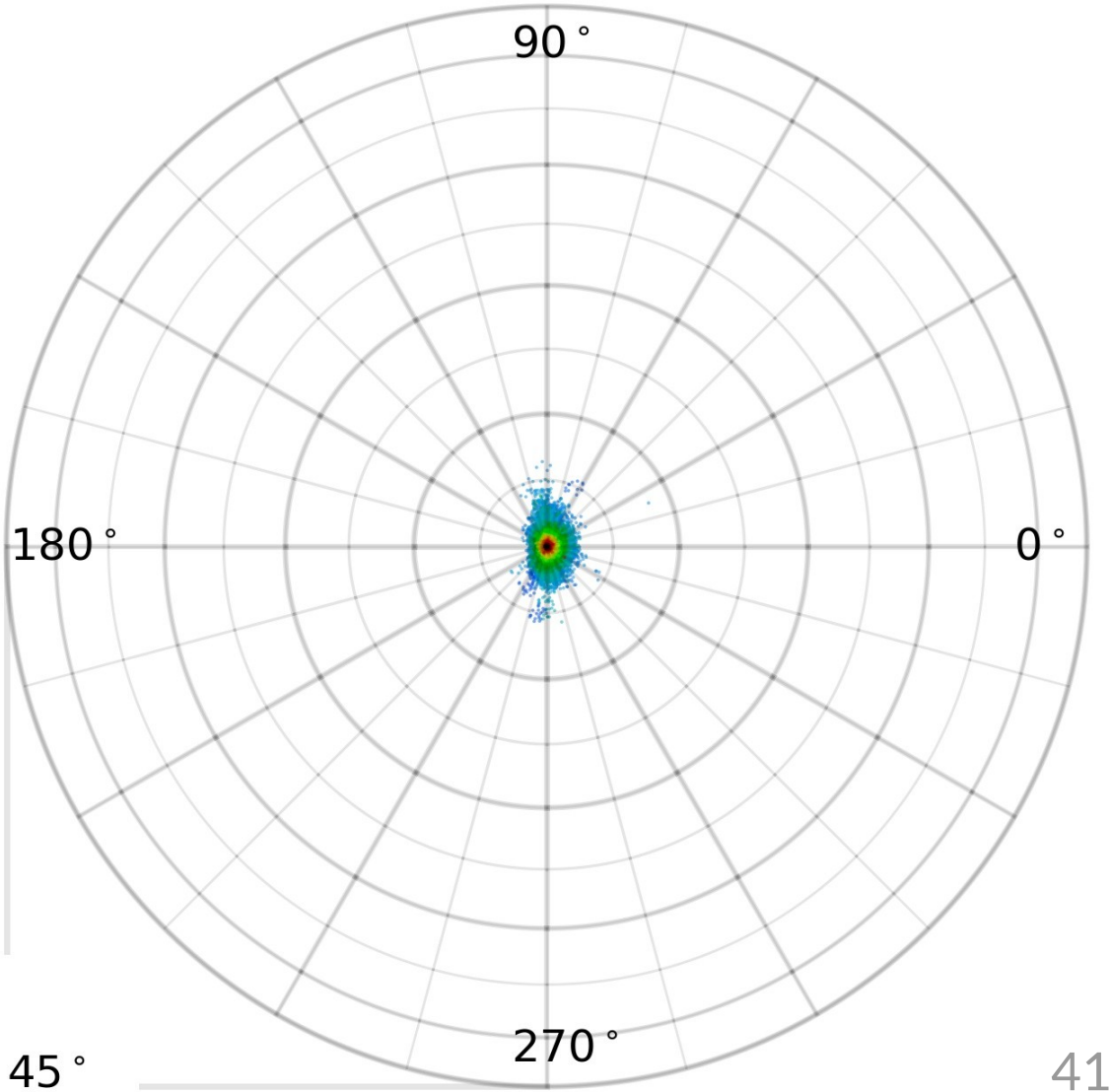

Deflection of shower

Gamma-ray

Gamsberg, Namibia

horizontal: 12.5uT
vertical: -25.9uT
2300m a.s.l.

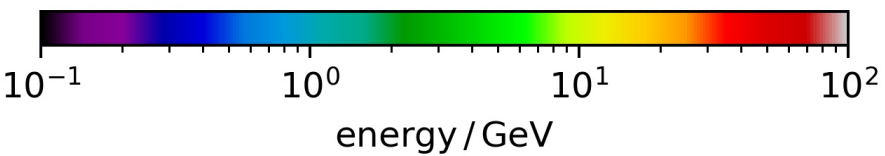

Direction of primary to get Cherenkov-light from zenith.

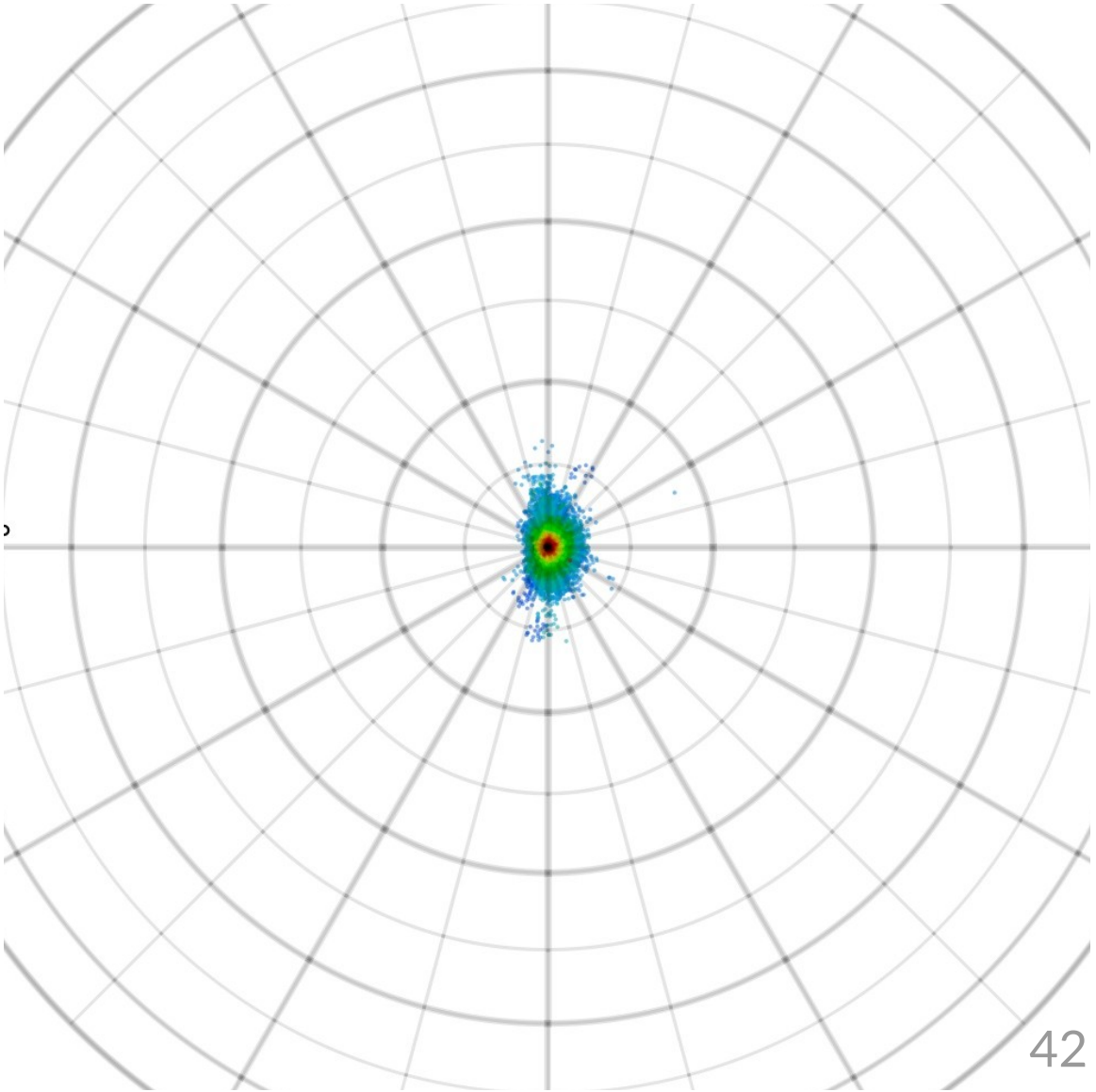

Deflection of shower

Gamma-ray

Gamsberg, Namibia

horizontal: 12.5uT
vertical: -25.9uT
2300m a.s.l.

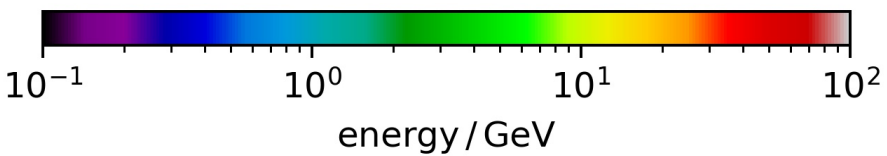

Direction of primary to get Cherenkov-light from zenith.

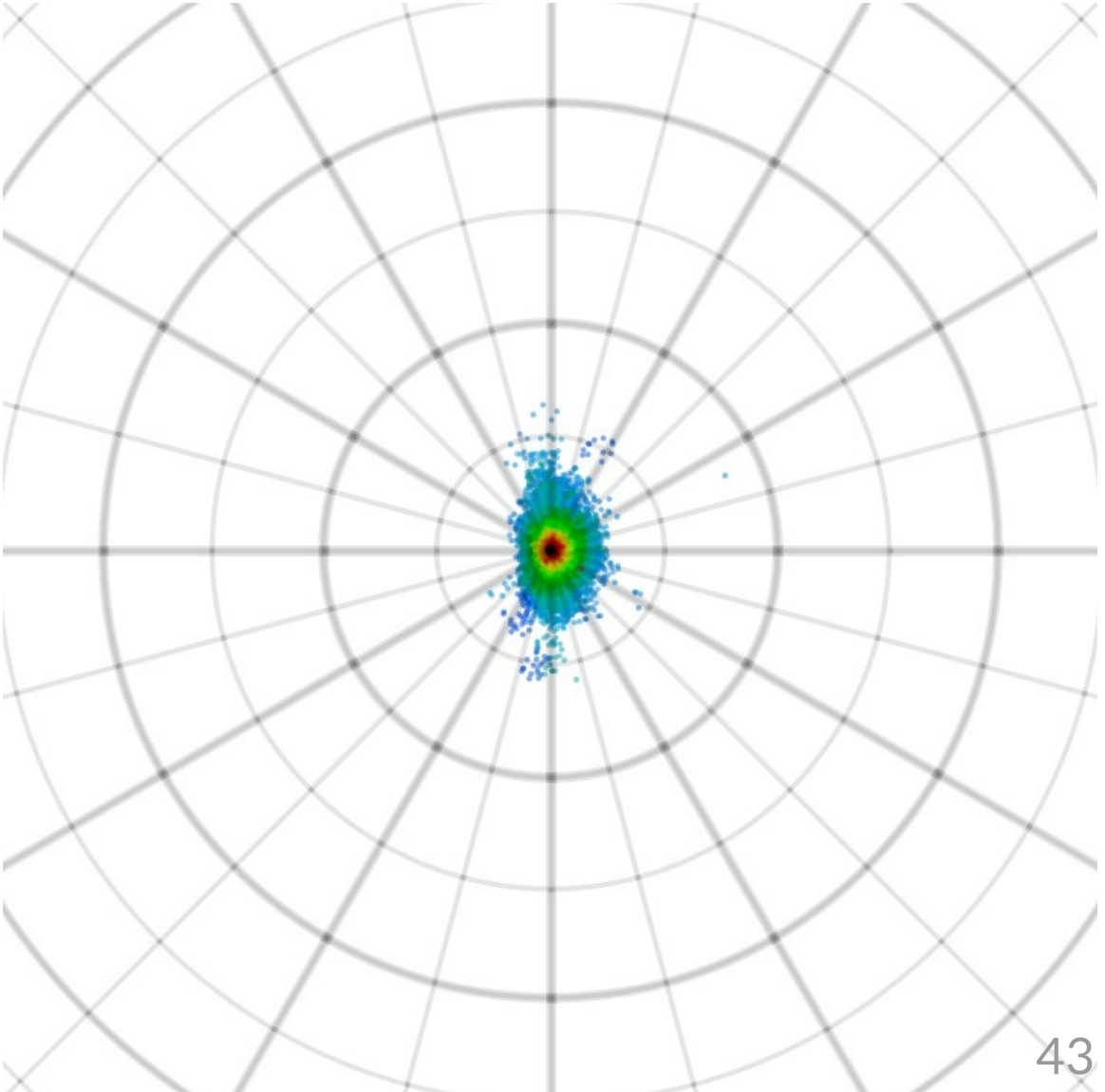

Deflection of shower

Gamma-ray

Gamsberg, Namibia

horizontal: 12.5uT
vertical: -25.9uT
2300m a.s.l.

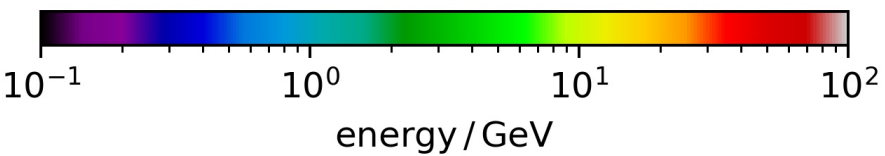

Direction of primary to get Cherenkov-light from zenith.

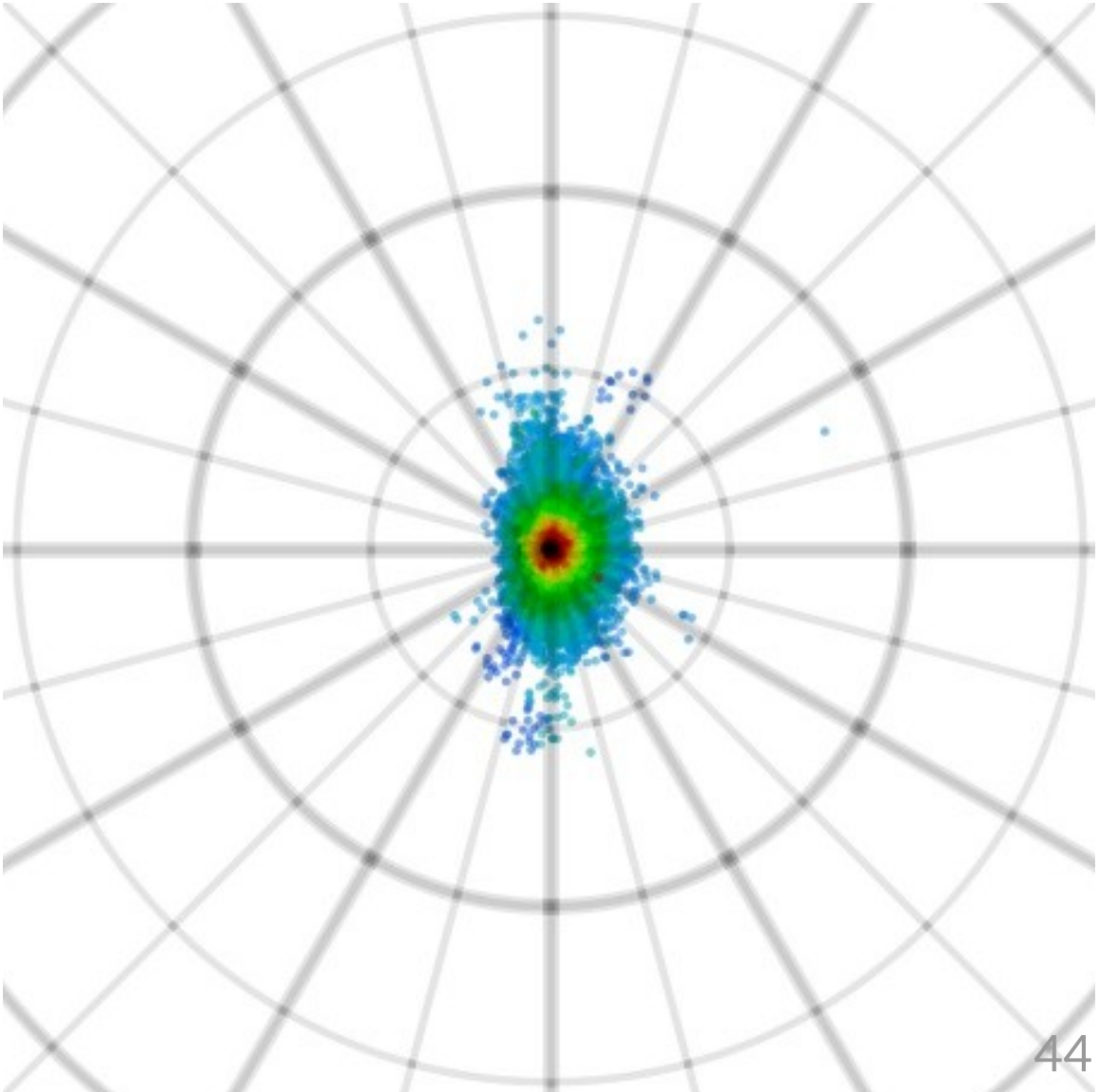

Deflection of shower

Gamma-ray

Gamsberg, Namibia

horizontal: 12.5uT
vertical: -25.9uT
2300m a.s.l.

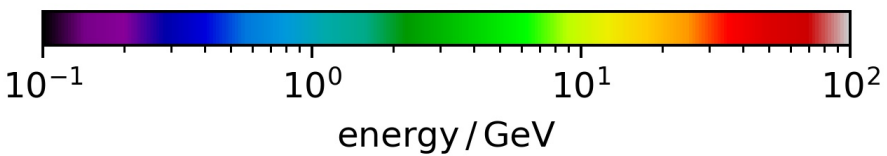

Direction of primary to get Cherenkov-light from zenith.

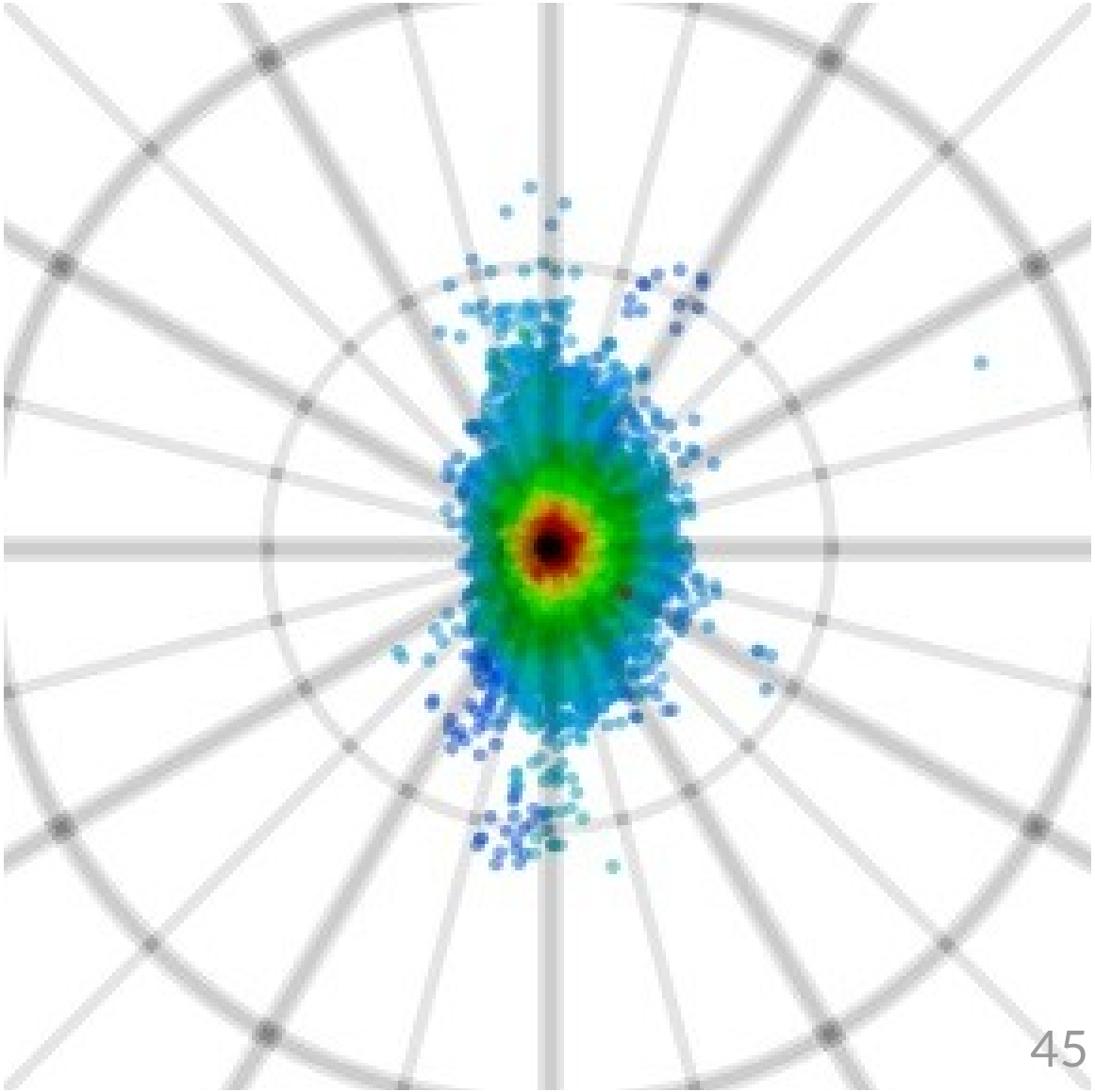

Deflection of shower

Gamma-ray

Gamsberg, Namibia

horizontal: 12.5uT
vertical: -25.9uT
2300m a.s.l.

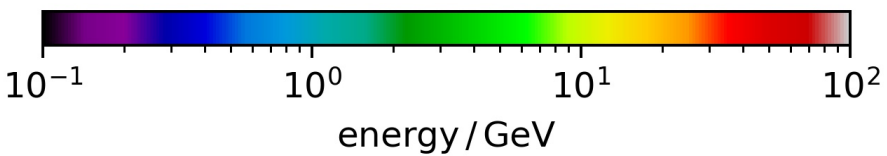

Direction of primary to get Cherenkov-light from zenith.

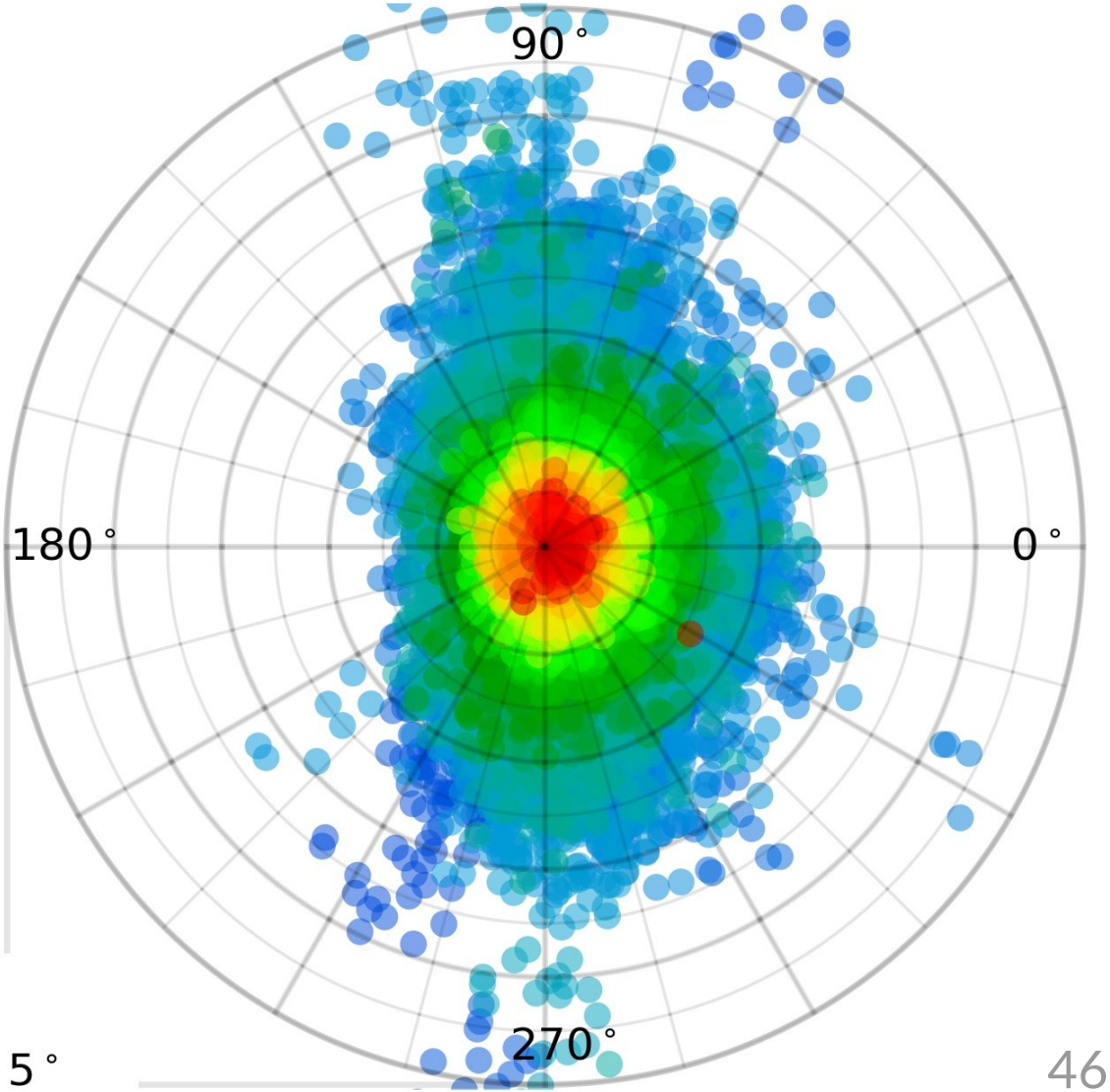

Deflection of shower

Gamma-ray

Chajnantor, Chile

horizontal: 20.8uT
vertical: -11.4uT
5000m a.s.l.

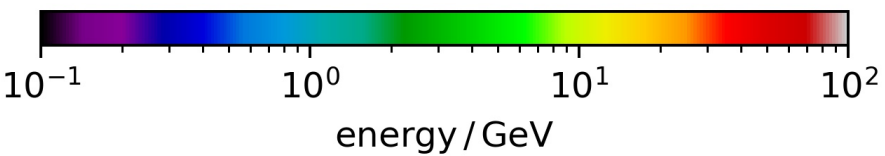

Direction of primary to get Cherenkov-light from zenith.

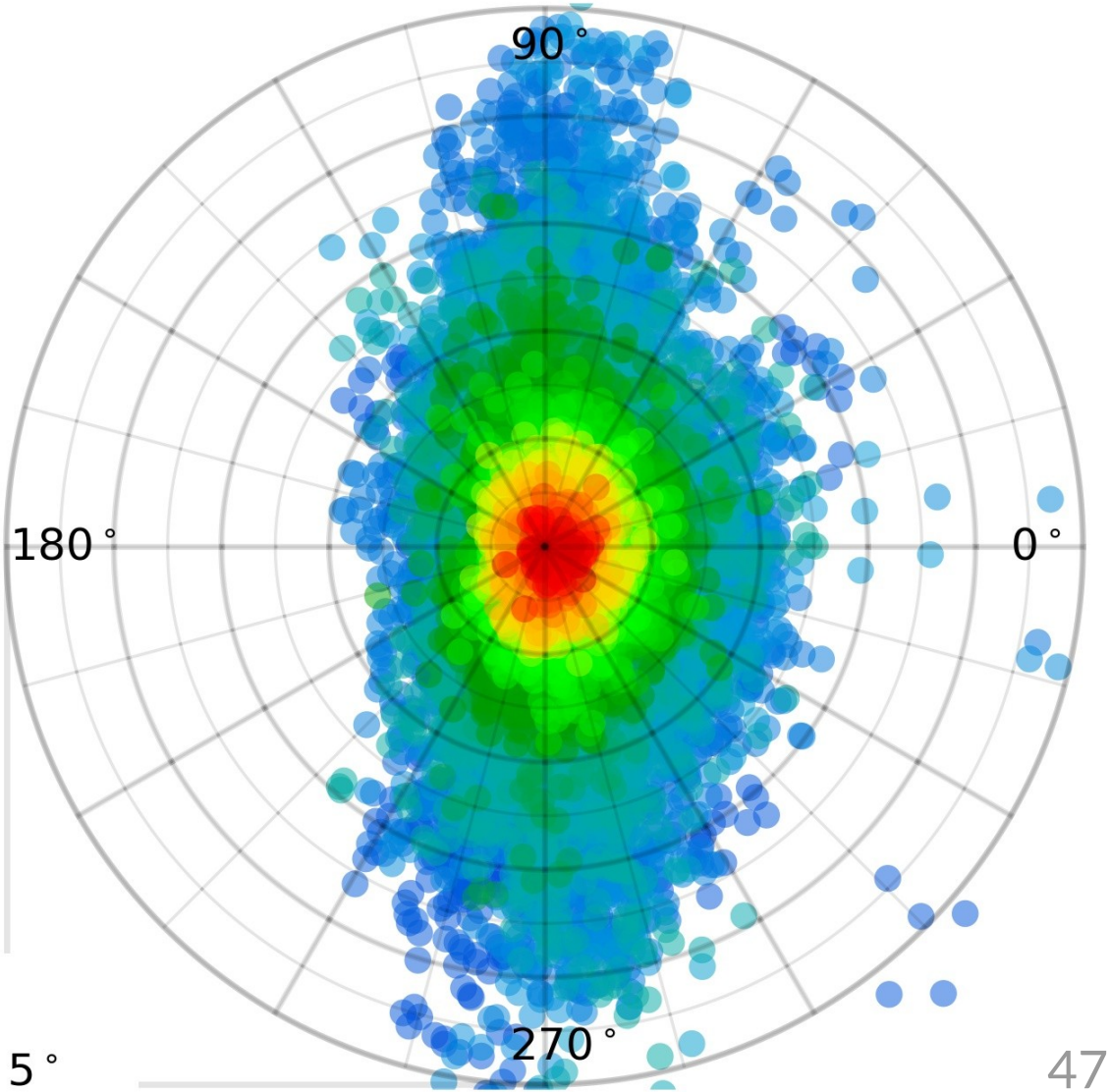

Deflection of shower

Gamma-ray

Roque, La Palma

horizontal: 30.4uT
vertical: -23.8uT
2200m a.s.l.

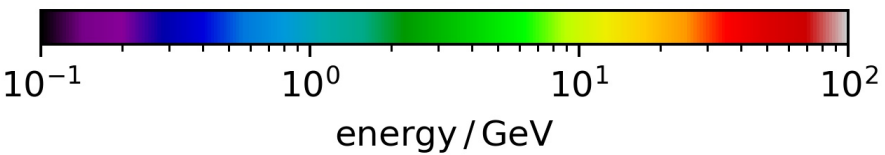

Direction of primary to get Cherenkov-light from zenith.

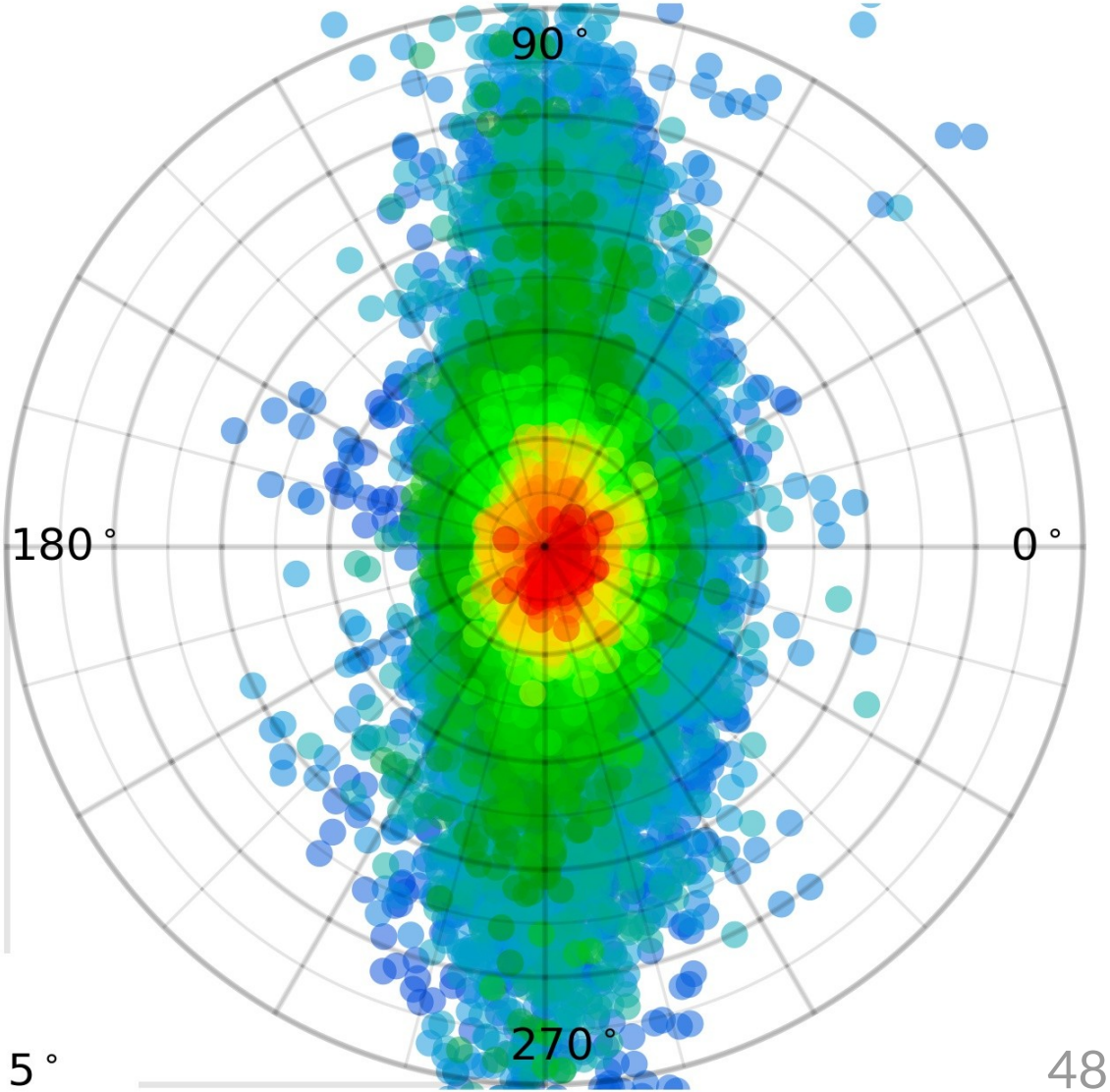

Background from Airshowers

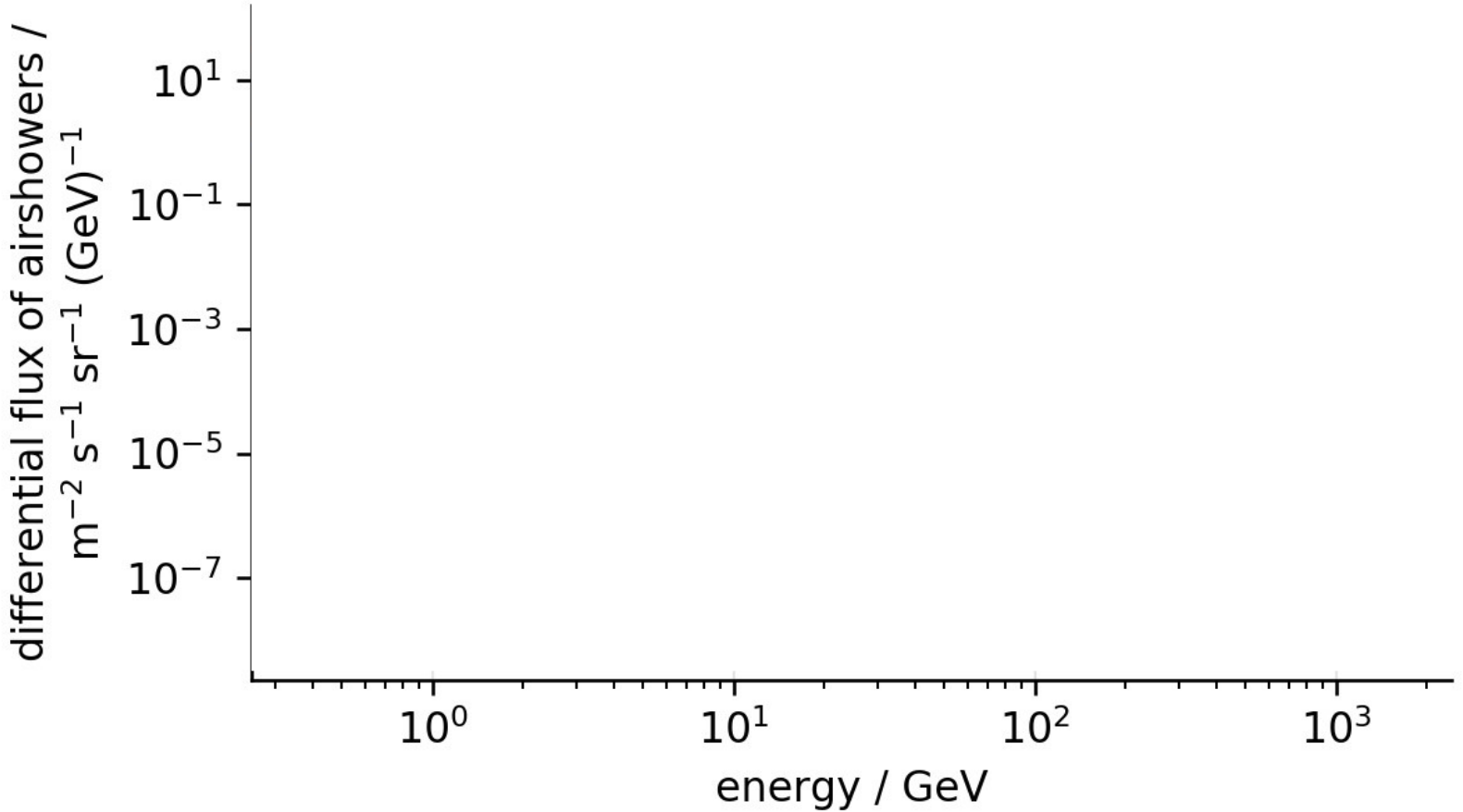

Background from Airshowers

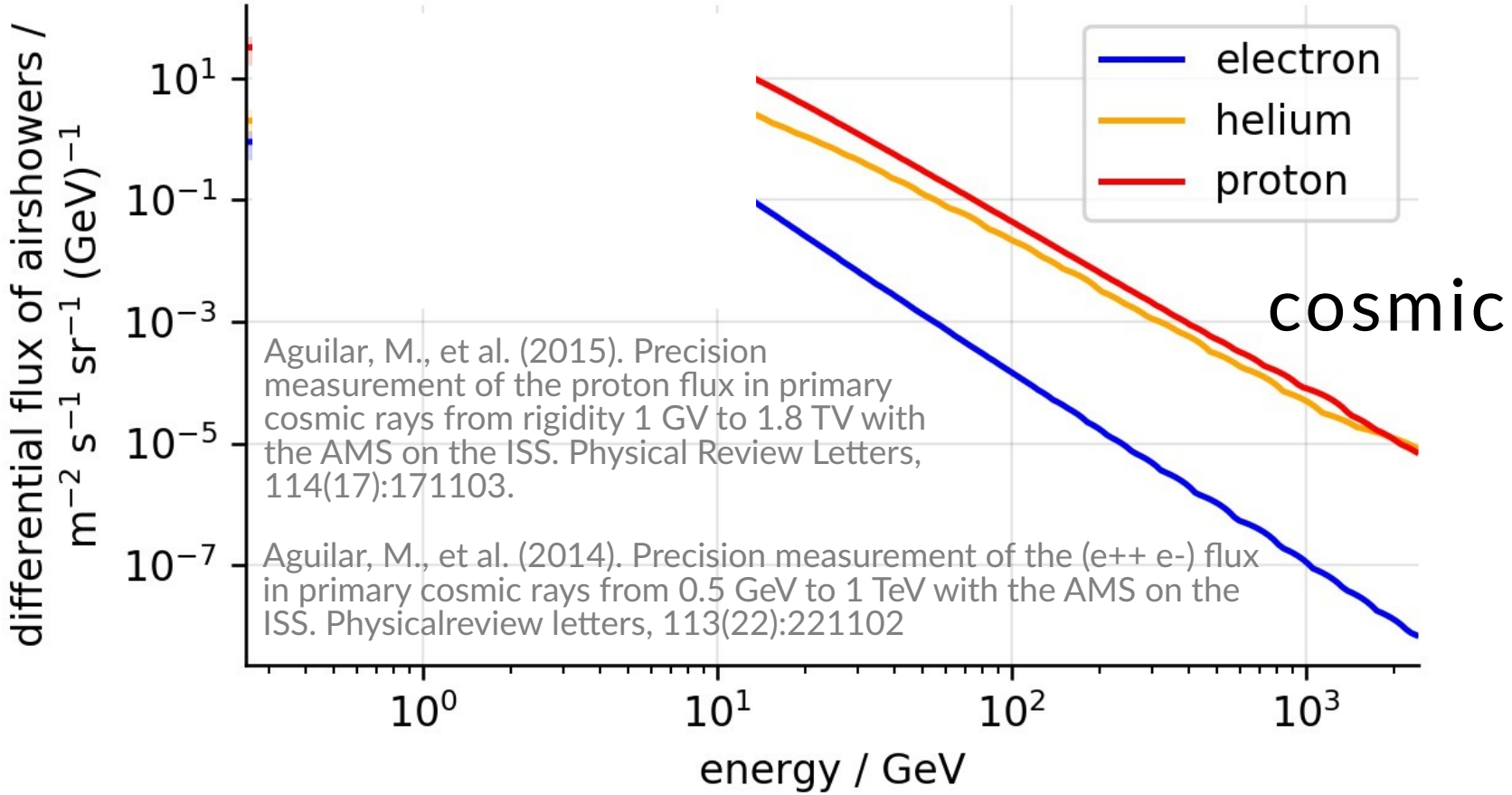

Background from Airshowers

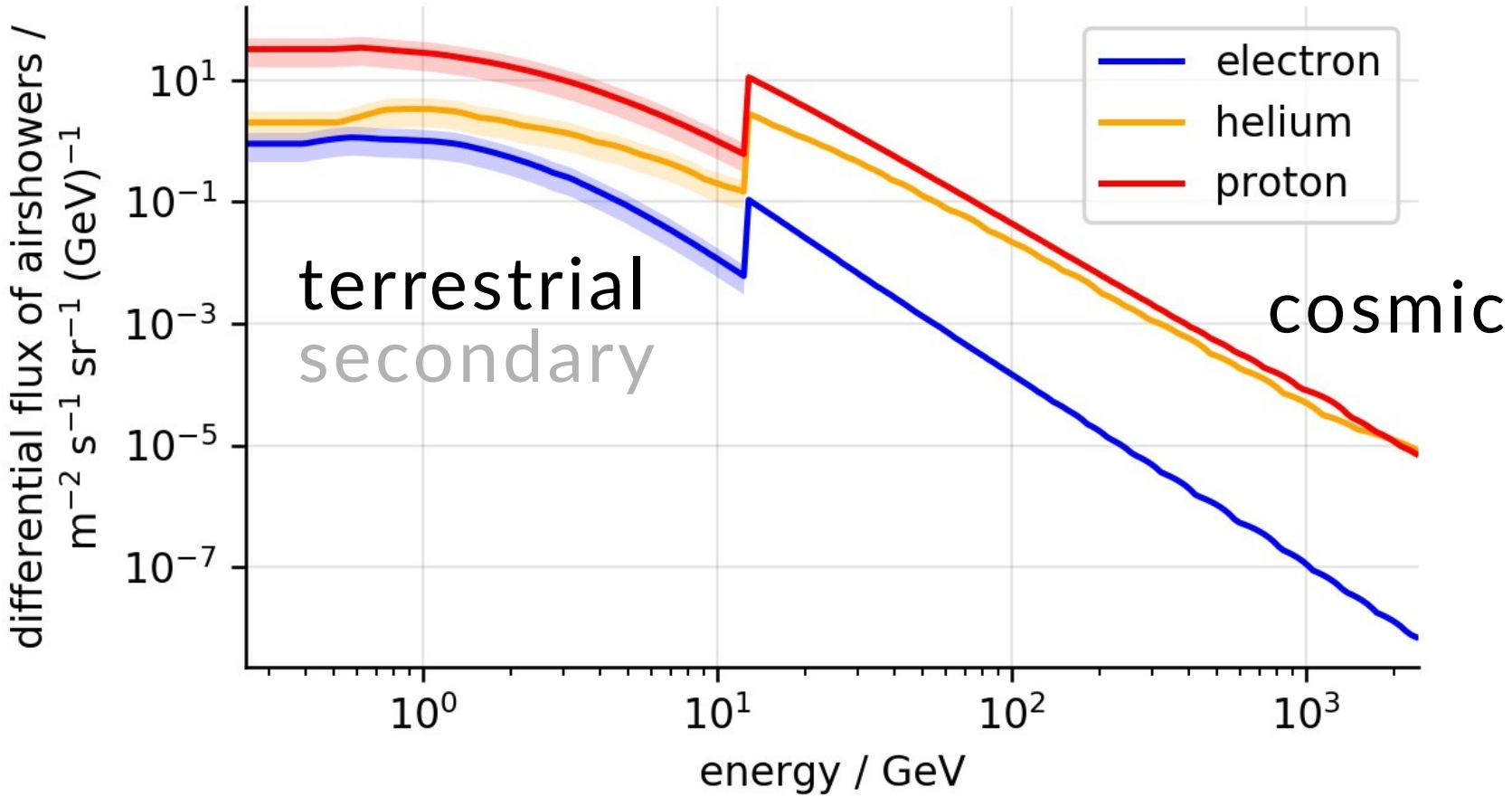

Background from Airshowers

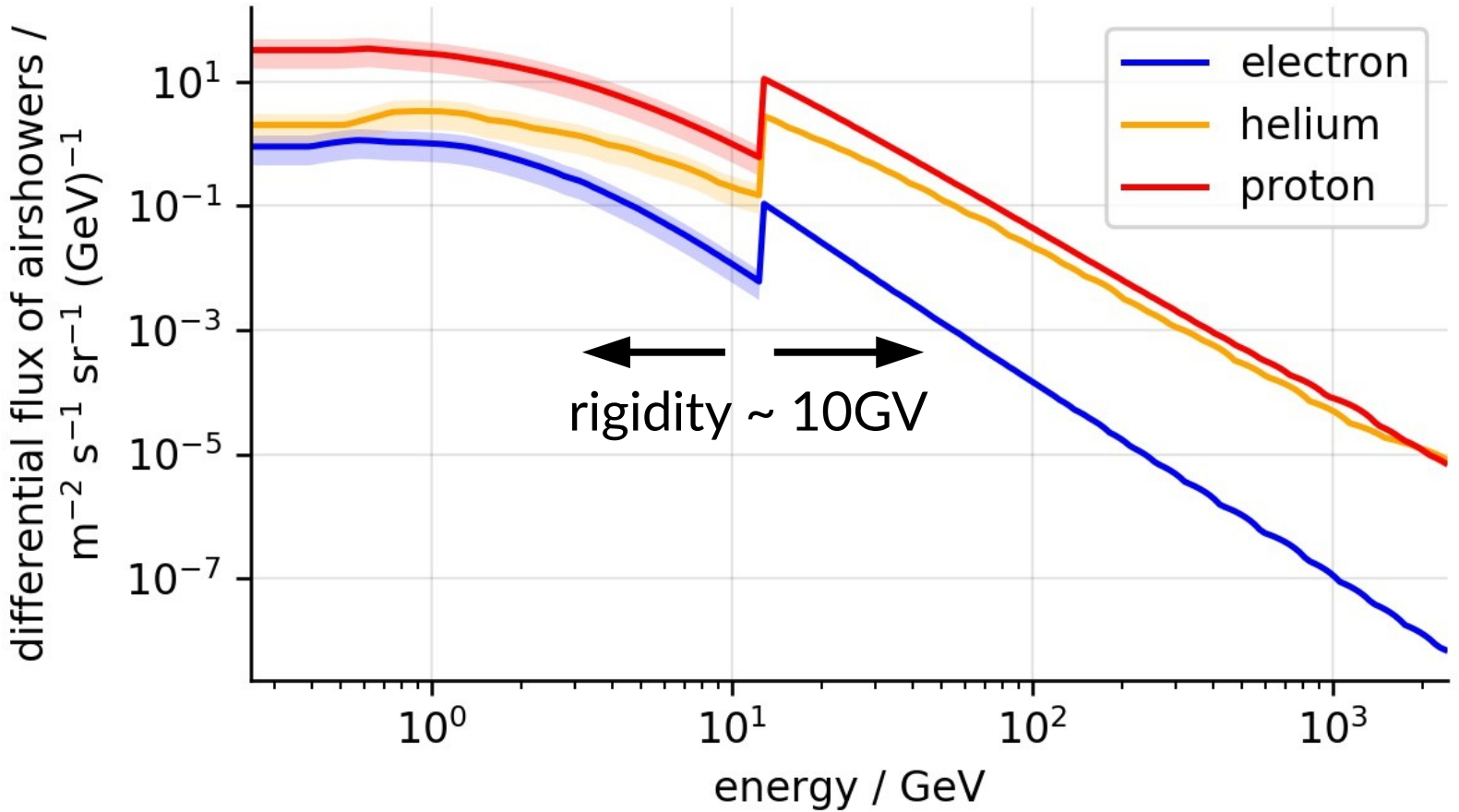

Background from Airshowers

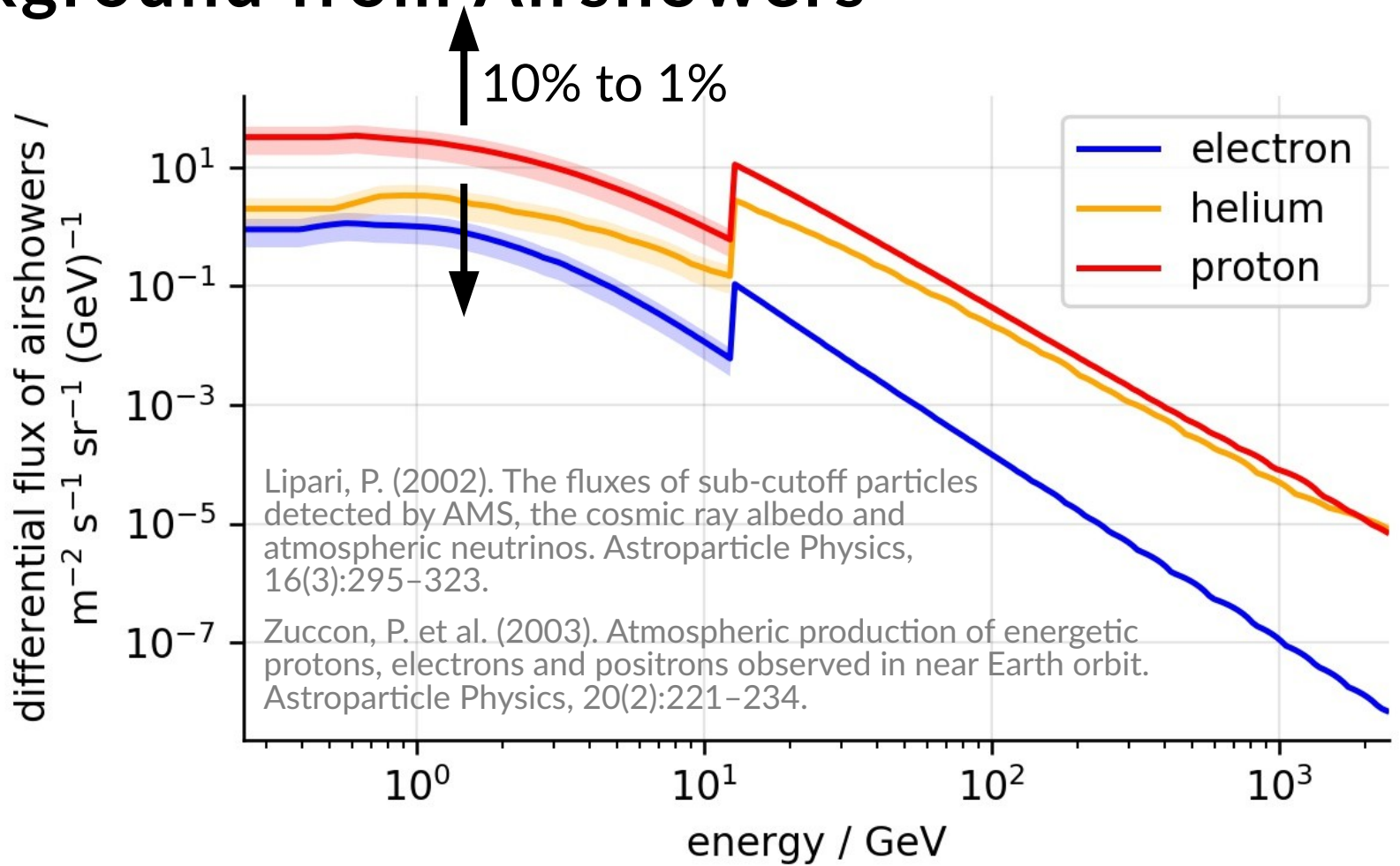

Background from Airshowers

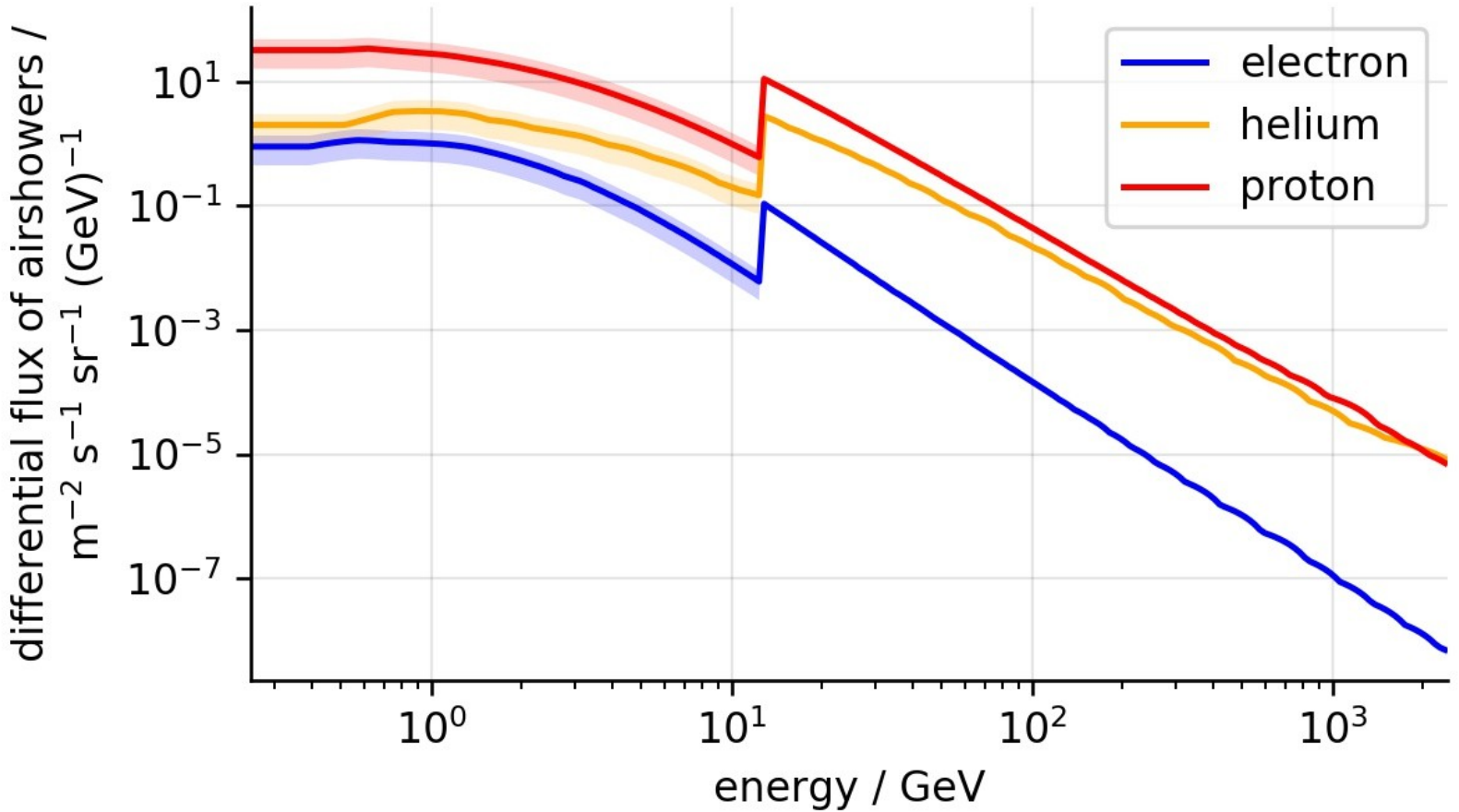

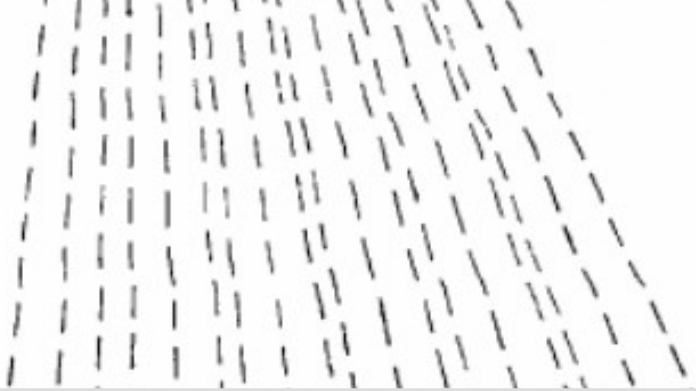

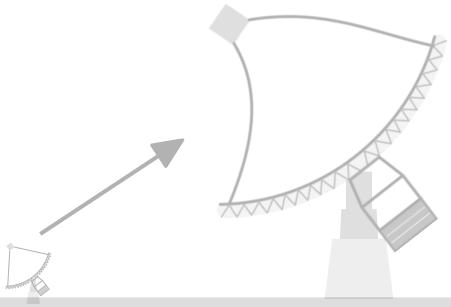

Plenoptic Perception

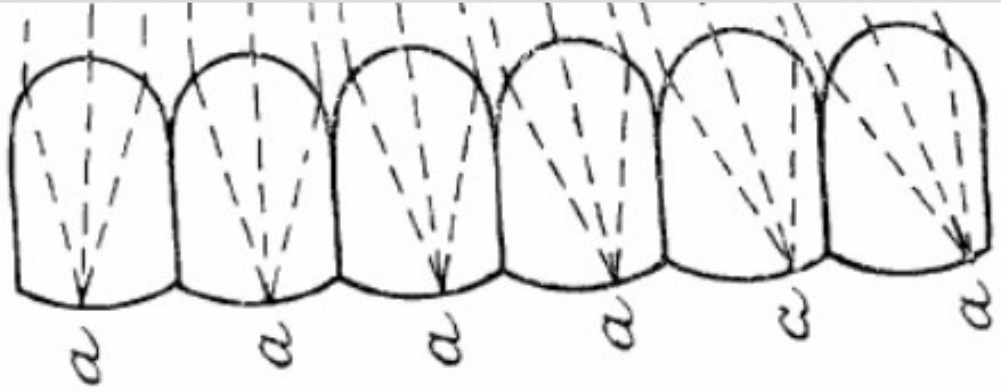

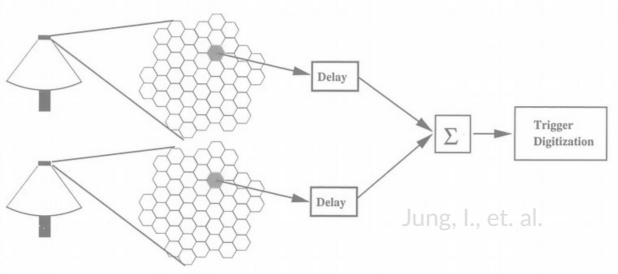

Jung, I., et. al.

Plenoptics

Telescope

Plenoptics

Telescope

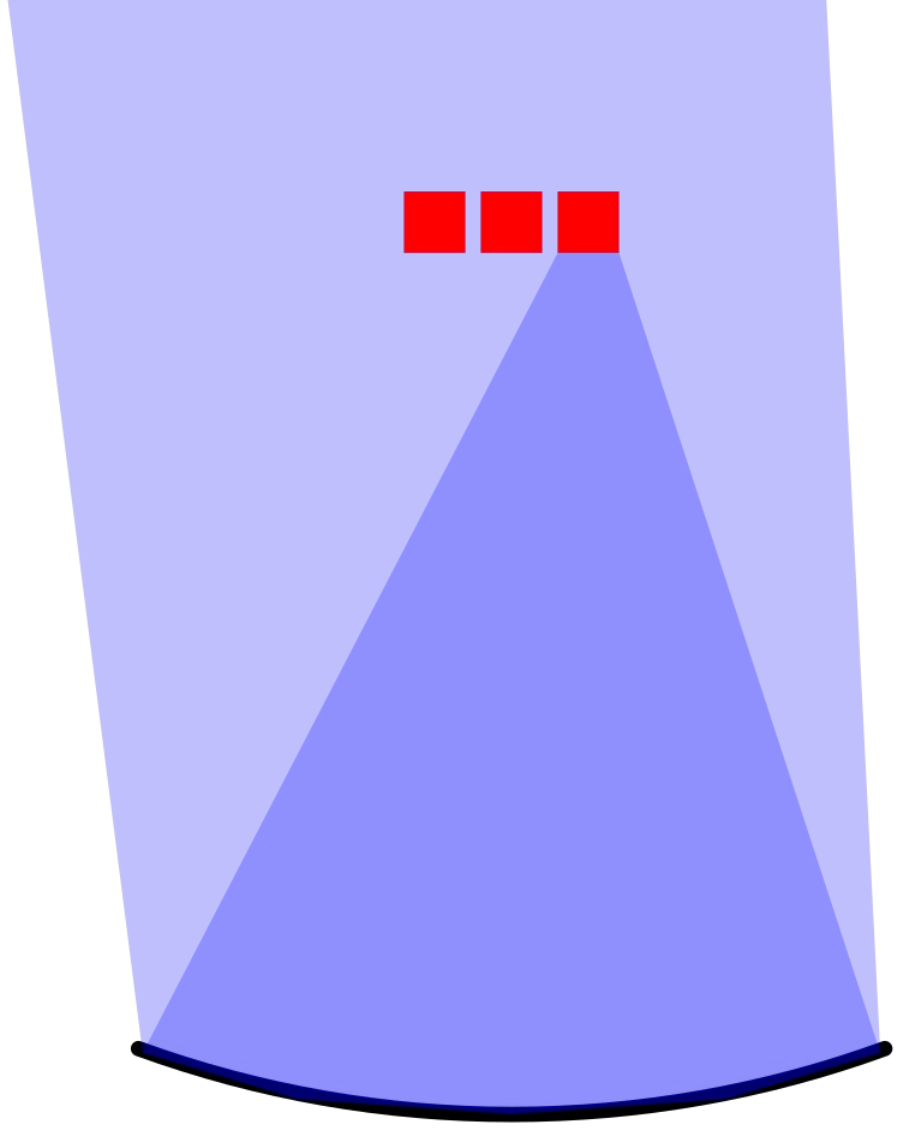

Plenoptics

Telescope

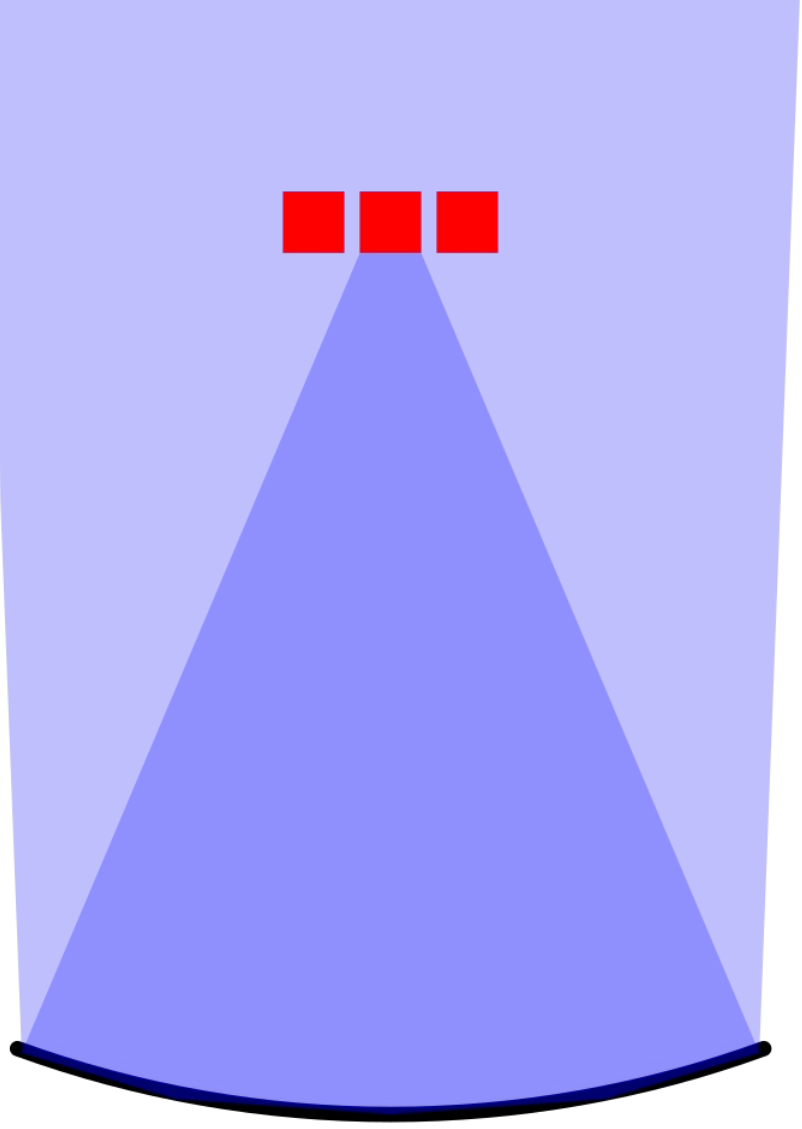

Plenoptics

Telescope

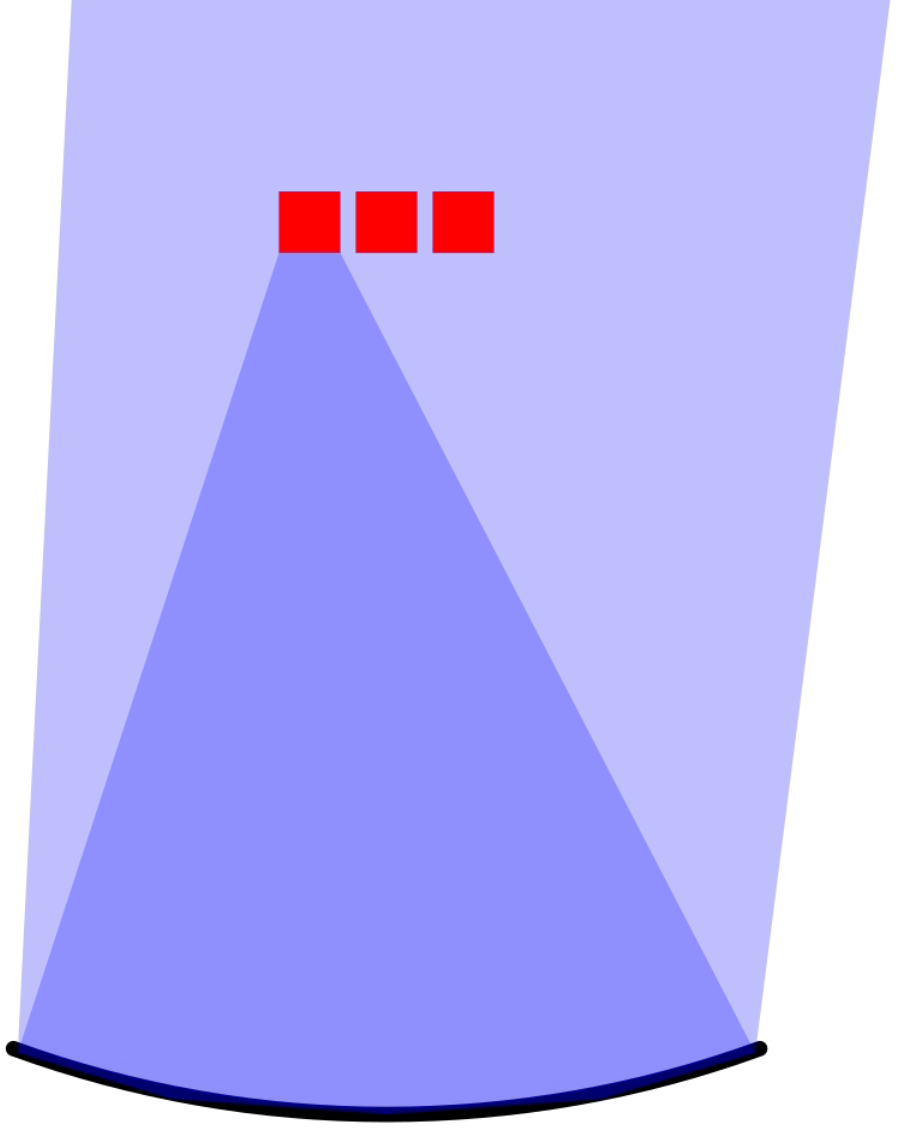

Plenoptics

Telescope

Plenoptics

Telescope
Plenoscope

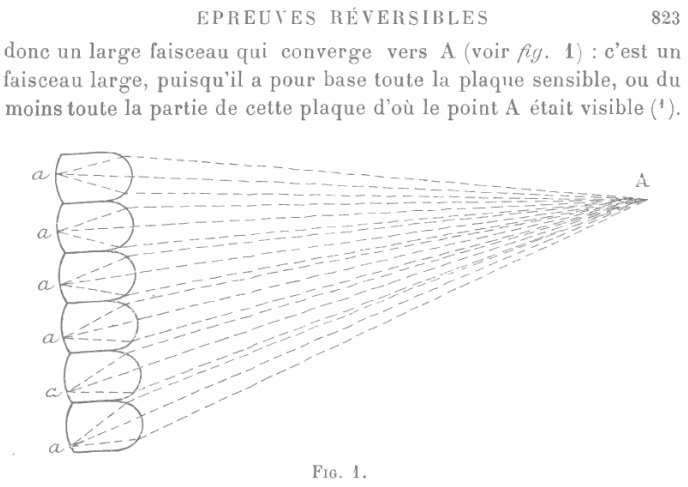

EPREUVES RÉVERSIBLES 823

donc un large faisceau qui converge vers A (voir *fig.* 1) : c'est un faisceau large, puisqu'il a pour base toute la plaque sensible, ou du moins toute la partie de cette plaque d'où le point A était visible (¹).

FIG. 1.

Par M. G. Lippmann, (**1908**),
Epreuves reversibles donnant la sensation du relief,
Phys. Theor. Appl. 7, p.821-825

Plenoptics

Plenoscope

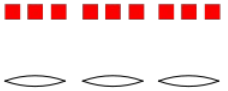

EPREUVES RÉVERSIBLES 823

donc un large faisceau qui converge vers A (voir *fig.* 1) : c'est un faisceau large, puisqu'il a pour base toute la plaque sensible, ou du moins toute la partie de cette plaque d'où le point A était visible (¹).

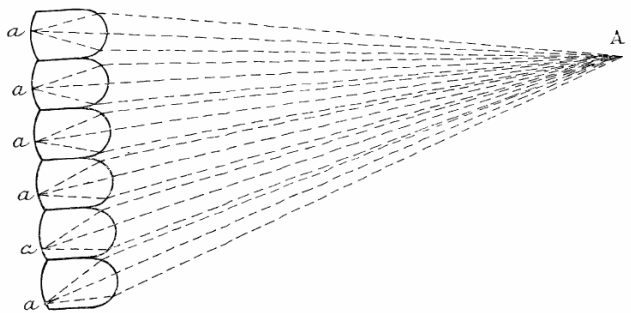

FIG. 1.

Par M. G. Lippmann, (**1908**),
Epreuves reversibles donnant la sensation du relief,
Phys. Theor. Appl. 7, p.821-825

Plenoptics

Plenoscope

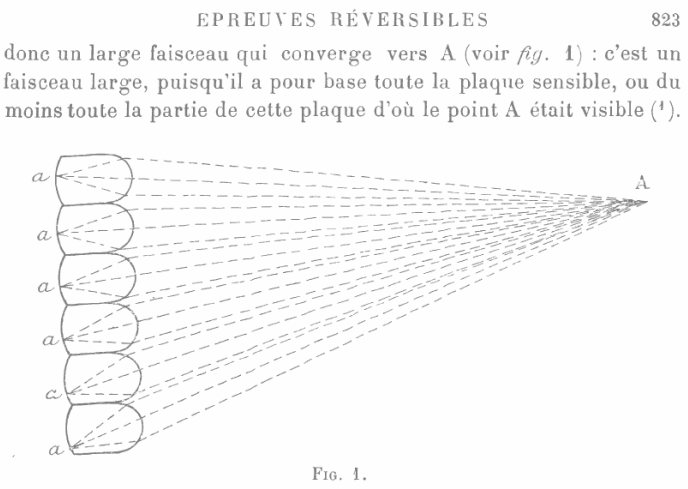
EPREUVES RÉVERSIBLES 823

donc un large faisceau qui converge vers A (voir *fig.* 1) : c'est un faisceau large, puisqu'il a pour base toute la plaque sensible, ou du moins toute la partie de cette plaque d'où le point A était visible (¹).

FIG. 1.

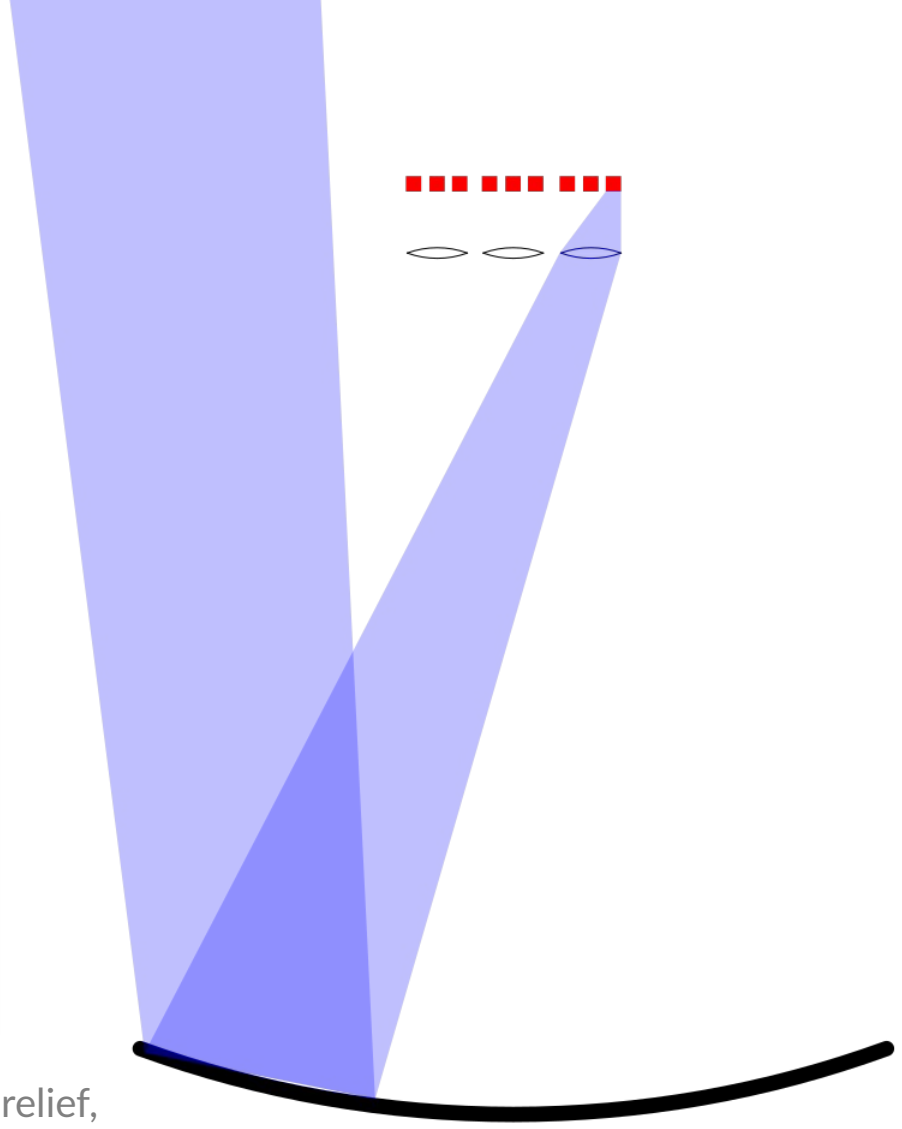

Par M. G. Lippmann, (**1908**),
Epreuves reversibles donnant la sensation du relief,
Phys. Theor. Appl. 7, p.821-825

Plenoptics

Plenoscope

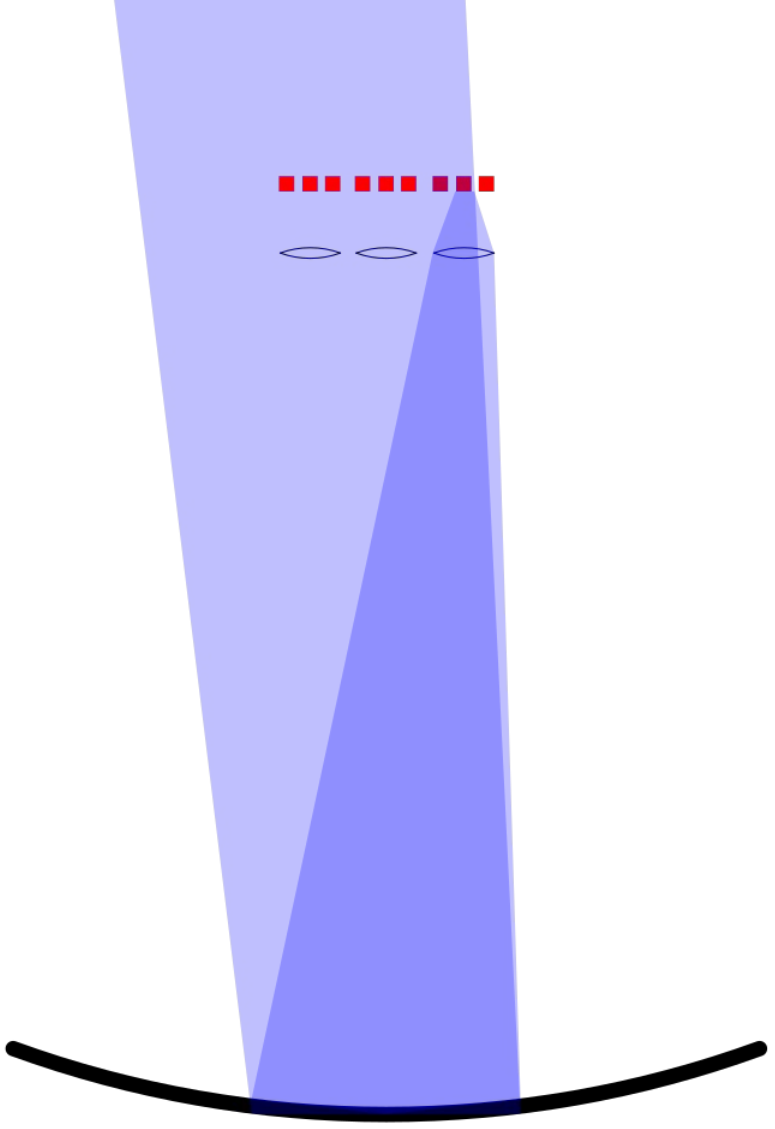

Plenoptics

Plenoscope

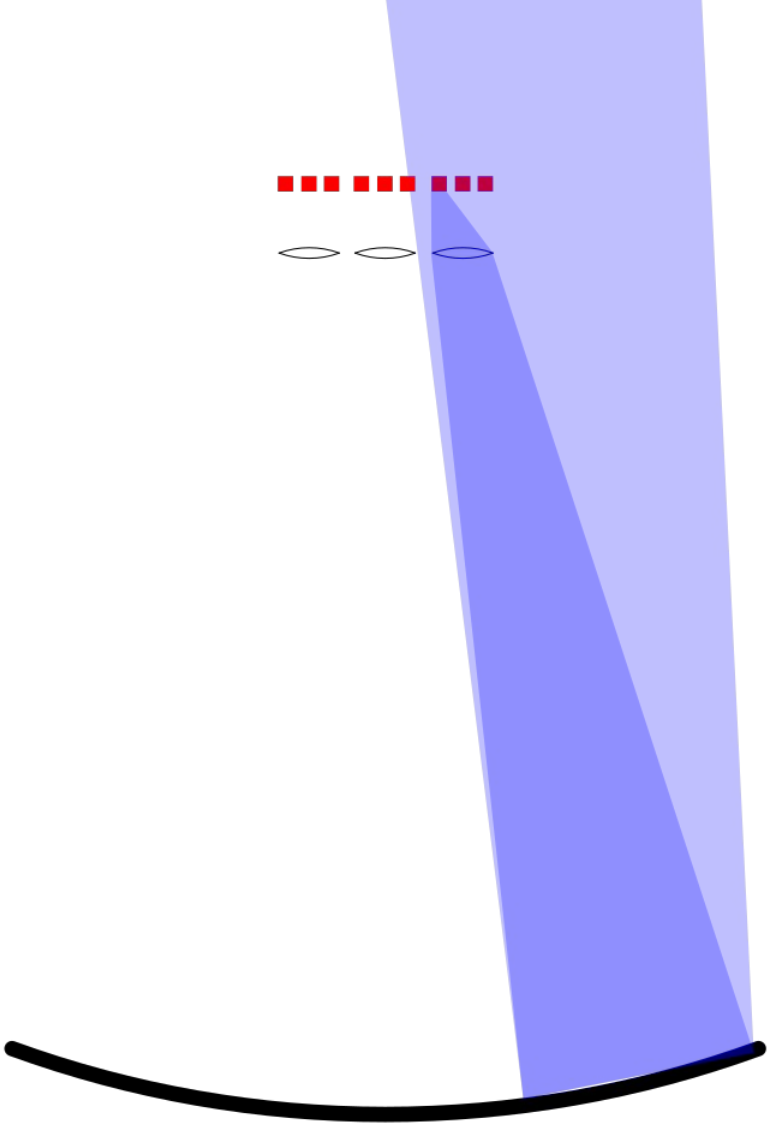

Plenoptics

Plenoscope

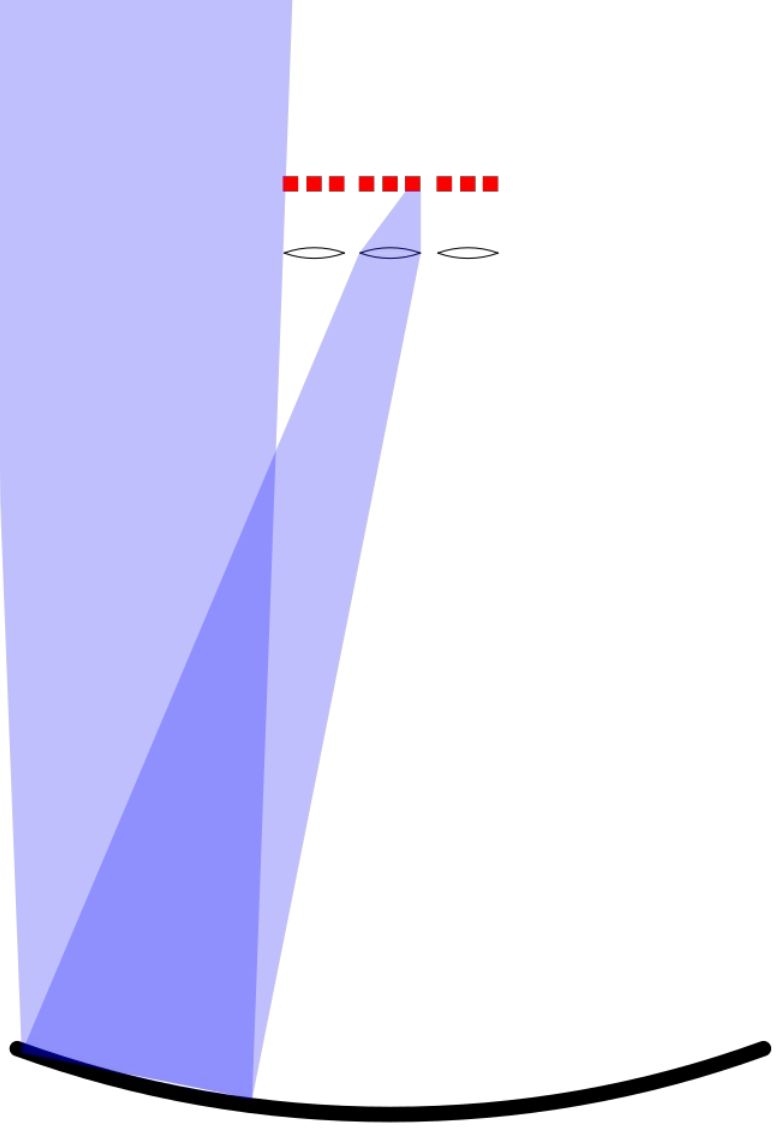

Plenoptics

Plenoscope

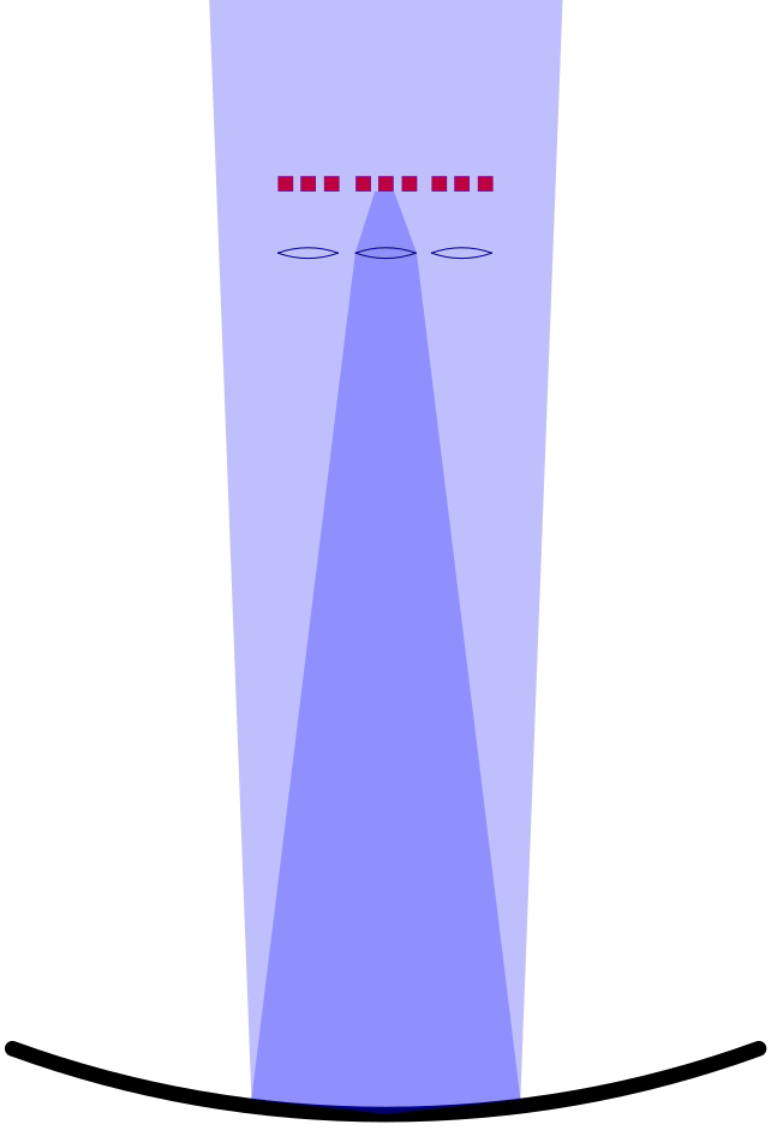

Plenoptics

Plenoscope

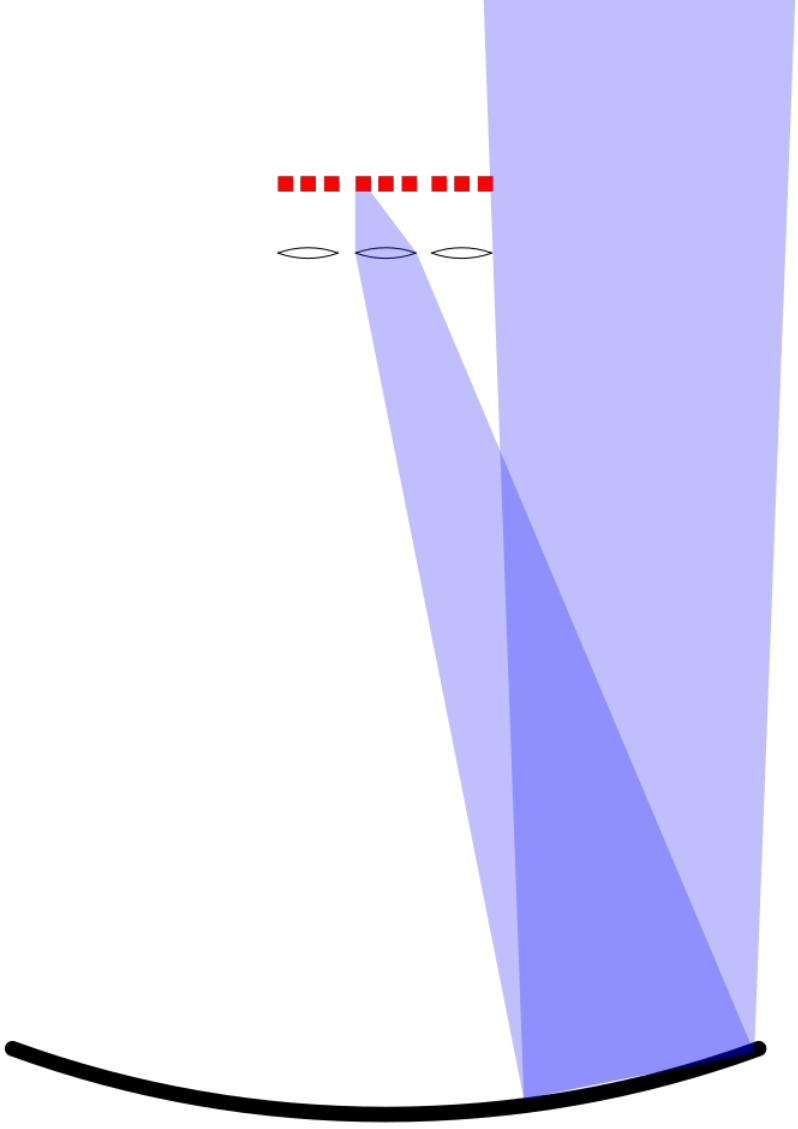

Plenoptics

Plenoscope

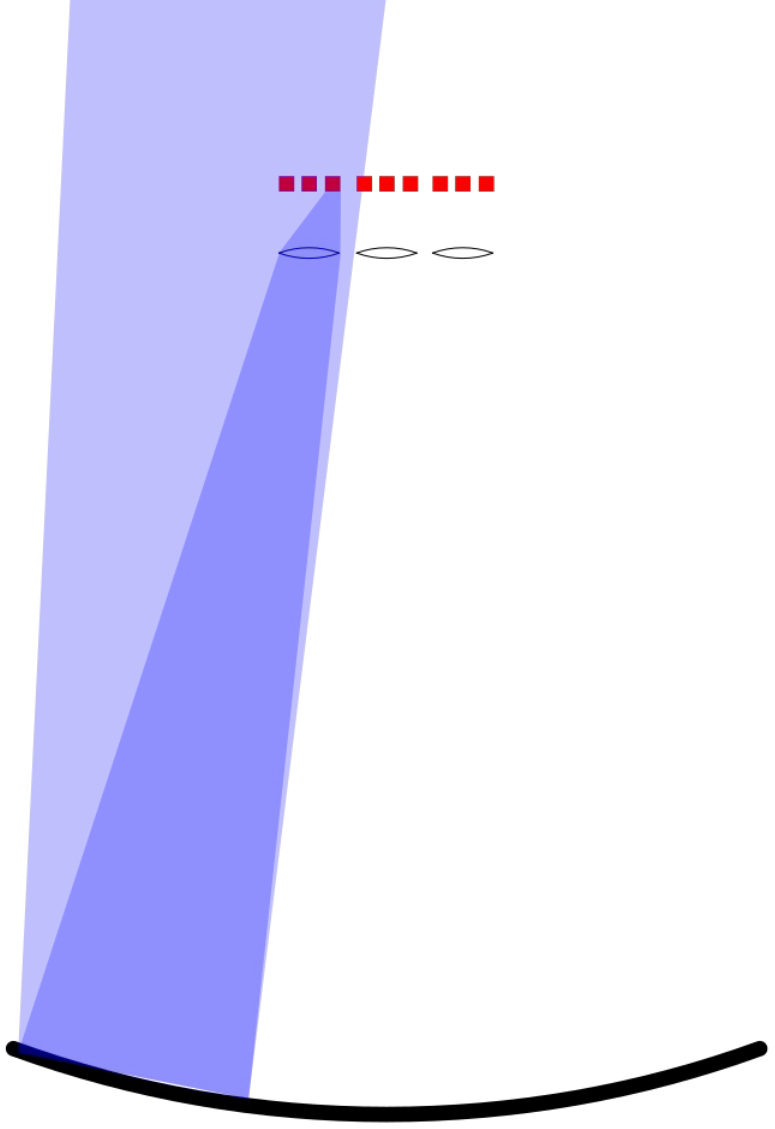

Plenoptics

Plenoscope

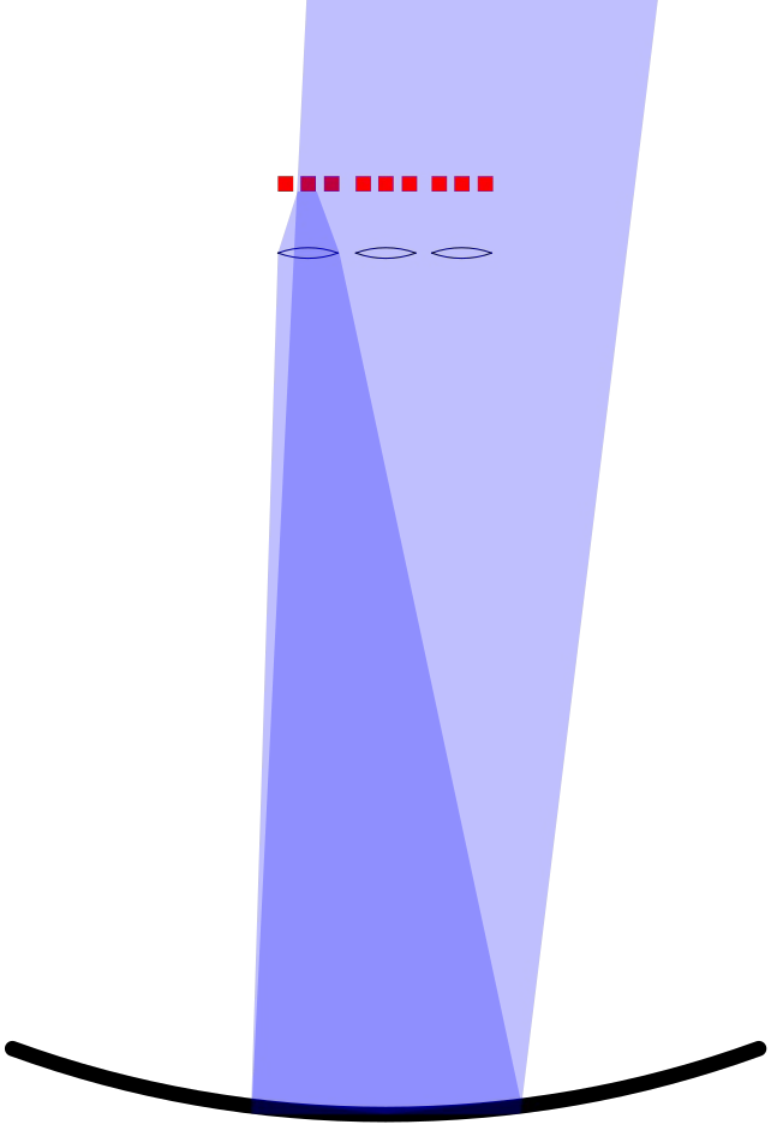

Plenoptics

Plenoscope

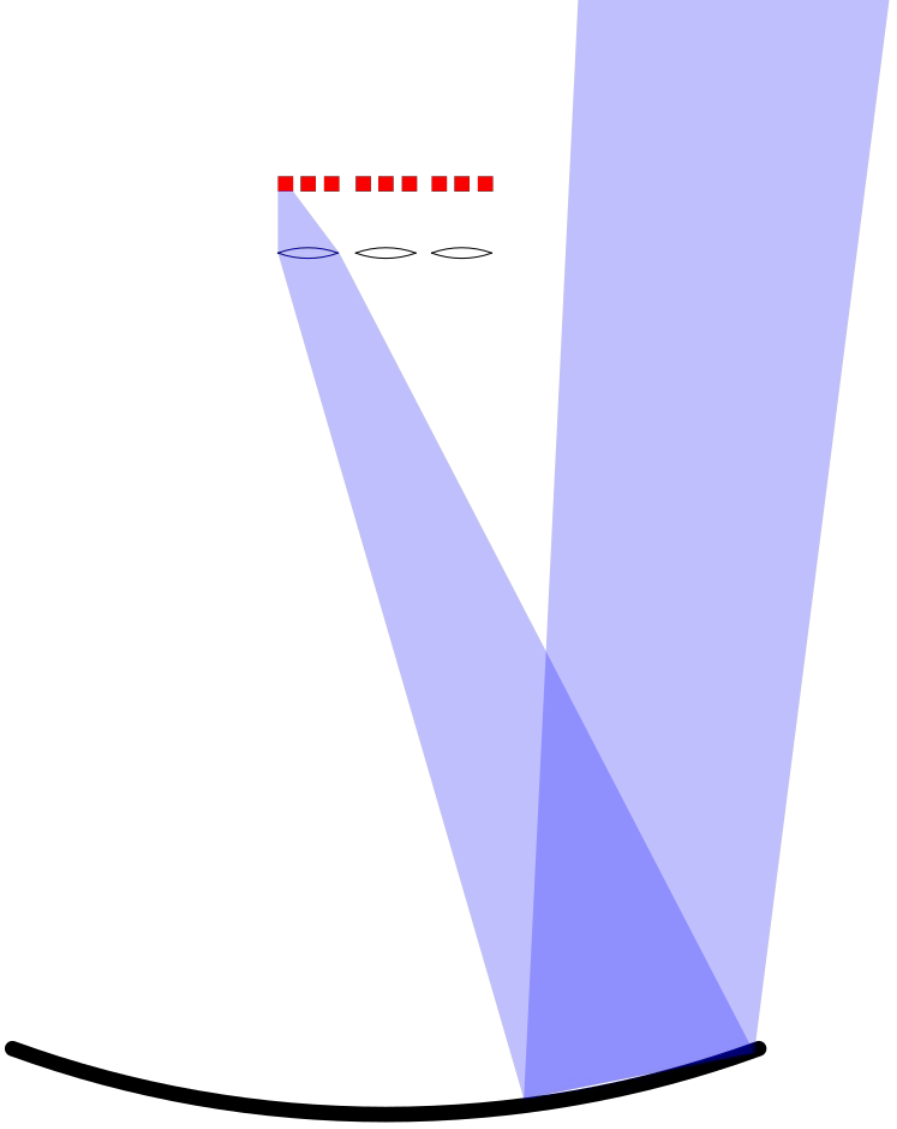

Plenoptics

Plenoscope

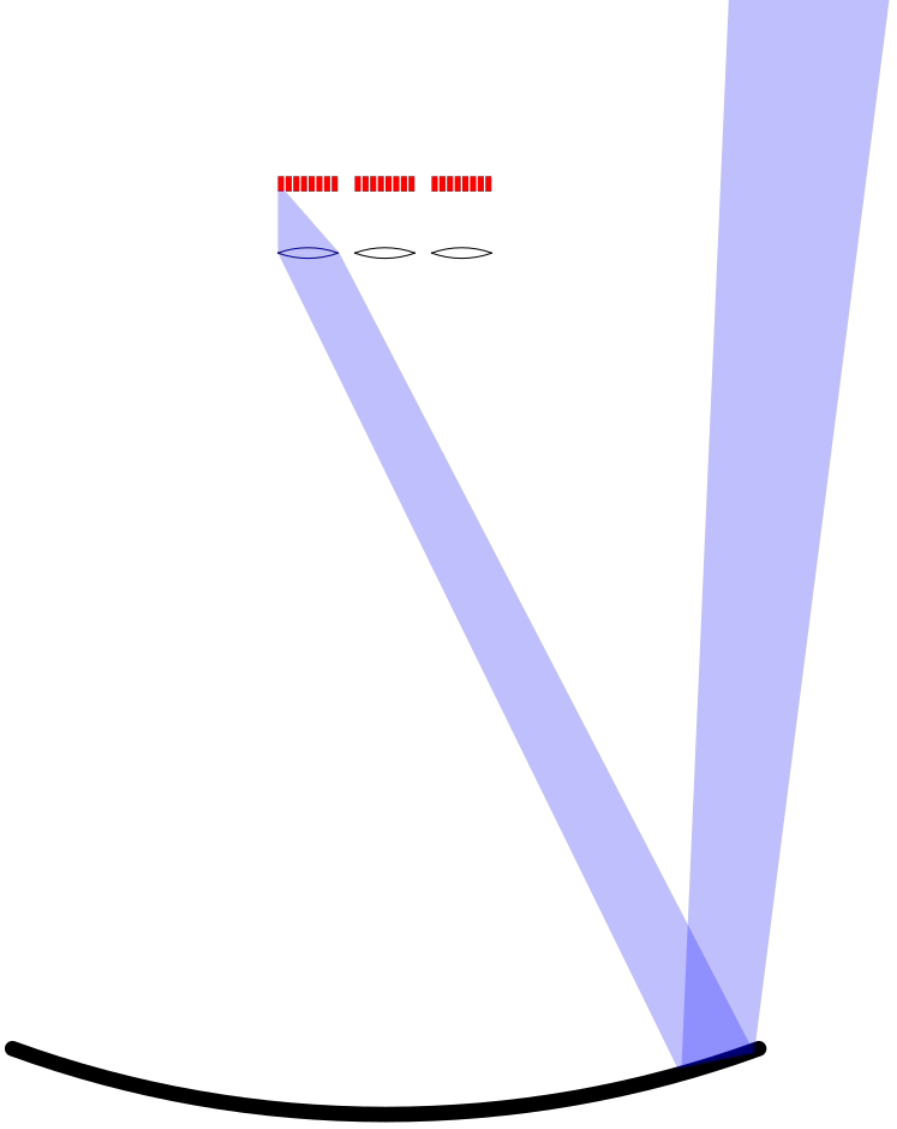

Plenoptics

Plenoscope

thin lens

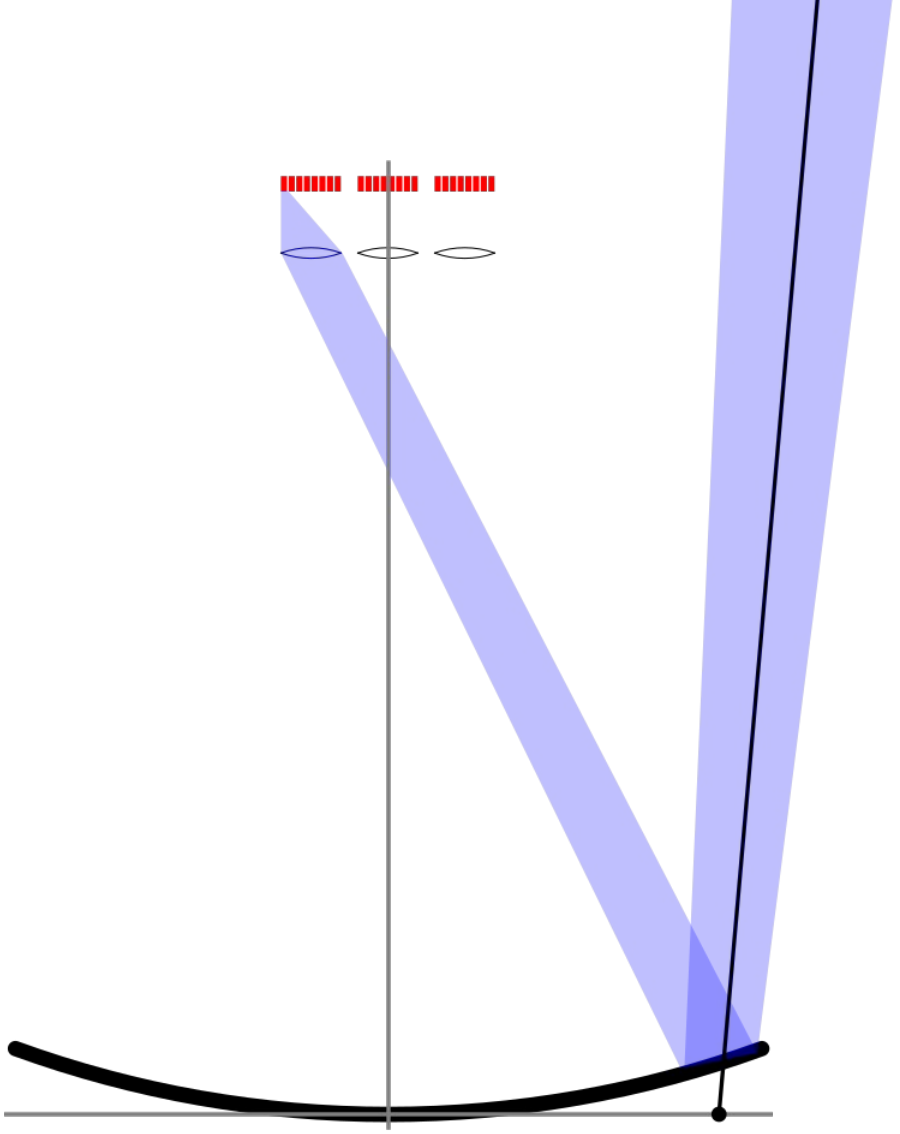

Plenoptics

thin lens

$$\frac{1}{\text{focal-length}} = \frac{1}{\text{depth}} + \frac{1}{\text{image-distance}}$$

Equations: arXiv:1904.13368 (astro-ph)

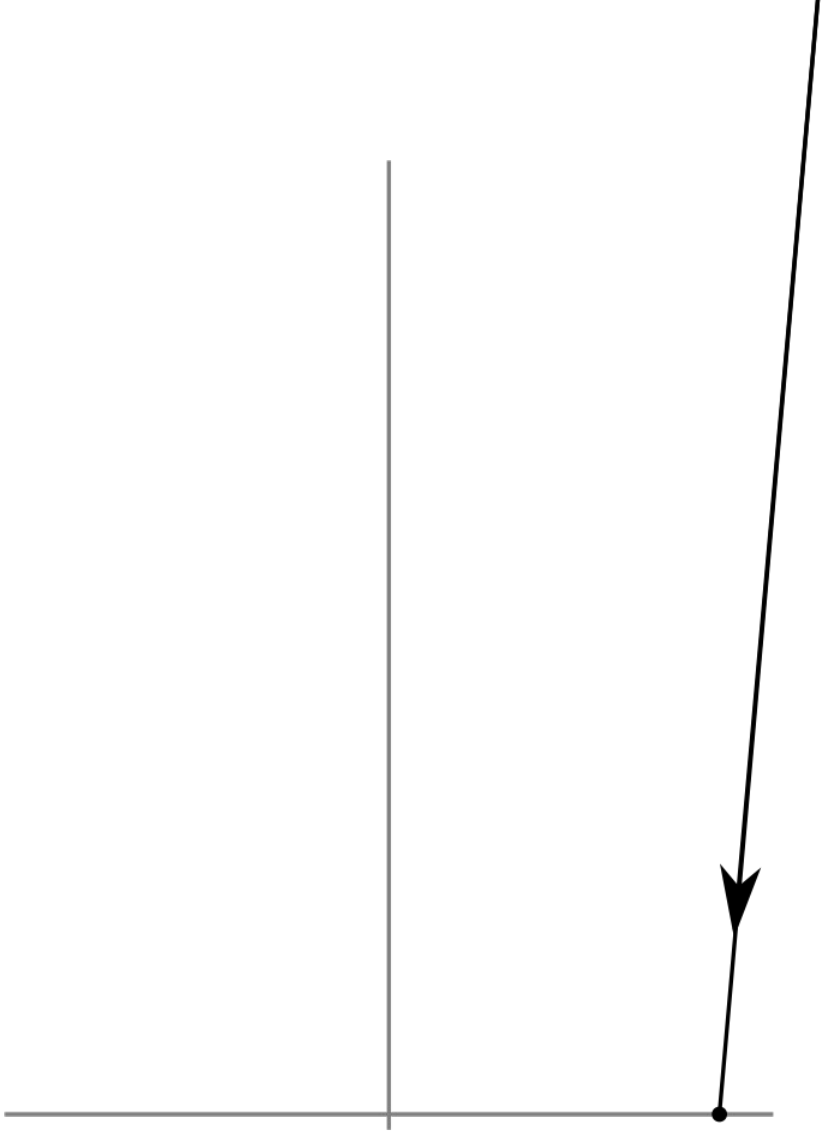

Plenoptics

thin lens

$$\frac{1}{\text{focal-length}} = \frac{1}{\text{depth}} + \frac{1}{\text{image-distance}}$$

Equations: arXiv:1904.13368 (astro-ph)

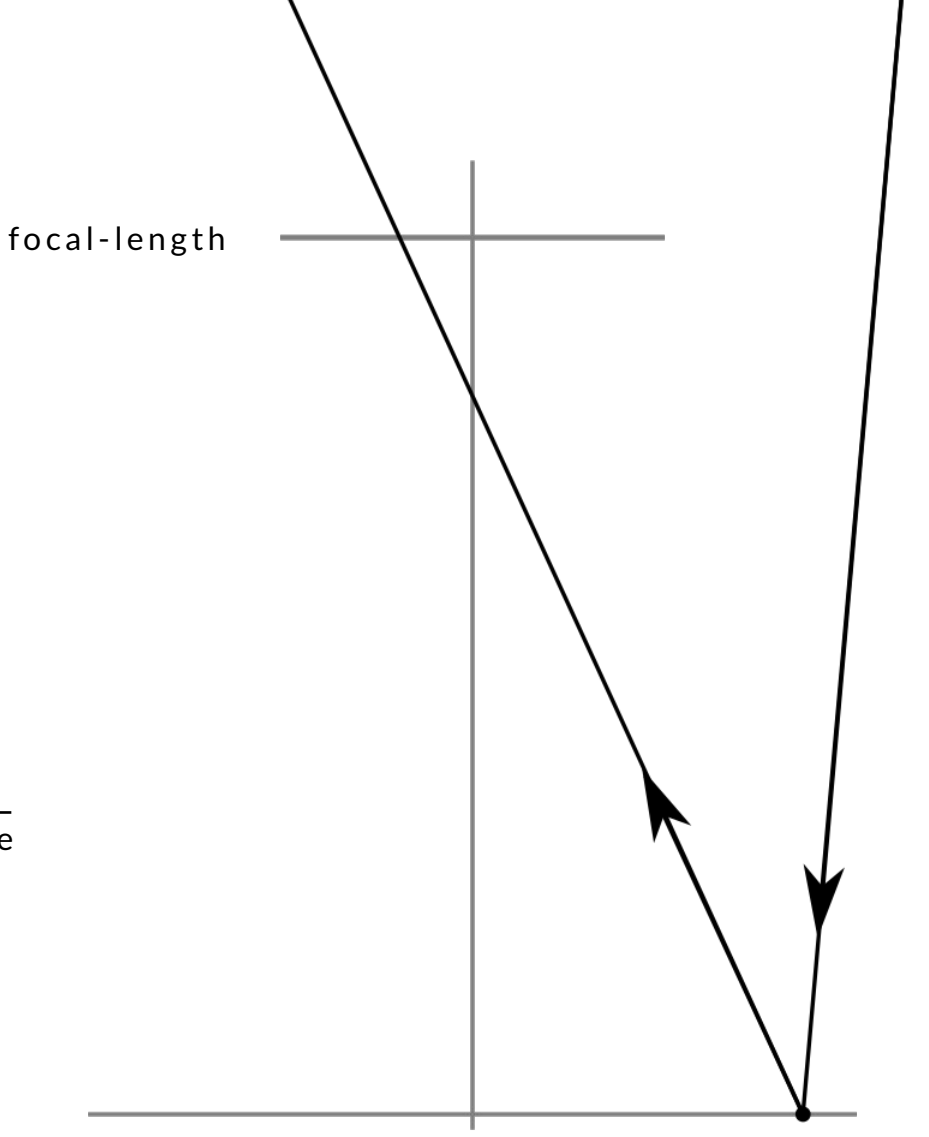

Plenoptics

thin lens

$$\frac{1}{\text{focal-length}} = \frac{1}{\text{depth}} + \frac{1}{\text{image-distance}}$$

Equations: arXiv:1904.13368 (astro-ph)

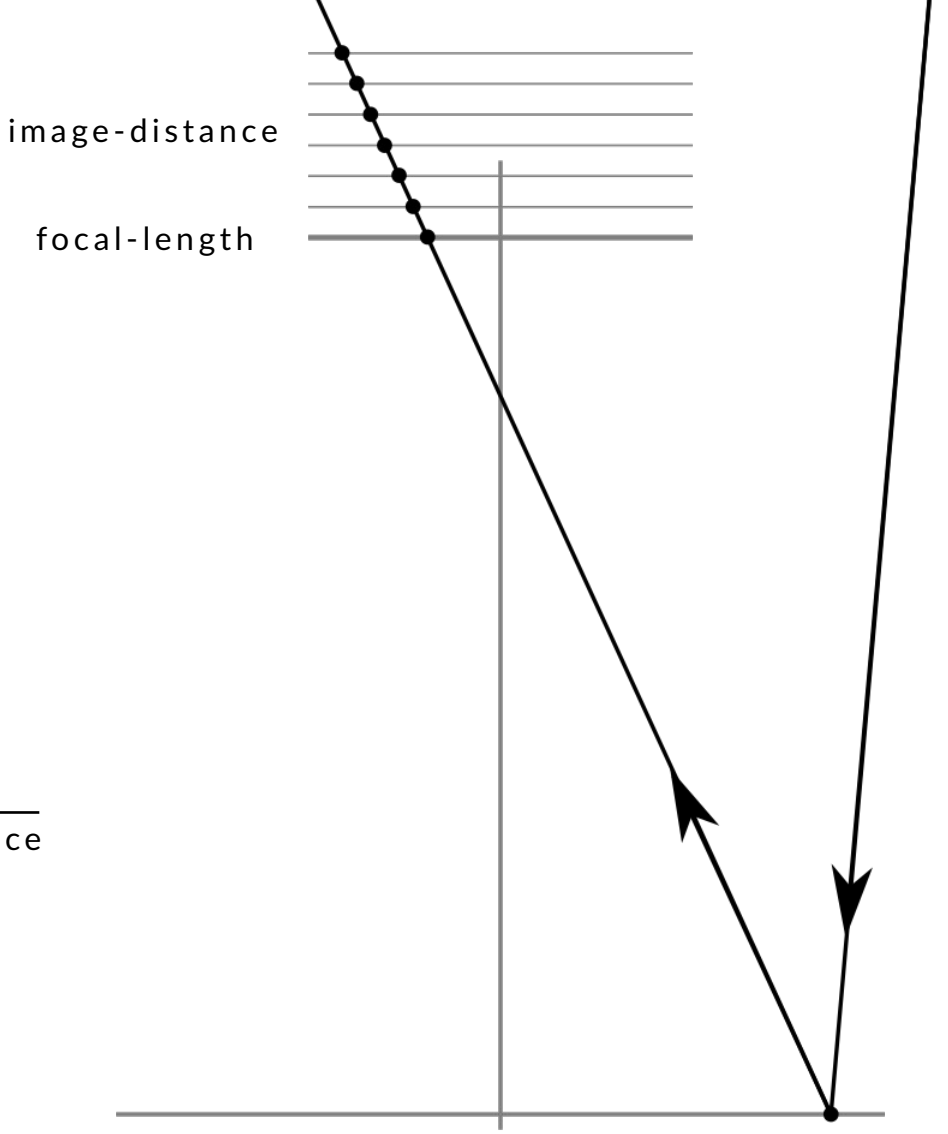

Plenoptics

Plenoscope

thin lens

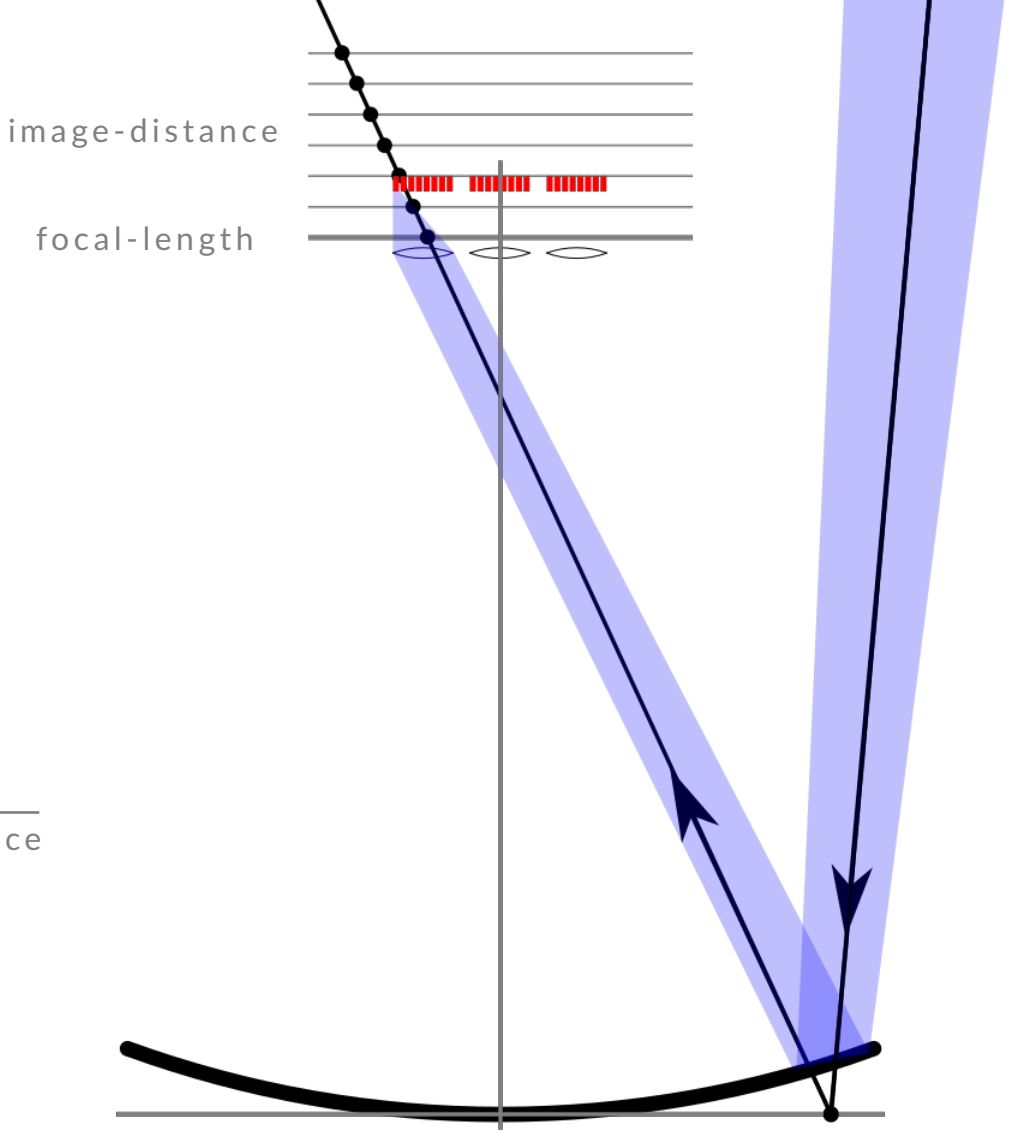

$$\frac{1}{\text{focal-length}} = \frac{1}{\text{depth}} + \frac{1}{\text{image-distance}}$$

Equations: arXiv:1904.13368 (astro-ph)

Plenoptics

Plenoscope

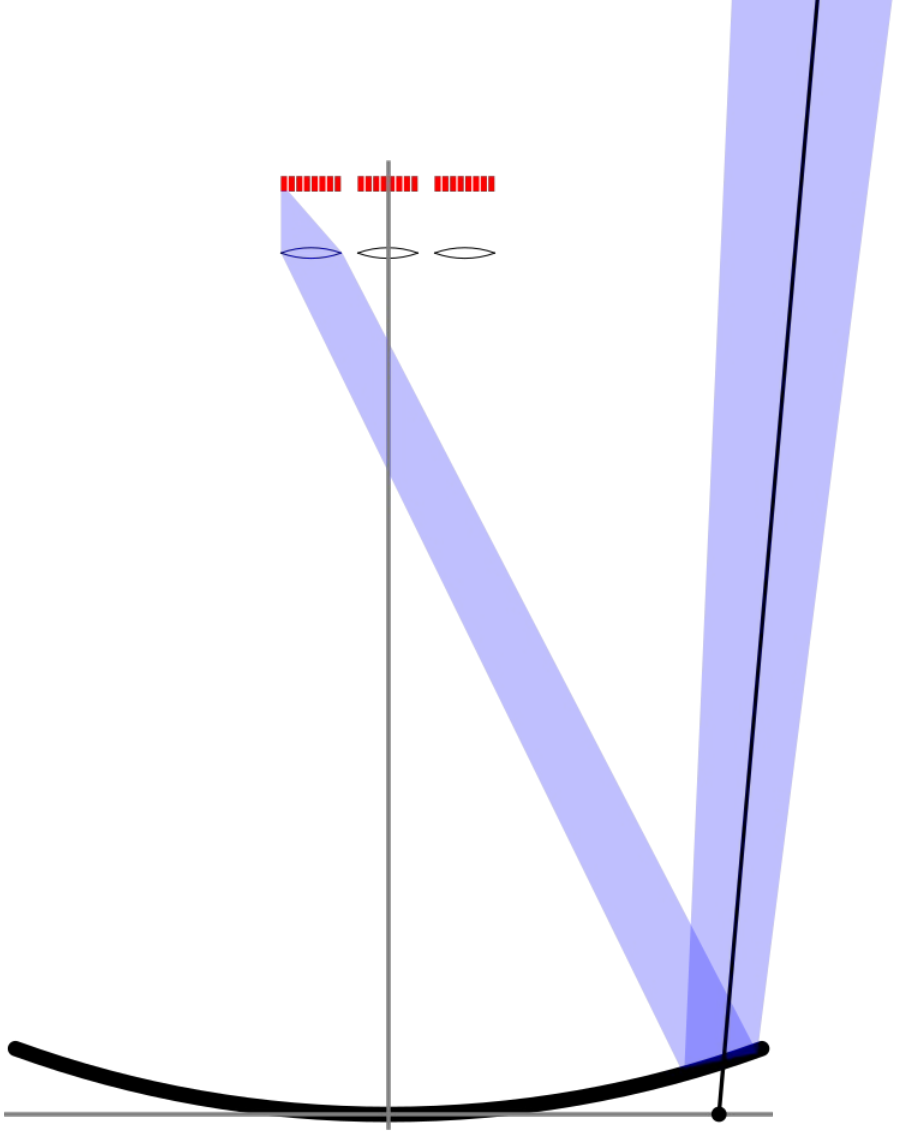

Plenoptics

Plenoscope

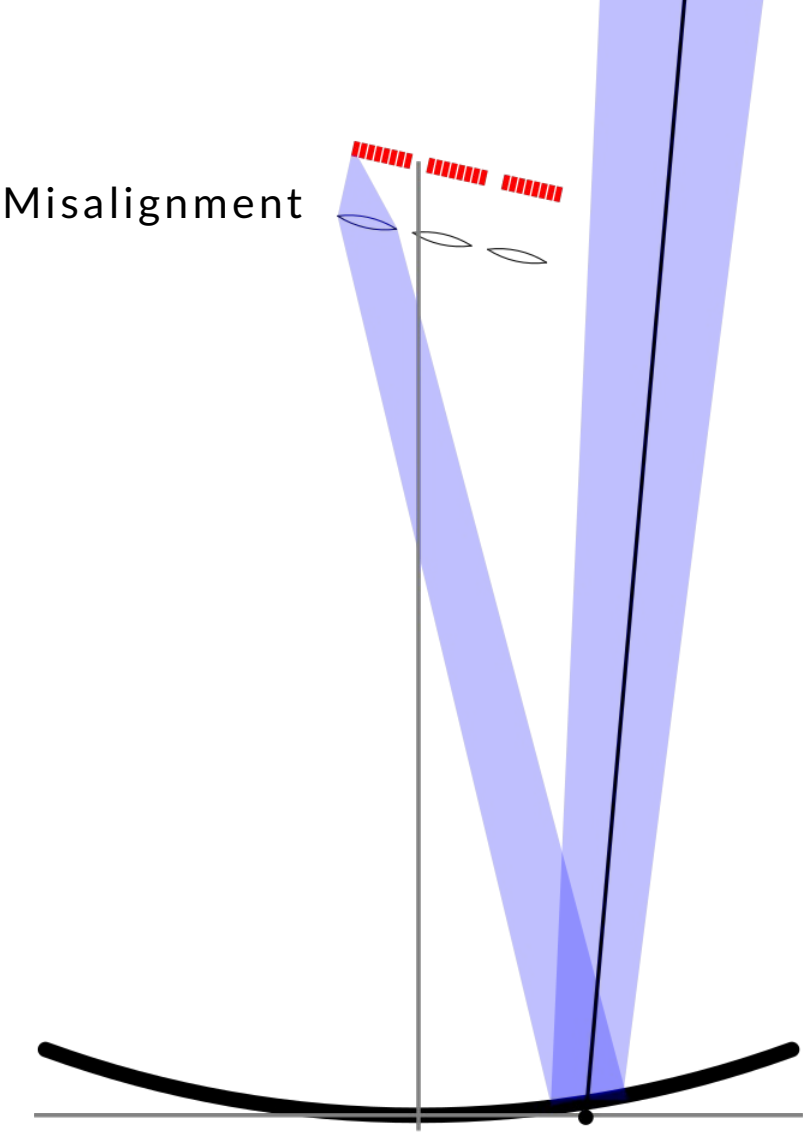

Plenoptics

Plenoscope

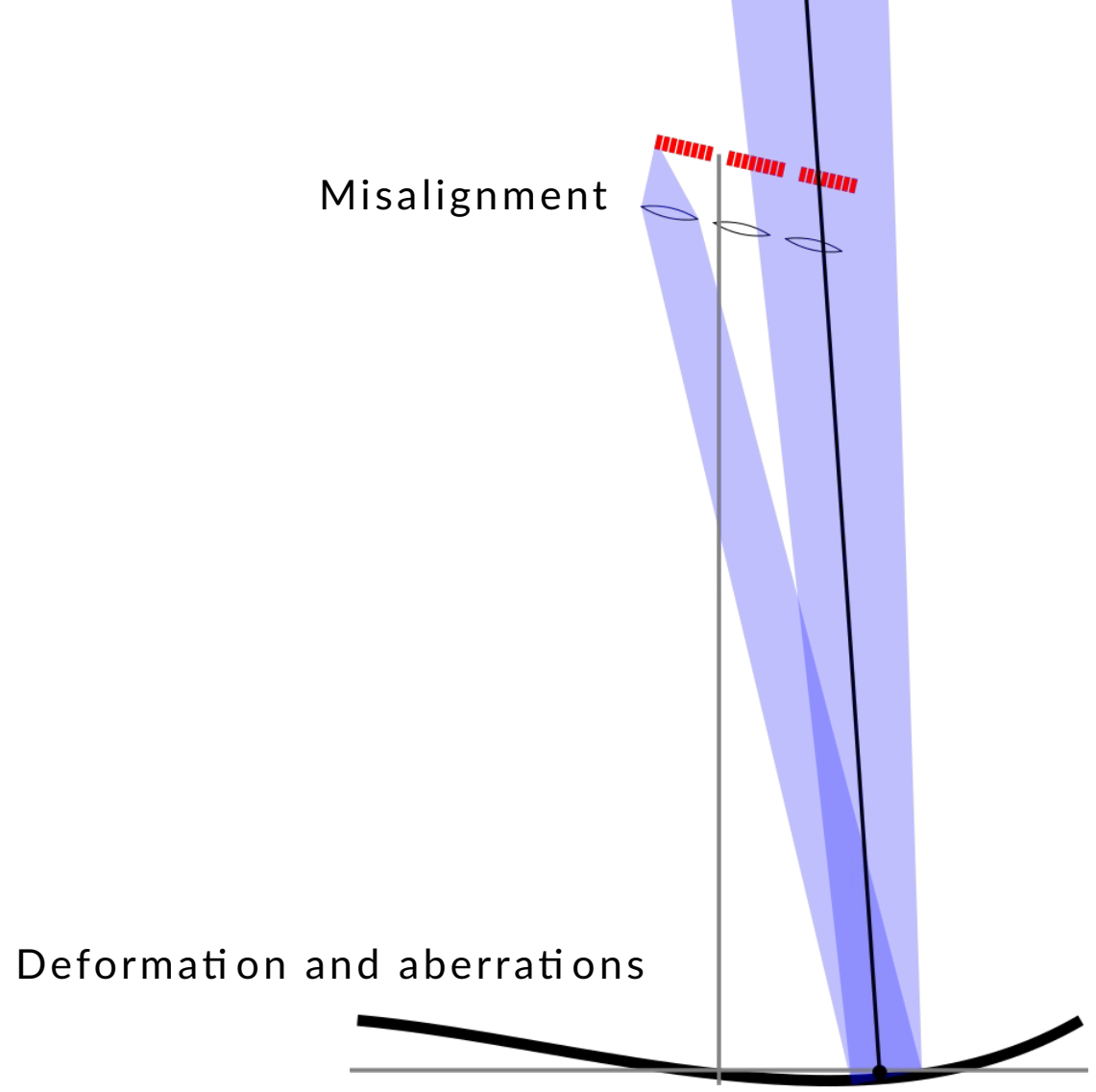

Plenoptics

Plenoscope

thin lens

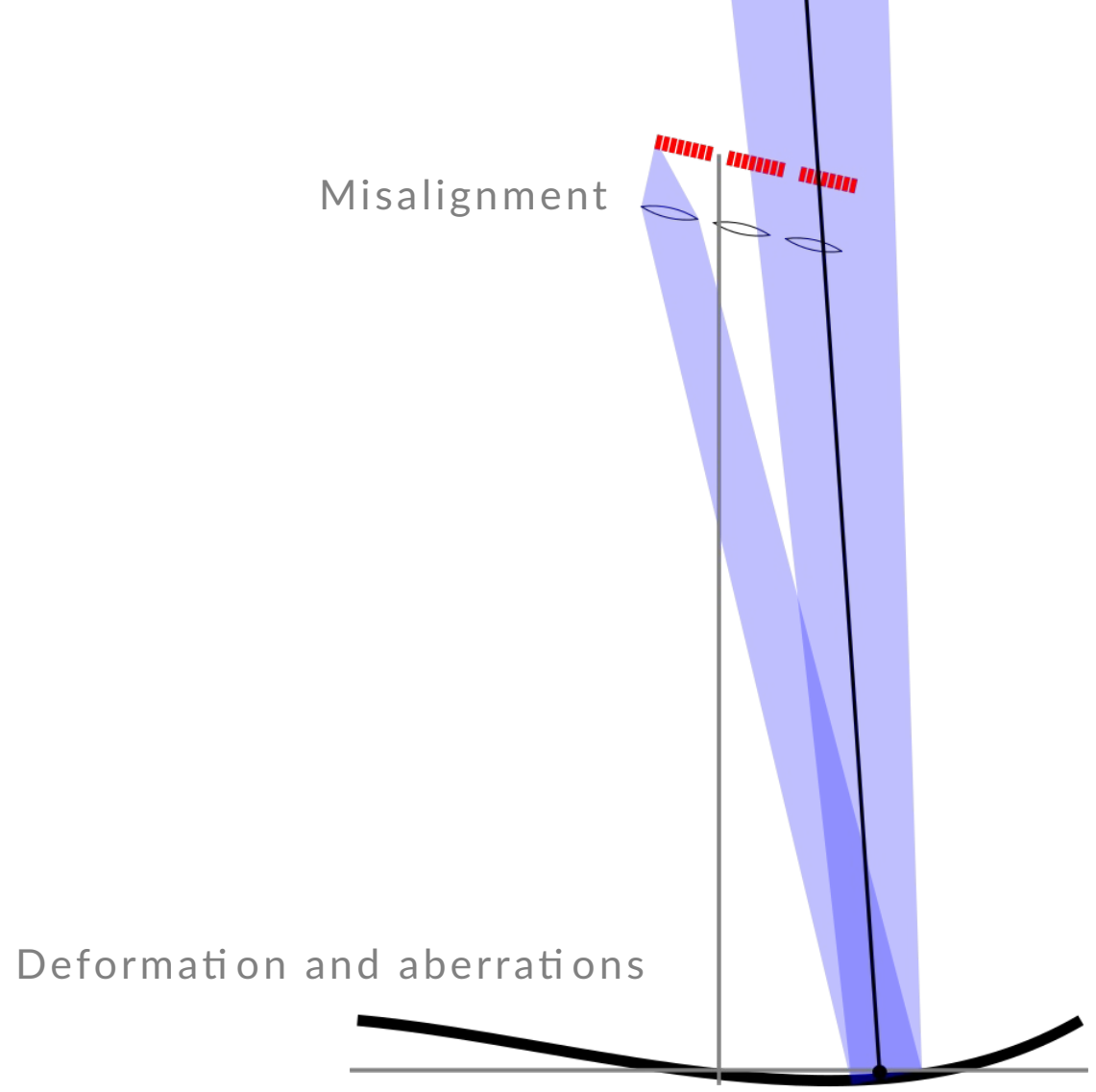

Plenoptics

thin lens

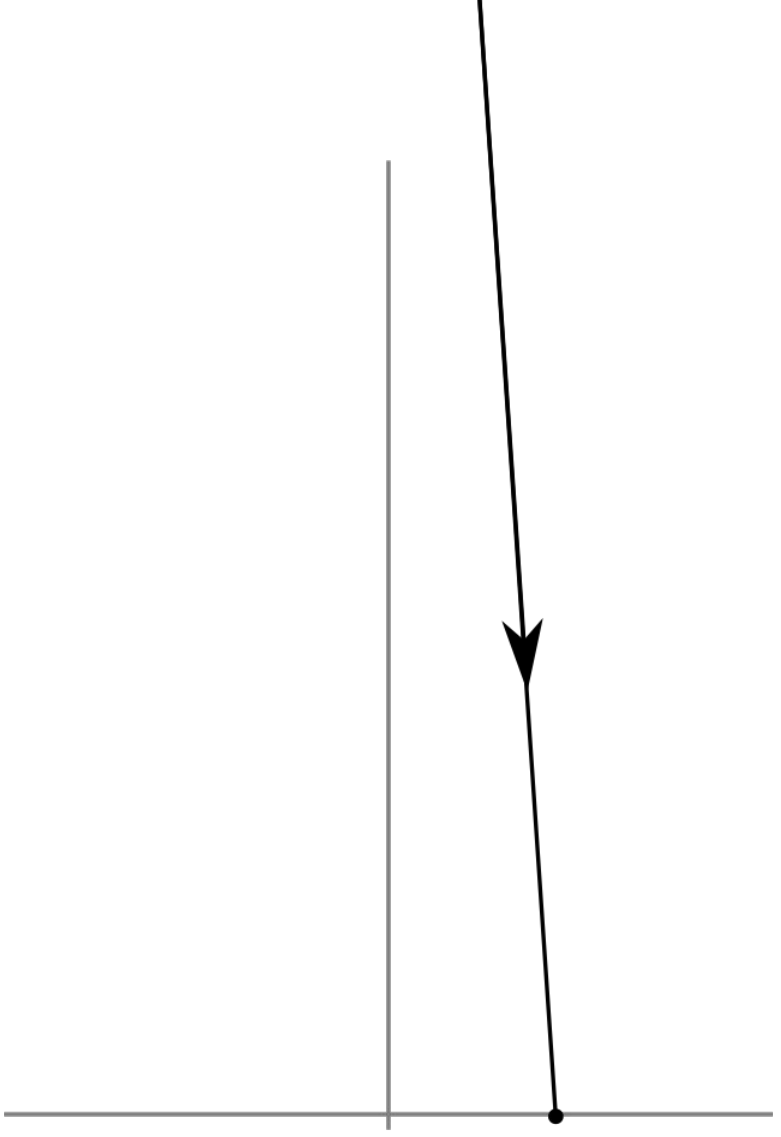

Plenoptics

thin lens

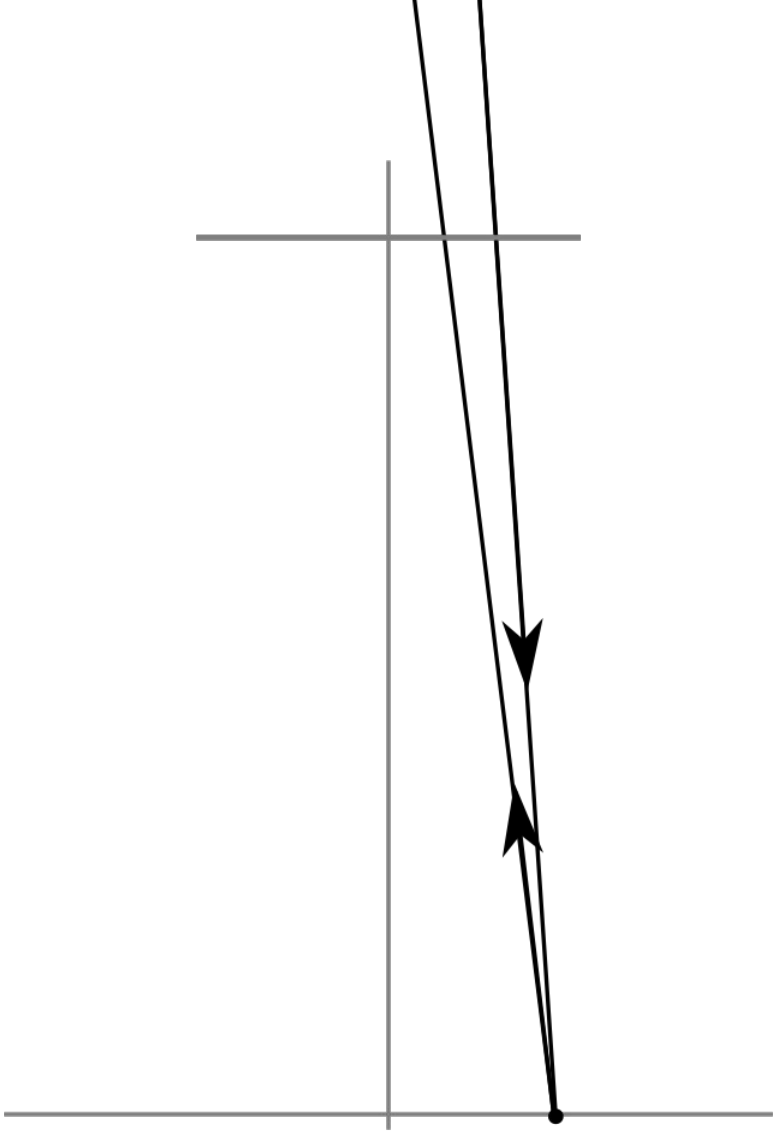

Plenoptics

thin lens

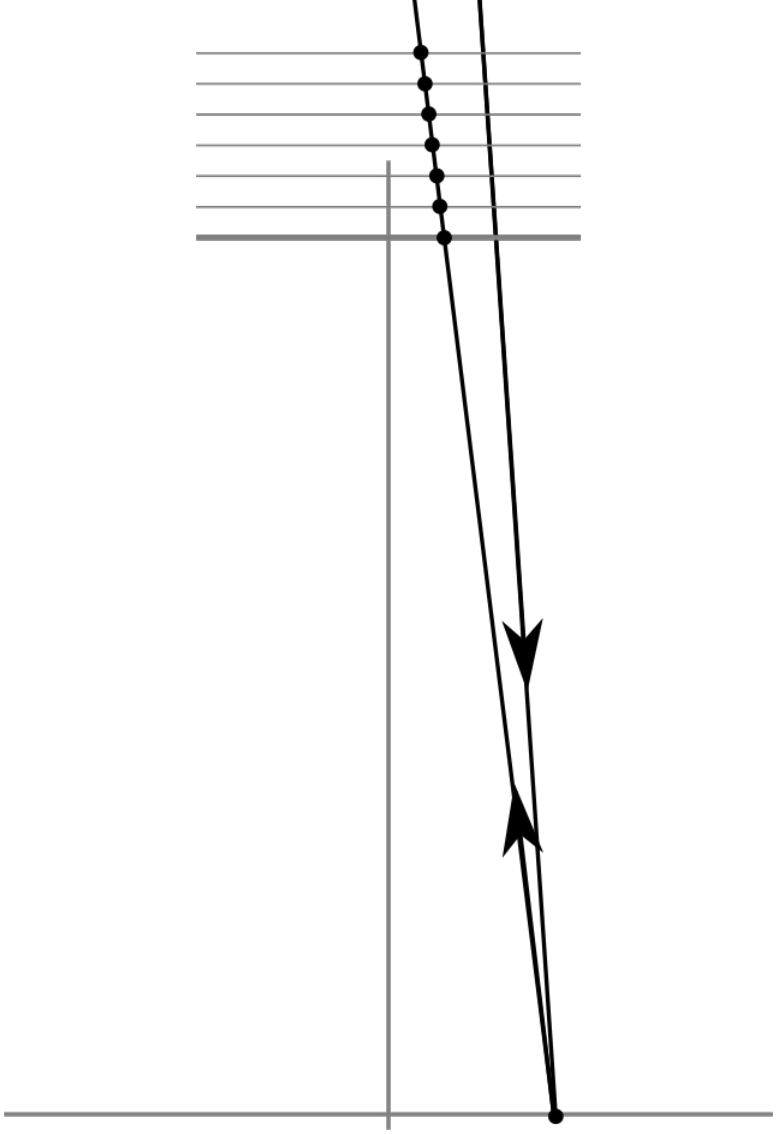

Plenoptics

Plenoscope

thin lens

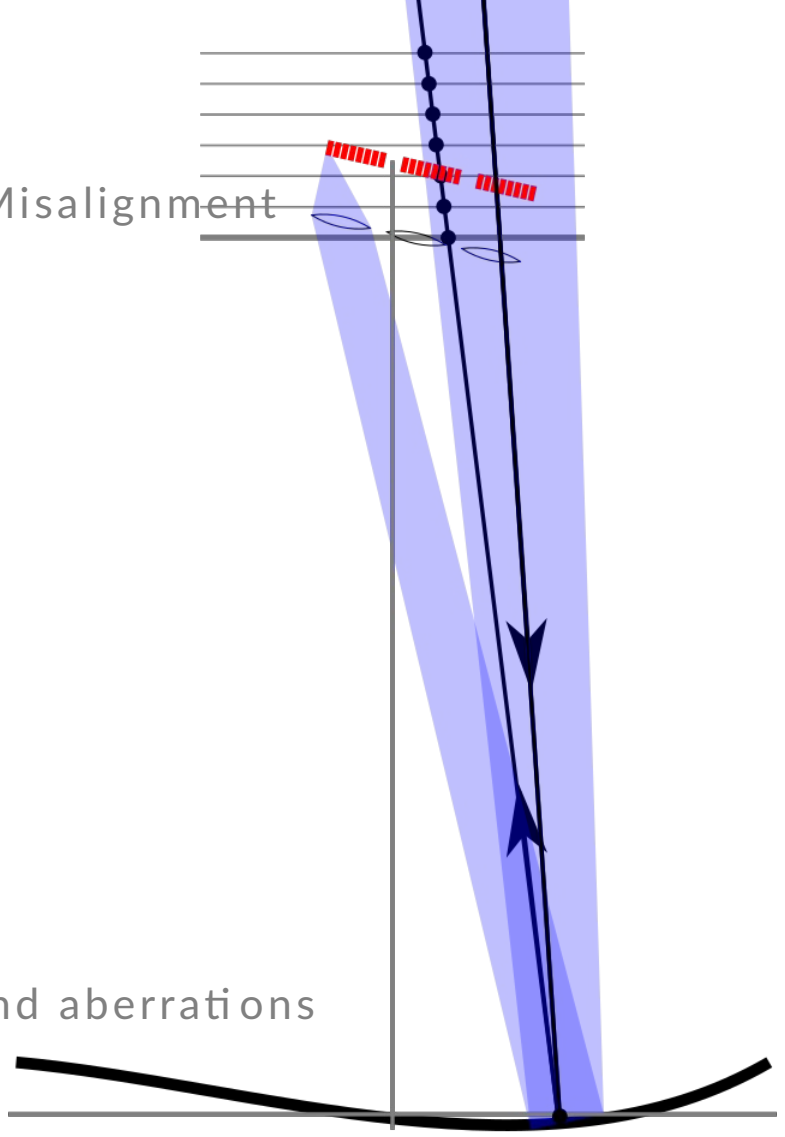

Plenoptics

Plenoscope

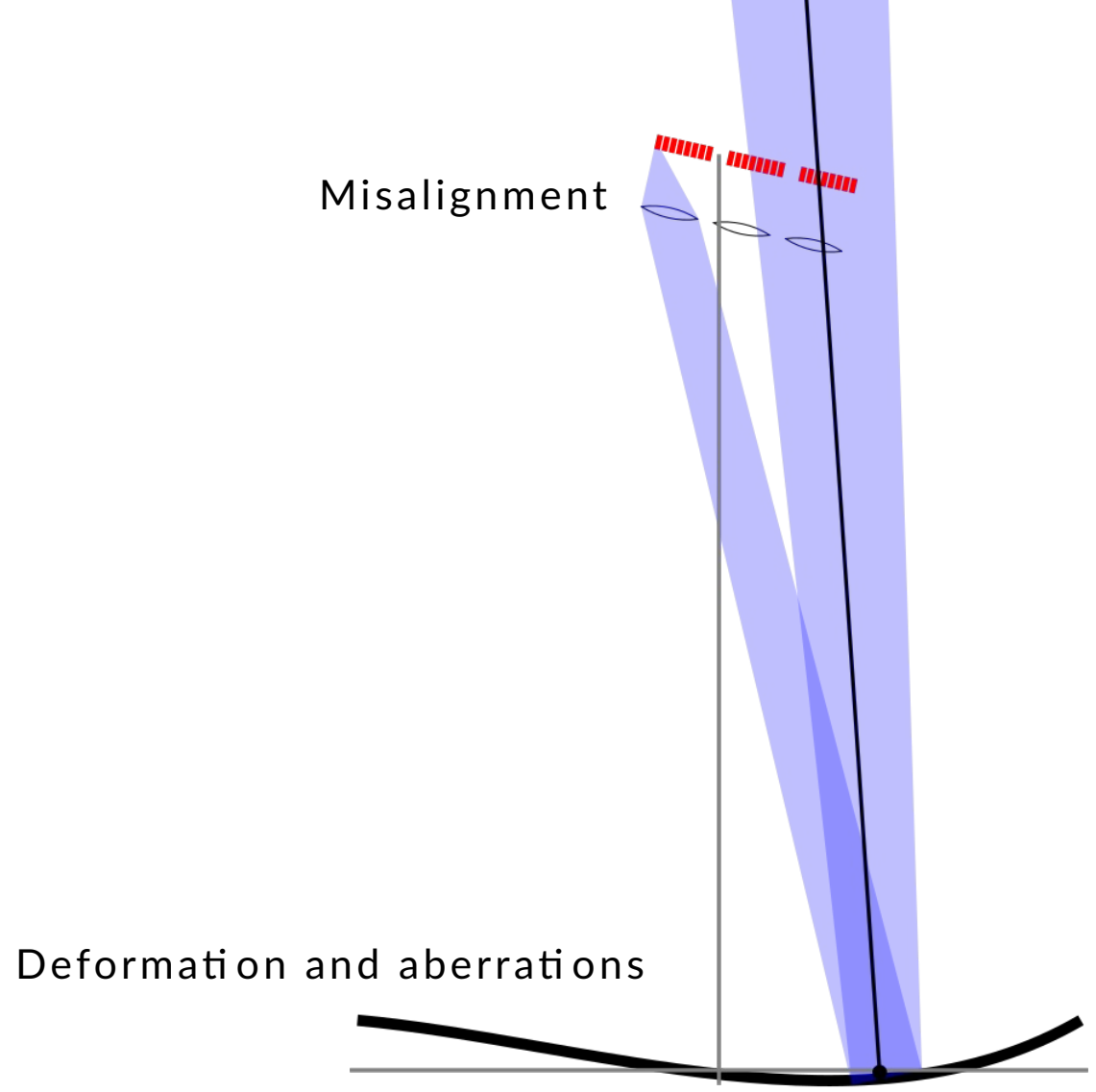

Plenoptics

Plenoscope

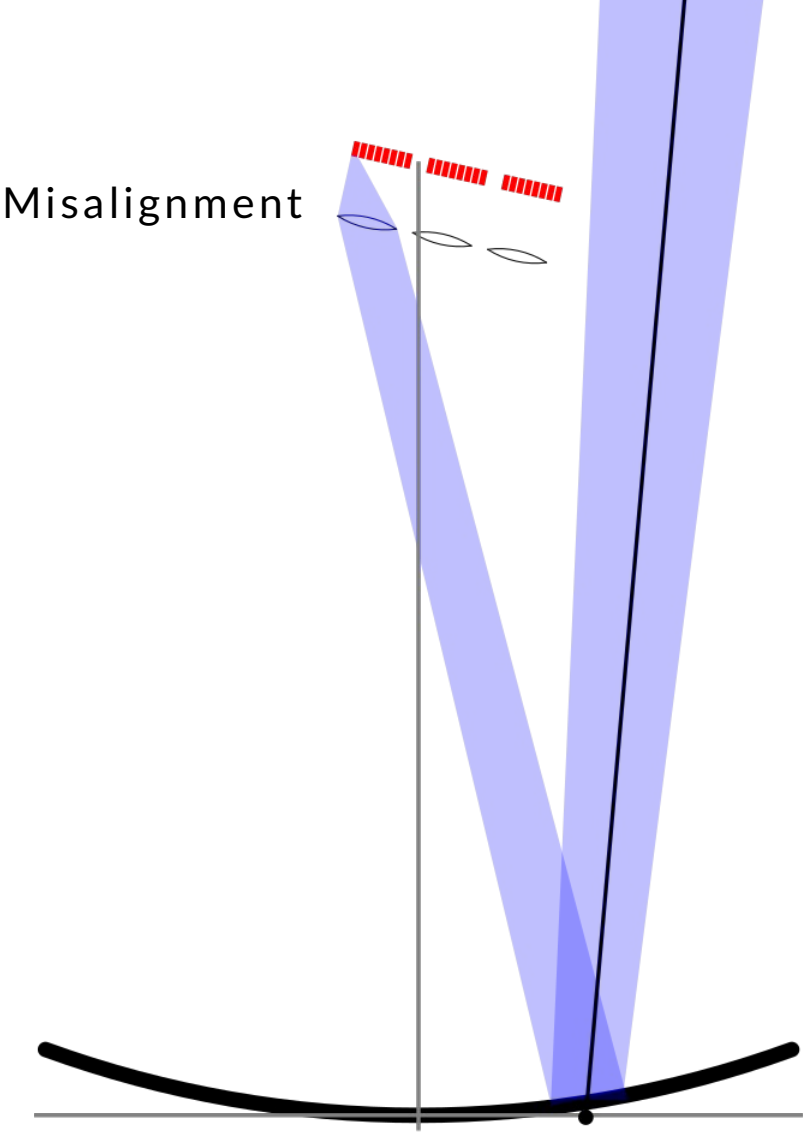

Plenoptics

Plenoscope

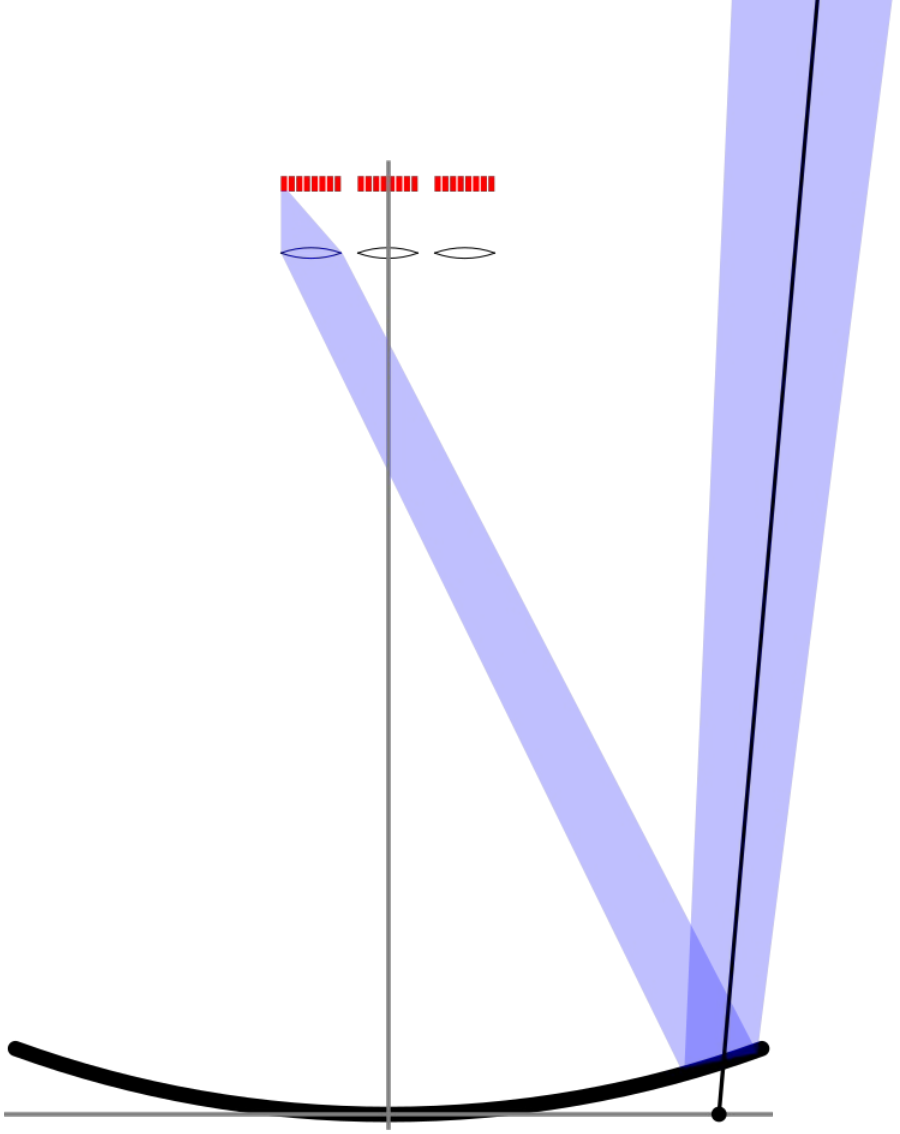

CHERENKOV-PLENOSCOPE

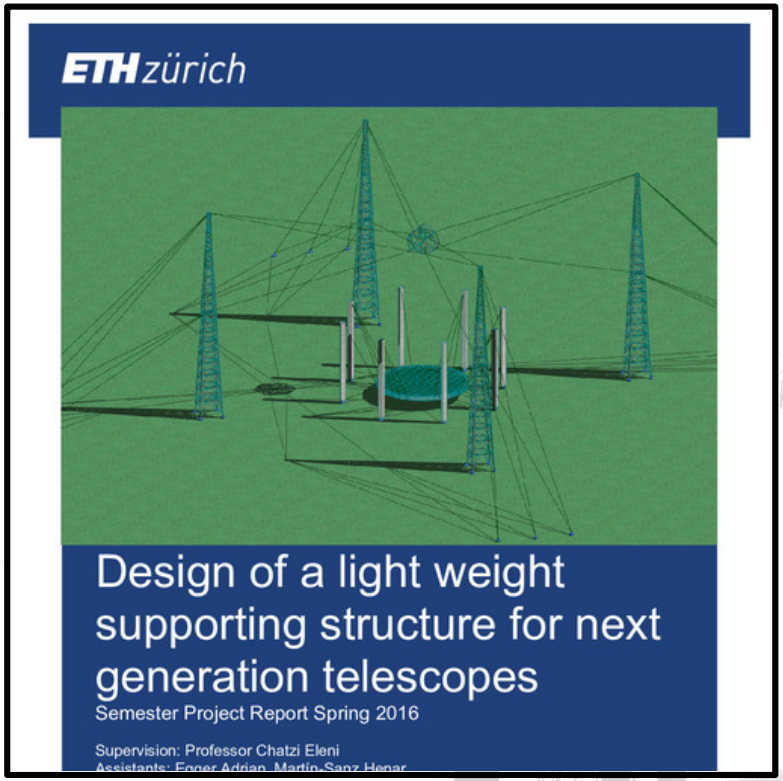

Georgios Zinas and Spyridon Daglas
Report (2016)

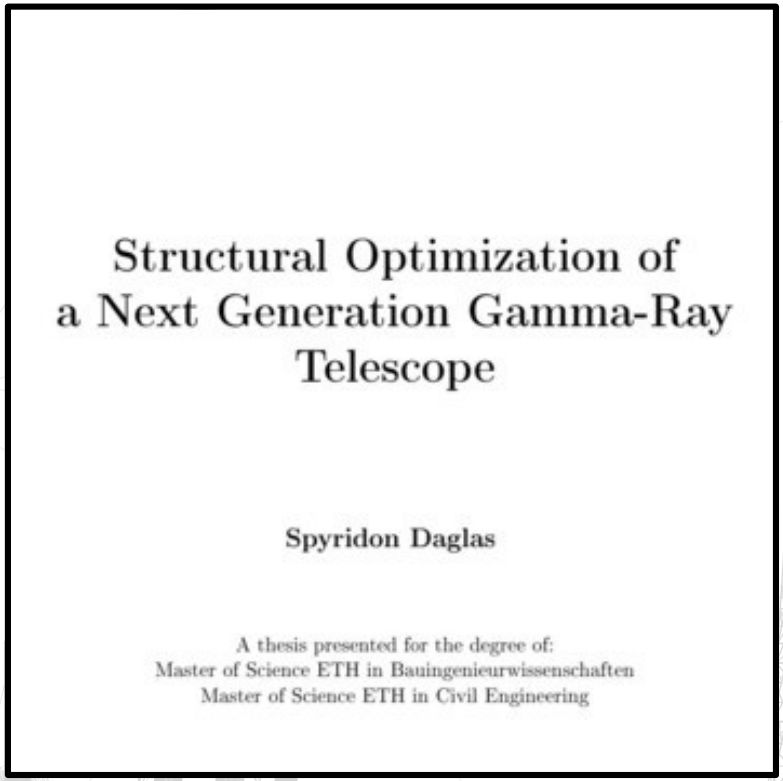

Spyridon Daglas
Master-thesis (2017)
in **Civil Engineering**

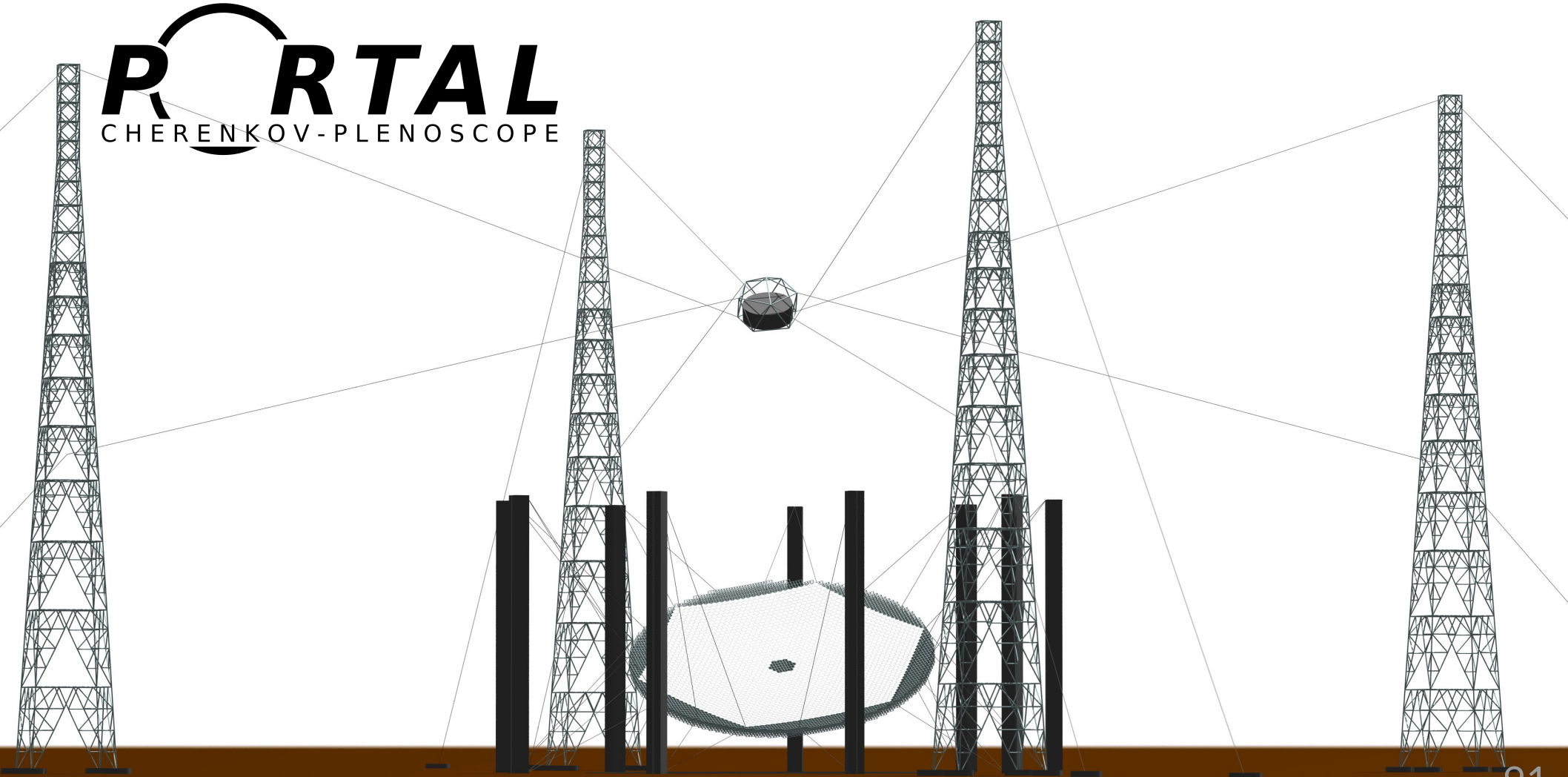
PORTAL
CHERENKOV-PLENOSCOPE

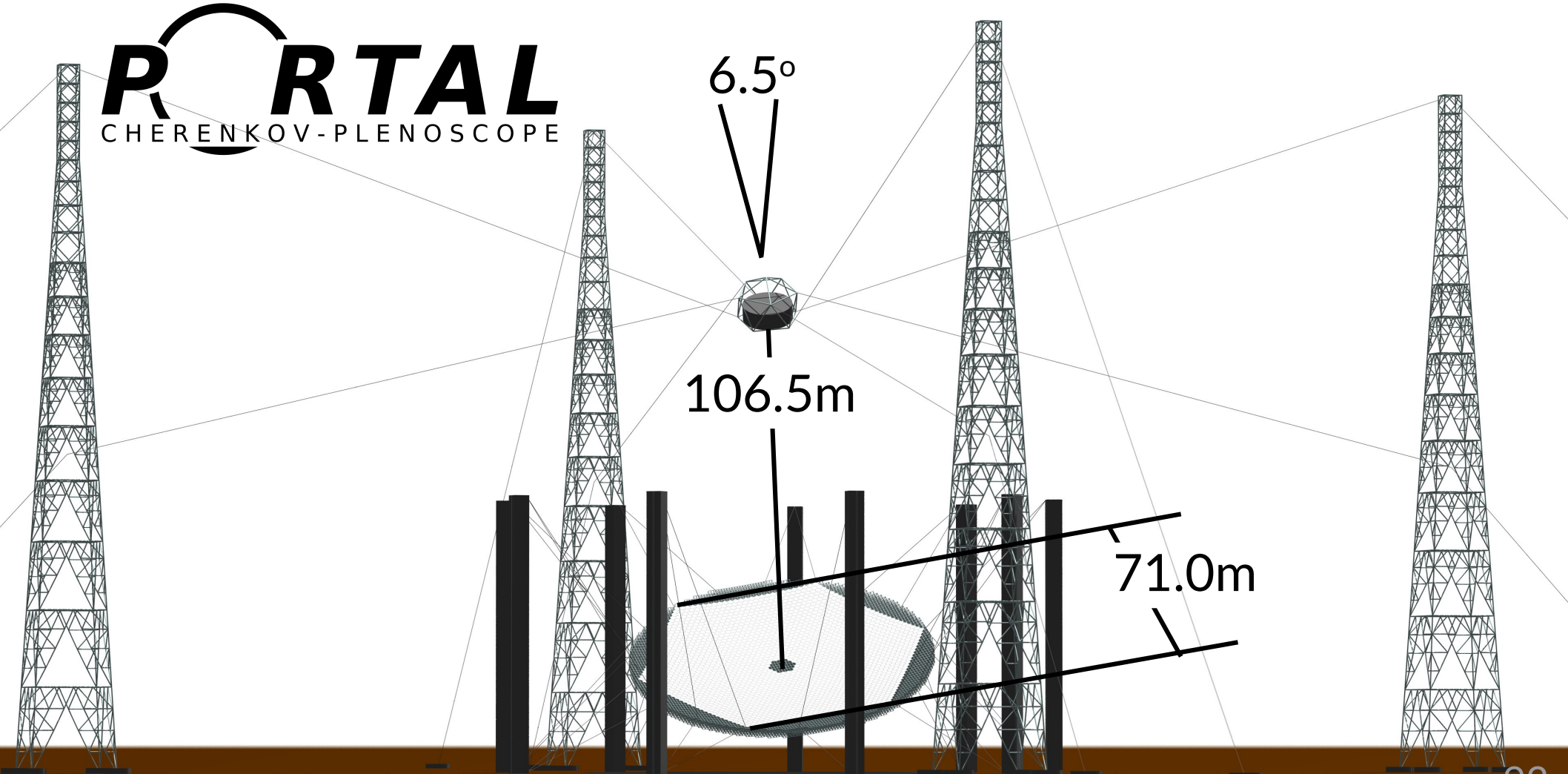
PORTAL
CHERENKOV-PLENOSCOPE
6.5°
106.5m
71.0m

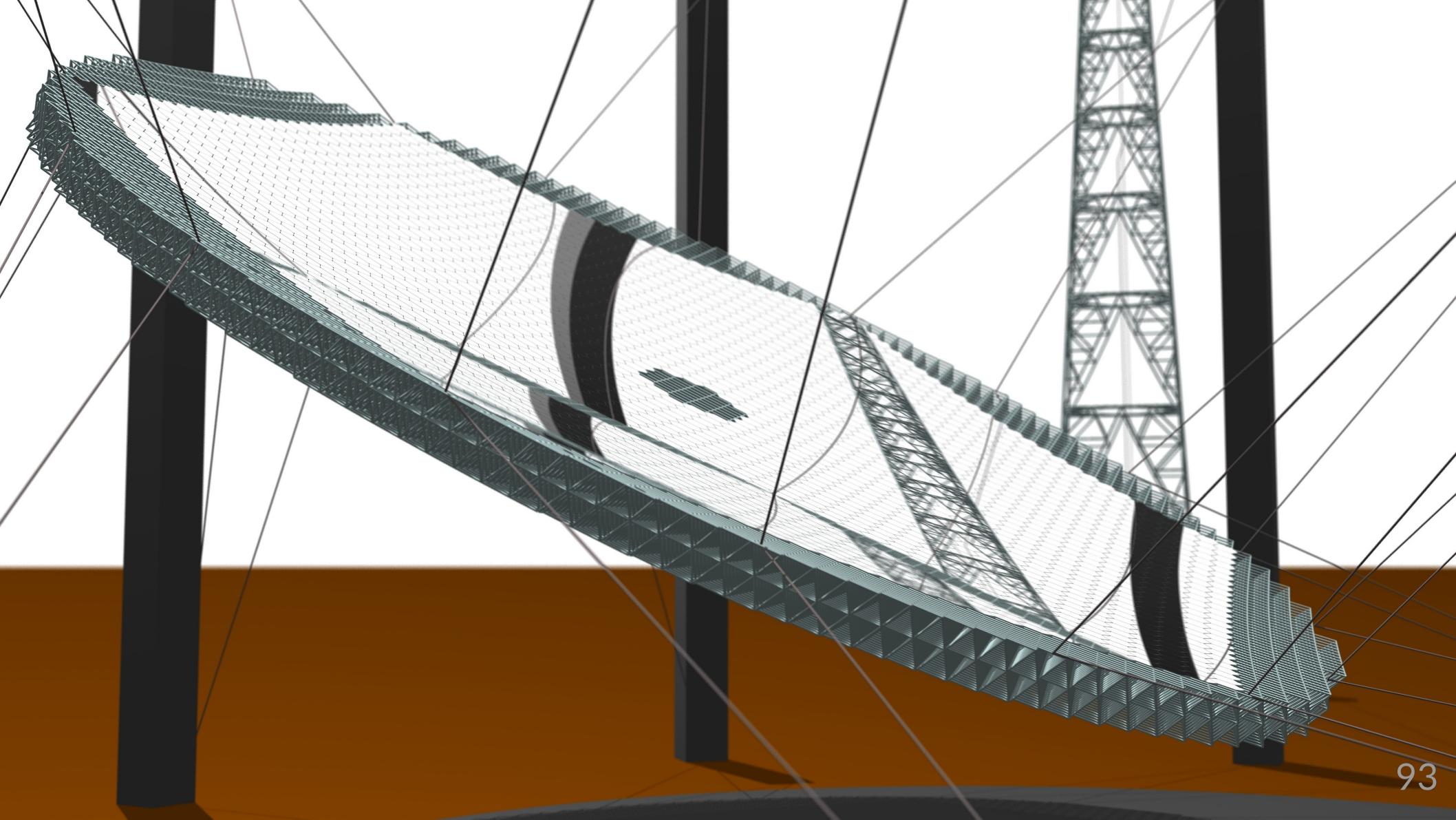

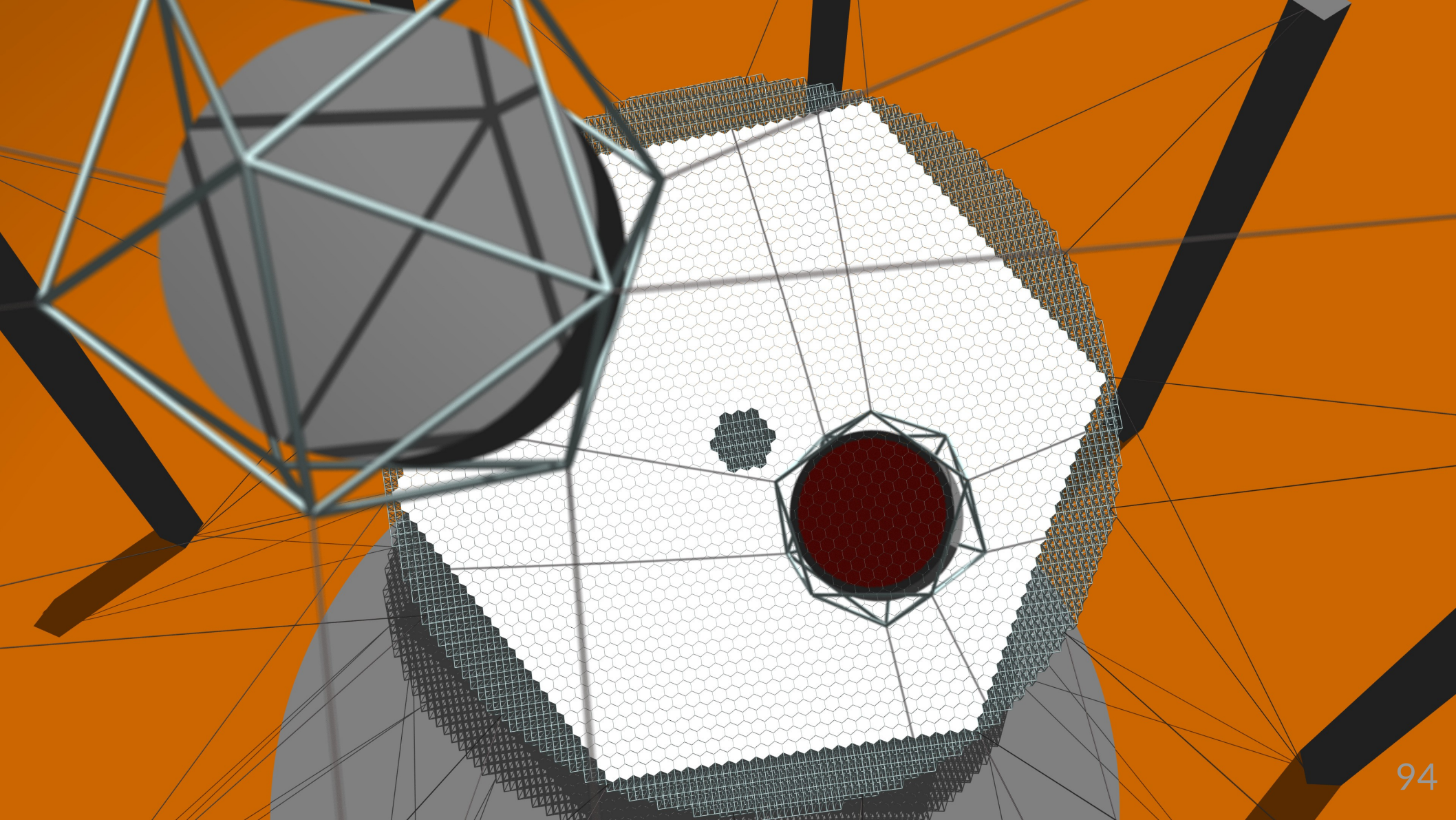

Miermeister, P., et al. (2016). The CableRobot Simulator: Large Scale Motion Platform Based on Cable Robot Technology. In IEEE/RSJ International Conference on Intelligent Robots and Systems.

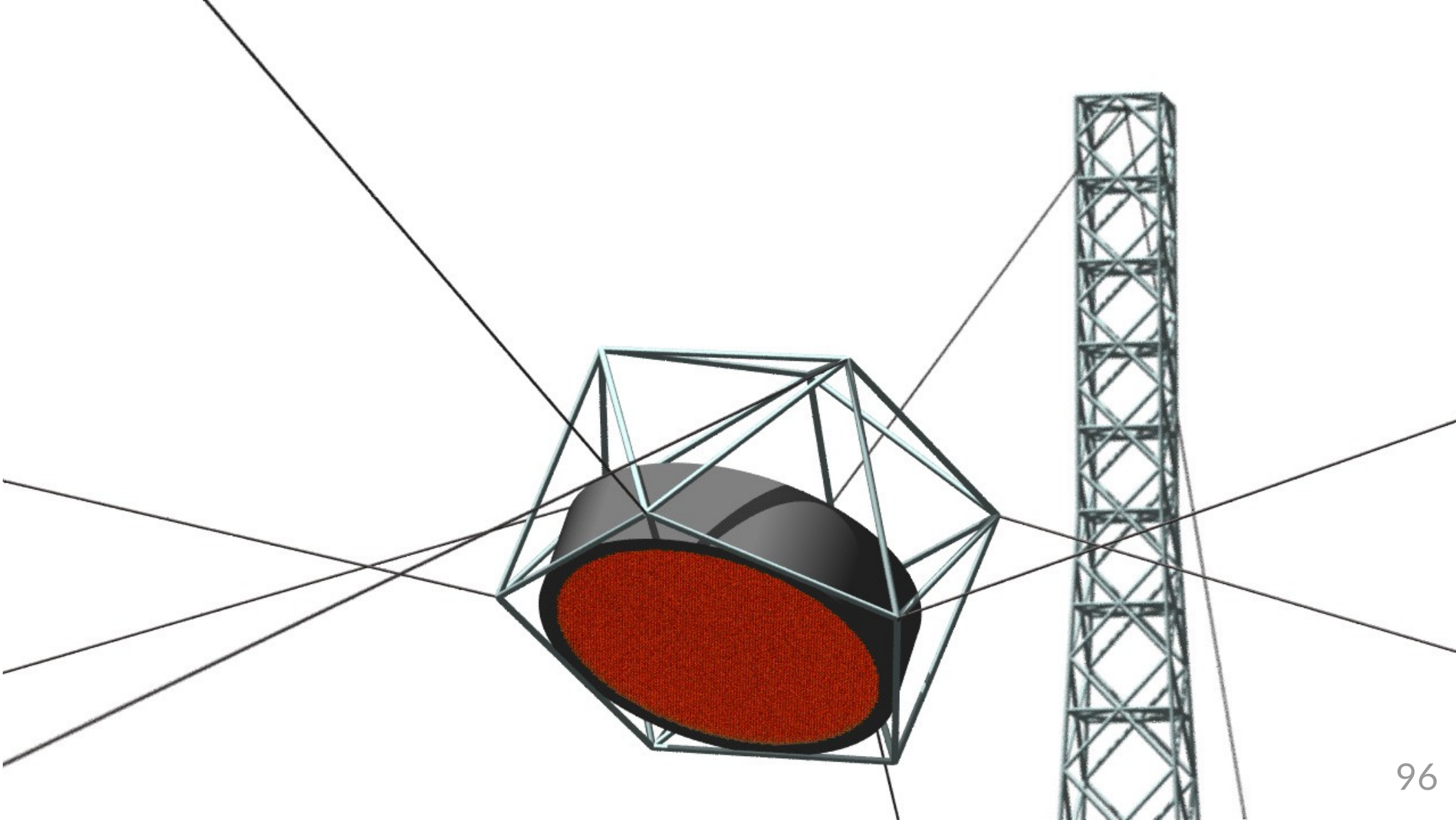

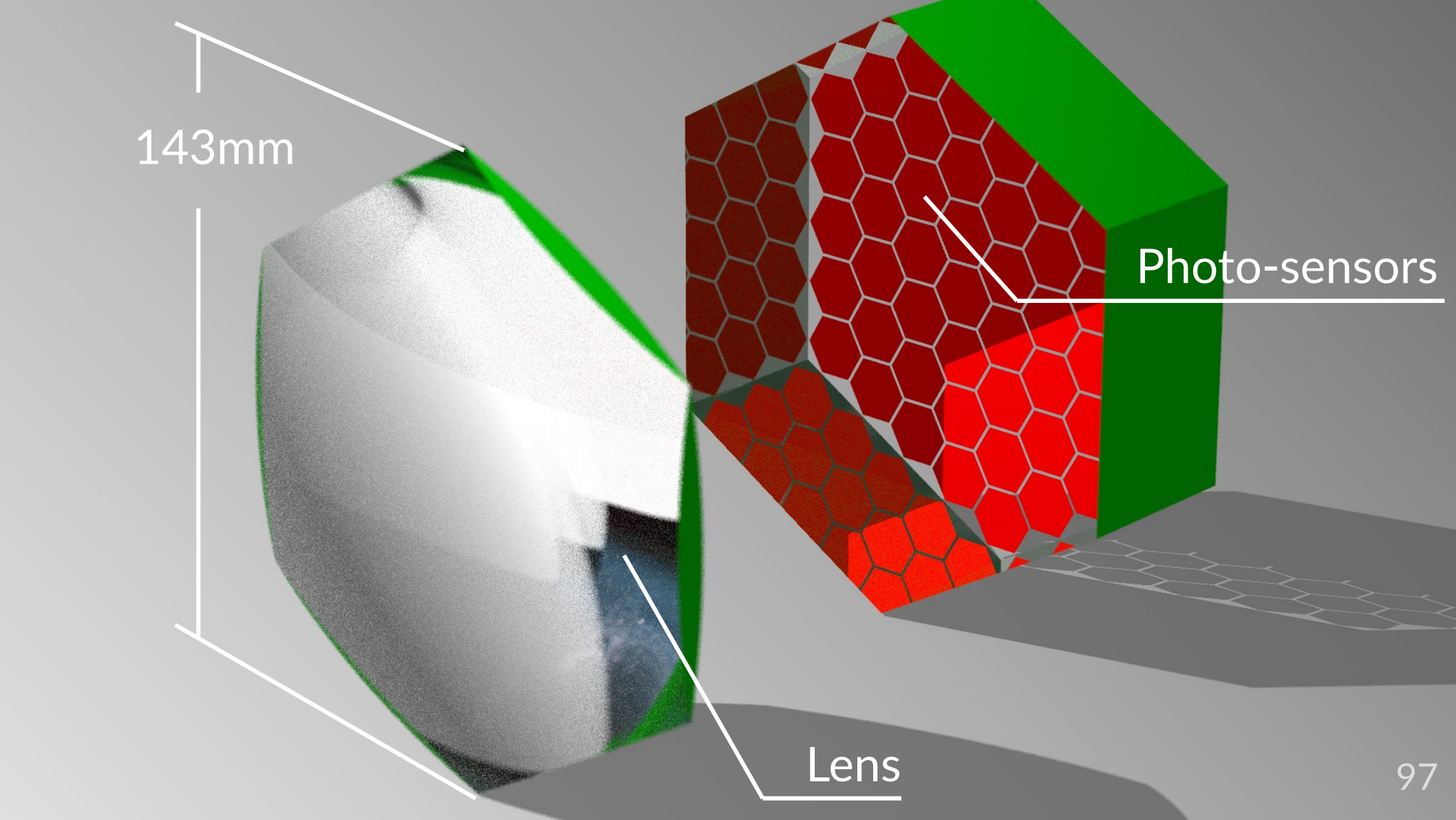
143mm
Photo-sensors
Lens

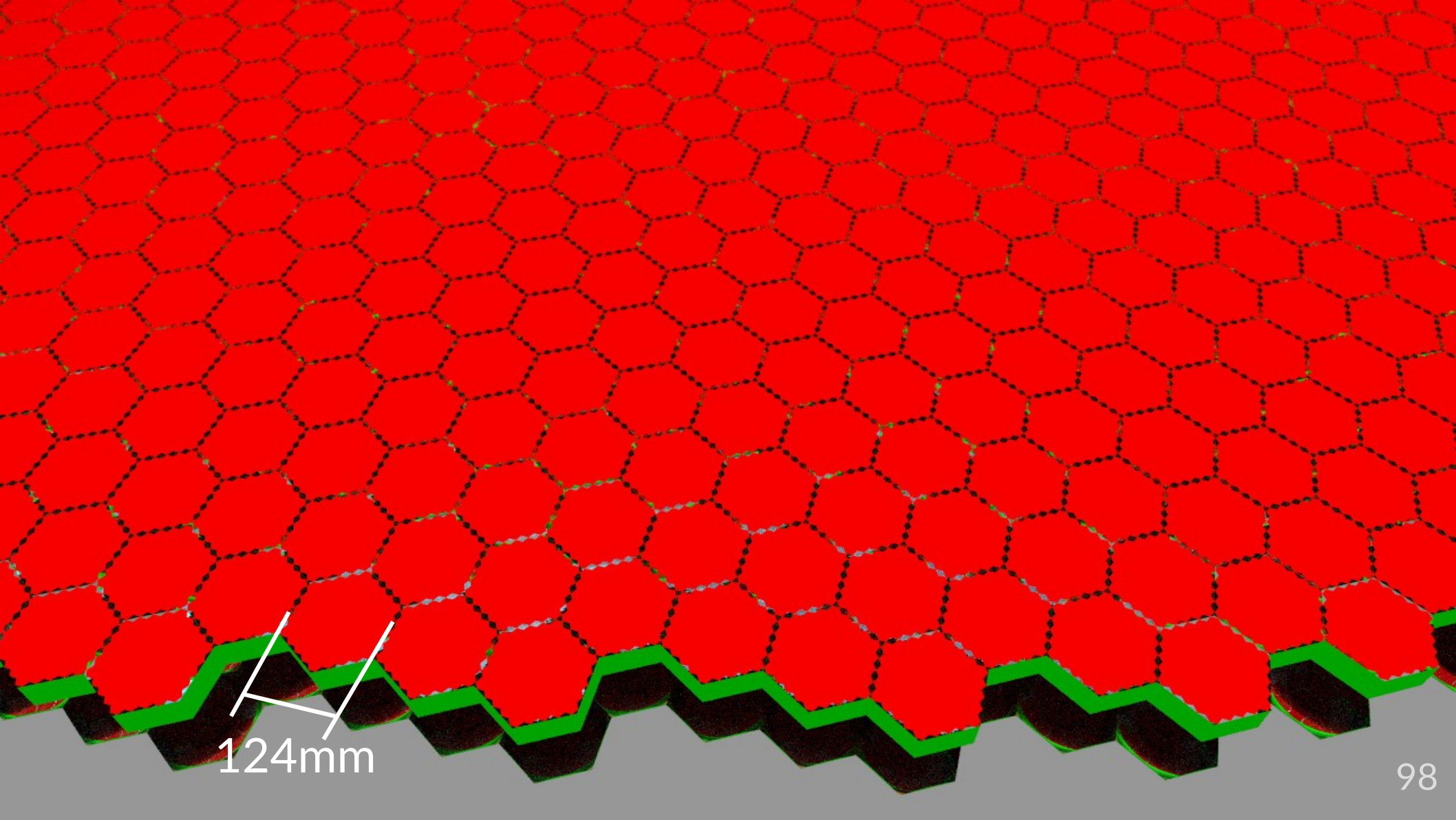
124mm

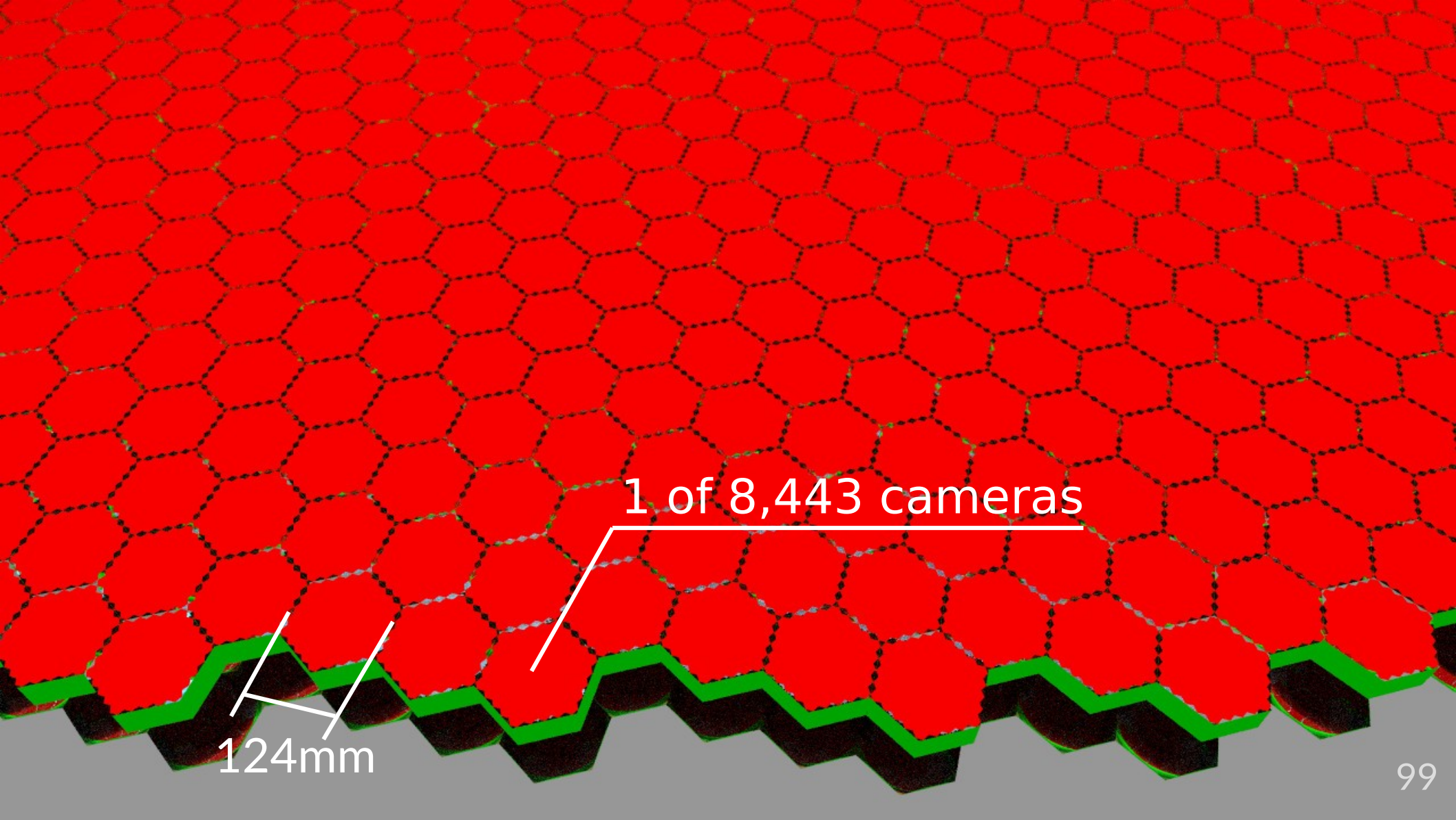
1 of 8,443 cameras
124mm

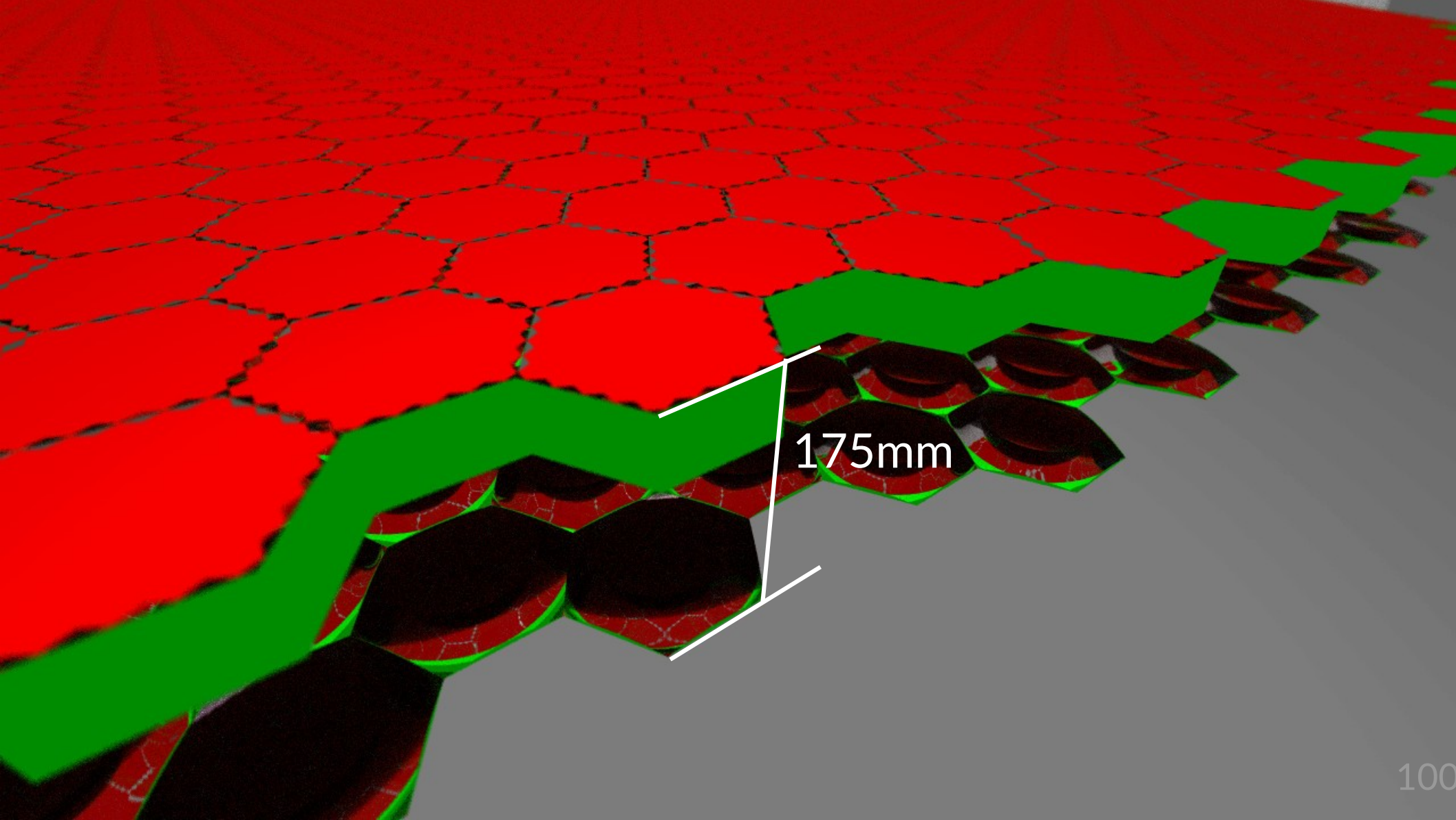
175mm

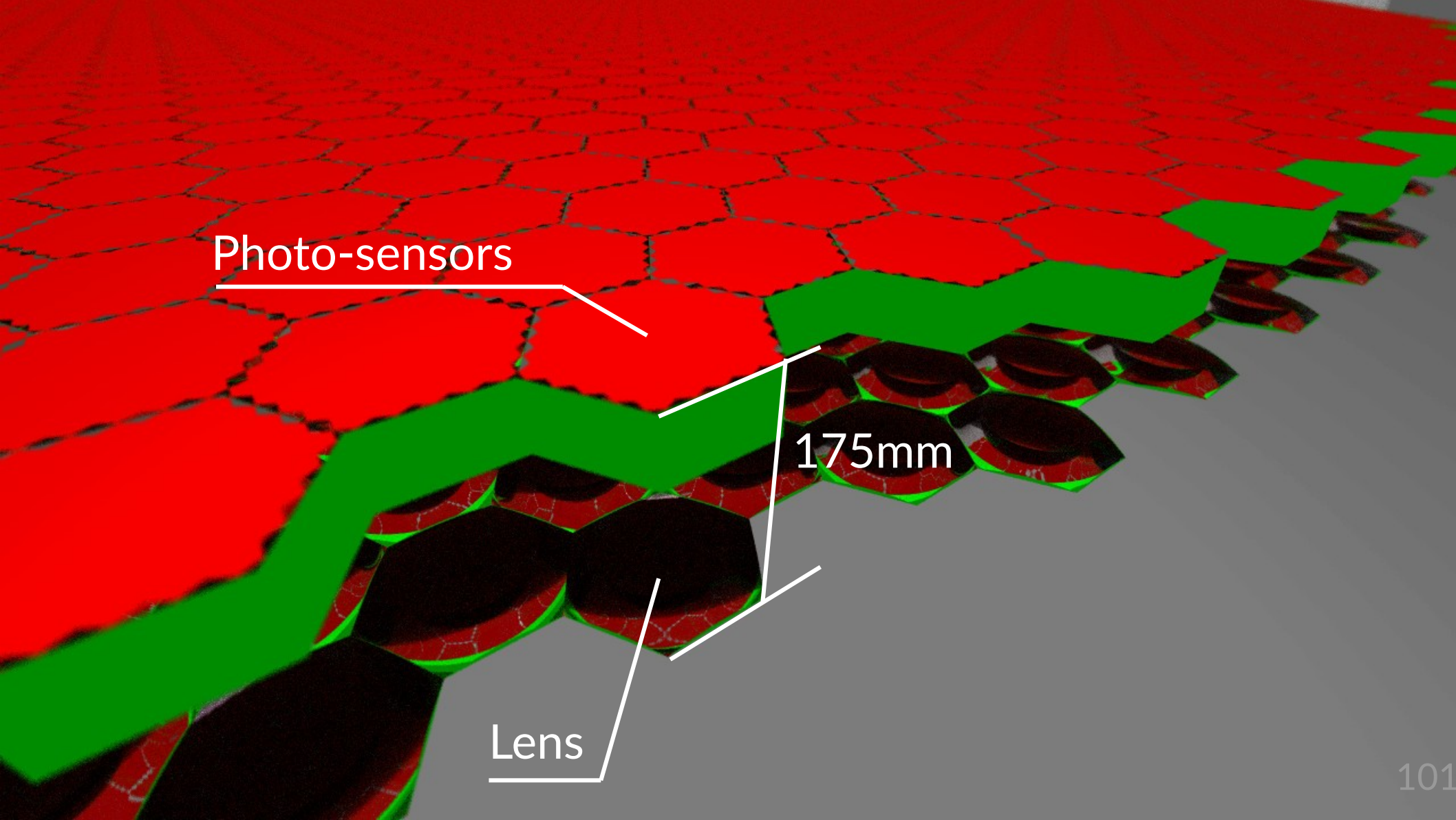
Photo-sensors
175mm
Lens

Pointing

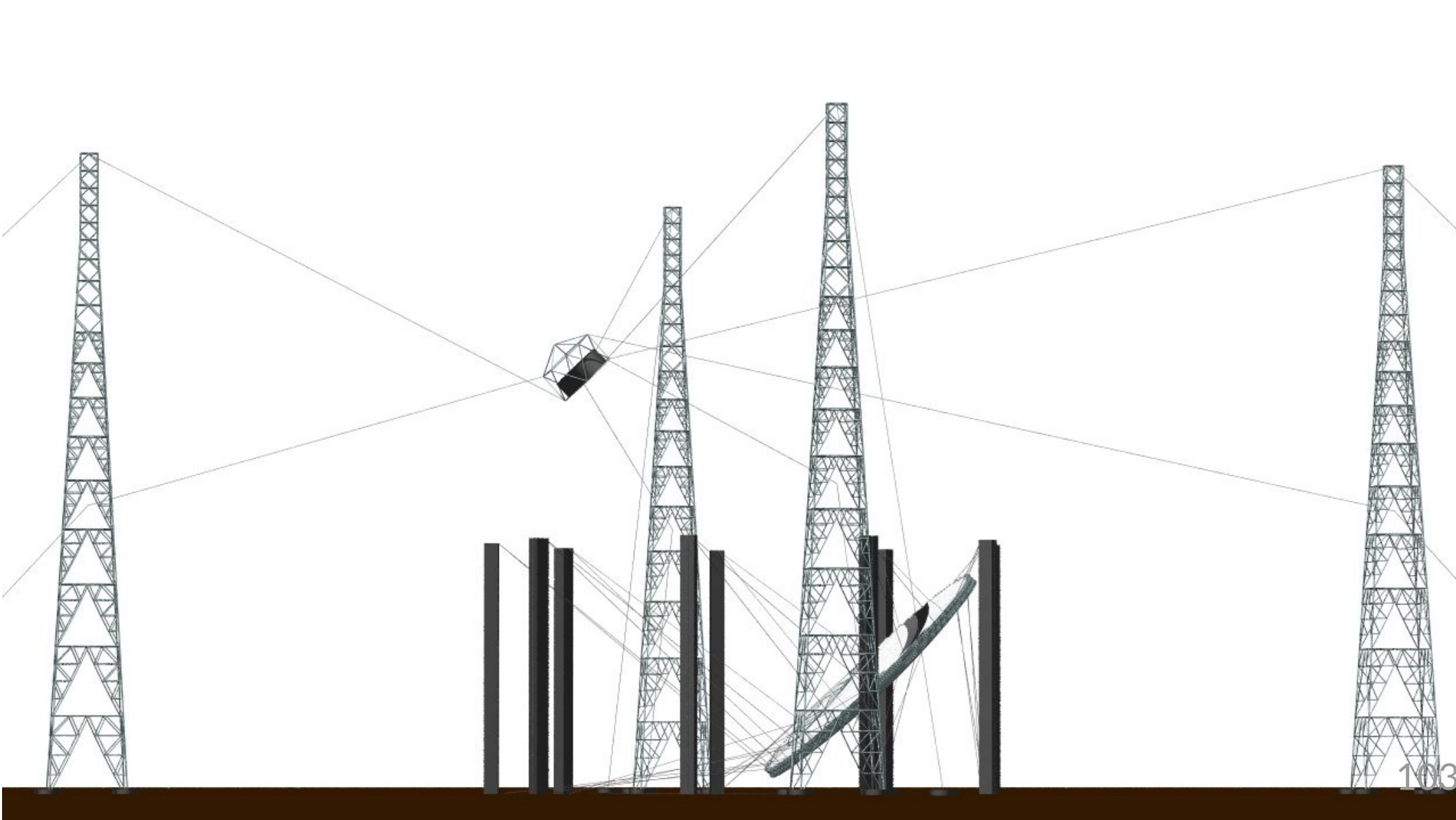

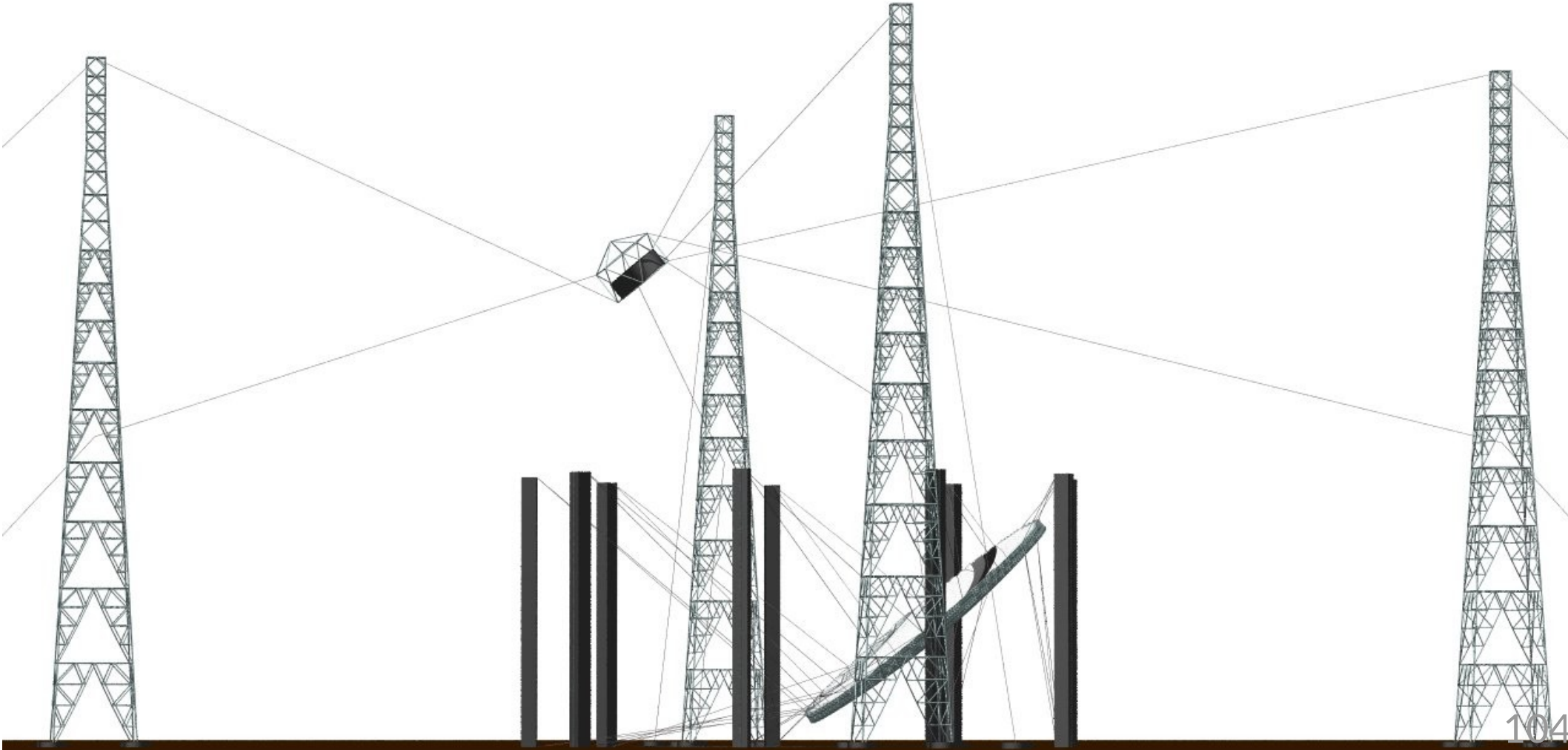

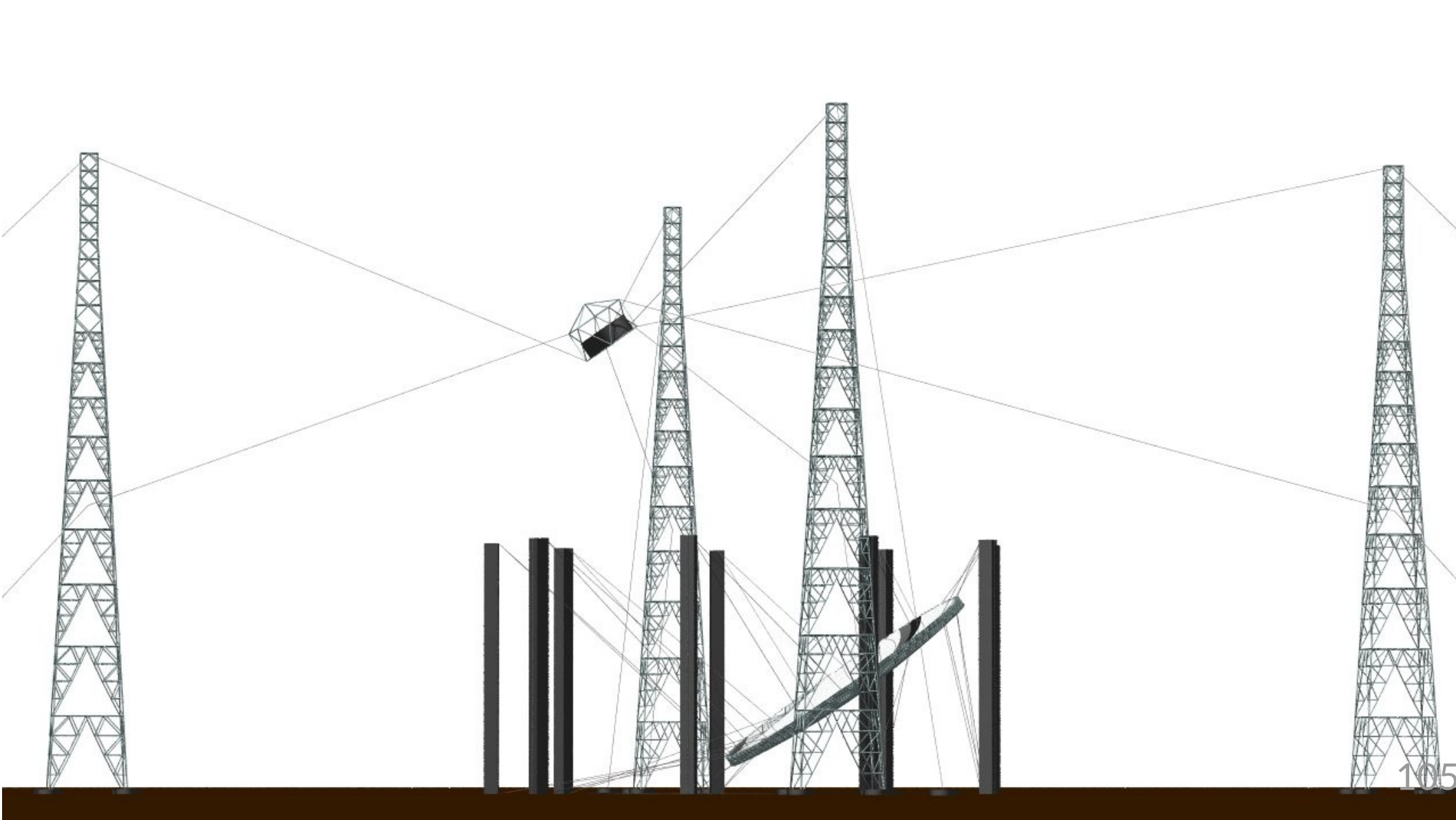

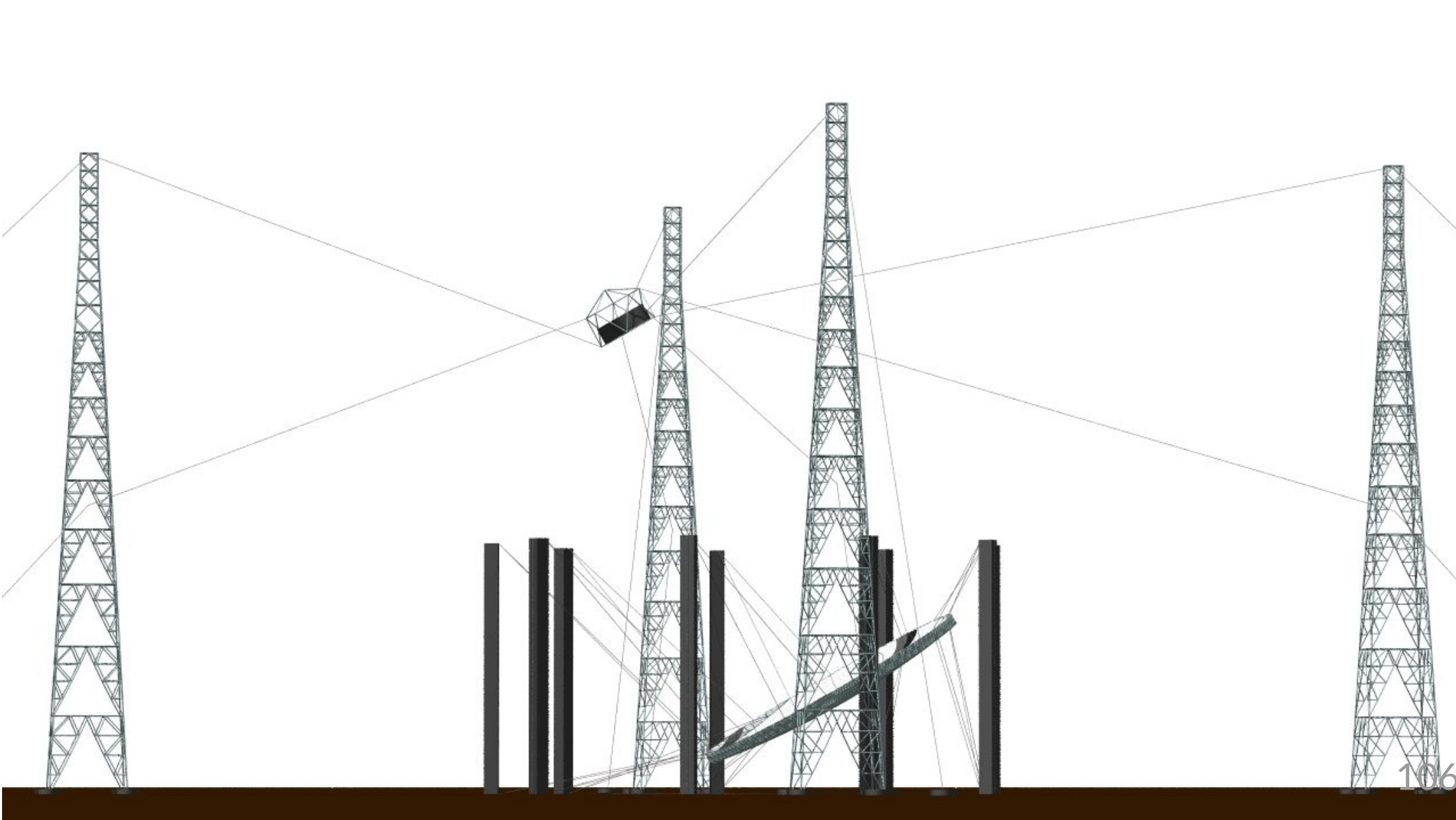

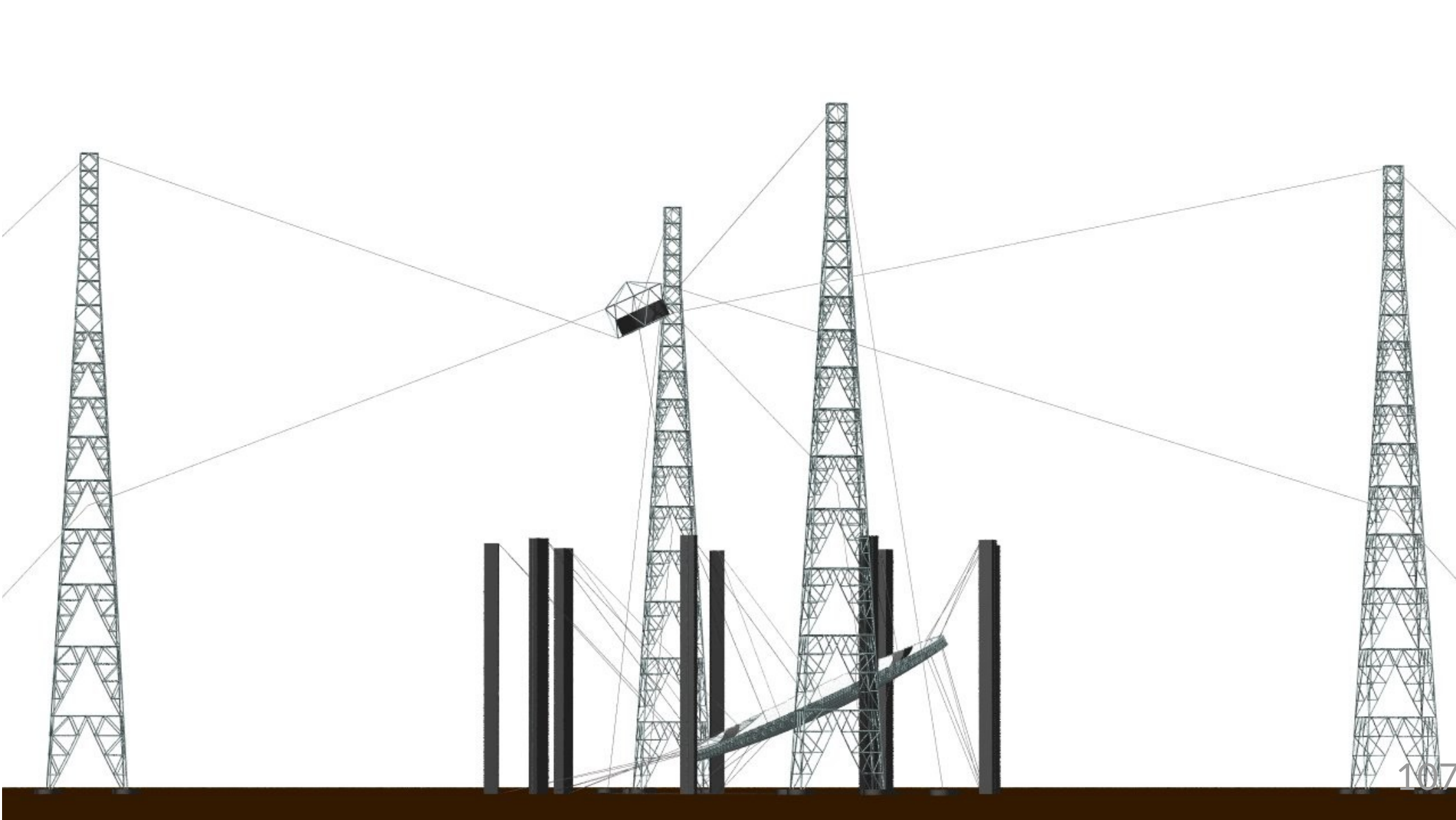

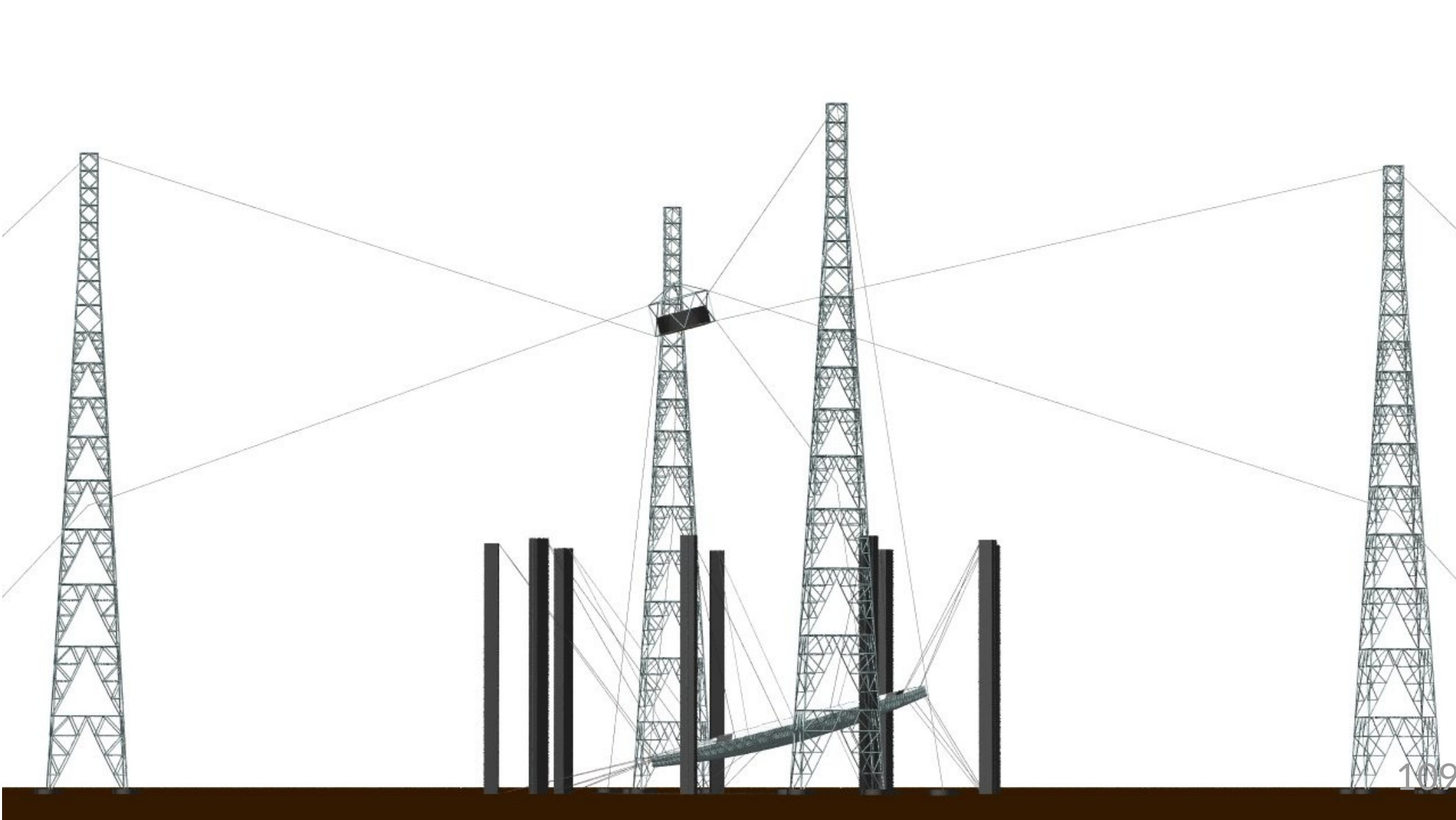

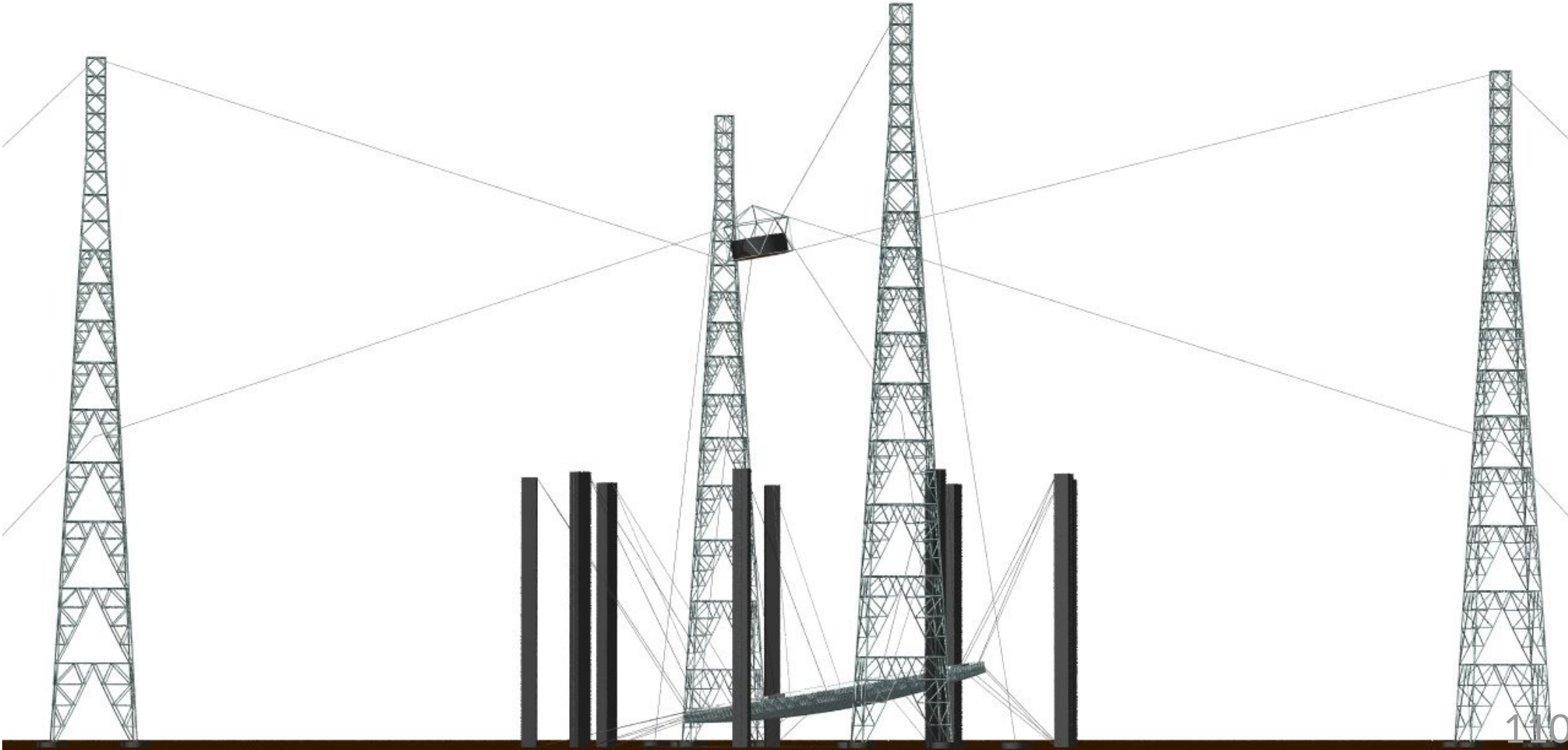

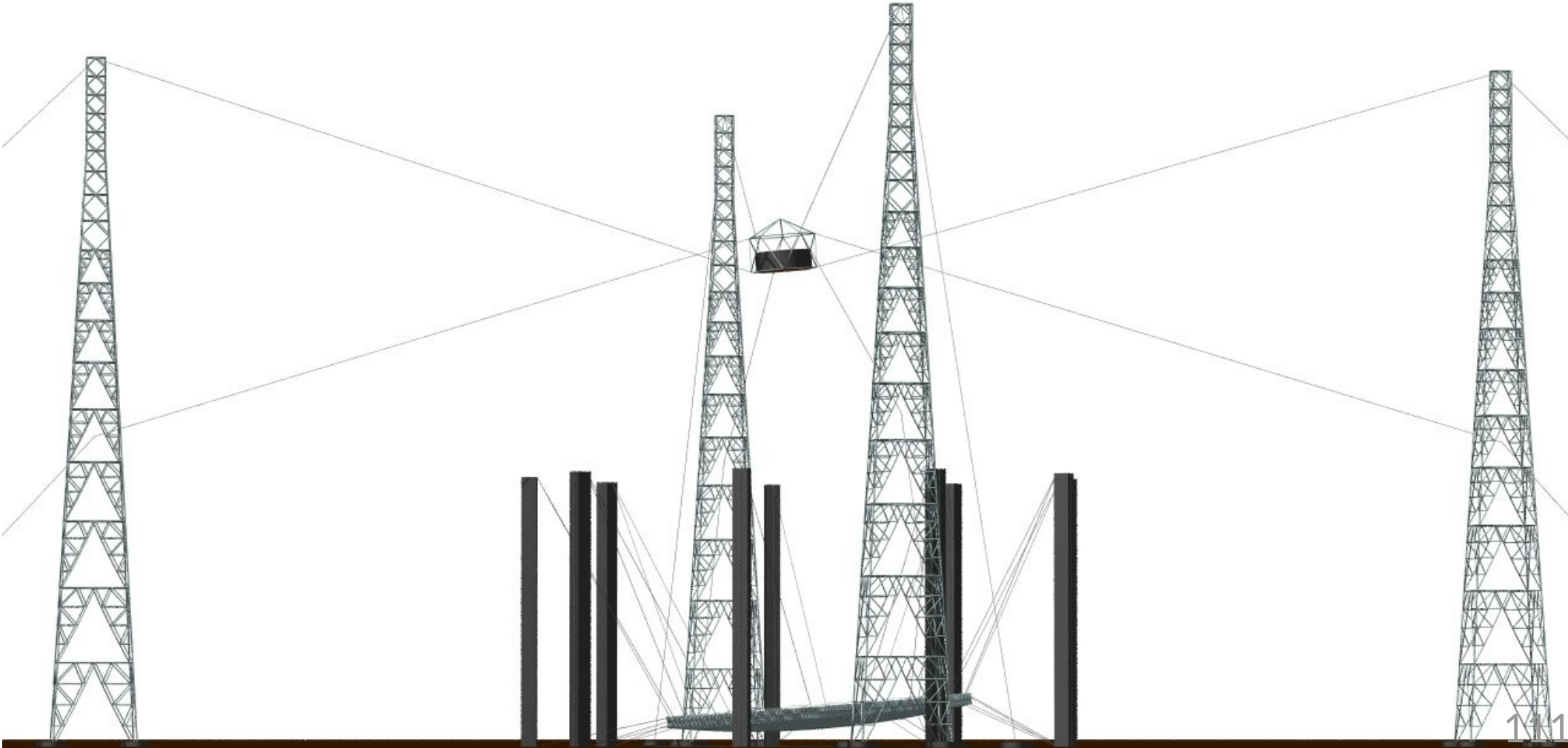

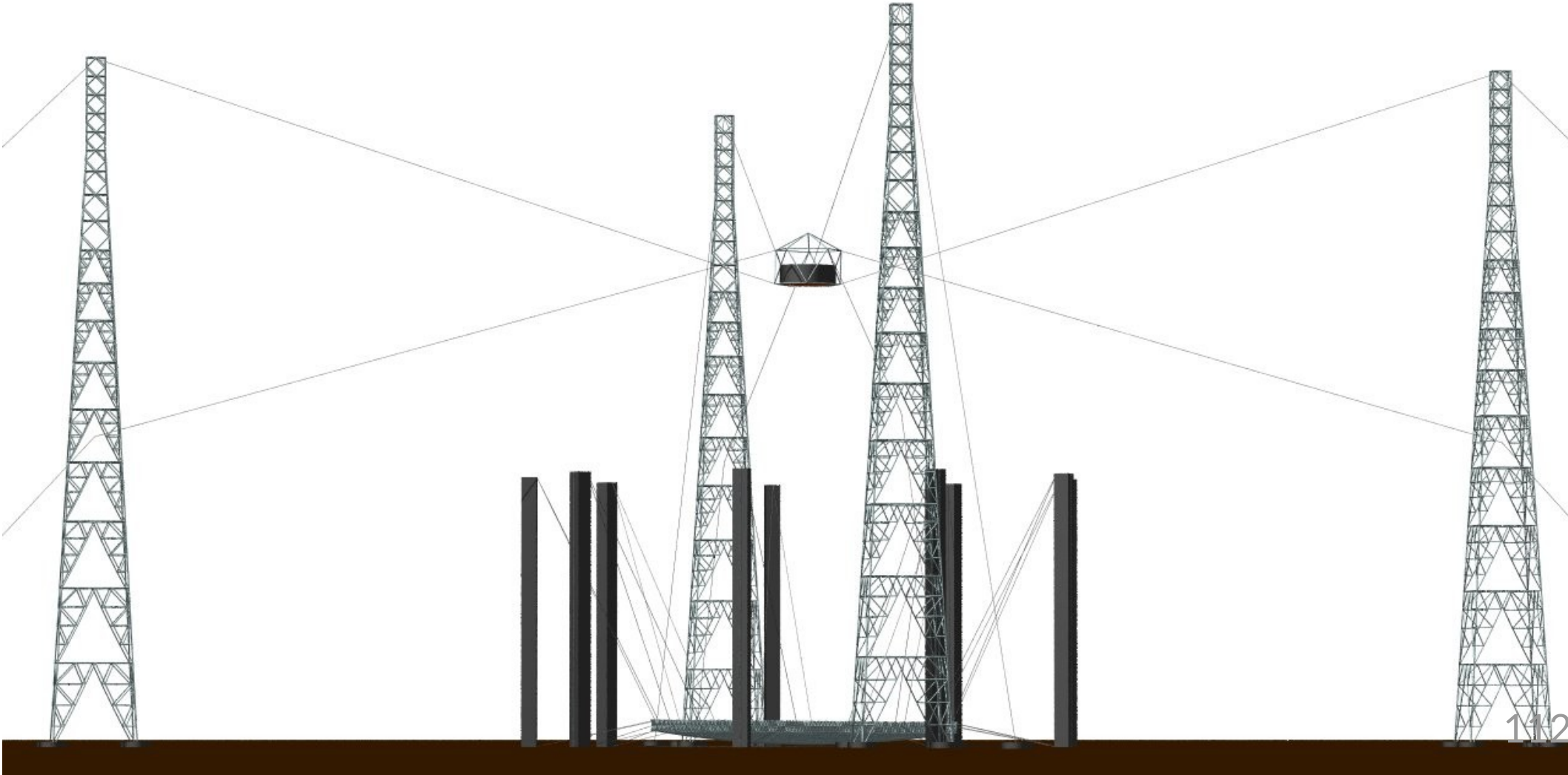

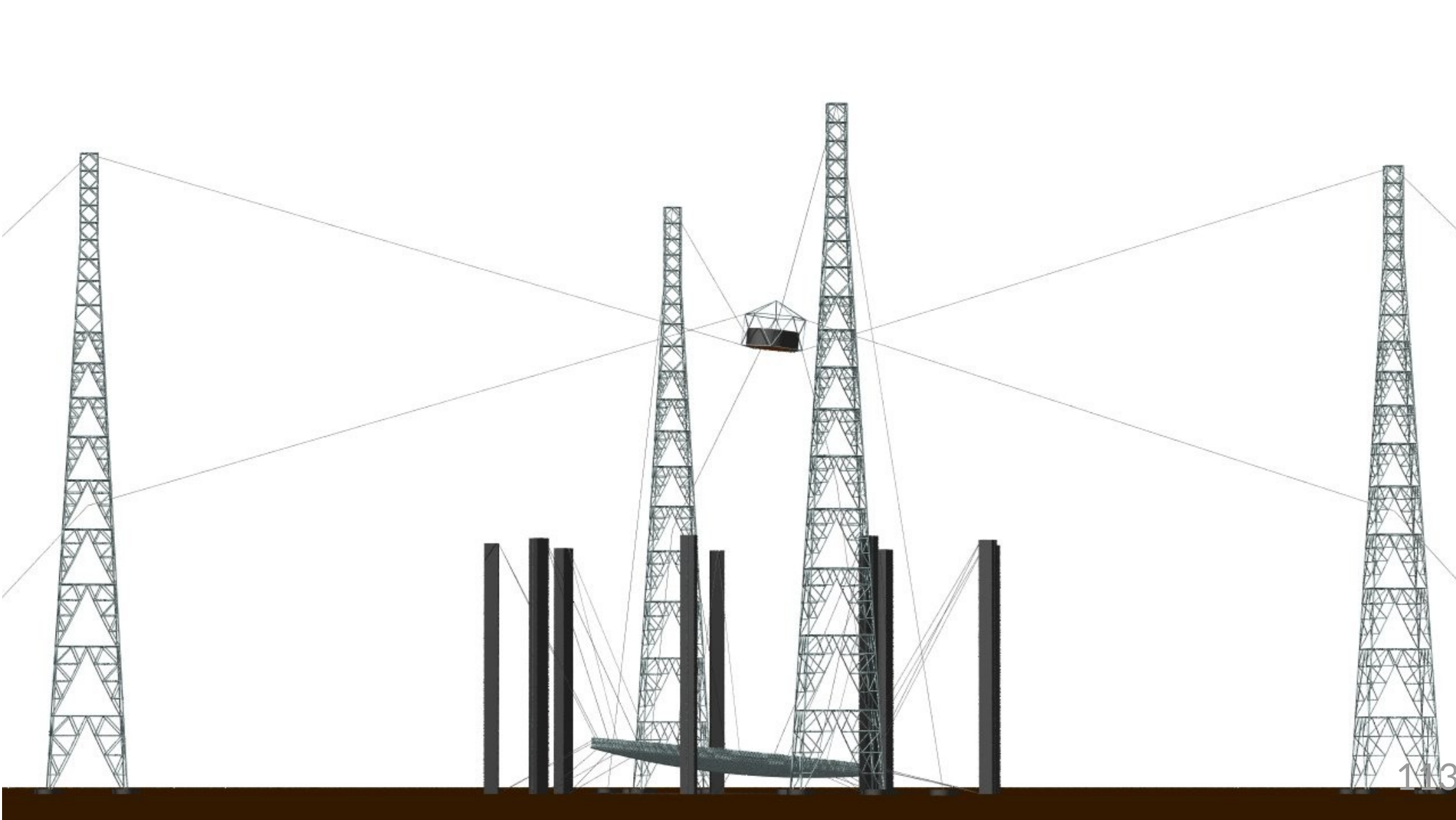

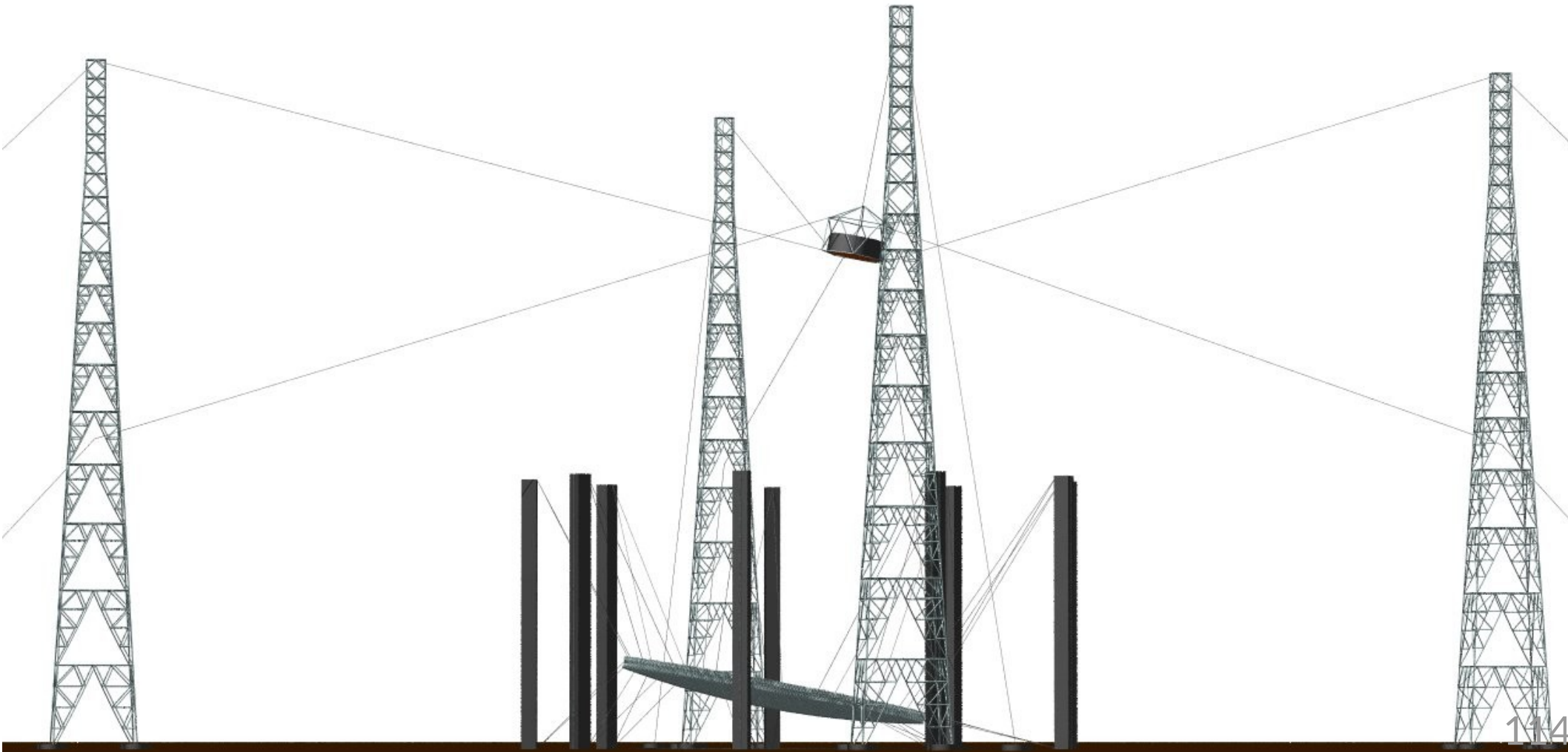

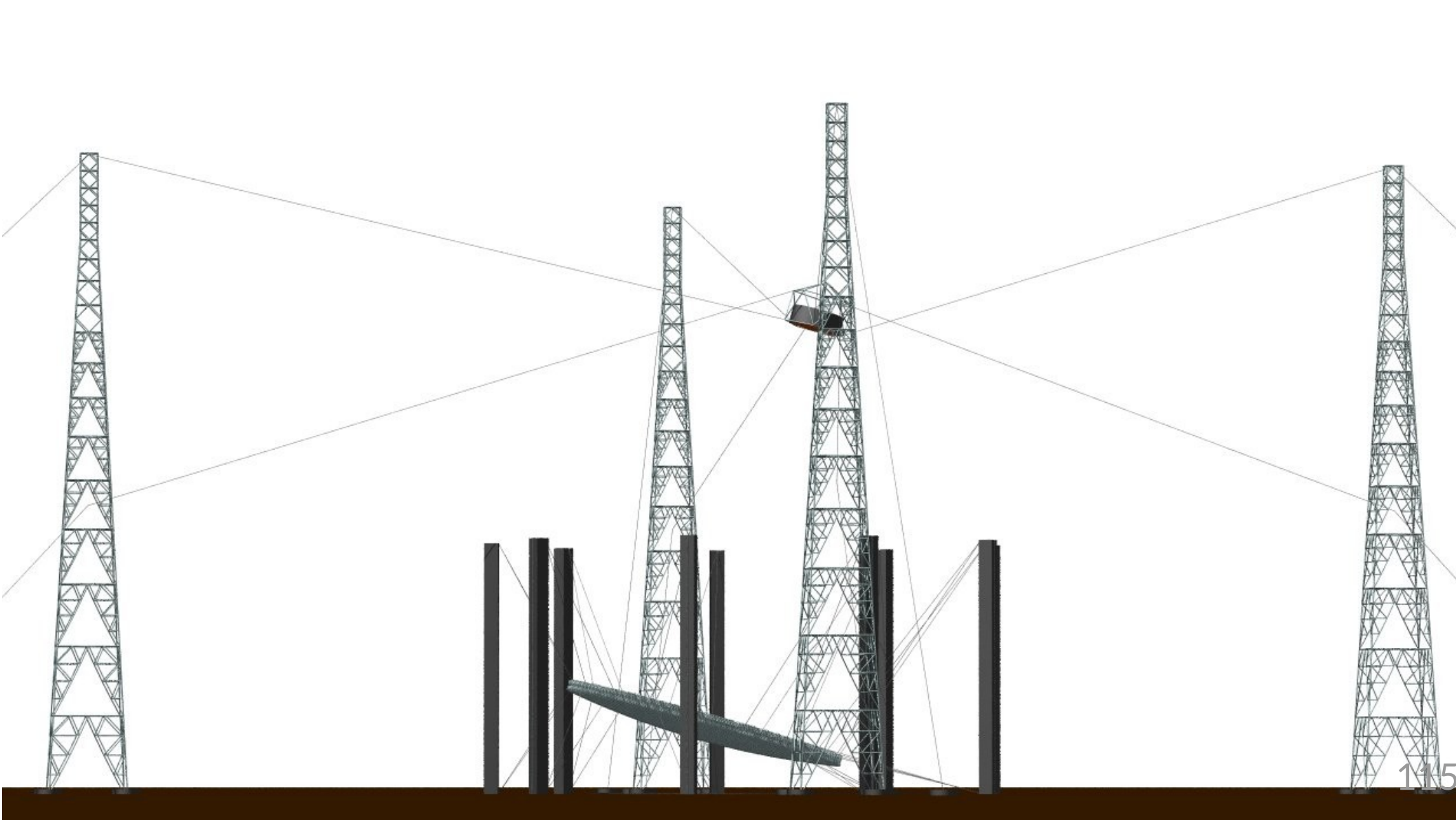

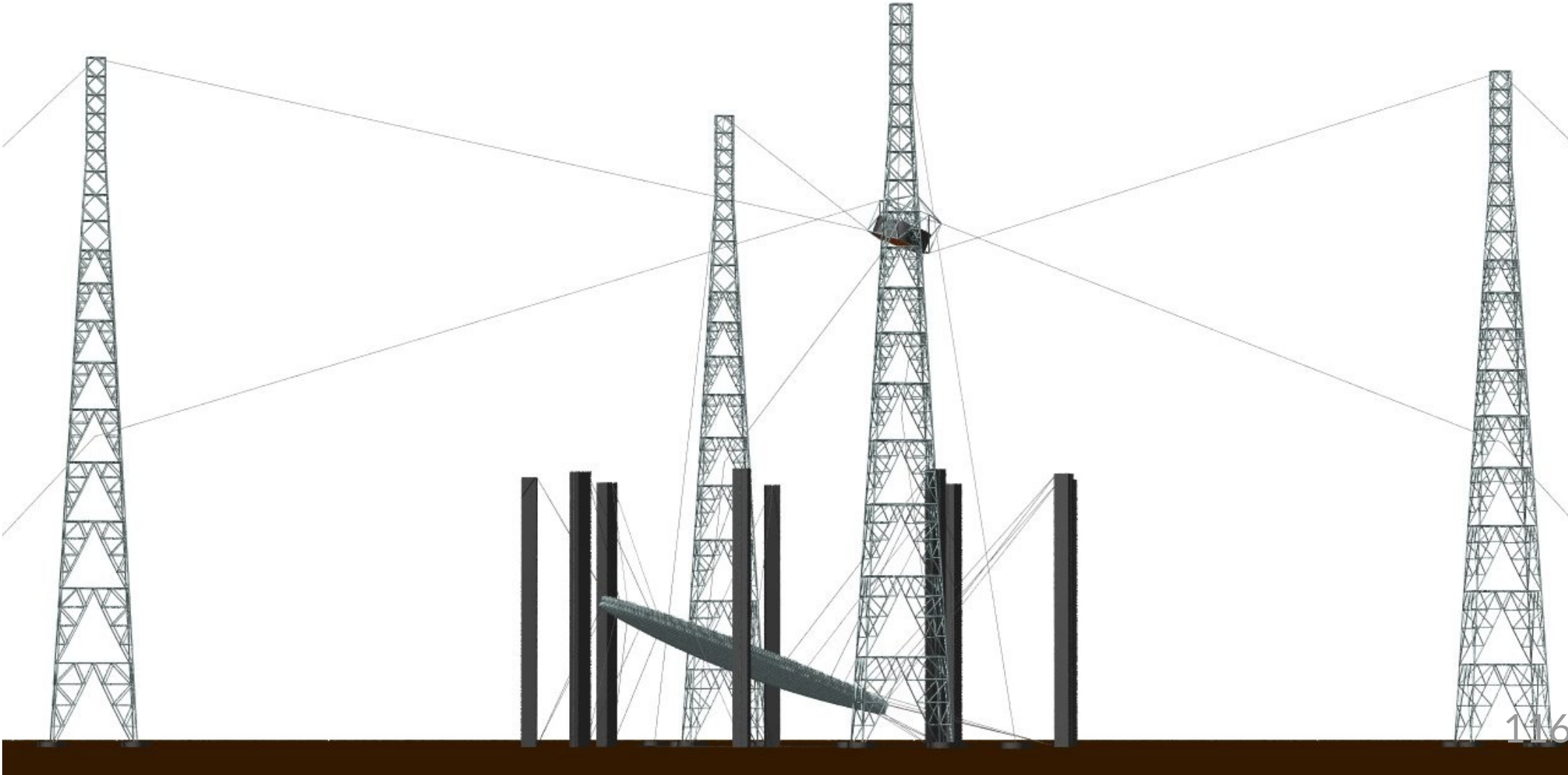

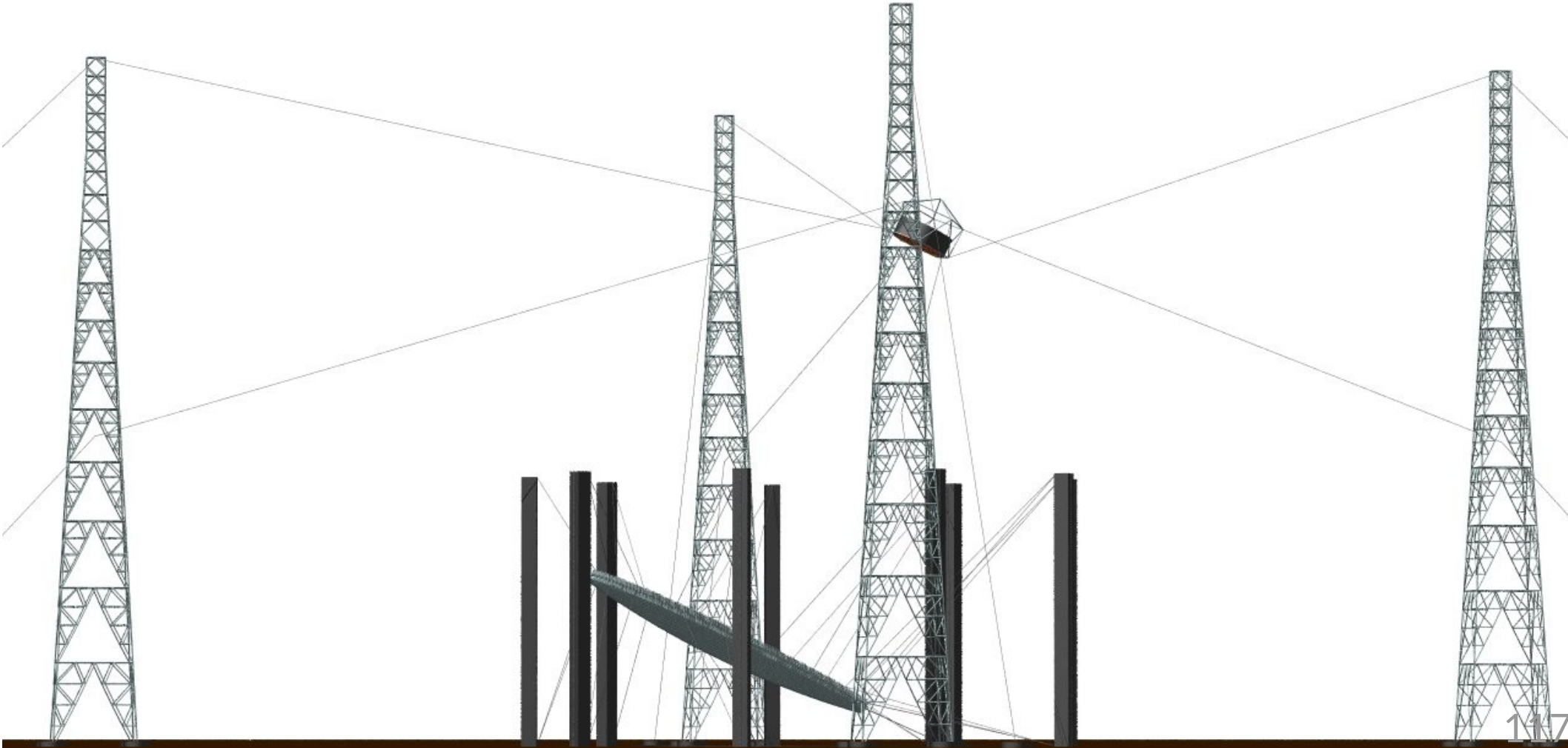

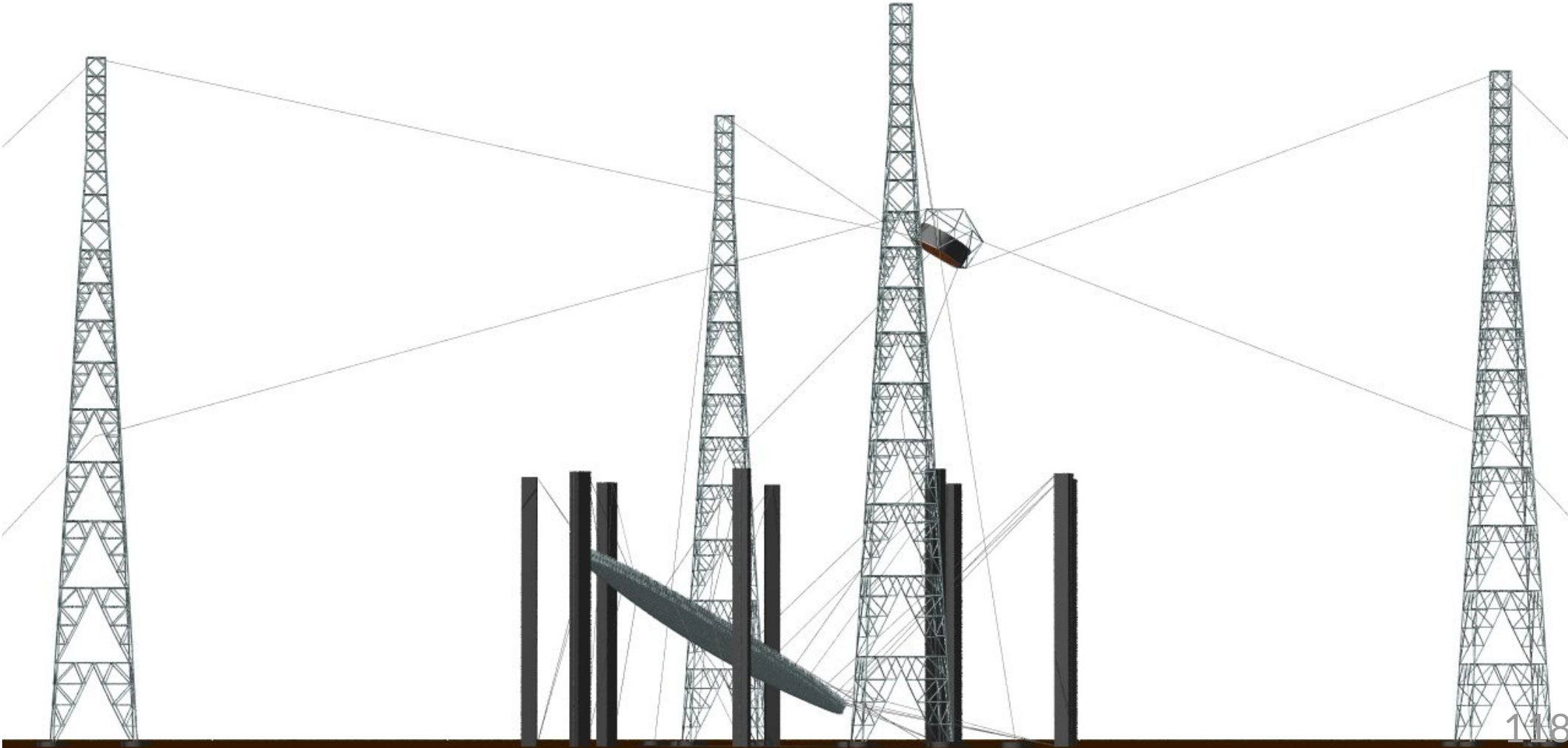

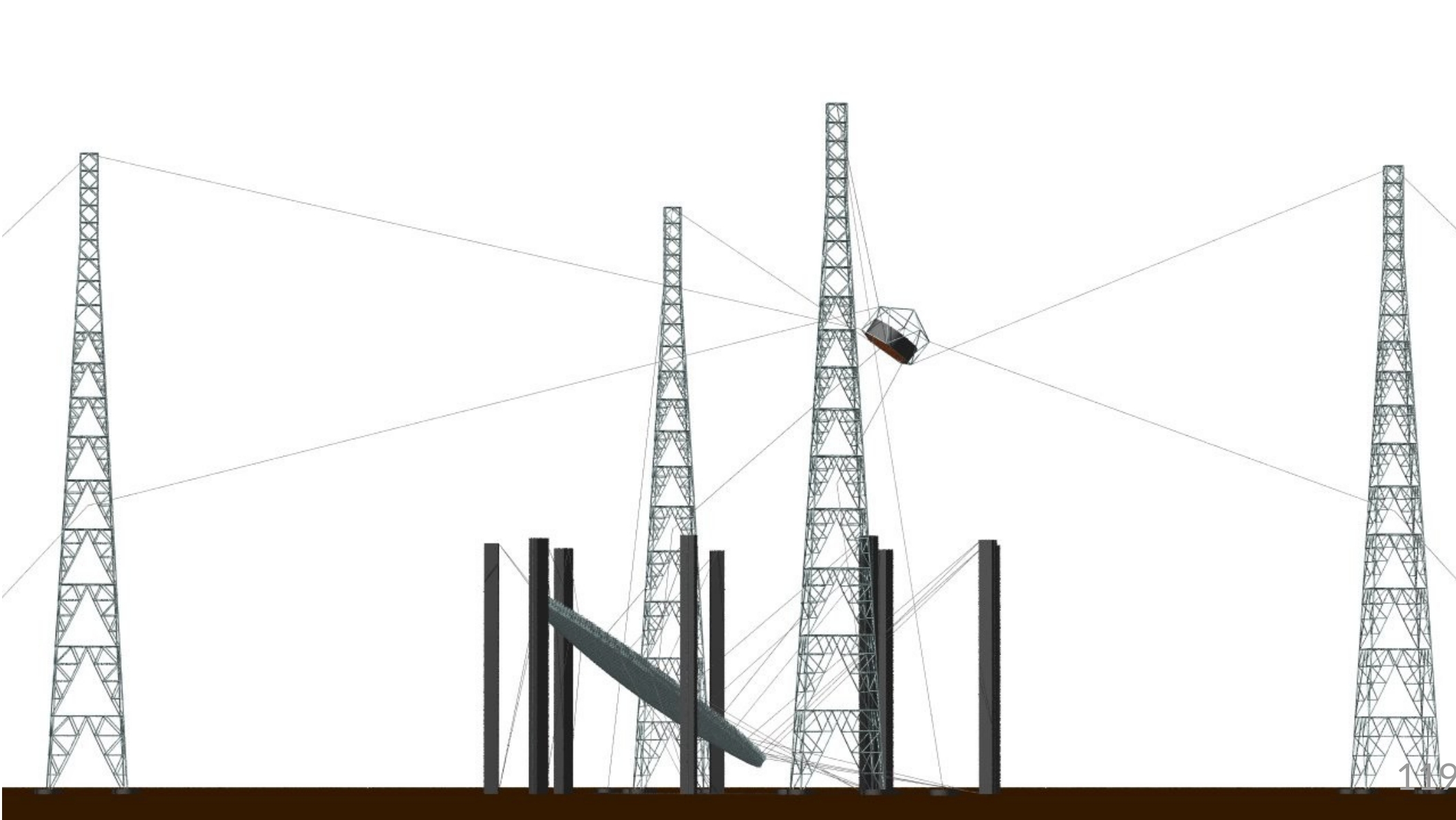

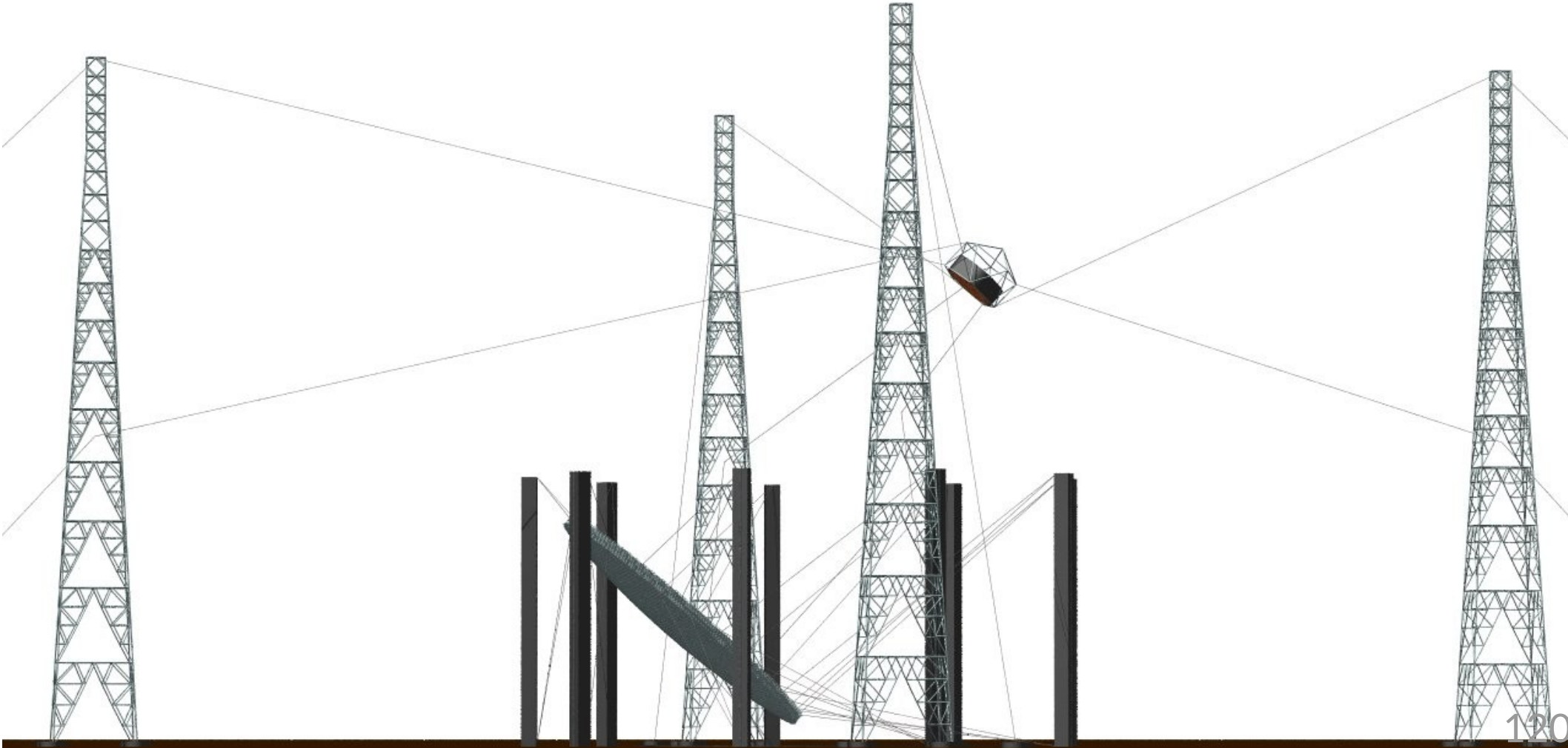

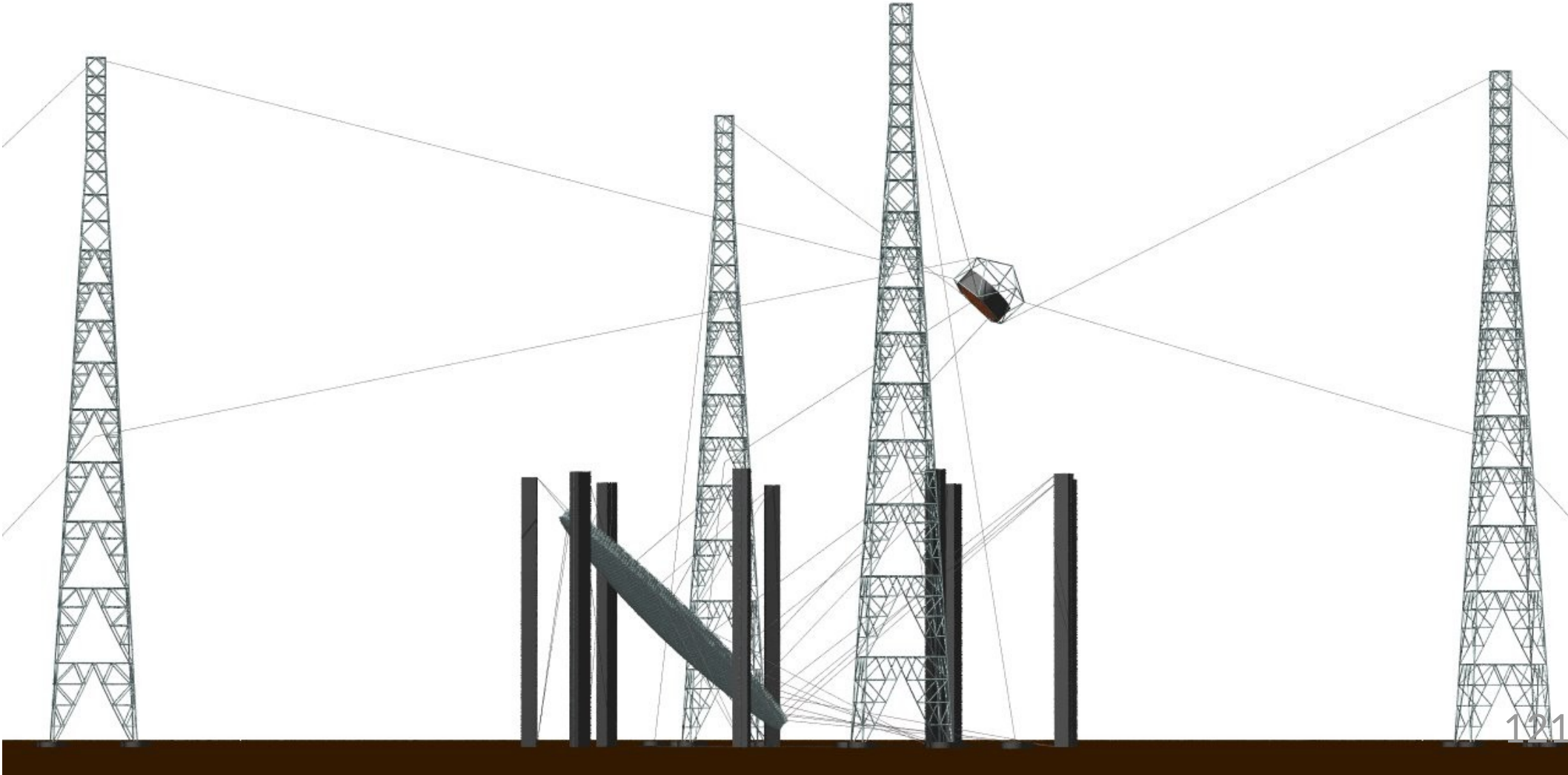

Phantom-Source

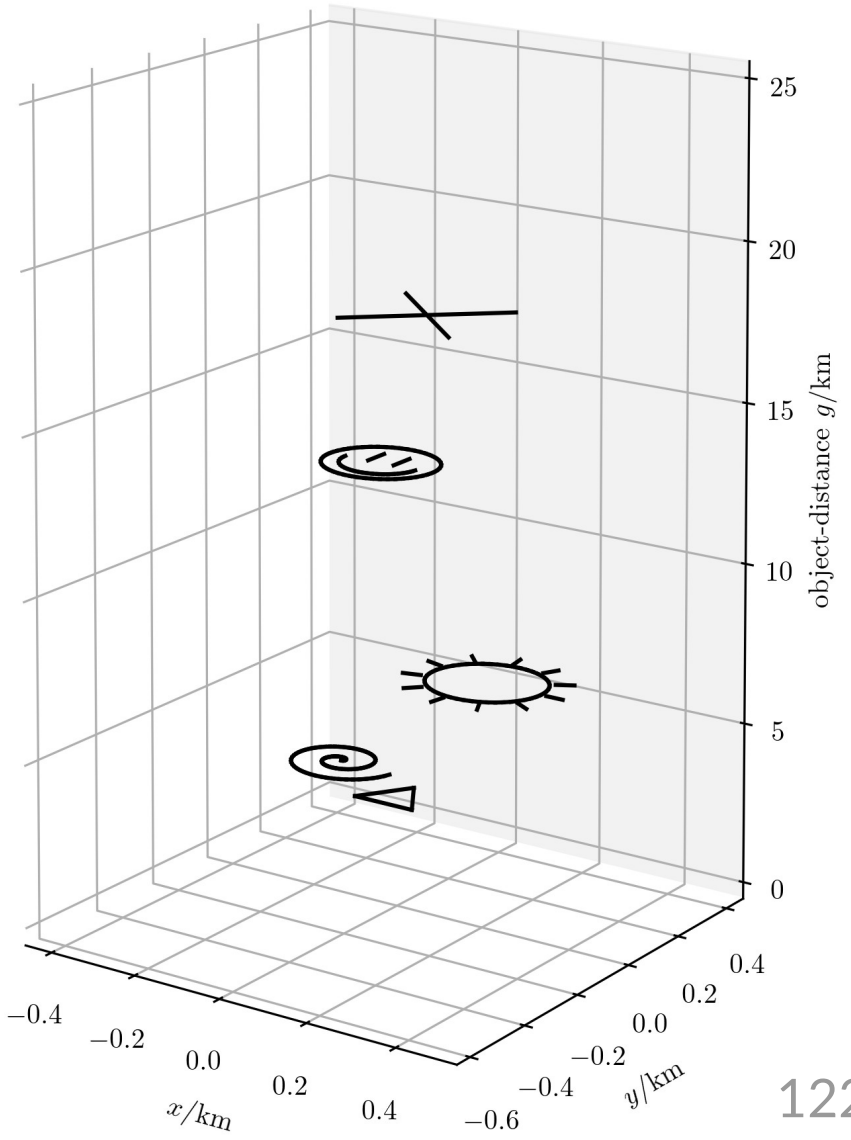

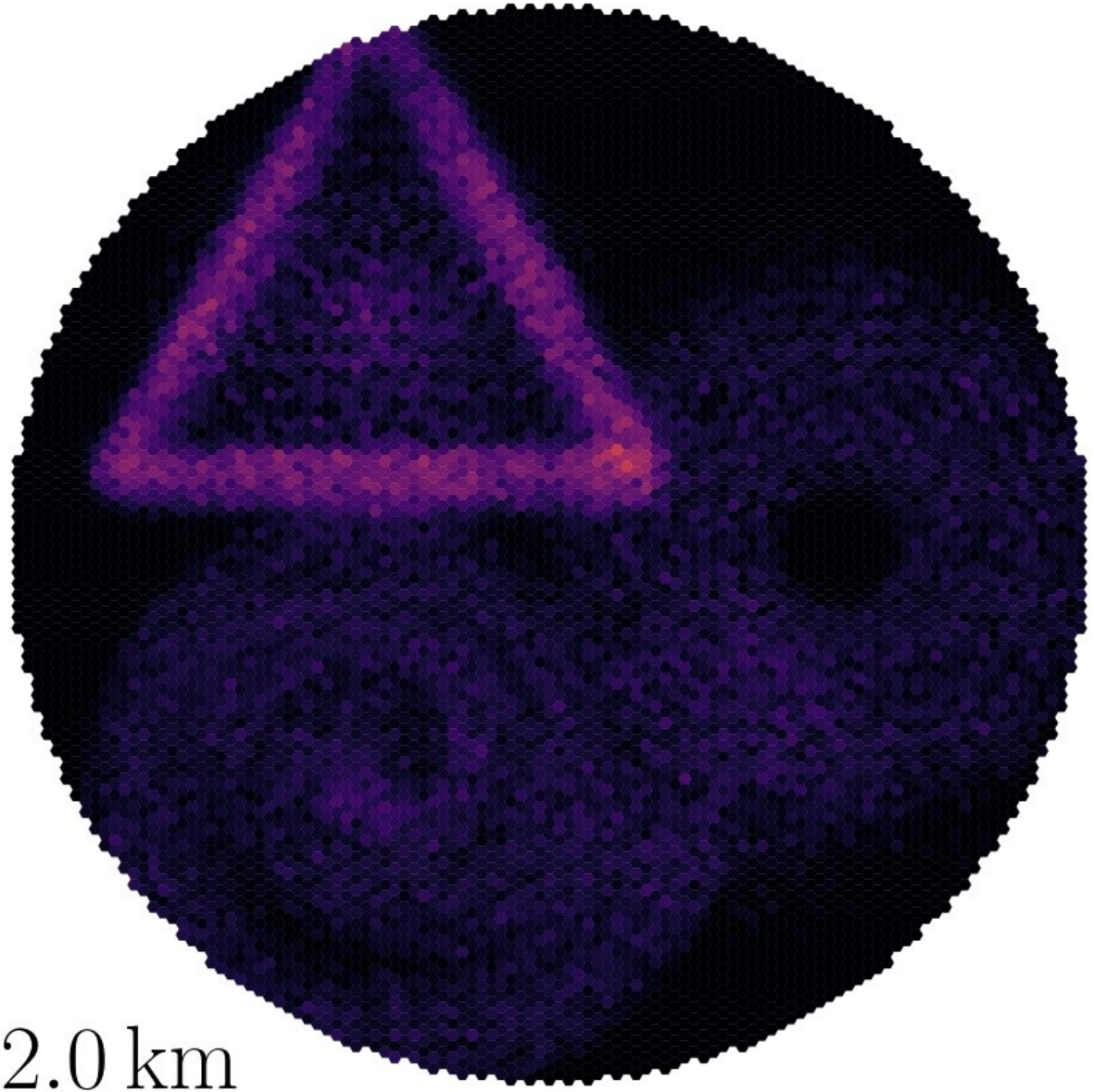

2.0 km

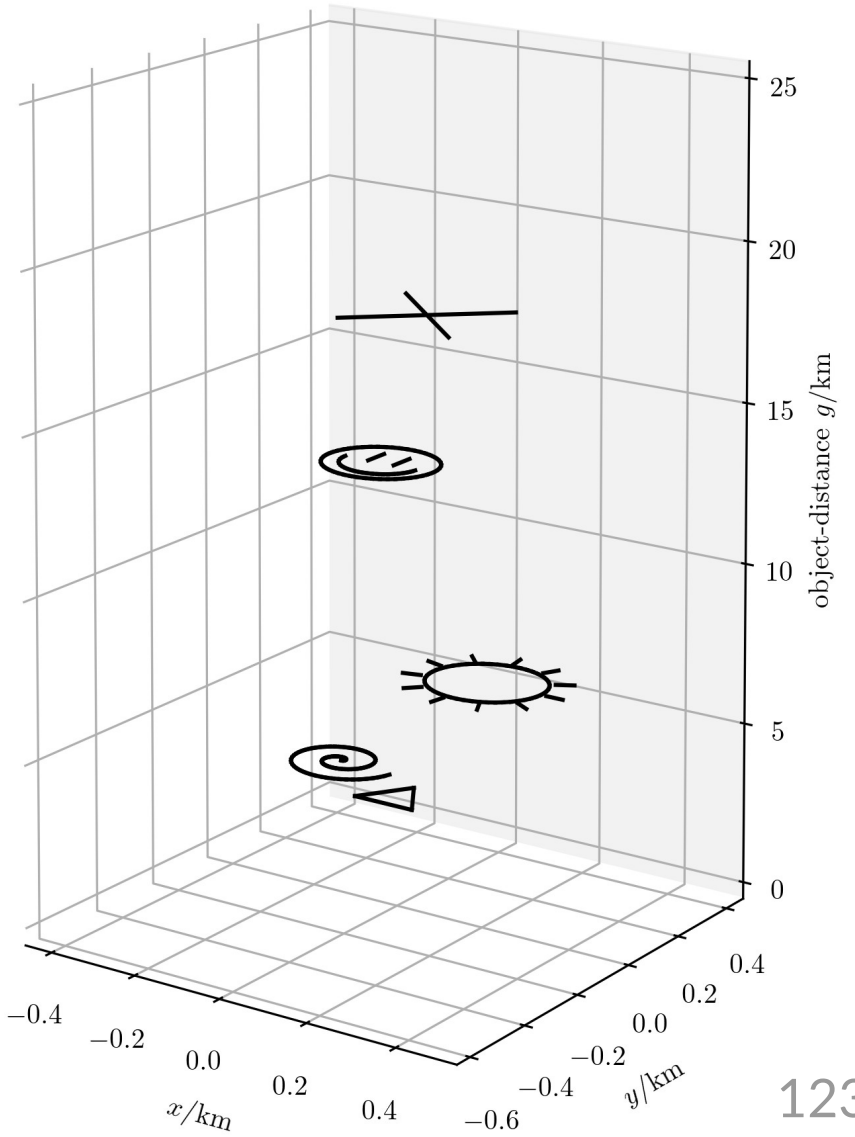
25
20
15
10
5
0
object-distance g/km
−0.4
−0.2
0.0
0.2
0.4
x/km
0.4
0.2
0.0
−0.2
−0.4
−0.6
y/km

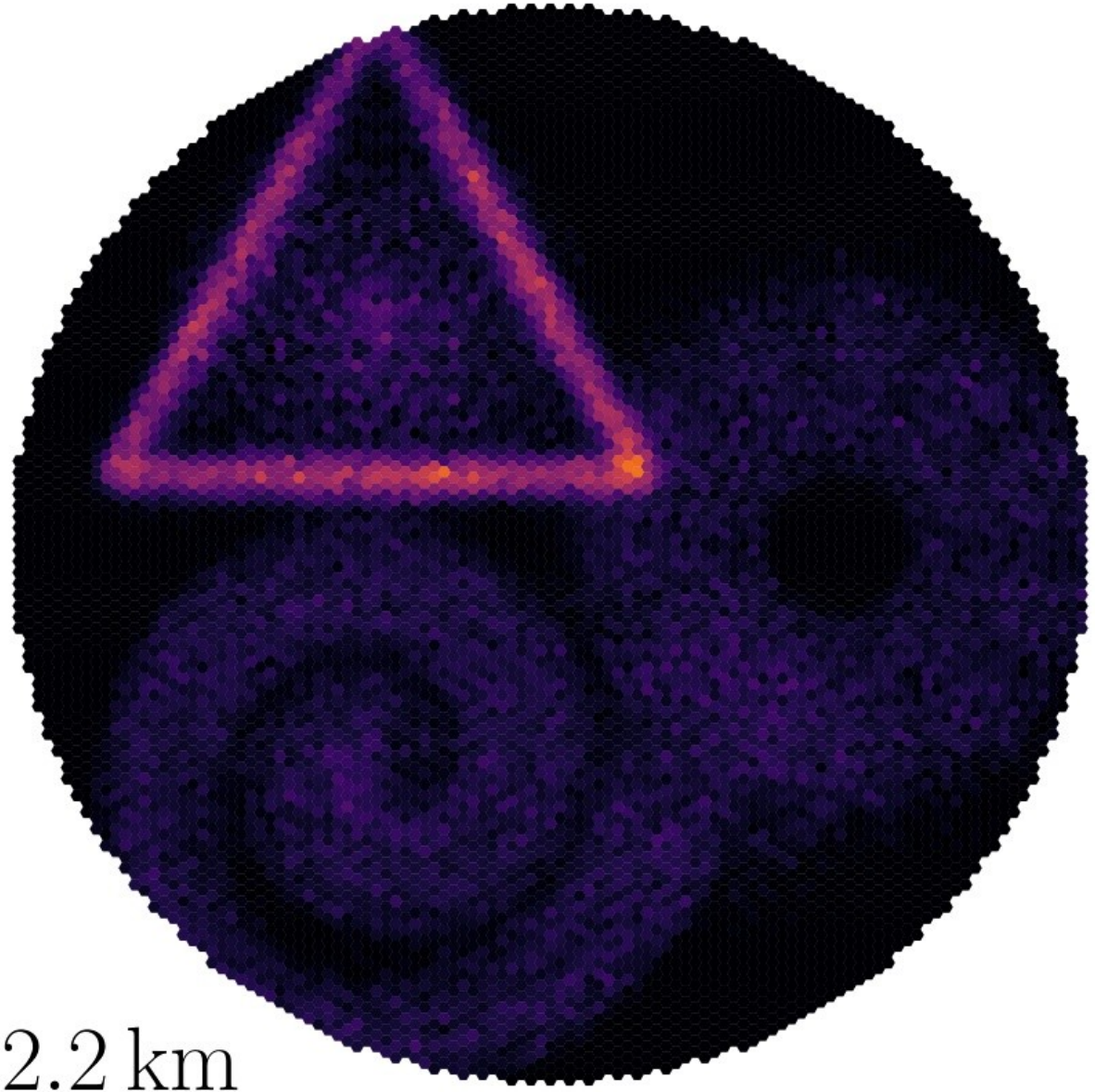

2.2 km

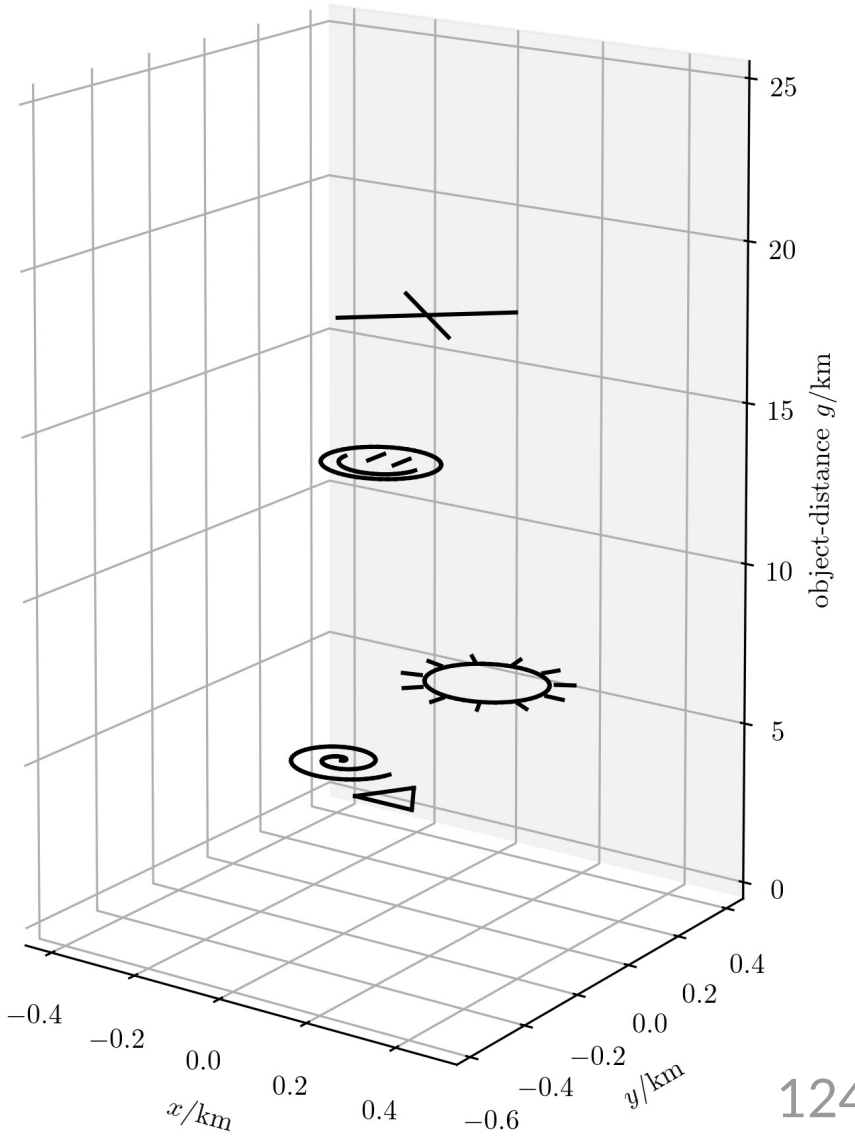
25
20
15
10
5
0
object-distance g/km
−0.4
−0.2
0.0
0.2
0.4
x/km
0.4
0.2
0.0
−0.2
−0.4
−0.6
y/km

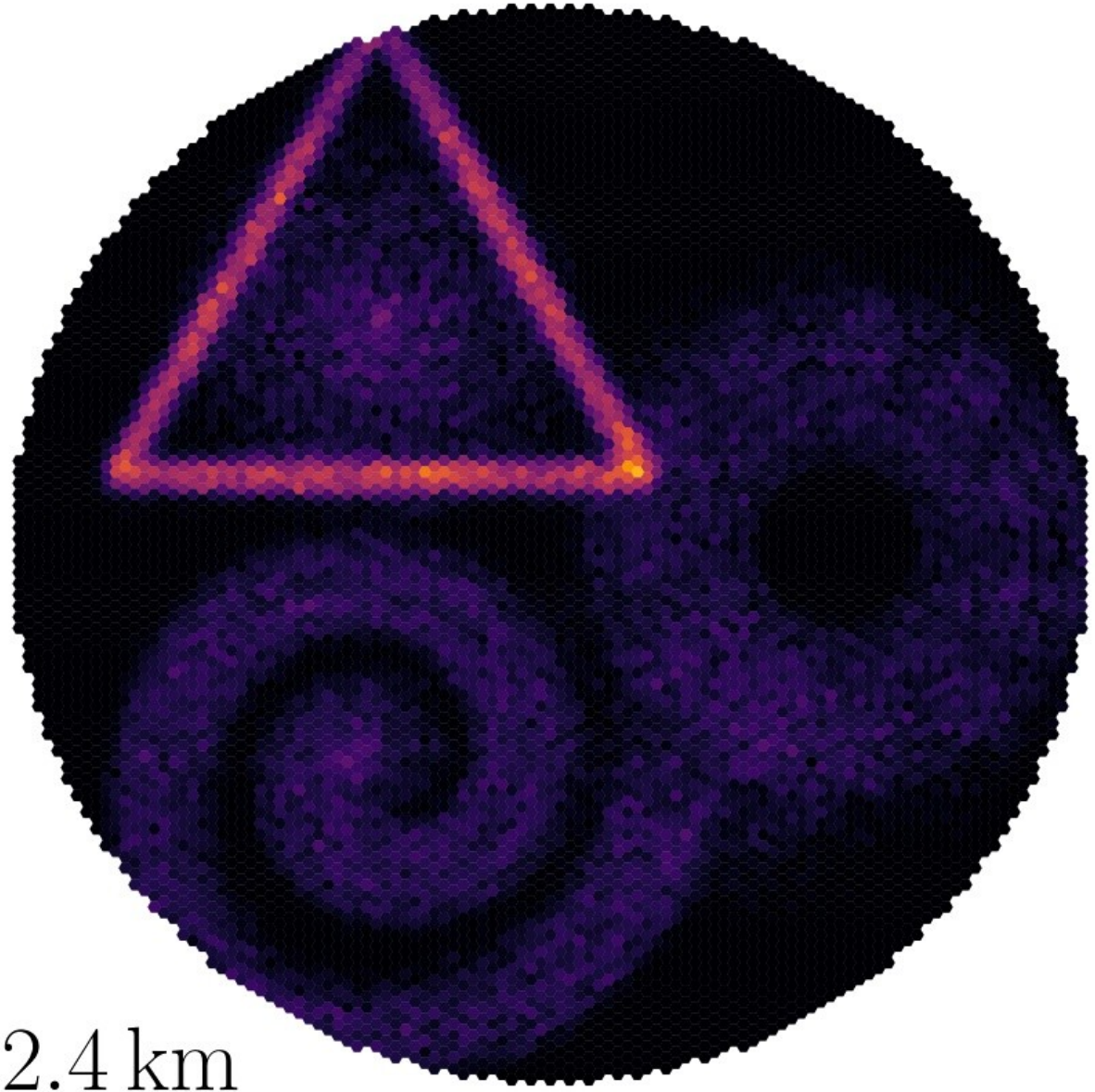

2.4 km

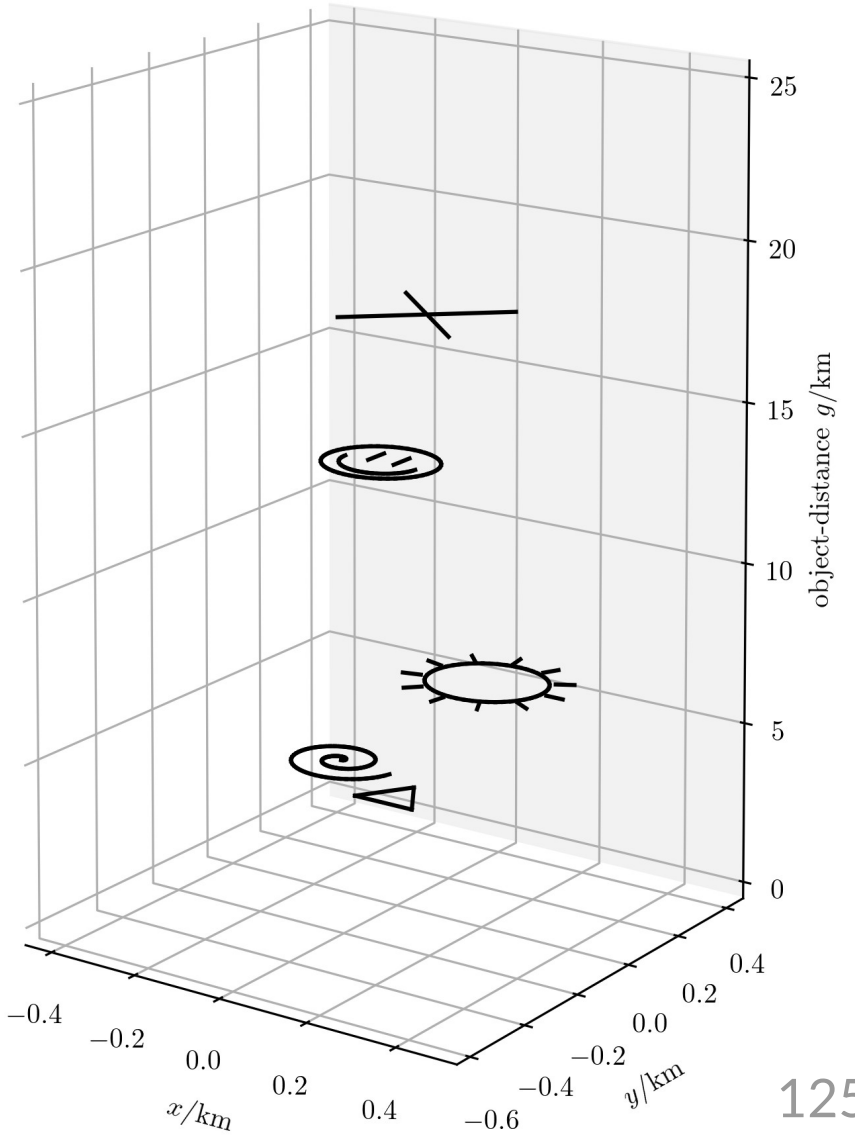
25
20
15
10
5
0
object-distance g/km
−0.4
−0.2
0.0
0.2
0.4
x/km
0.4
0.2
0.0
−0.2
−0.4
−0.6
y/km

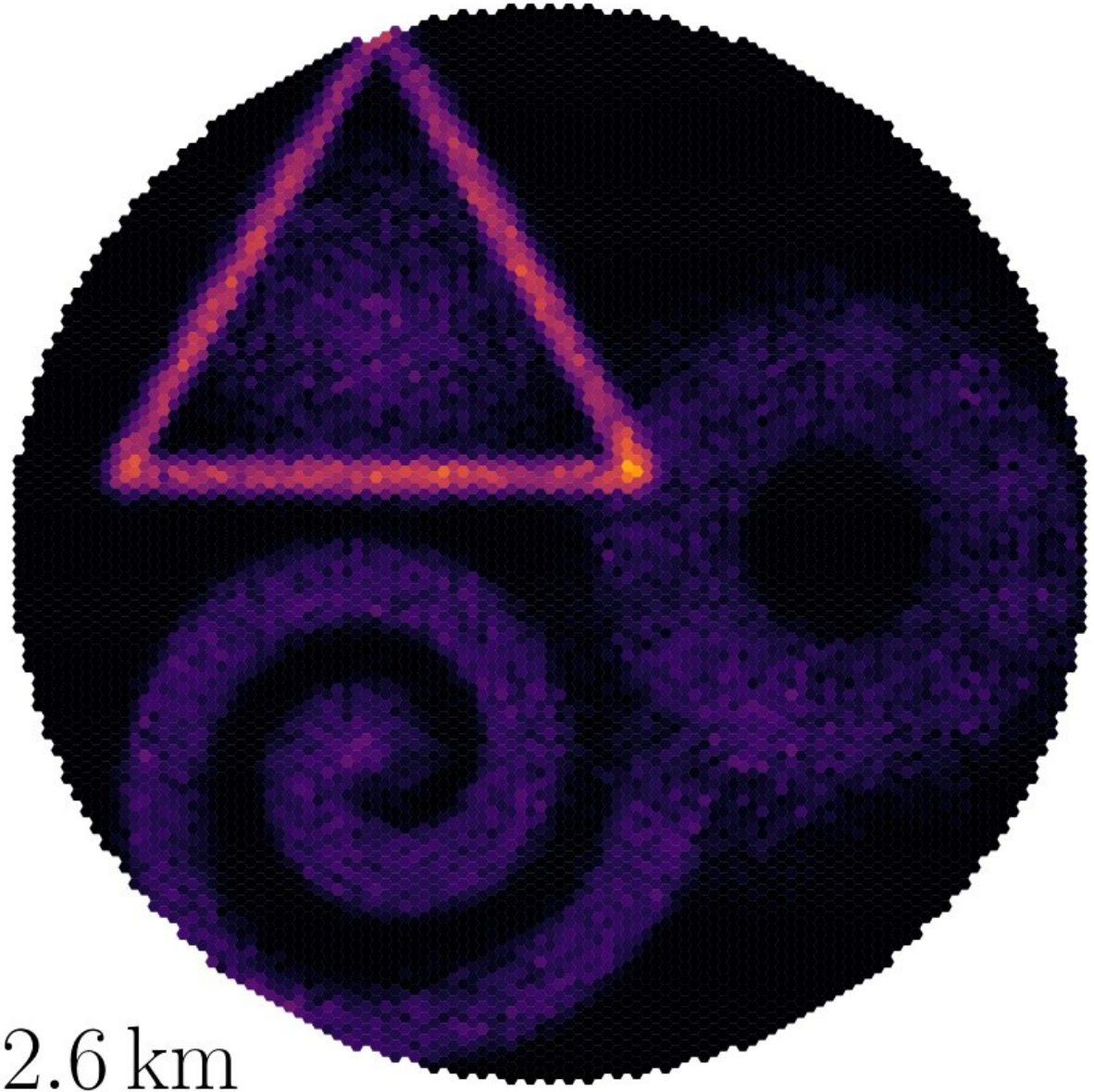

2.6 km

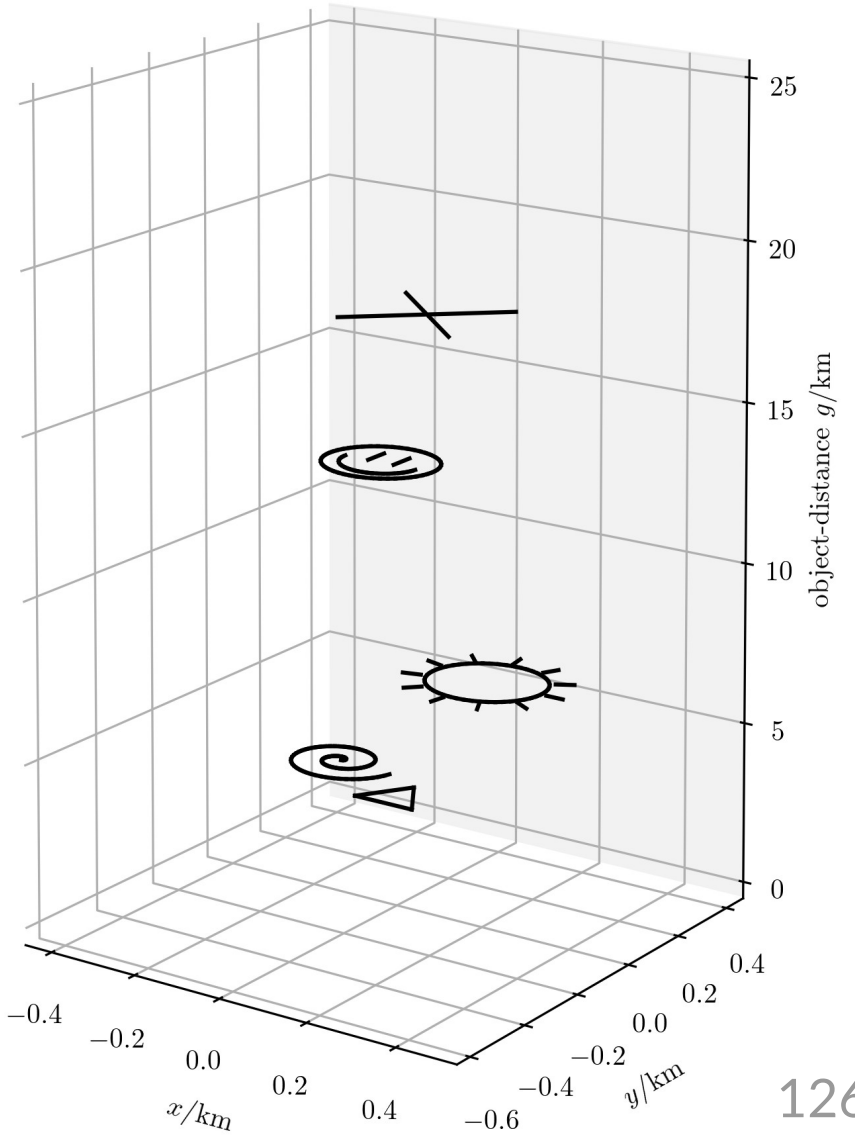
25
20
15
10
5
0
object-distance g/km
−0.4
−0.2
0.0
0.2
0.4
x/km
0.4
0.2
0.0
−0.2
−0.4
−0.6
y/km

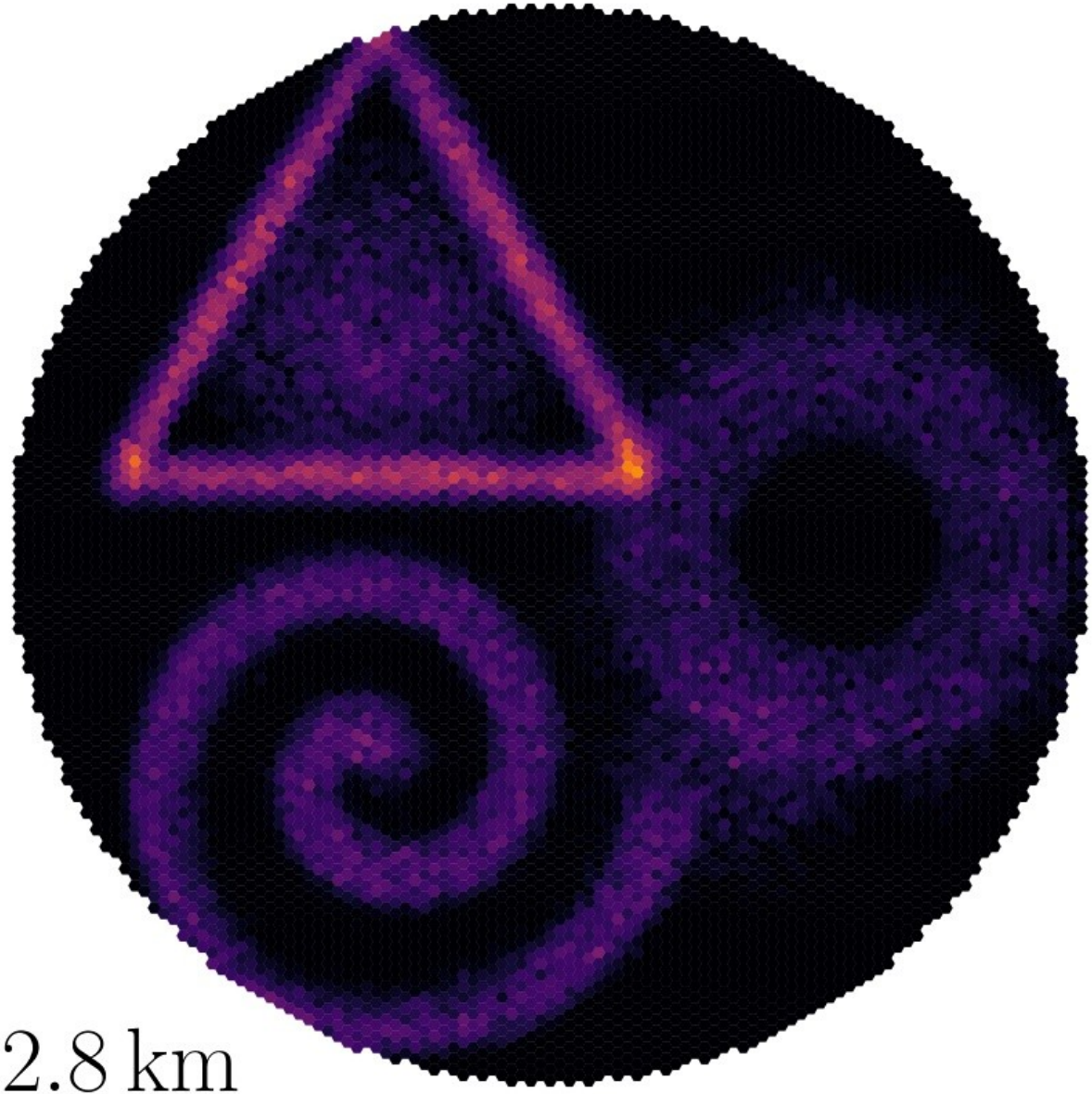

2.8 km

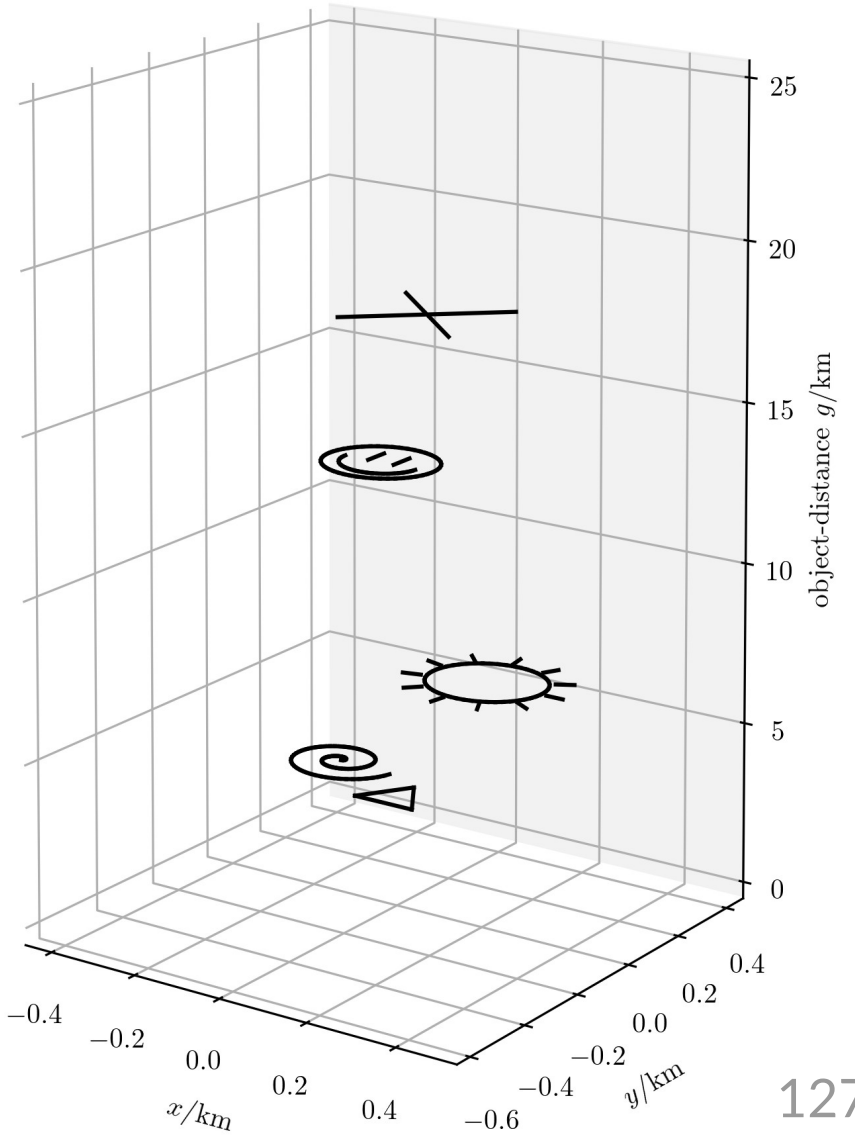
25
20
15
10
5
0
object-distance g/km
−0.4
−0.2
0.0
0.2
0.4
x/km
0.4
0.2
0.0
−0.2
−0.4
−0.6
y/km

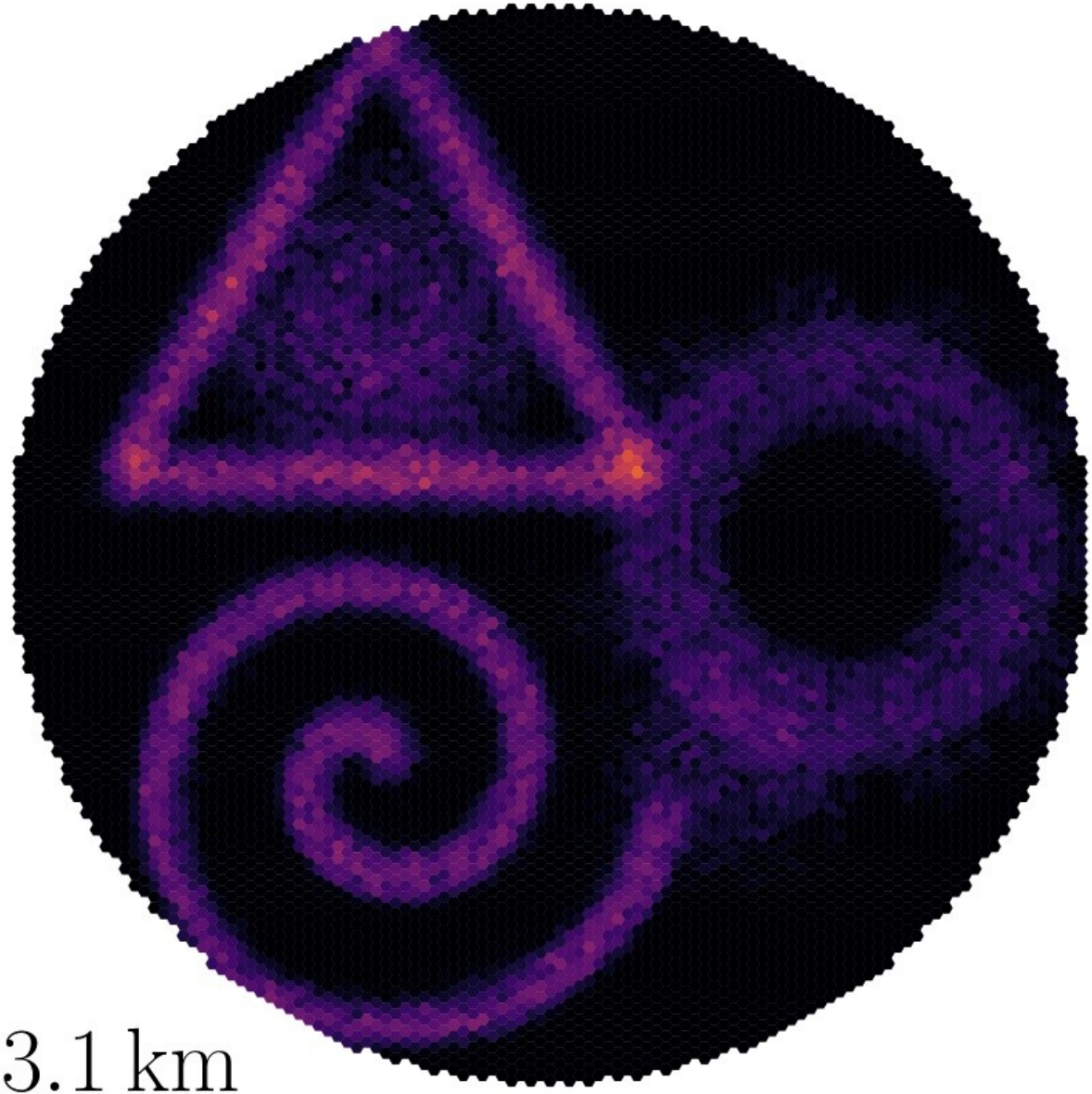

3.1 km

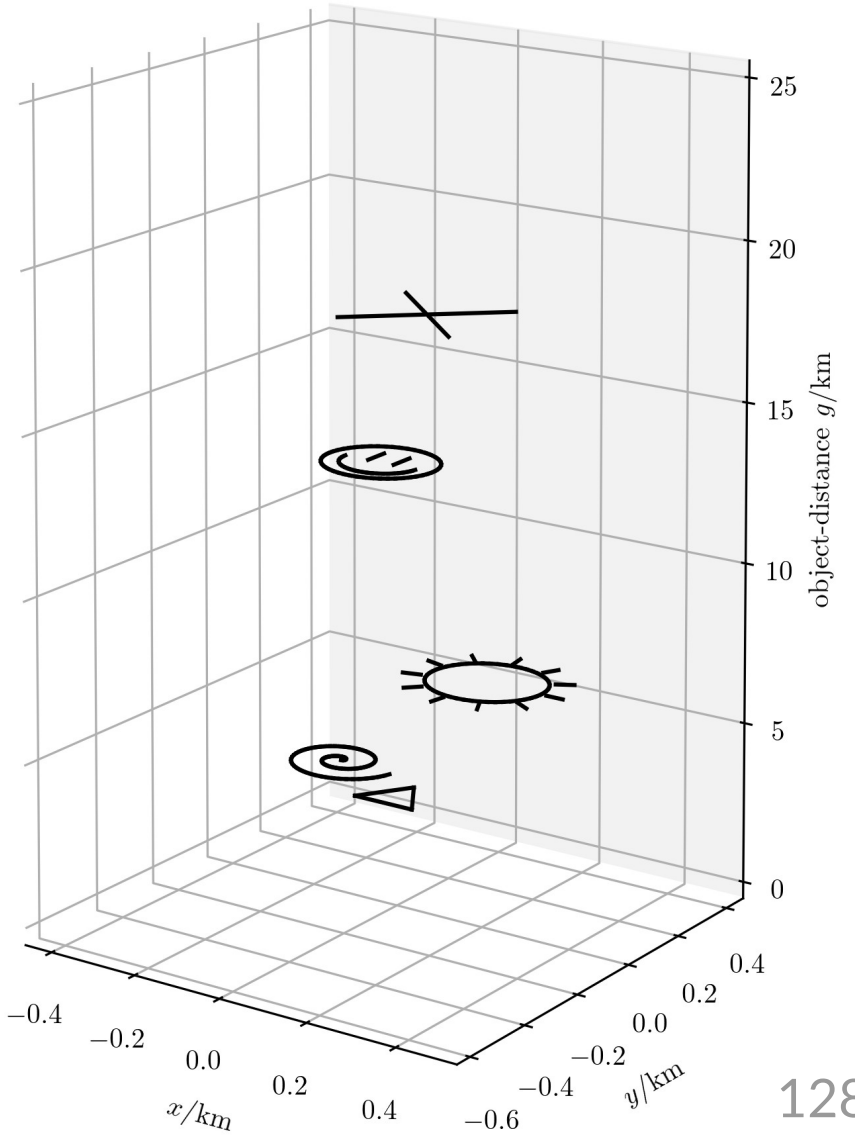
25
20
15
10
5
0
object-distance g/km
−0.4
−0.2
0.0
0.2
0.4
x/km
0.4
0.2
0.0
−0.2
−0.4
−0.6
y/km

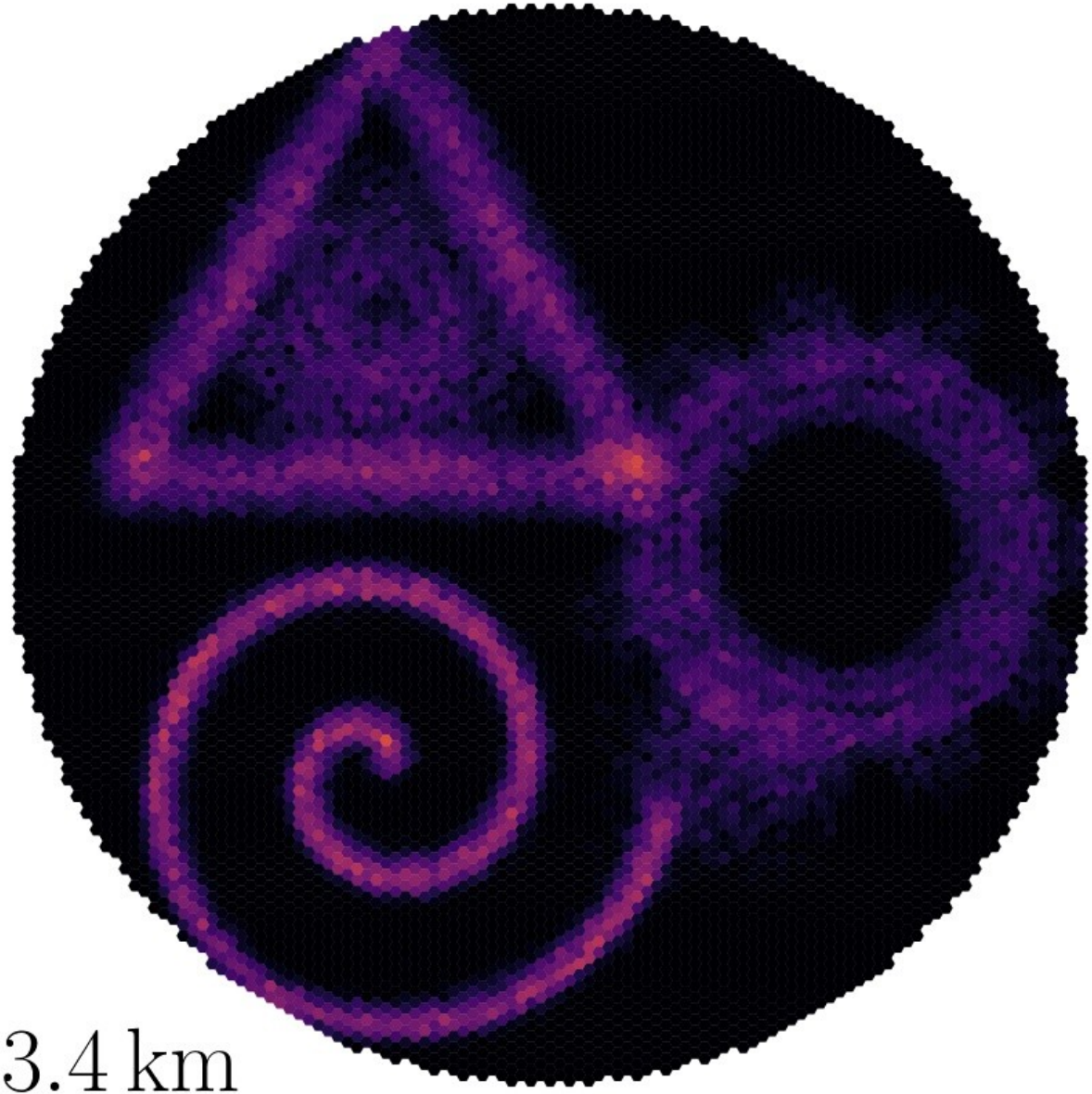

3.4 km

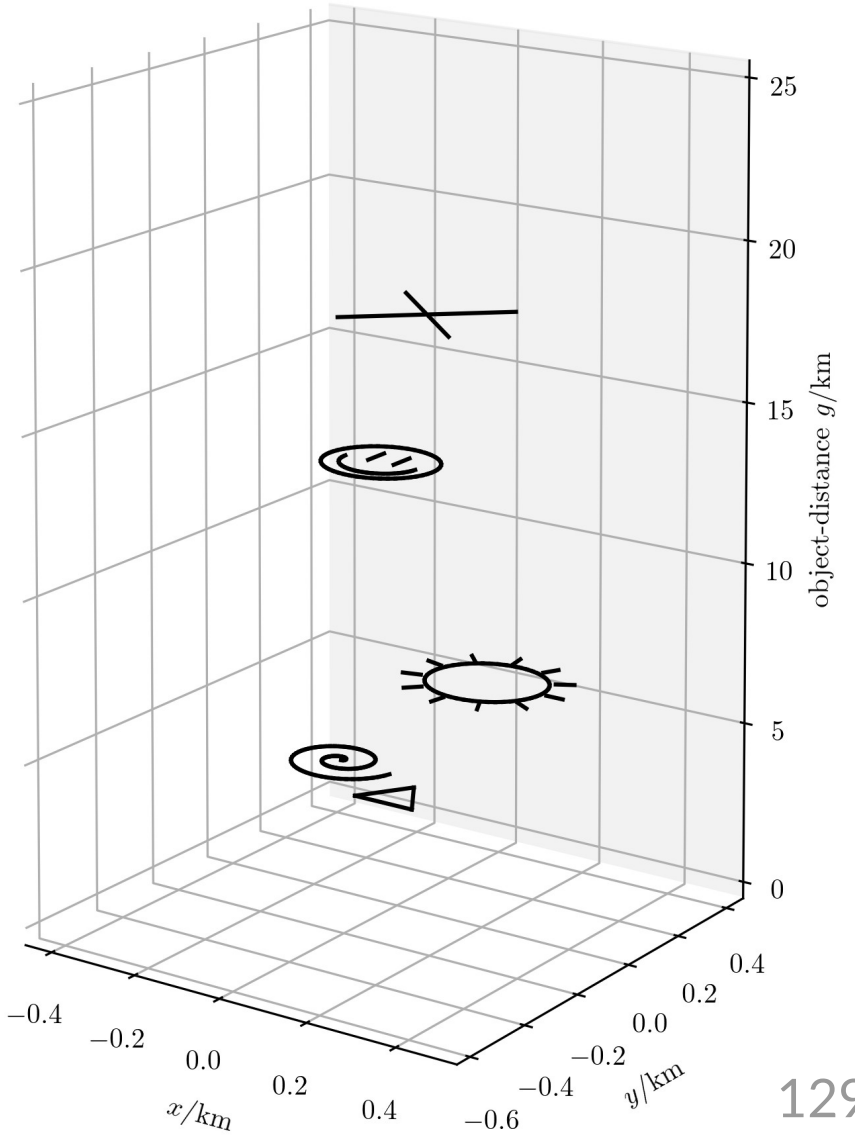
25
20
15
10
5
0
object-distance g/km
−0.4
−0.2
0.0
0.2
0.4
x/km
0.4
0.2
0.0
−0.2
−0.4
−0.6
y/km

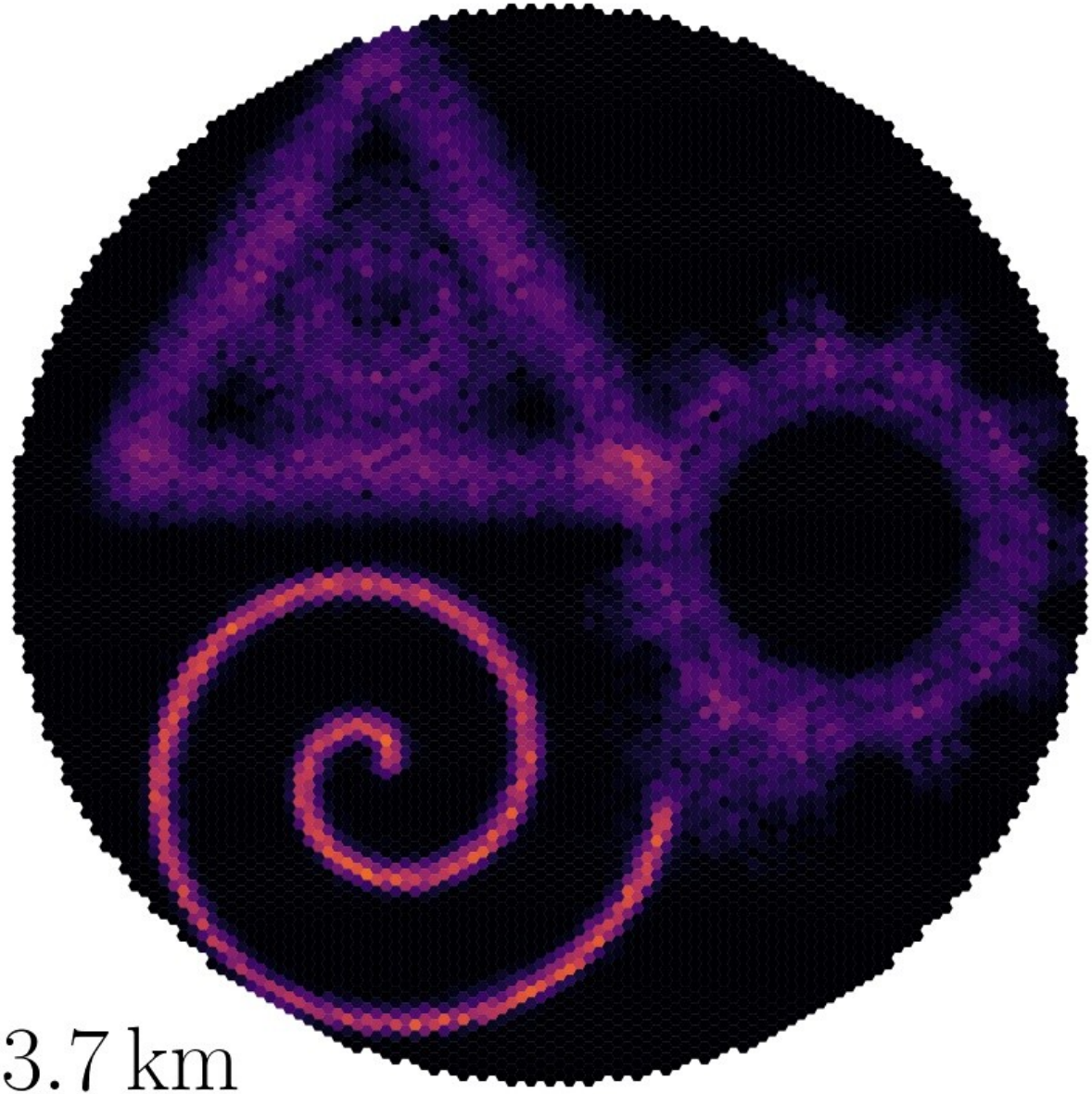

3.7 km

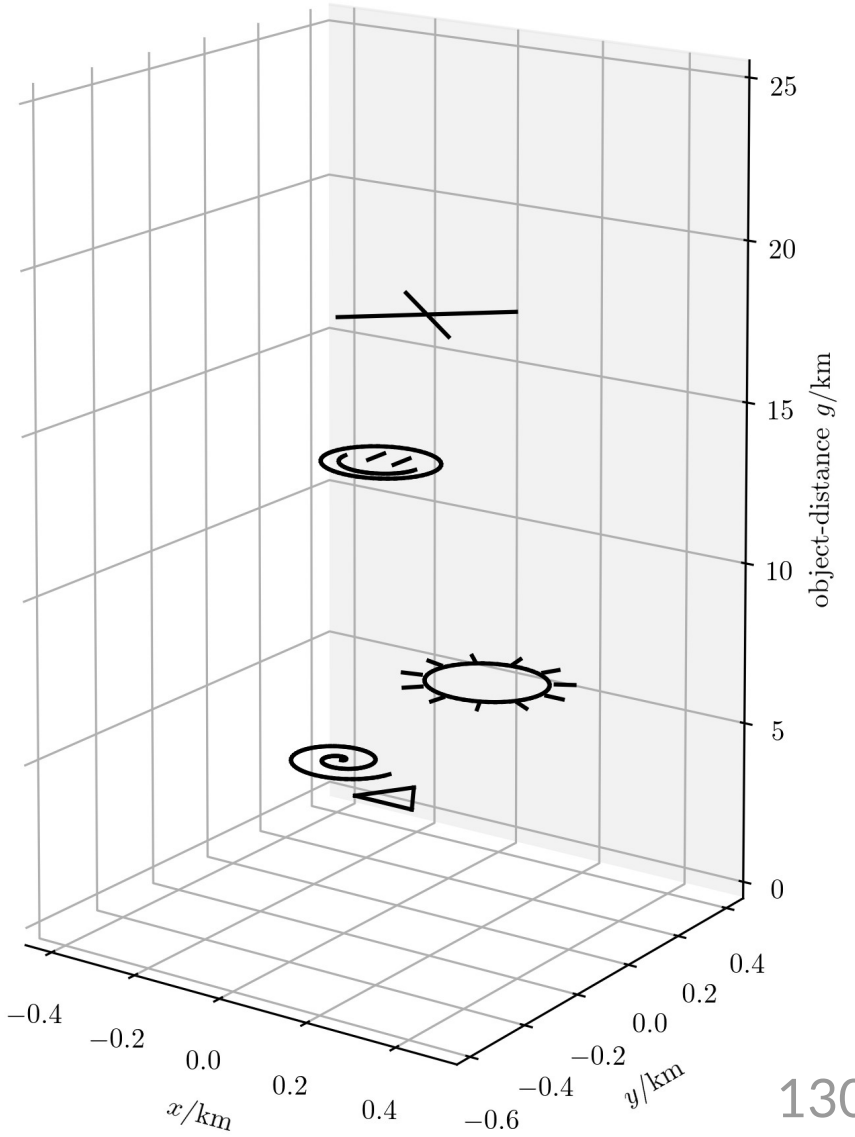
25
20
15
10
5
0
object-distance g/km
−0.4
−0.2
0.0
0.2
0.4
x/km
0.4
0.2
0.0
−0.2
−0.4
−0.6
y/km

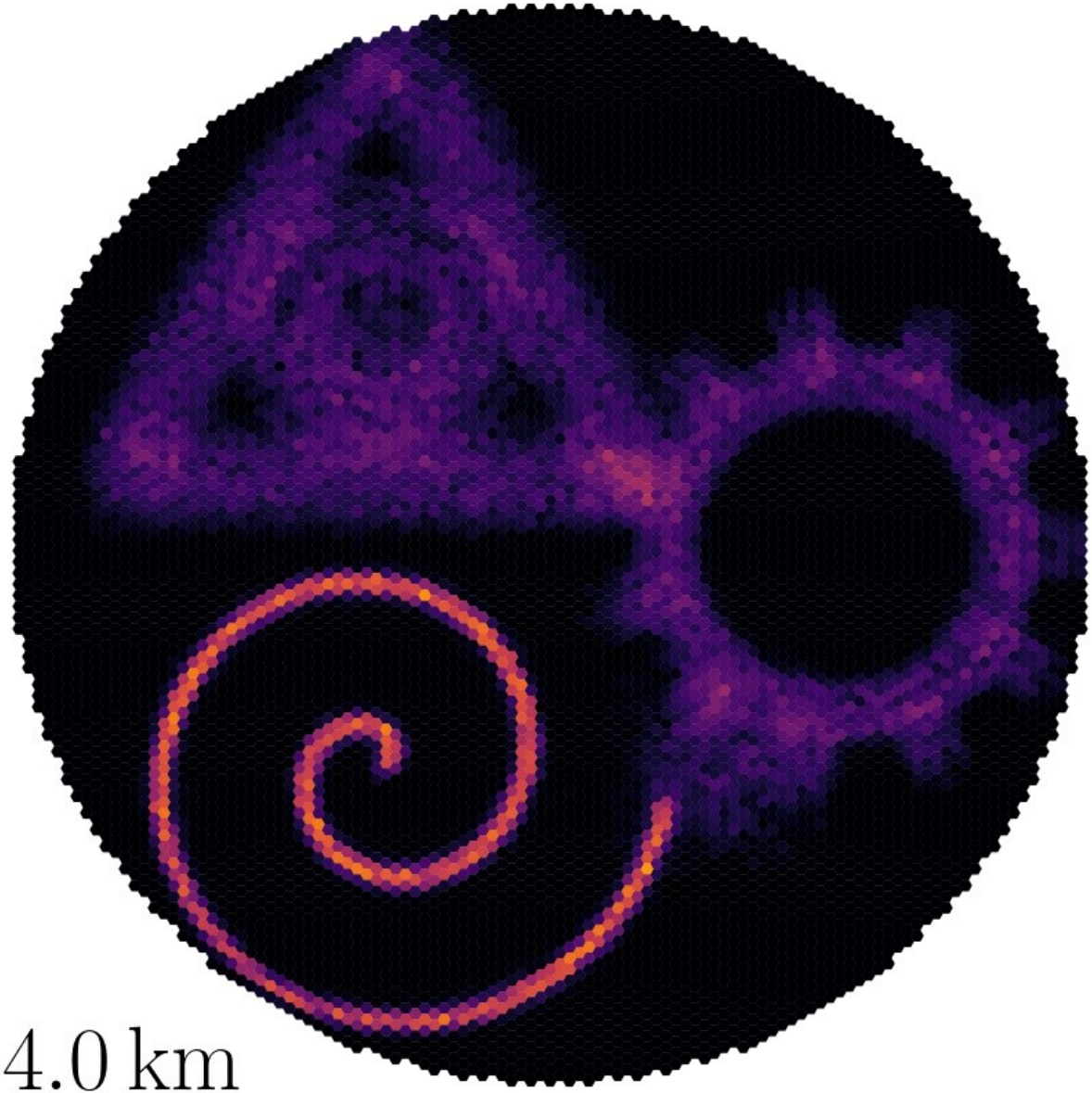

4.0 km

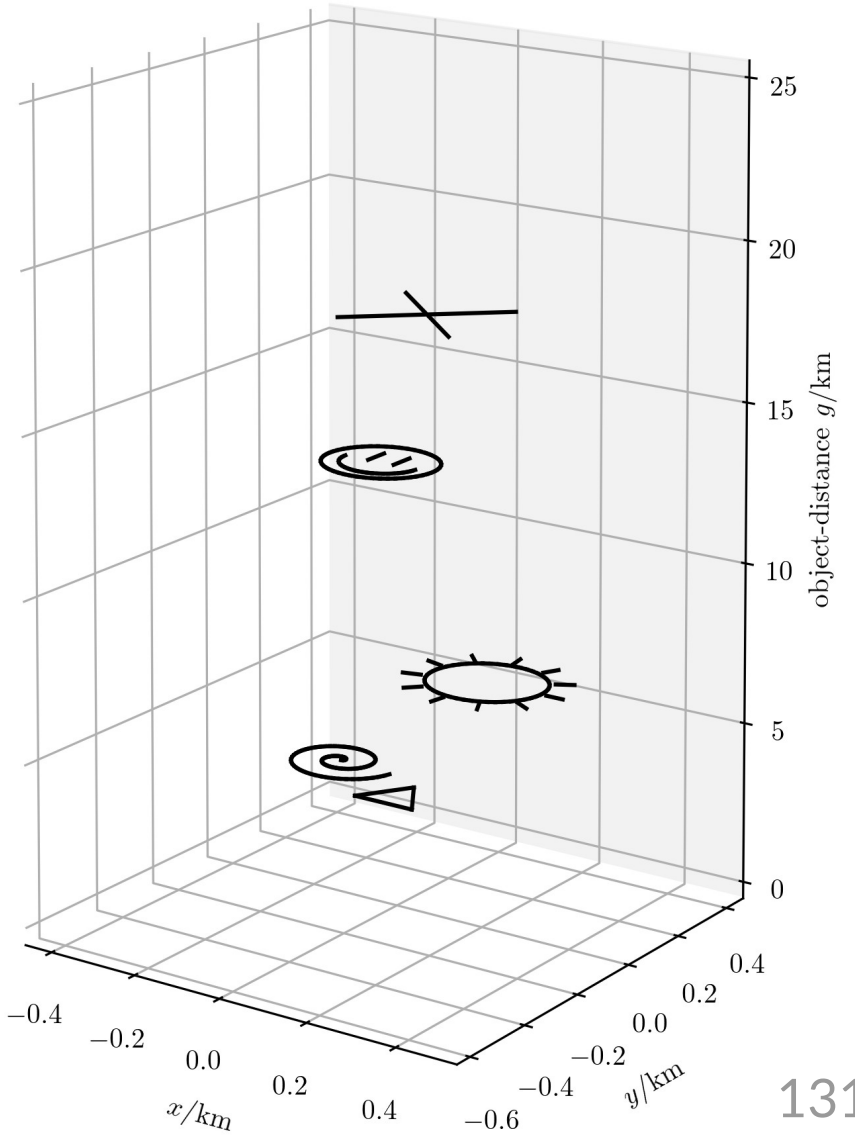
25
20
15
10
5
0
object-distance g/km
−0.4
−0.2
0.0
0.2
0.4
x/km
0.4
0.2
0.0
−0.2
−0.4
−0.6
y/km

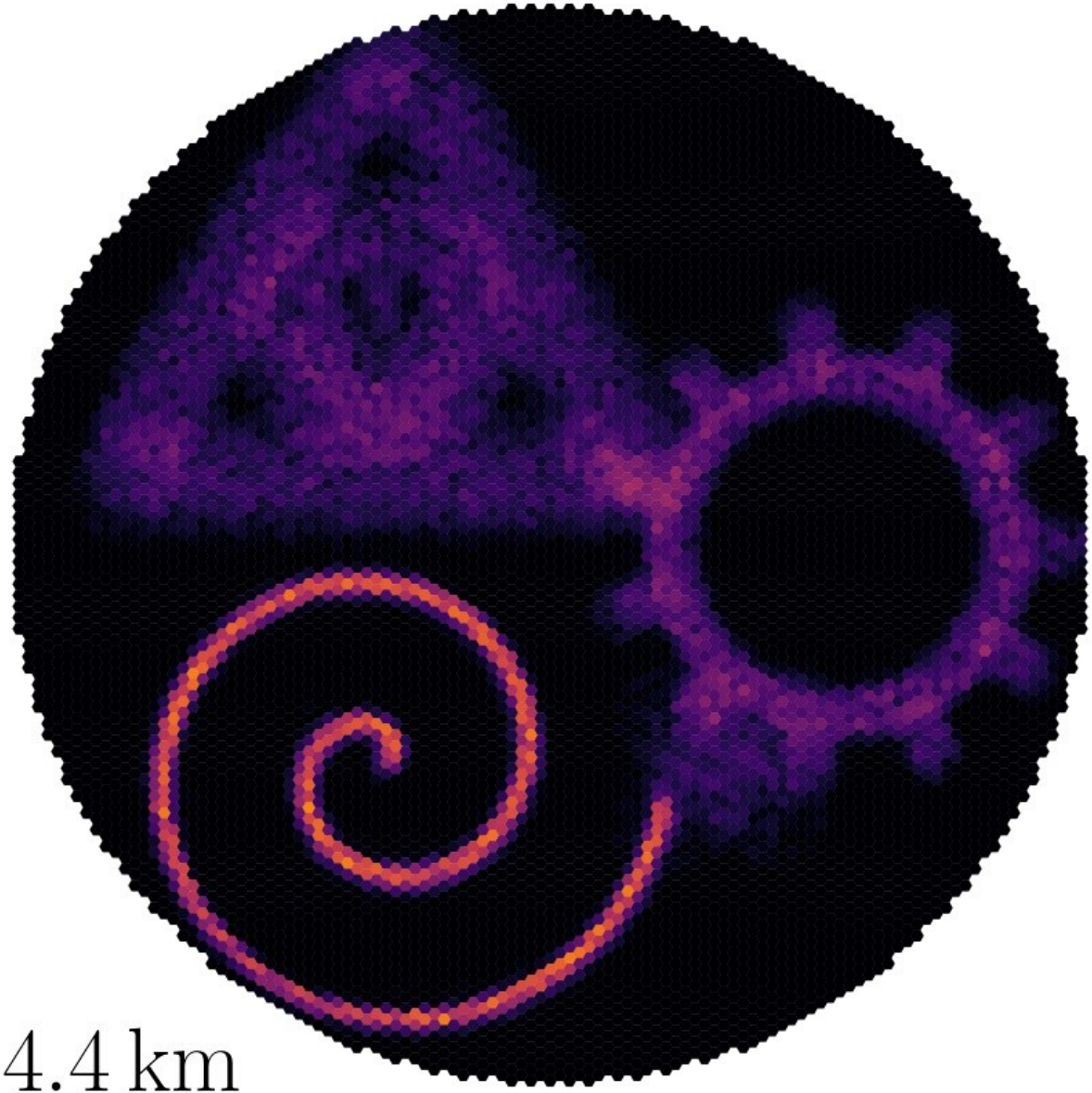

4.4 km

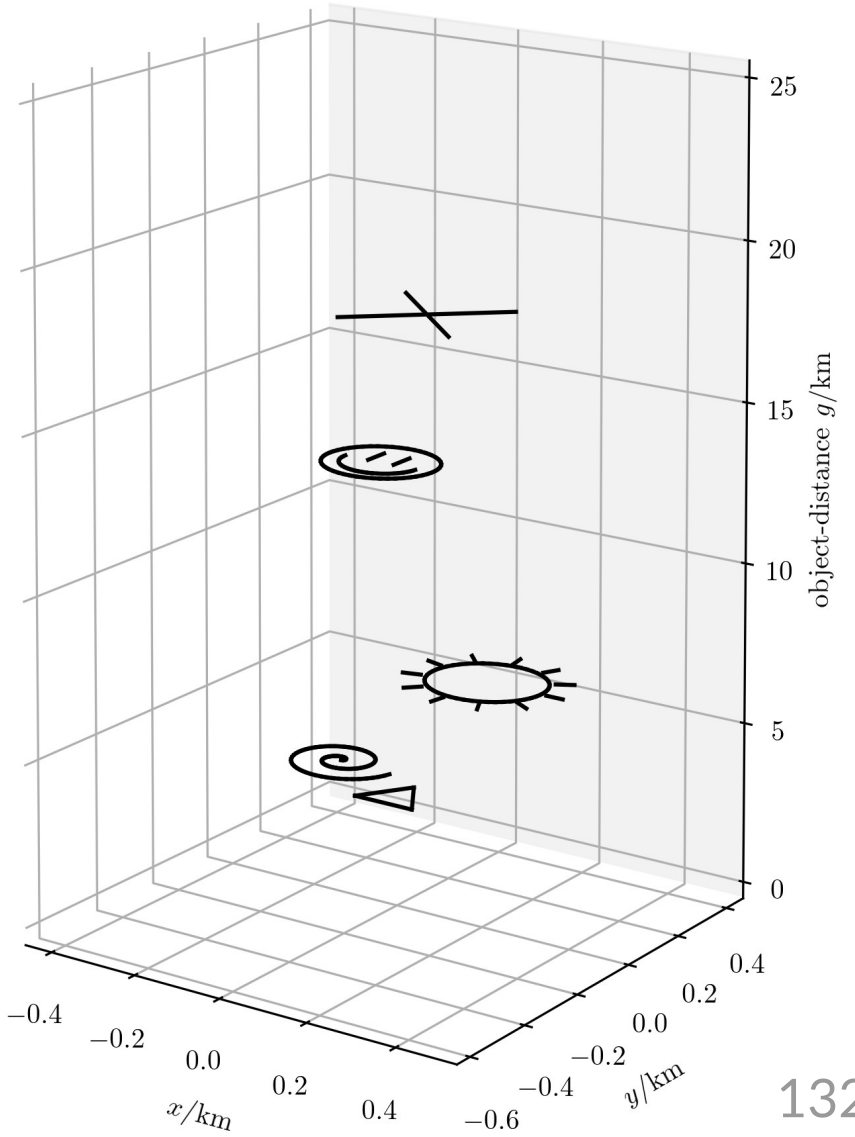
25
20
15
10
5
0
object-distance g/km
−0.4
−0.2
0.0
0.2
0.4
x/km
0.4
0.2
0.0
−0.2
−0.4
−0.6
y/km

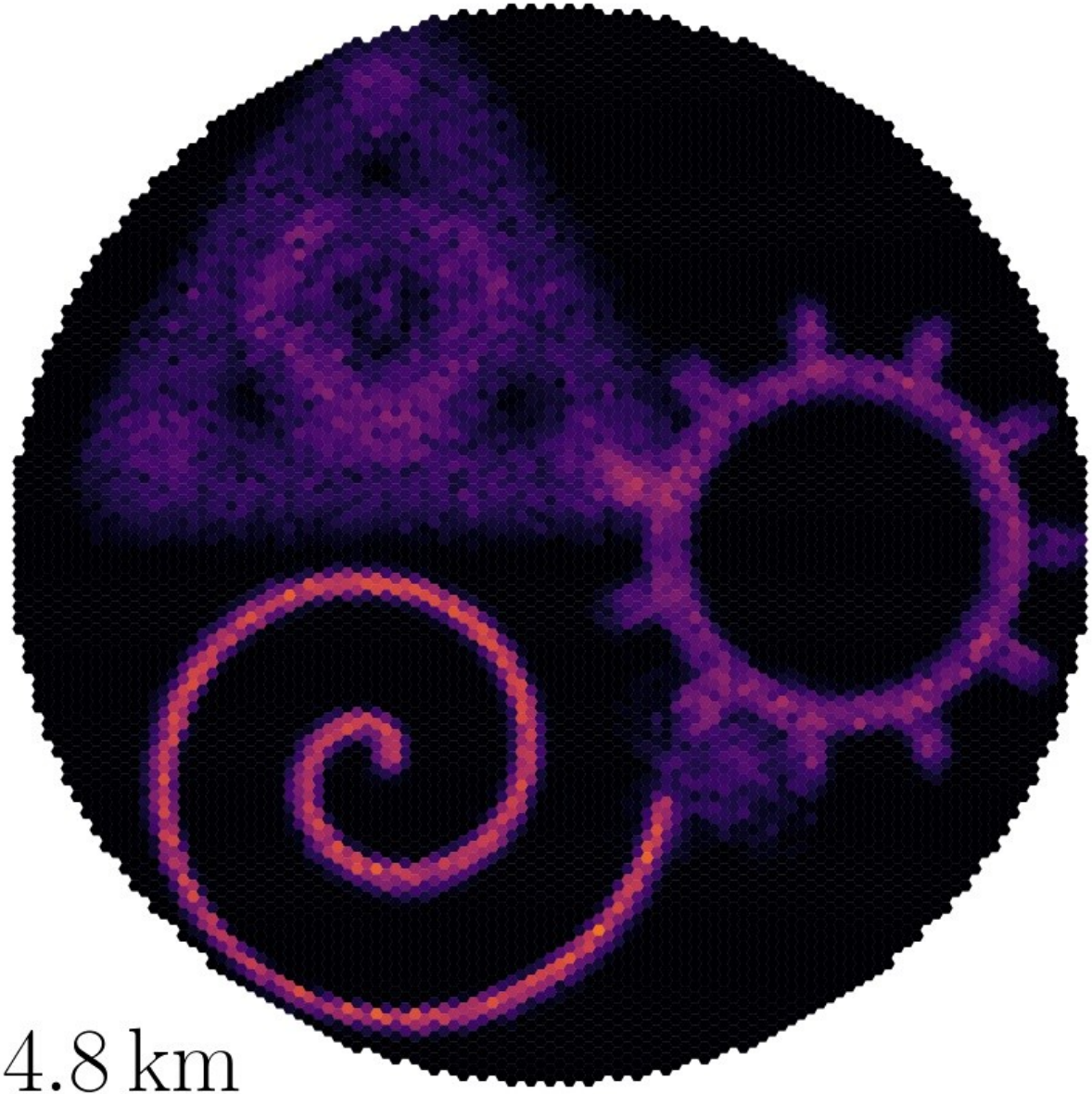

4.8 km

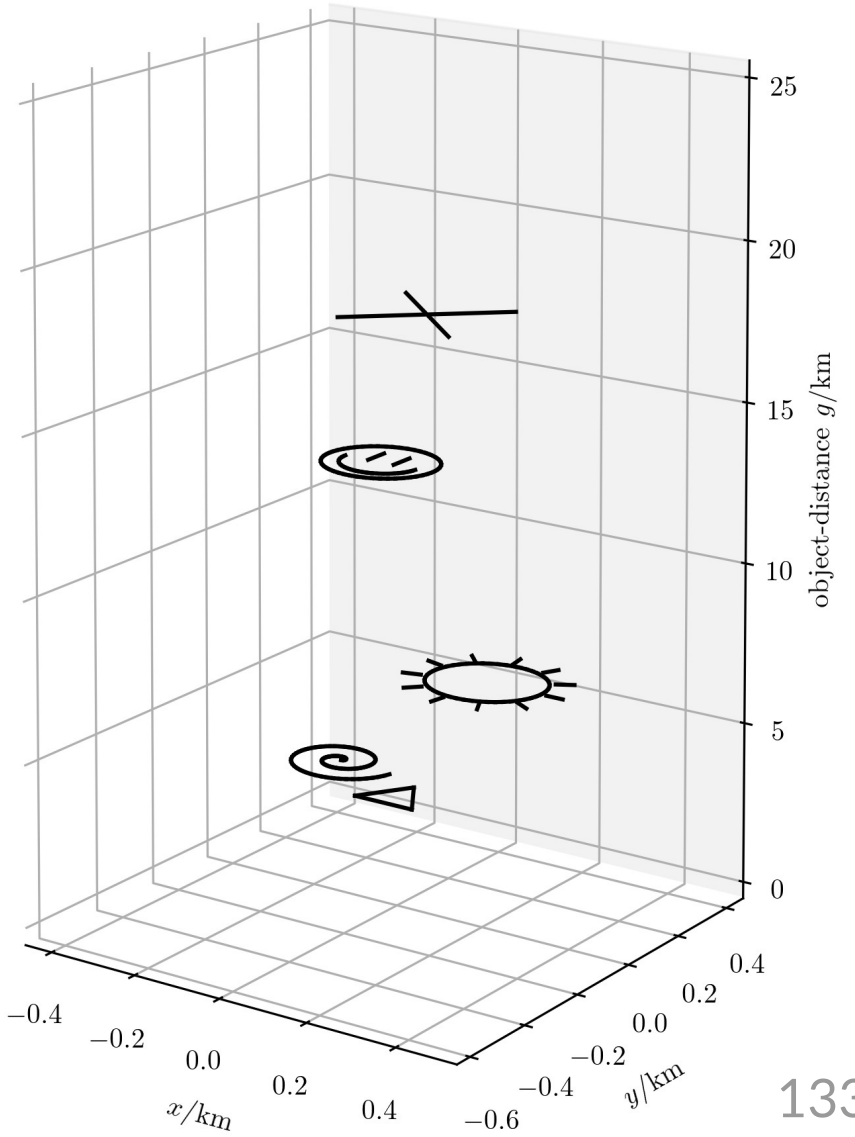
25
20
15
10
5
0
object-distance g/km
−0.4
−0.2
0.0
0.2
0.4
x/km
0.4
0.2
0.0
−0.2
−0.4
−0.6
y/km

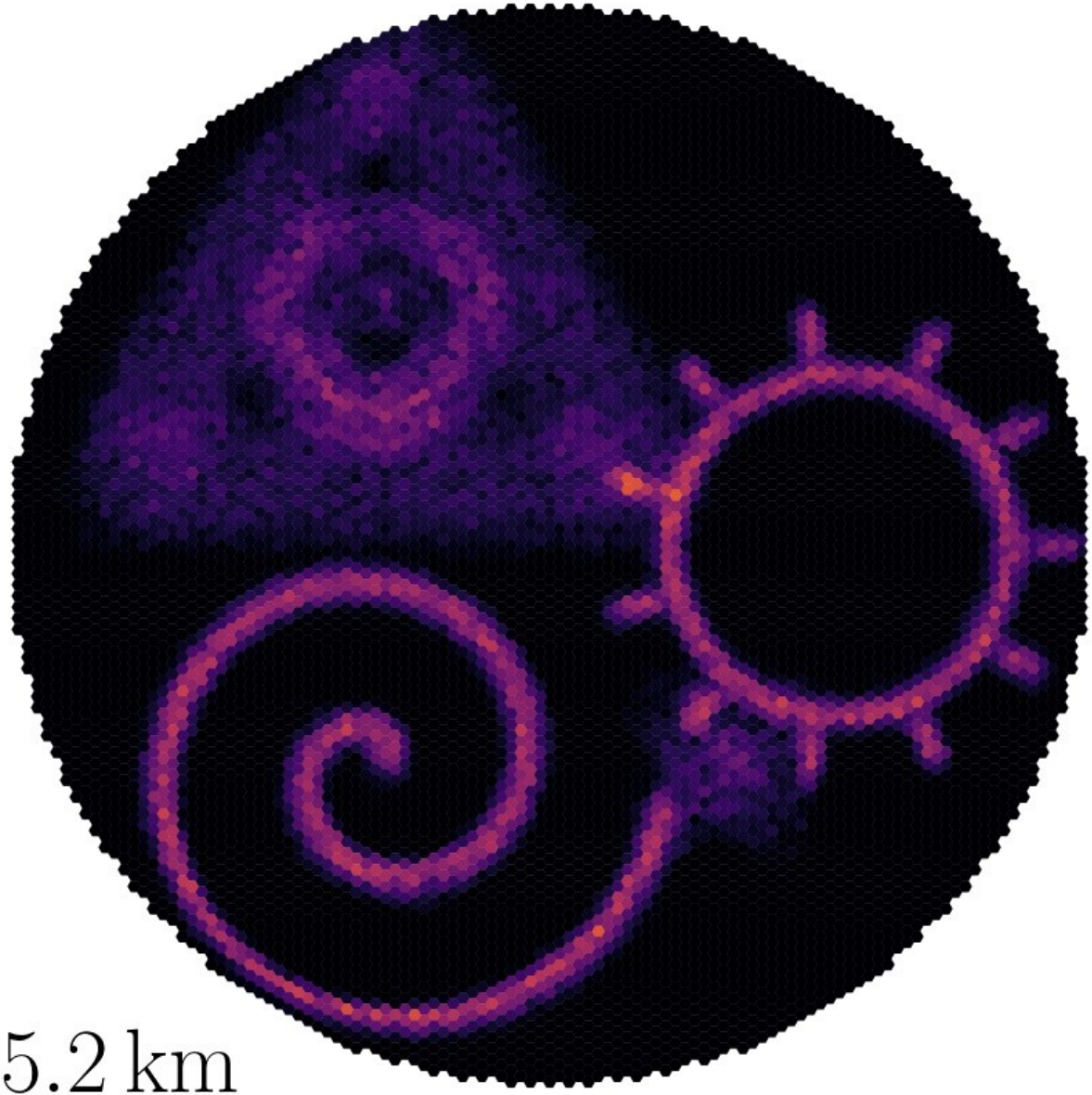

5.2 km

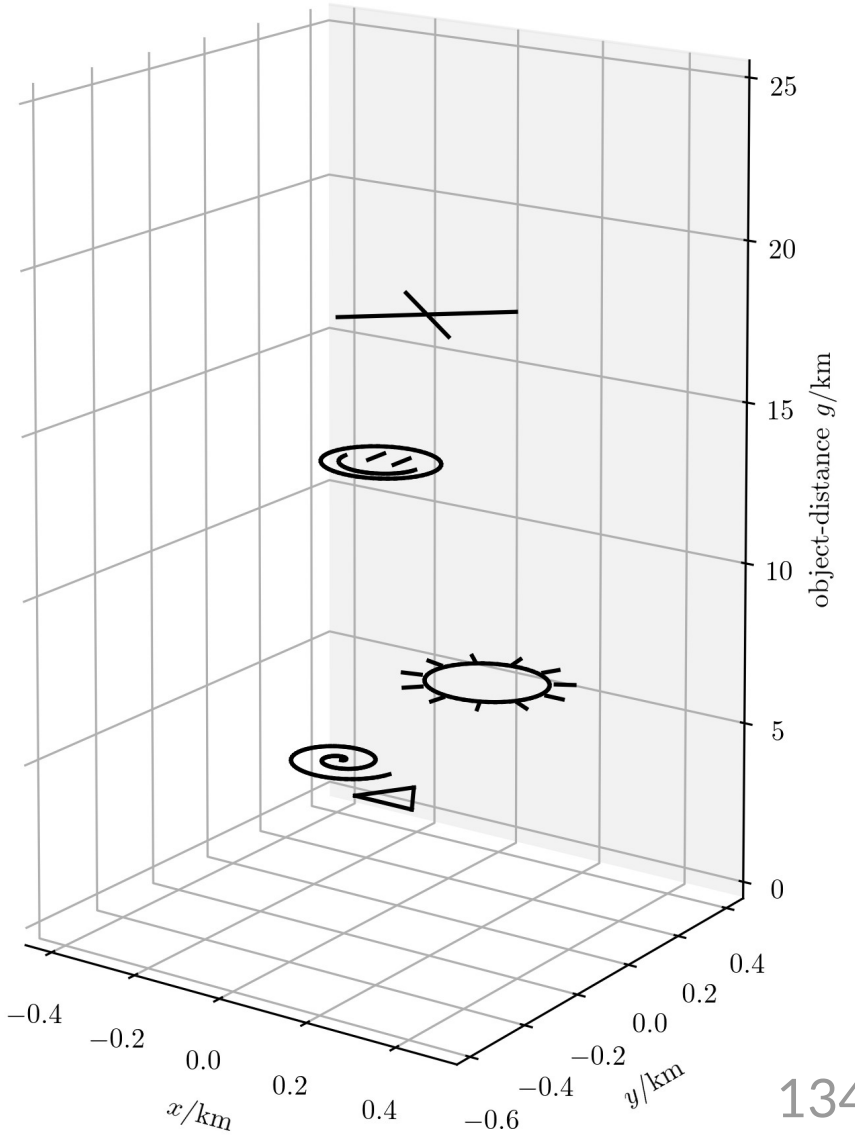
25
20
15
10
5
0
object-distance g/km
−0.4
−0.2
0.0
0.2
0.4
x/km
0.4
0.2
0.0
−0.2
−0.4
−0.6
y/km

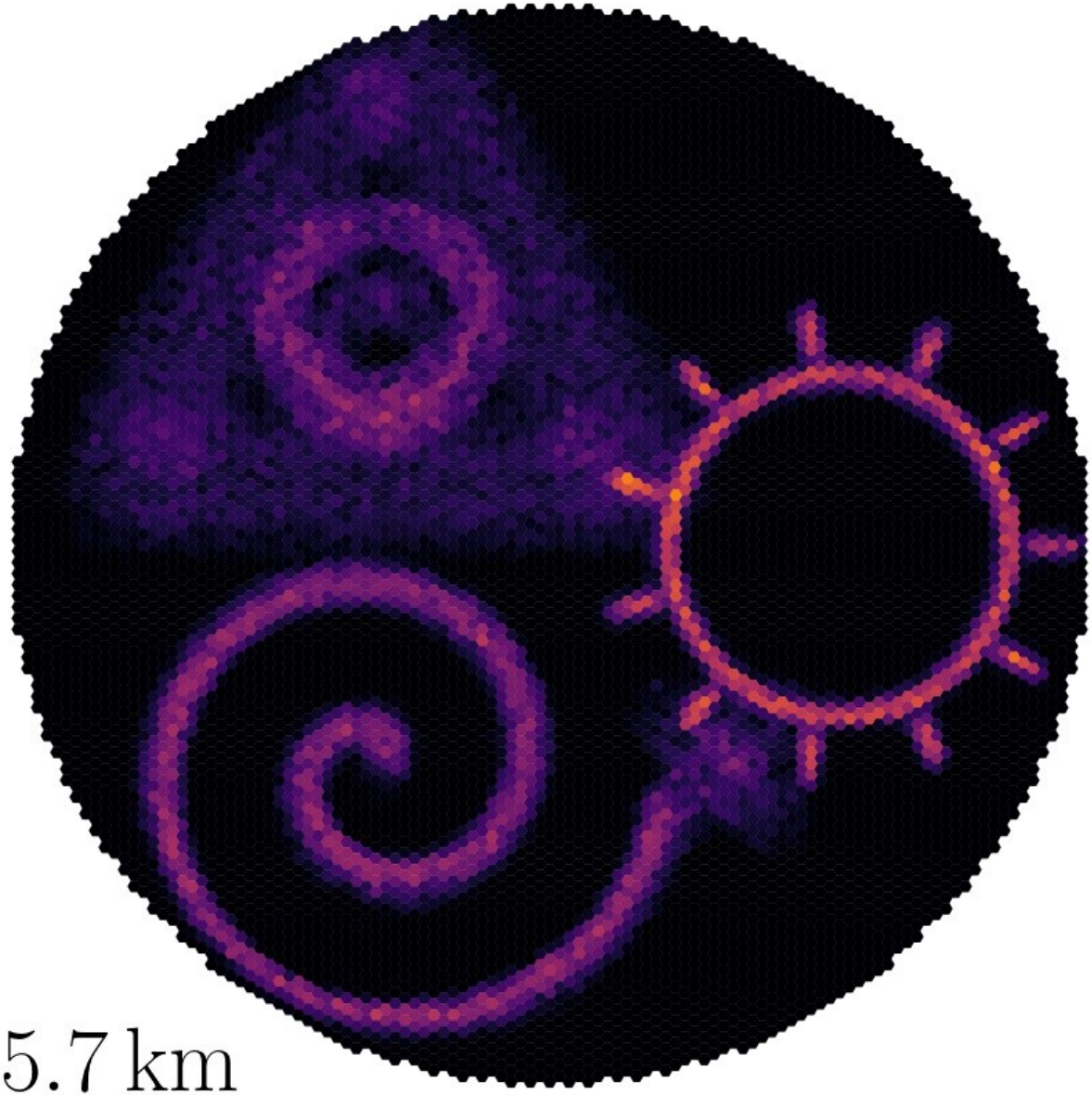

5.7 km

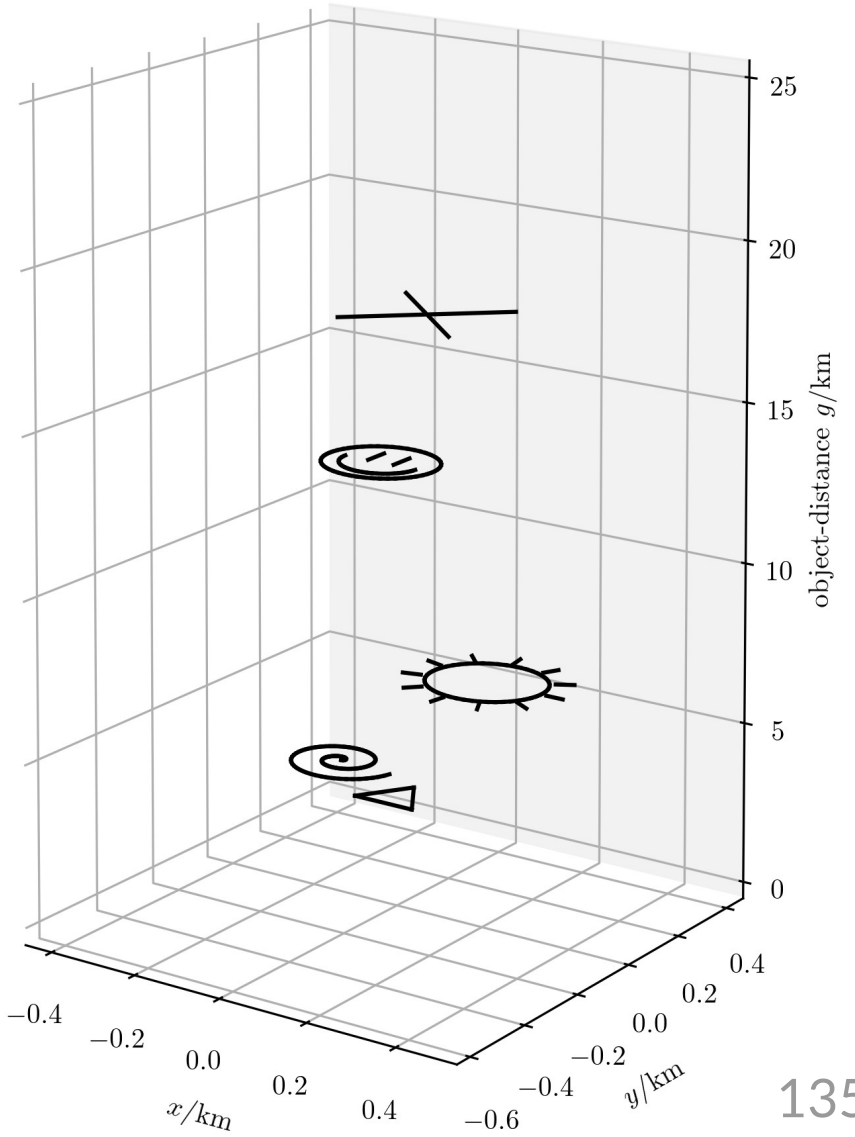
25
20
15
10
5
0
object-distance g/km
0.4
0.2
0.0
−0.2
−0.4
y/km
−0.4
−0.2
0.0
0.2
0.4
−0.6
x/km

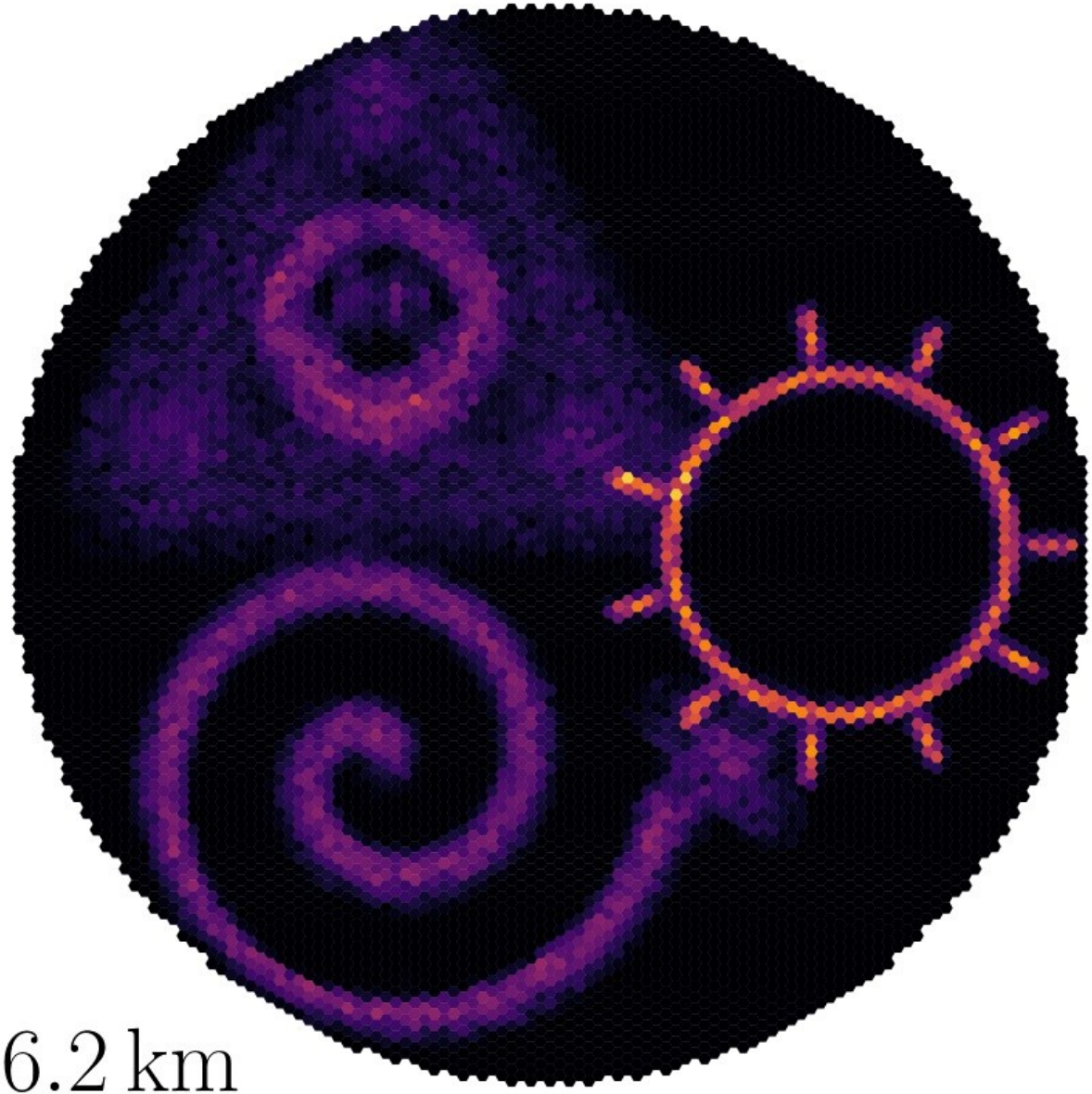

6.2 km

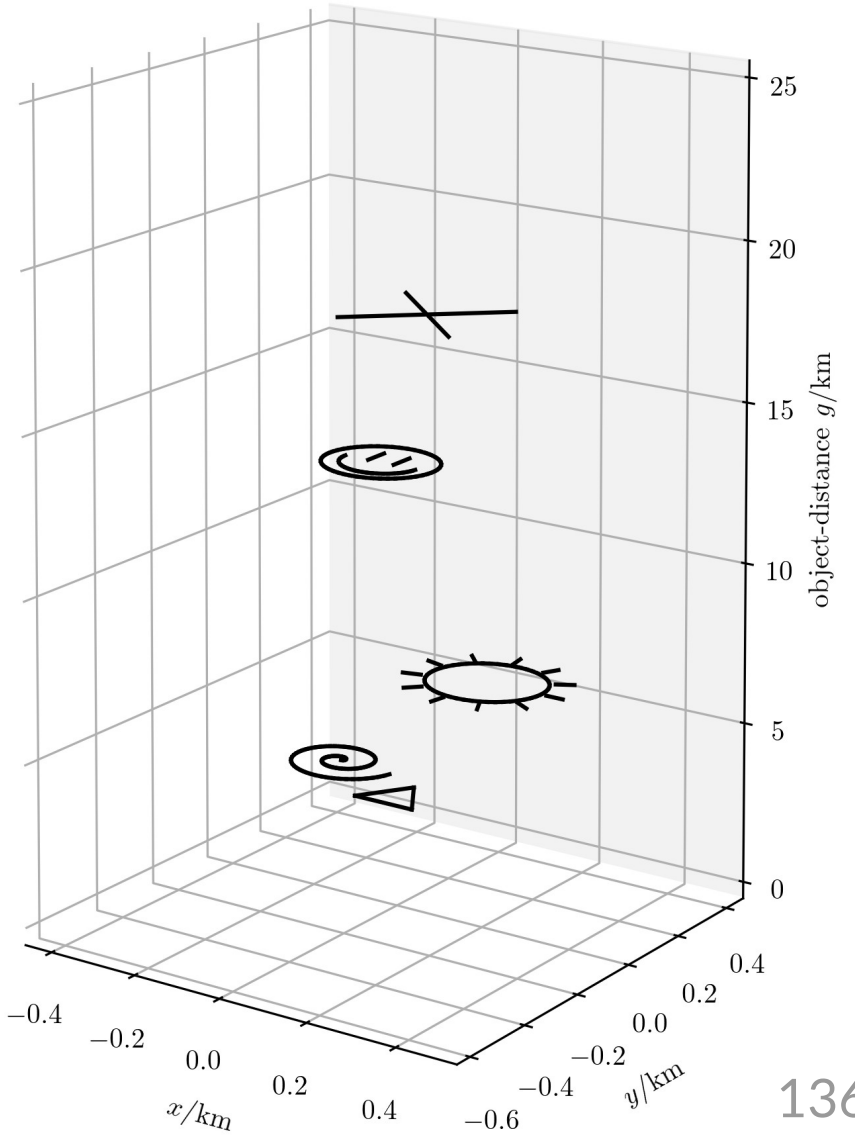
25
20
15
10
5
0
object-distance g/km
−0.4
−0.2
0.0
0.2
0.4
x/km
0.4
0.2
0.0
−0.2
−0.4
−0.6
y/km

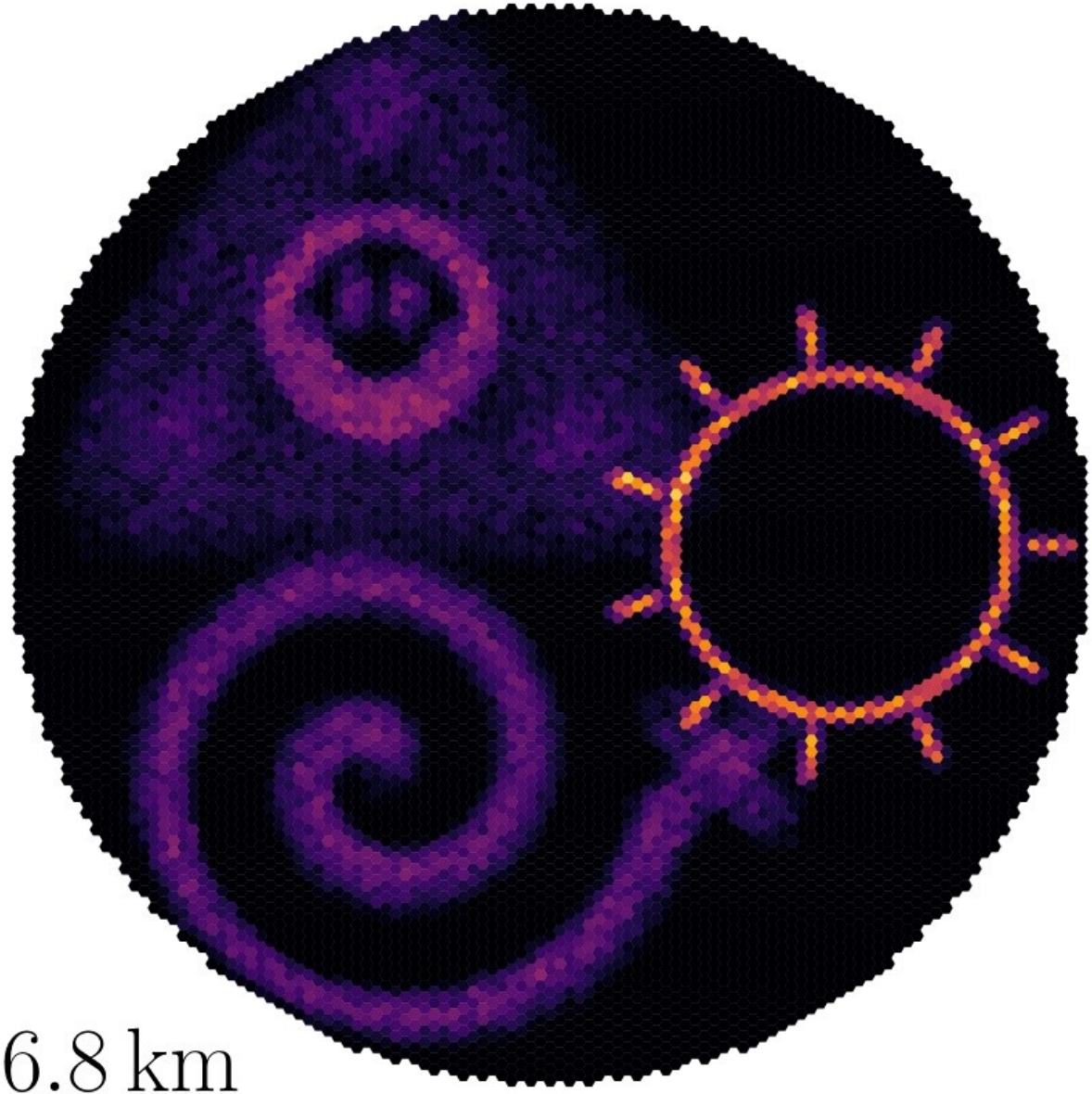

6.8 km

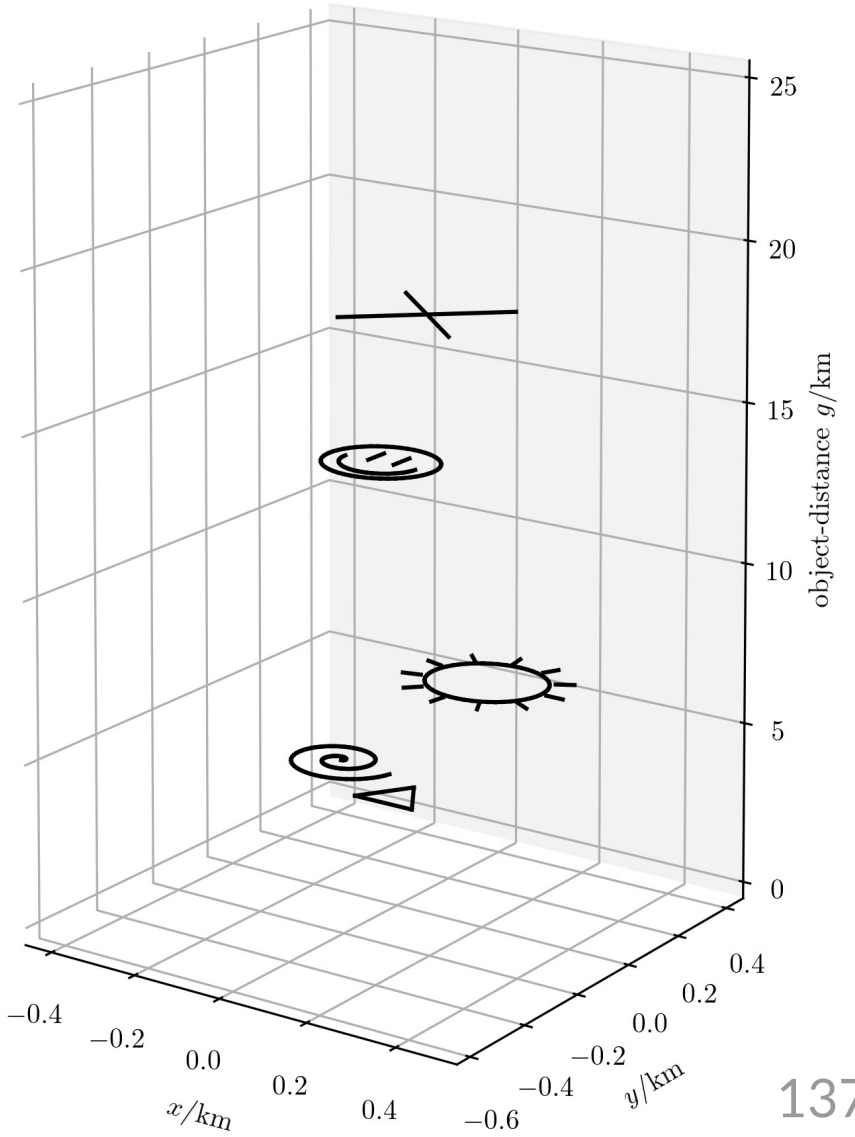
25
20
15
10
5
0
object-distance g/km
−0.4
−0.2
0.0
0.2
0.4
x/km
0.4
0.2
0.0
−0.2
−0.4
−0.6
y/km

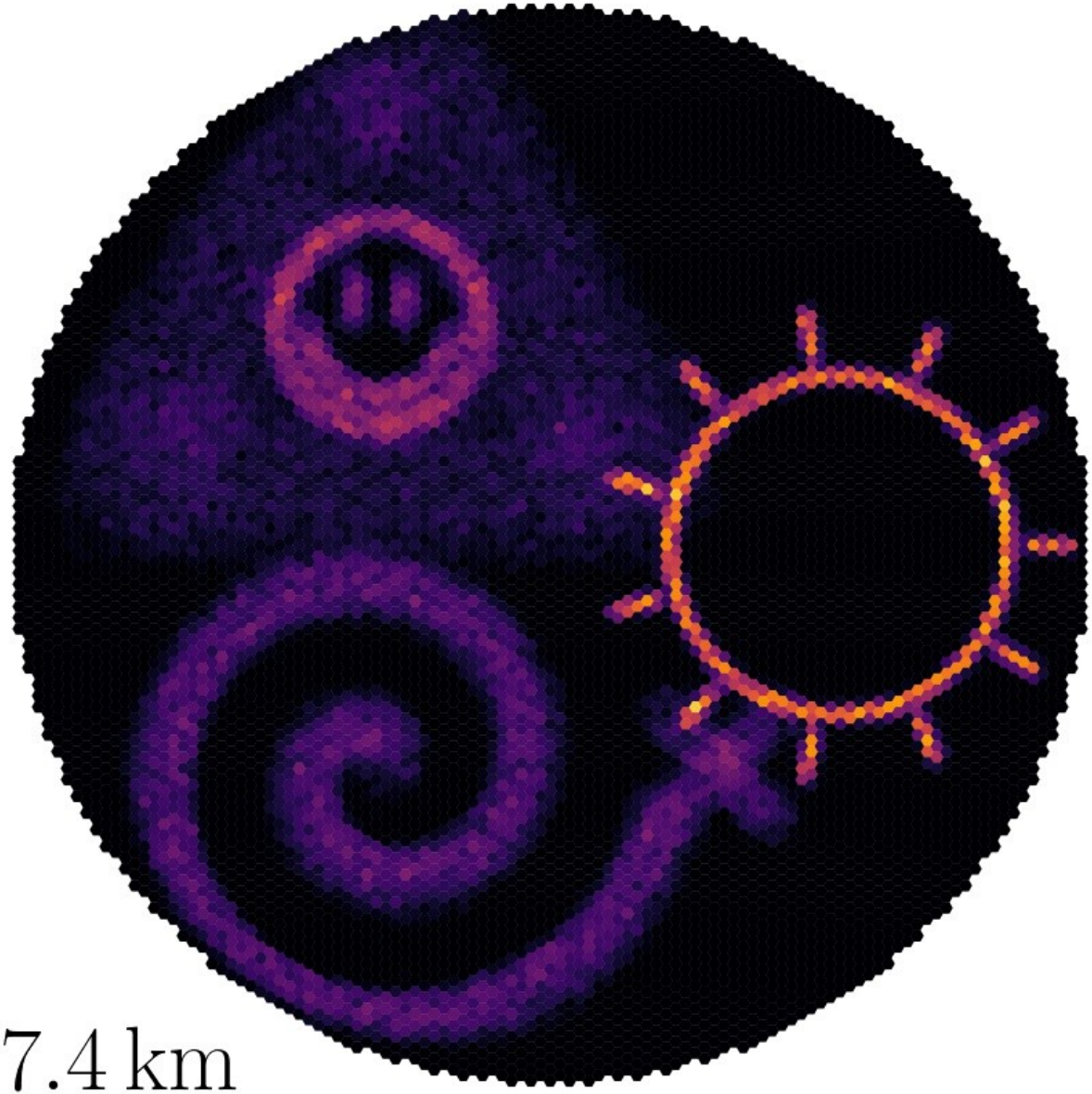

7.4 km

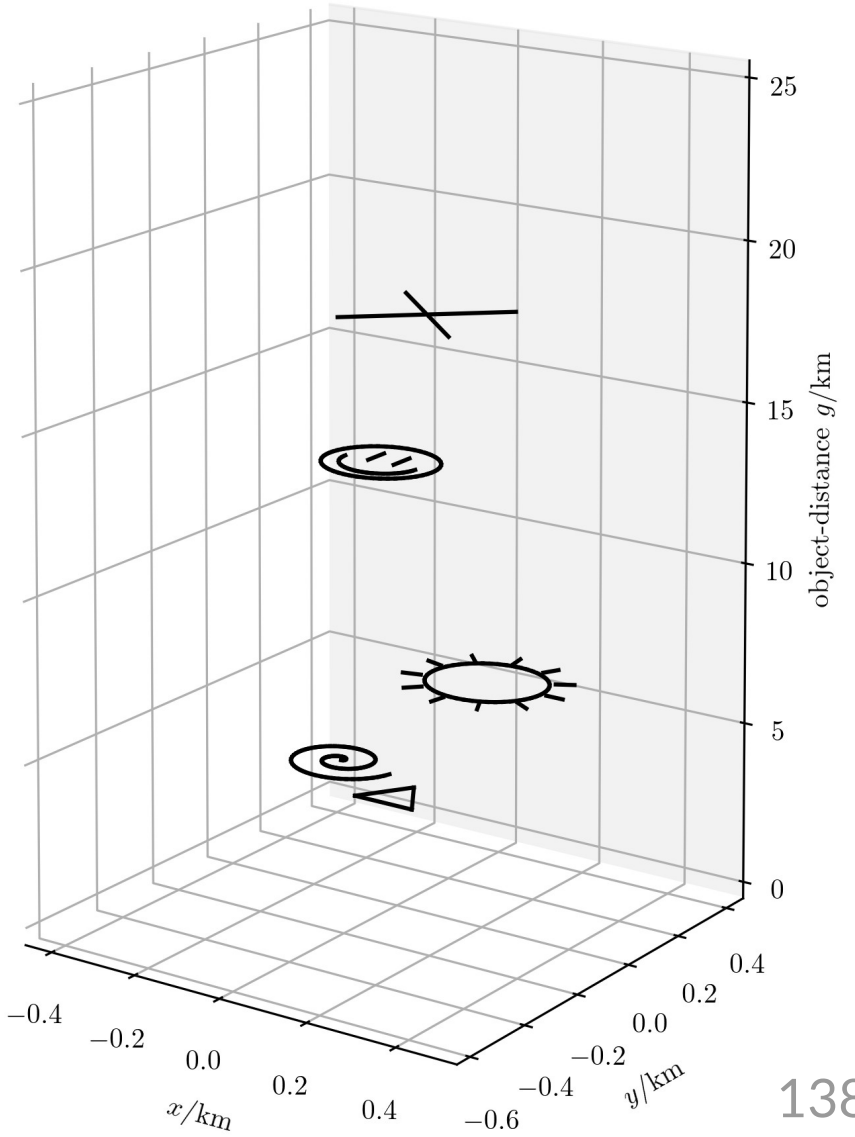
25
20
15
10
5
0
object-distance g/km
−0.4
−0.2
0.0
0.2
0.4
x/km
0.4
0.2
0.0
−0.2
−0.4
−0.6
y/km

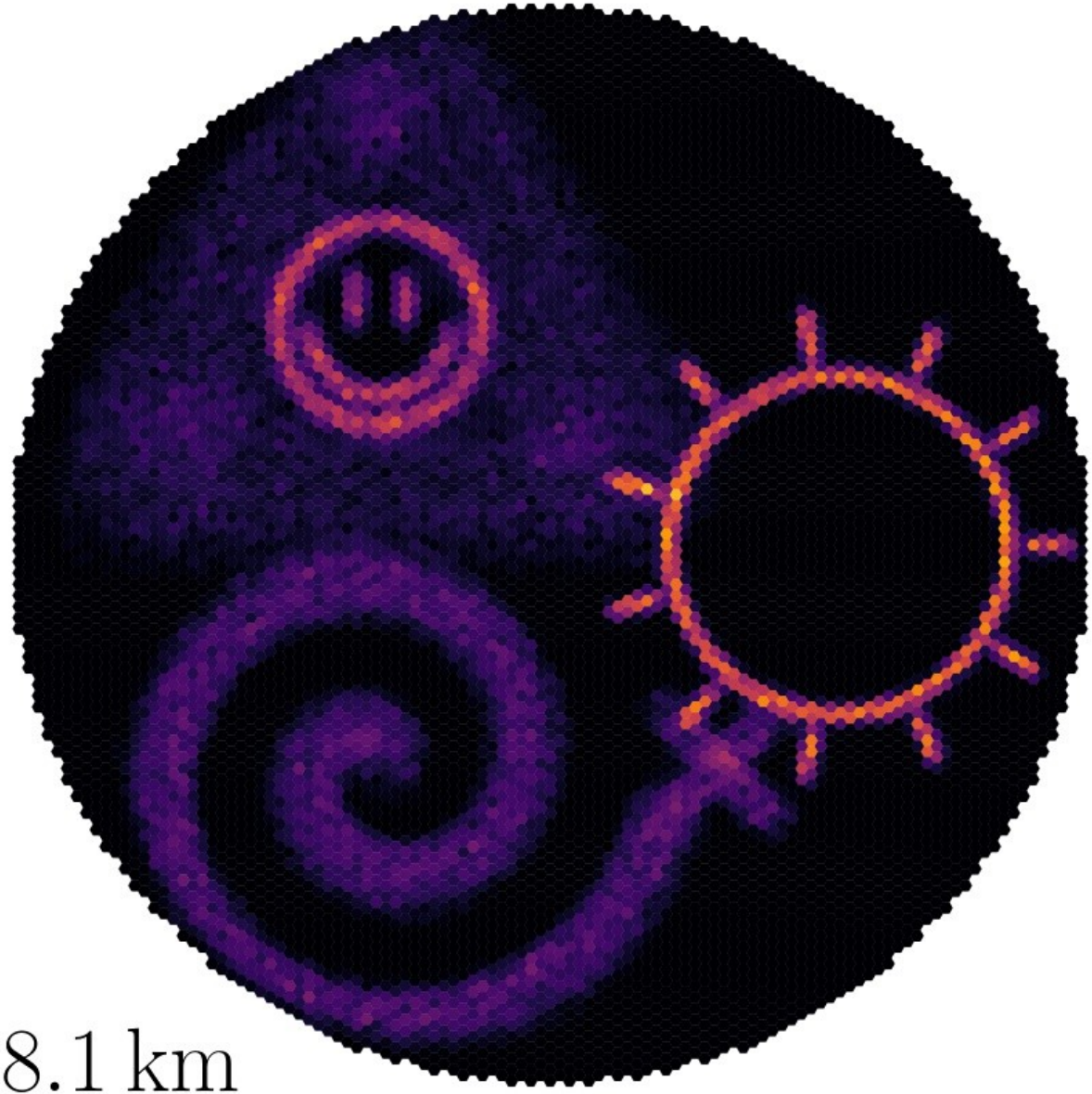

8.1 km

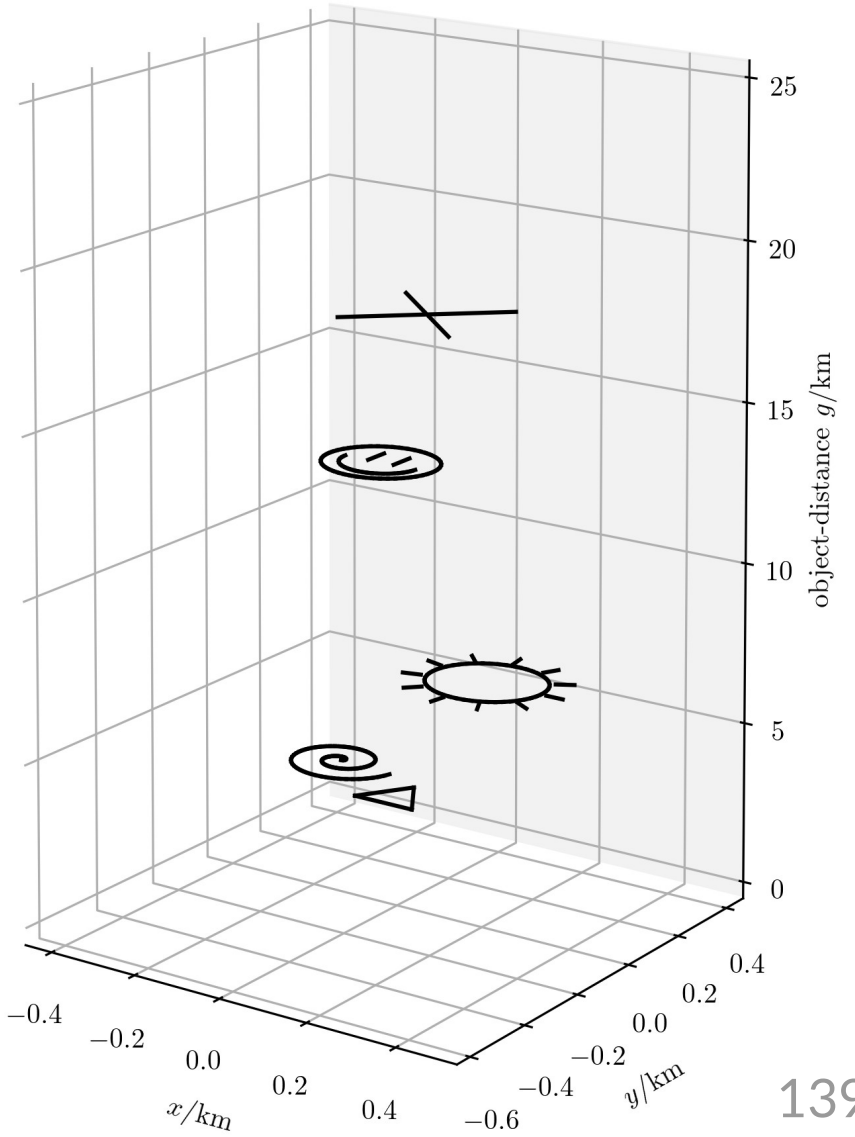
25
20
15
10
5
0
object-distance g/km
0.4
0.2
0.0
−0.2
−0.4
−0.6
y/km
−0.4
−0.2
0.0
0.2
0.4
x/km

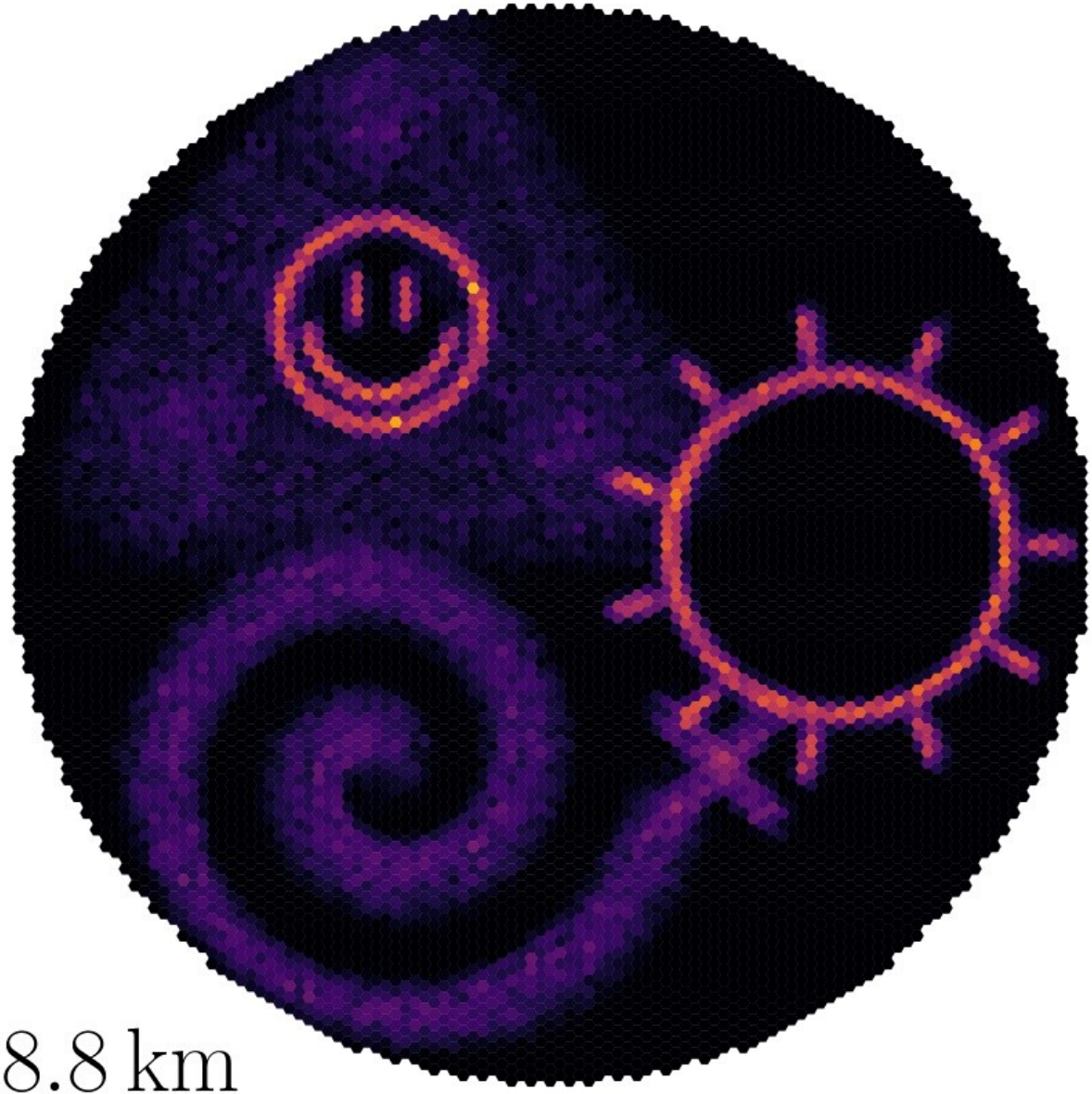

8.8 km

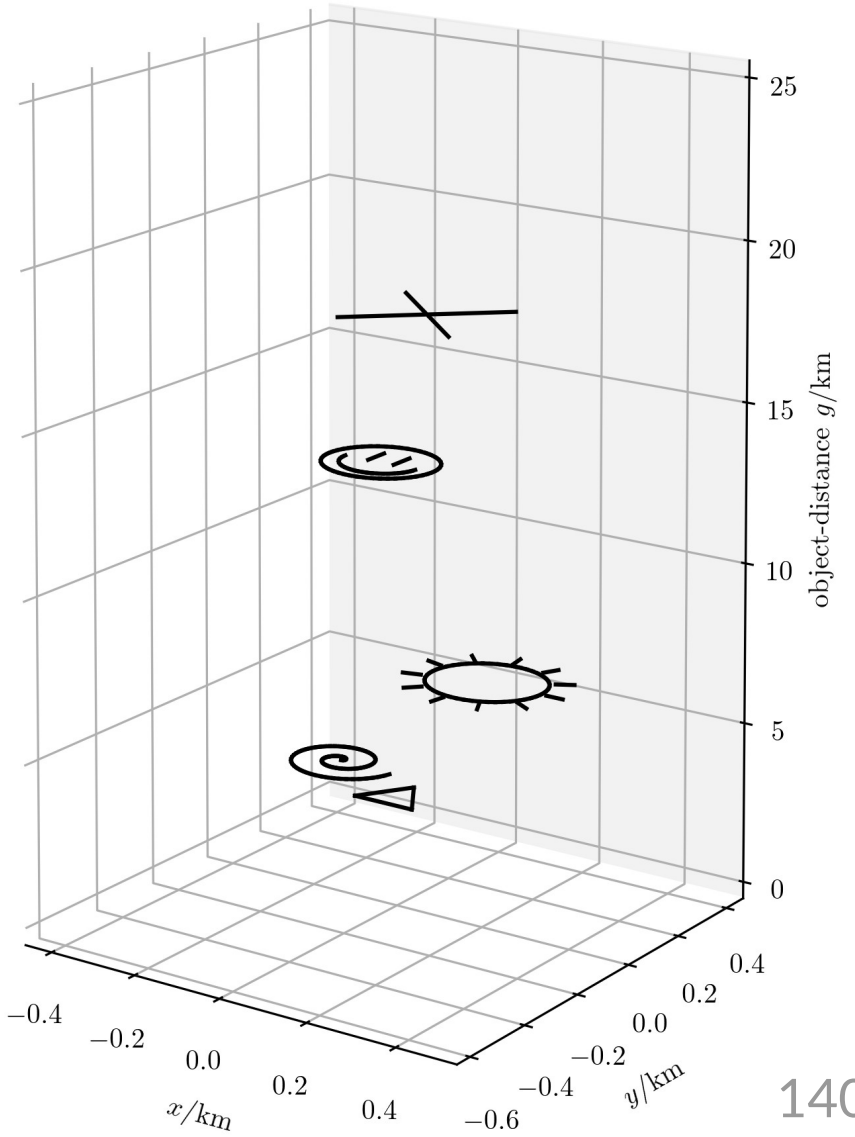
25
20
15
10
5
0
object-distance g/km
−0.4
−0.2
0.0
0.2
0.4
x/km
0.4
0.2
0.0
−0.2
−0.4
−0.6
y/km

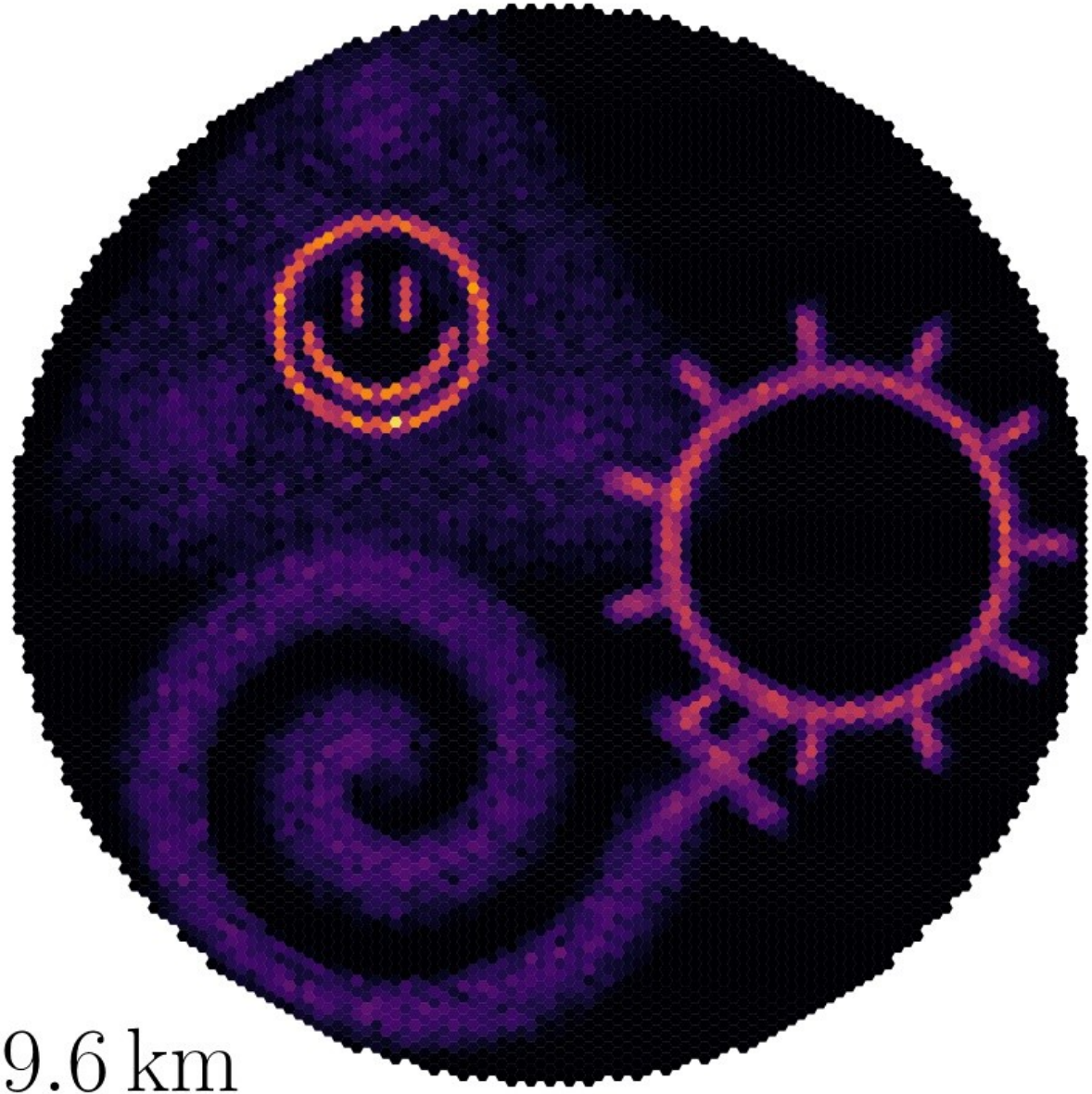

9.6 km

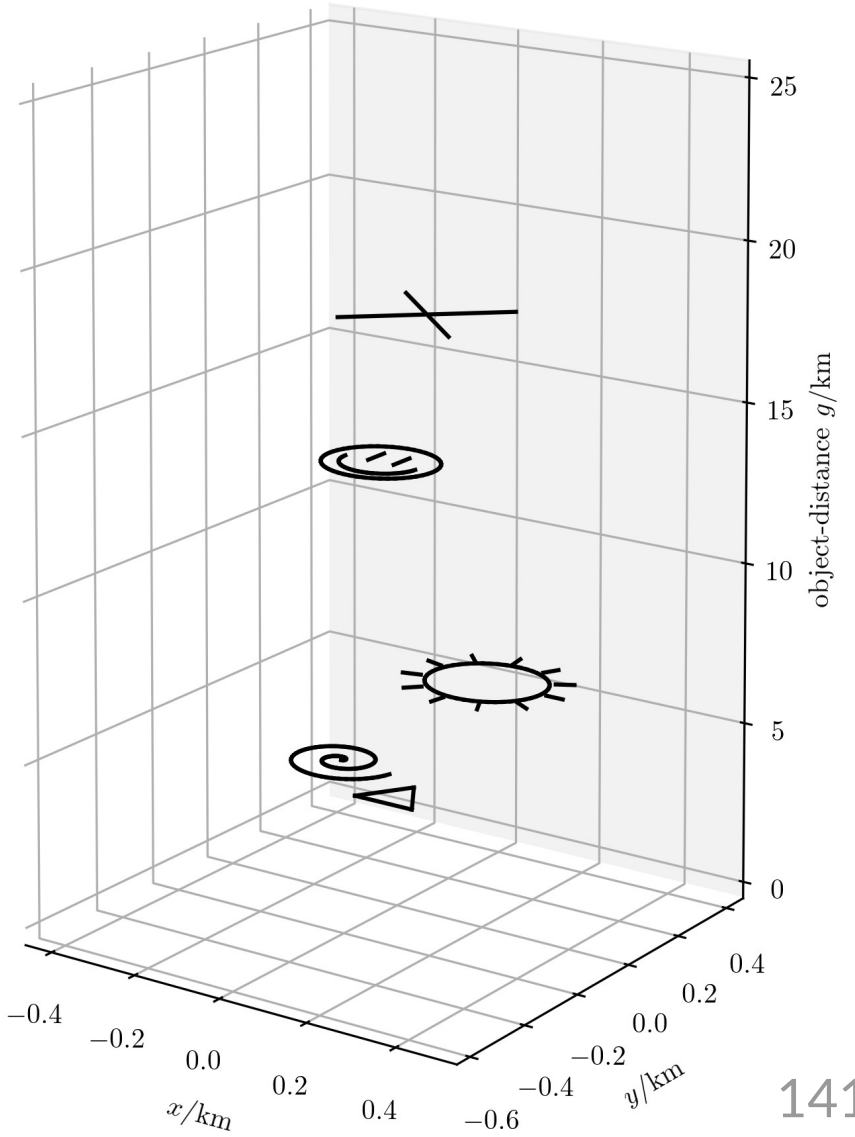
25
20
15
10
5
0
object-distance g/km
−0.4
−0.2
0.0
0.2
0.4
x/km
0.4
0.2
0.0
−0.2
−0.4
−0.6
y/km

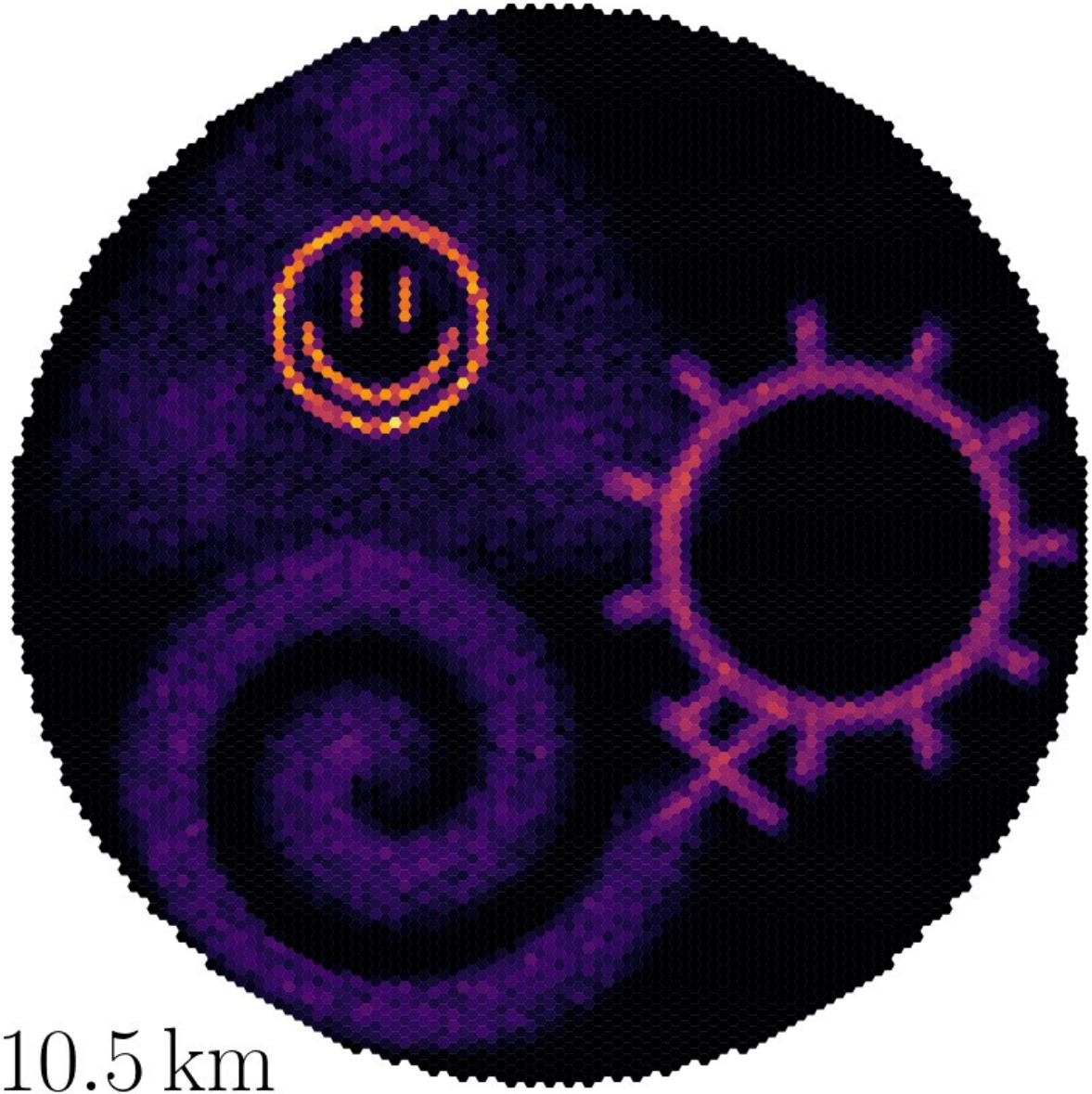

10.5 km

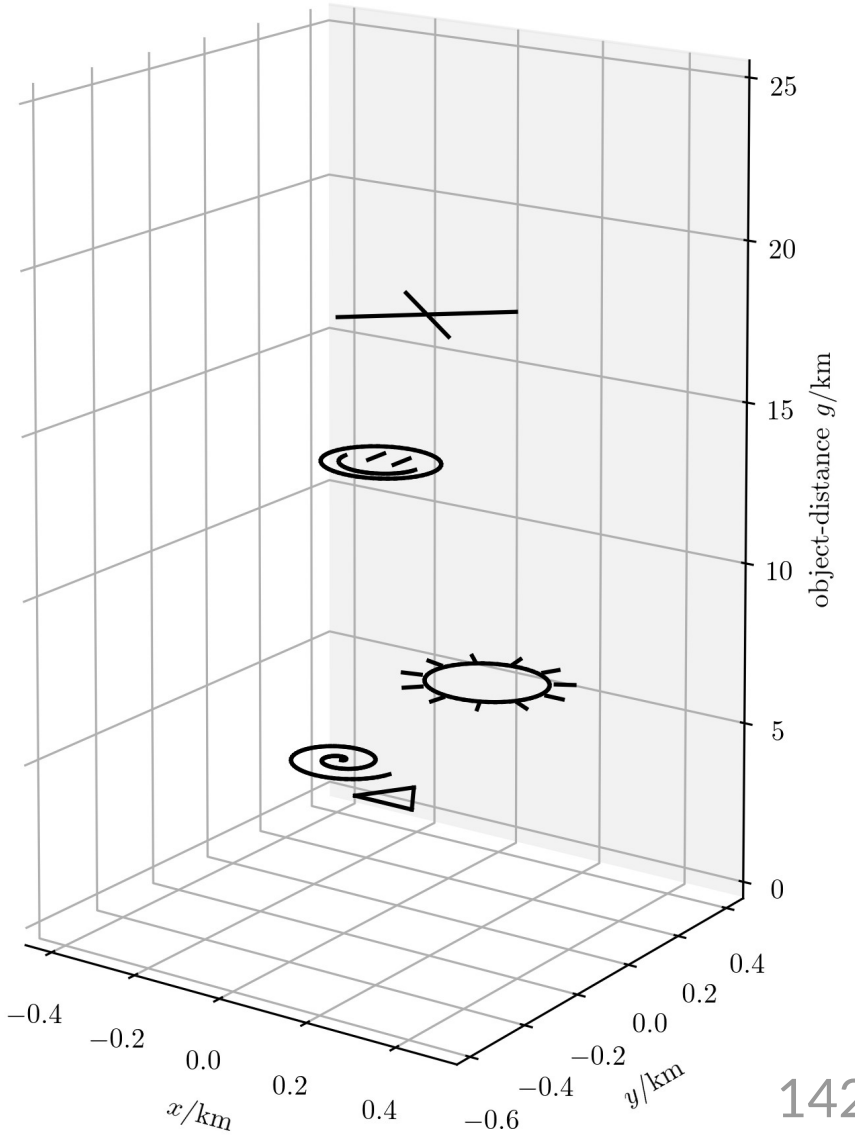
25
20
15
10
5
0
object-distance g/km
−0.4
−0.2
0.0
0.2
0.4
x/km
0.4
0.2
0.0
−0.2
−0.4
−0.6
y/km

11.4 km

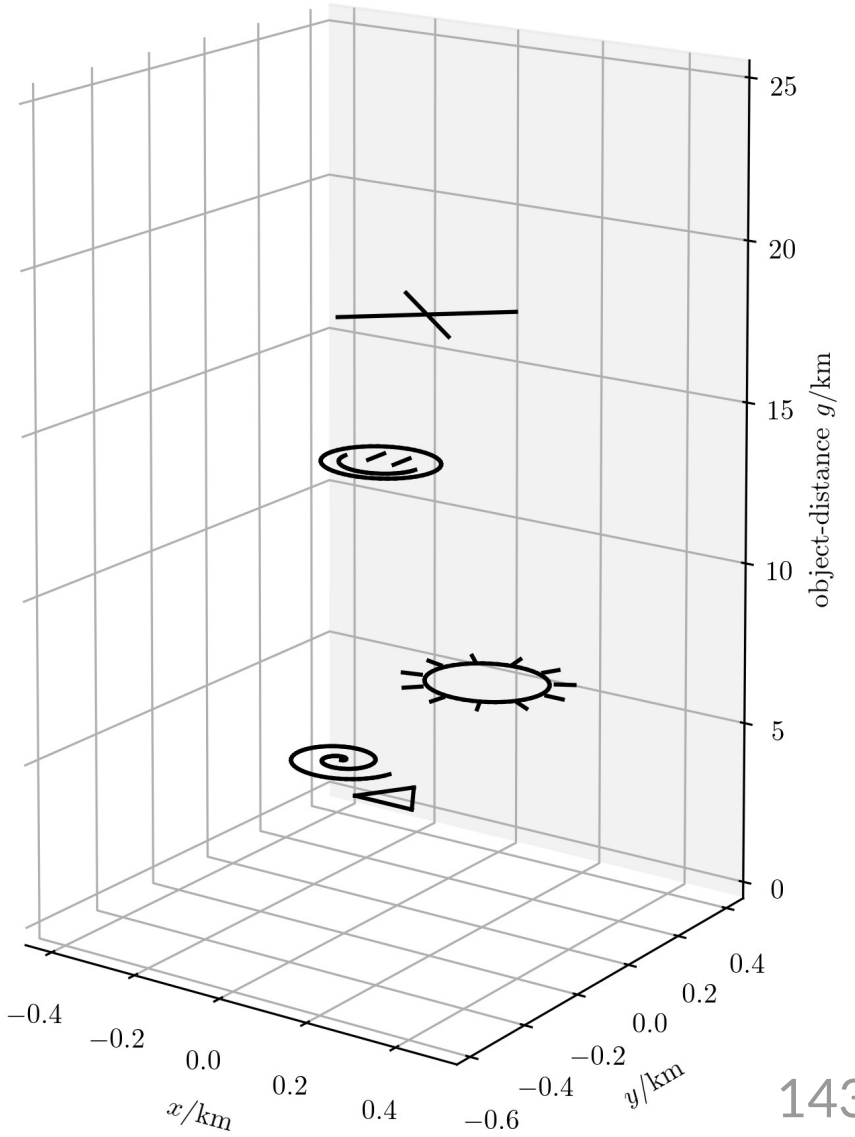
25
20
15
10
5
0
object-distance g/km
−0.4
−0.2
0.0
0.2
0.4
x/km
0.4
0.2
0.0
−0.2
−0.4
−0.6
y/km

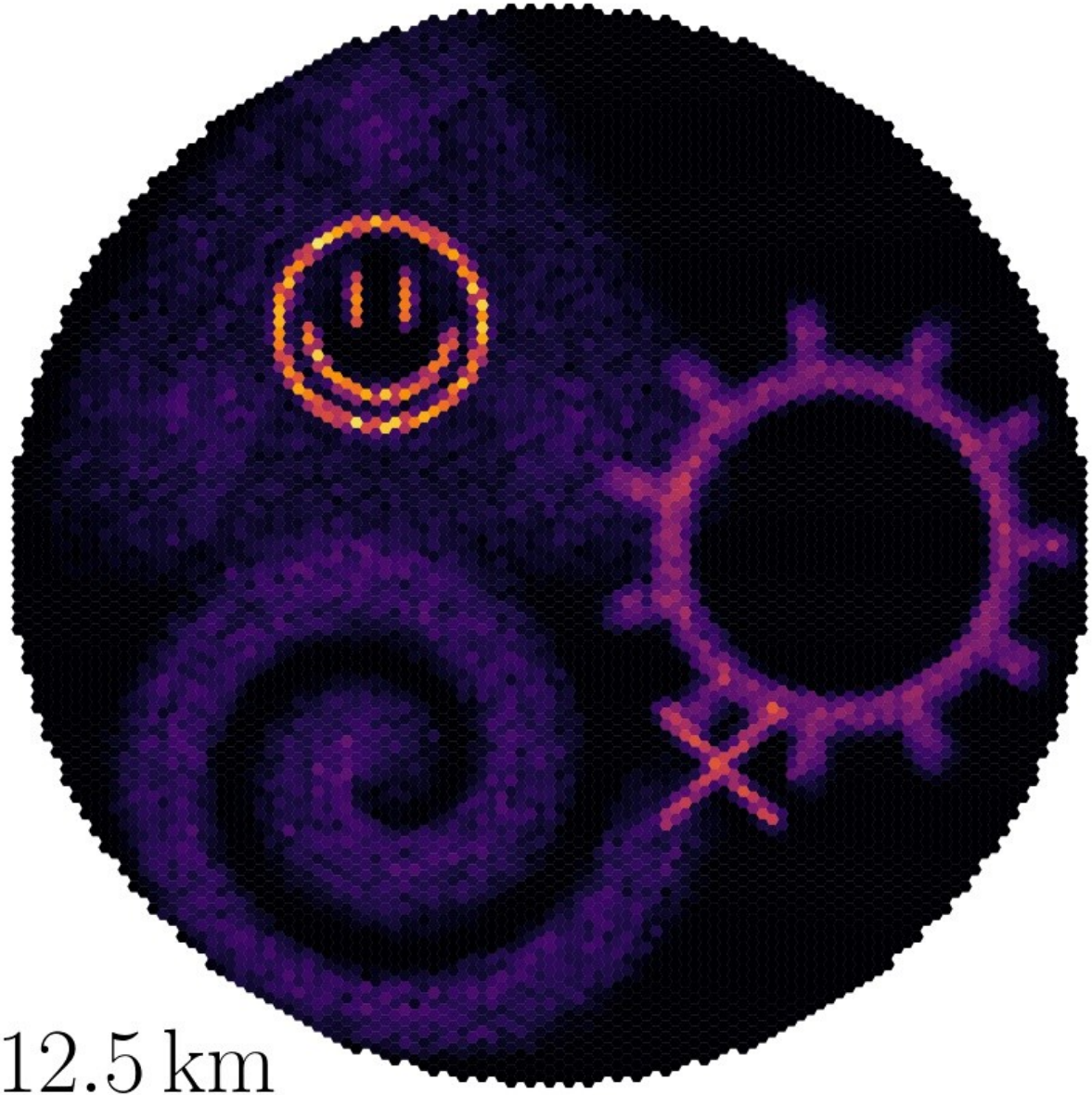

12.5 km

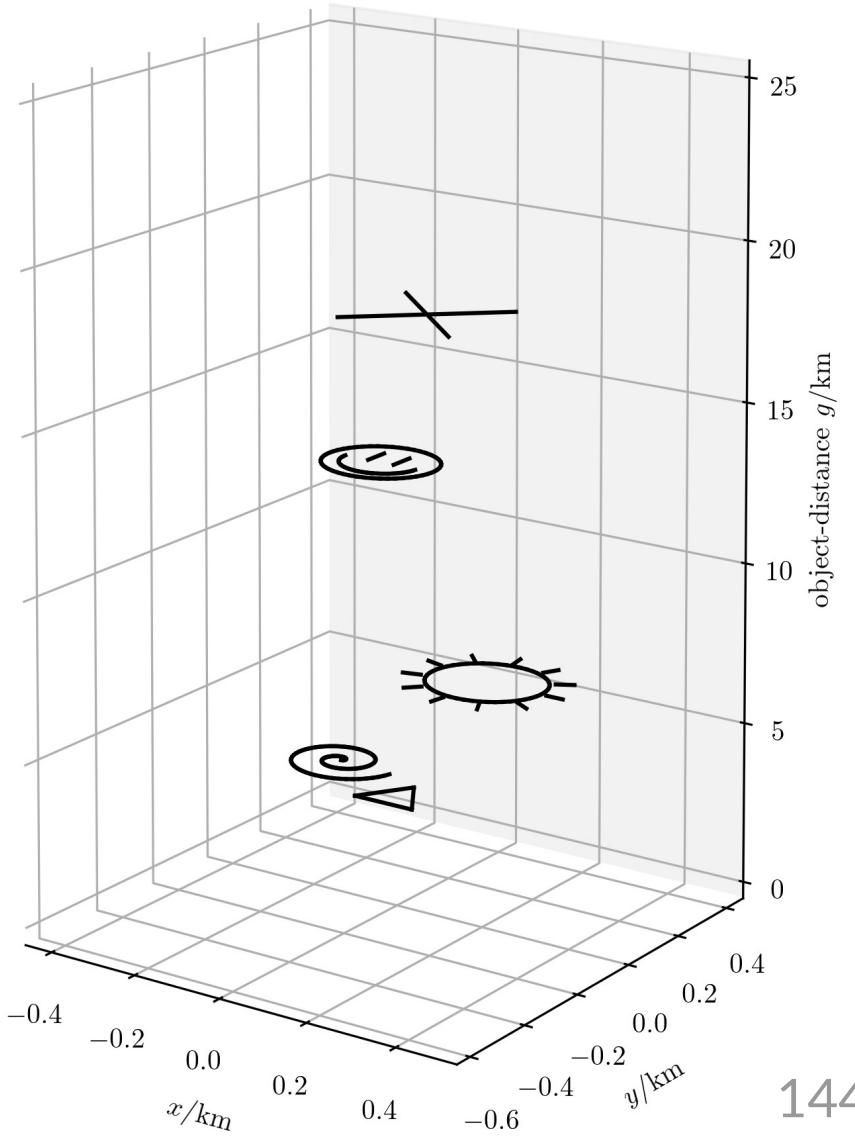
25
20
15
10
5
0
object-distance g/km
−0.4
−0.2
0.0
0.2
0.4
x/km
0.4
0.2
0.0
−0.2
−0.4
−0.6
y/km

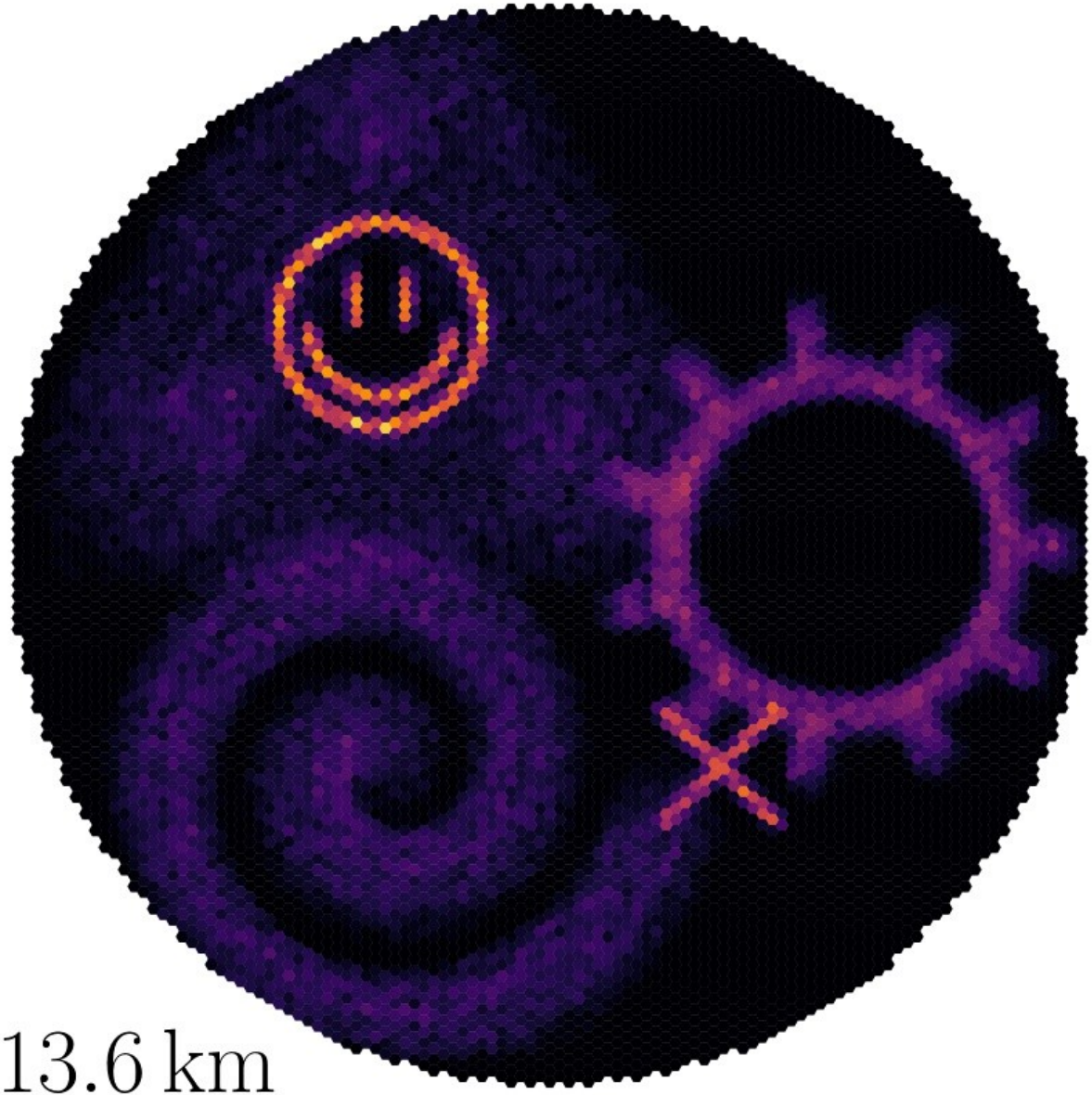

13.6 km

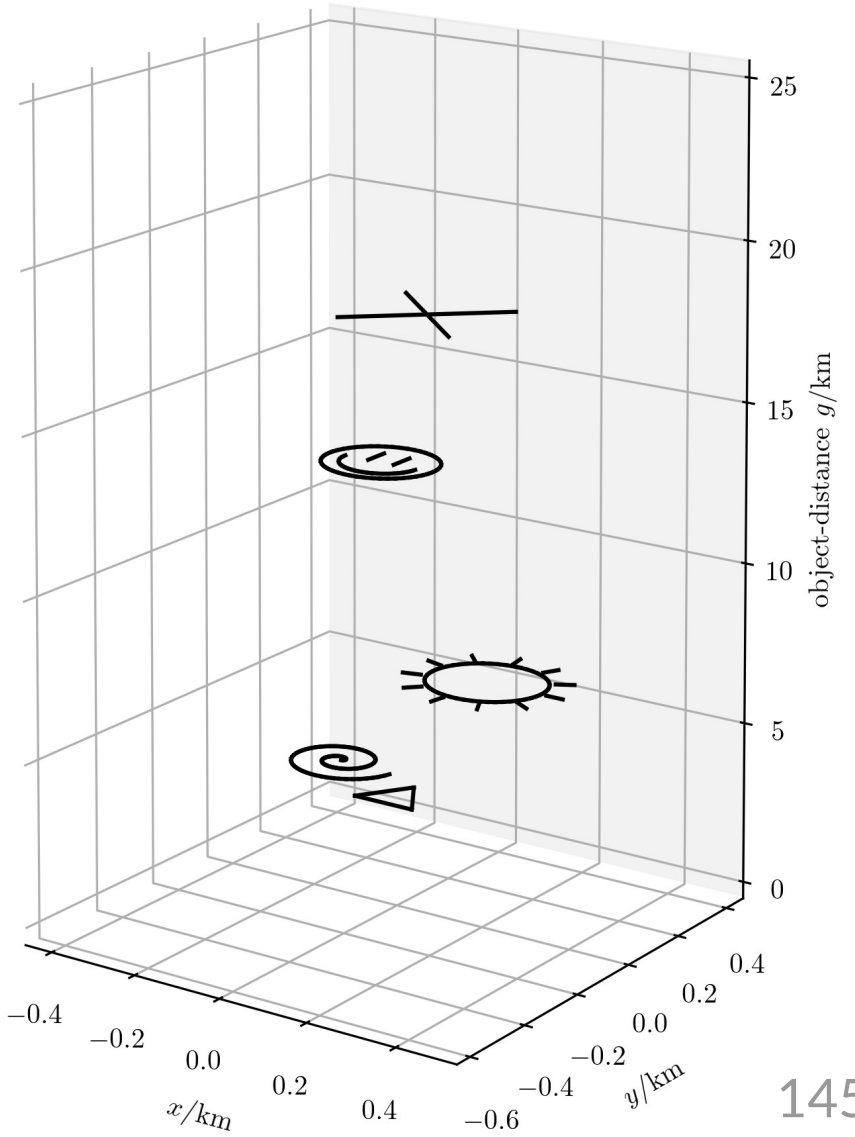
25
20
15
10
5
0
object-distance g/km
−0.4
−0.2
0.0
0.2
0.4
x/km
0.4
0.2
0.0
−0.2
−0.4
−0.6
y/km

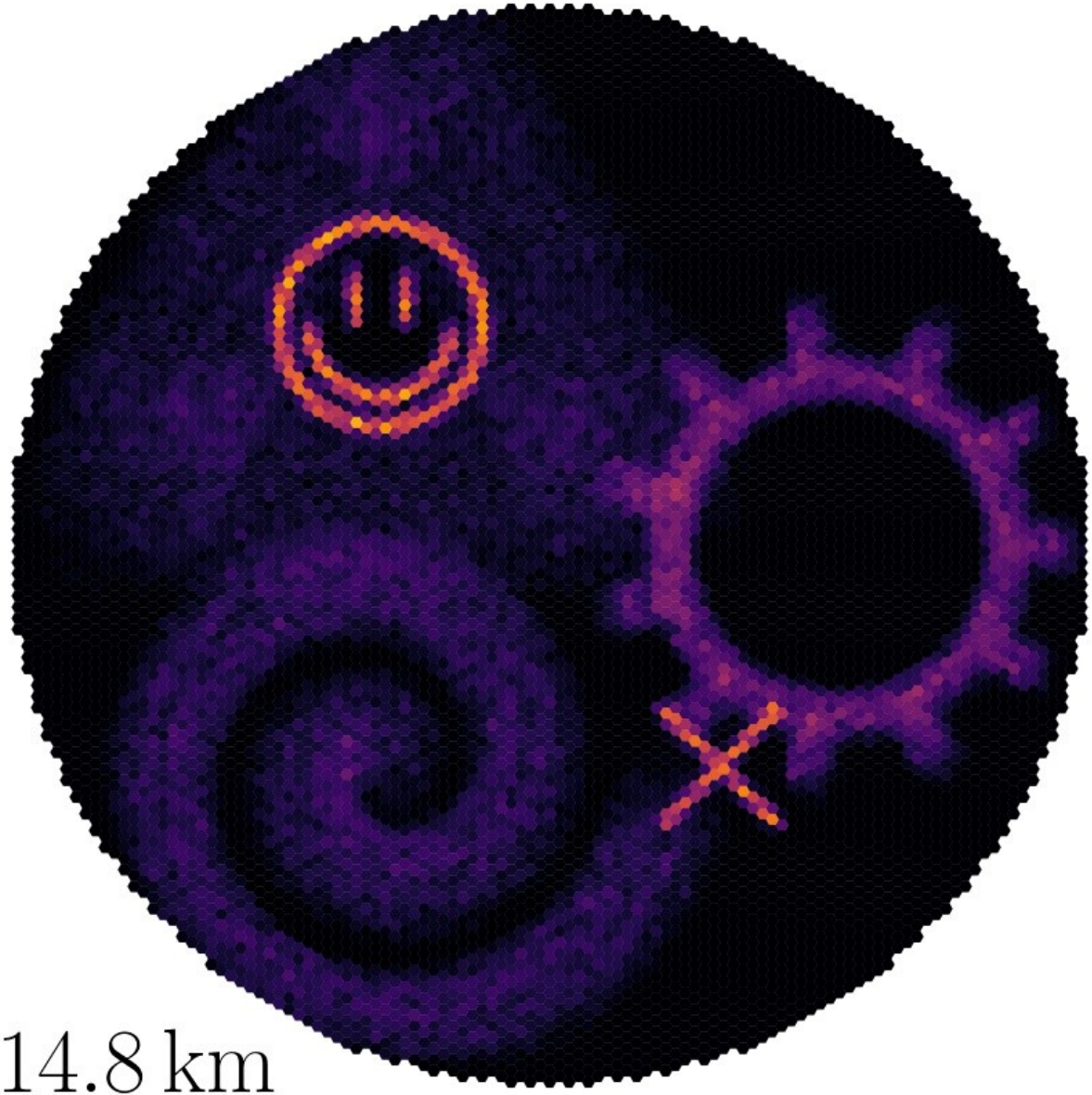

14.8 km

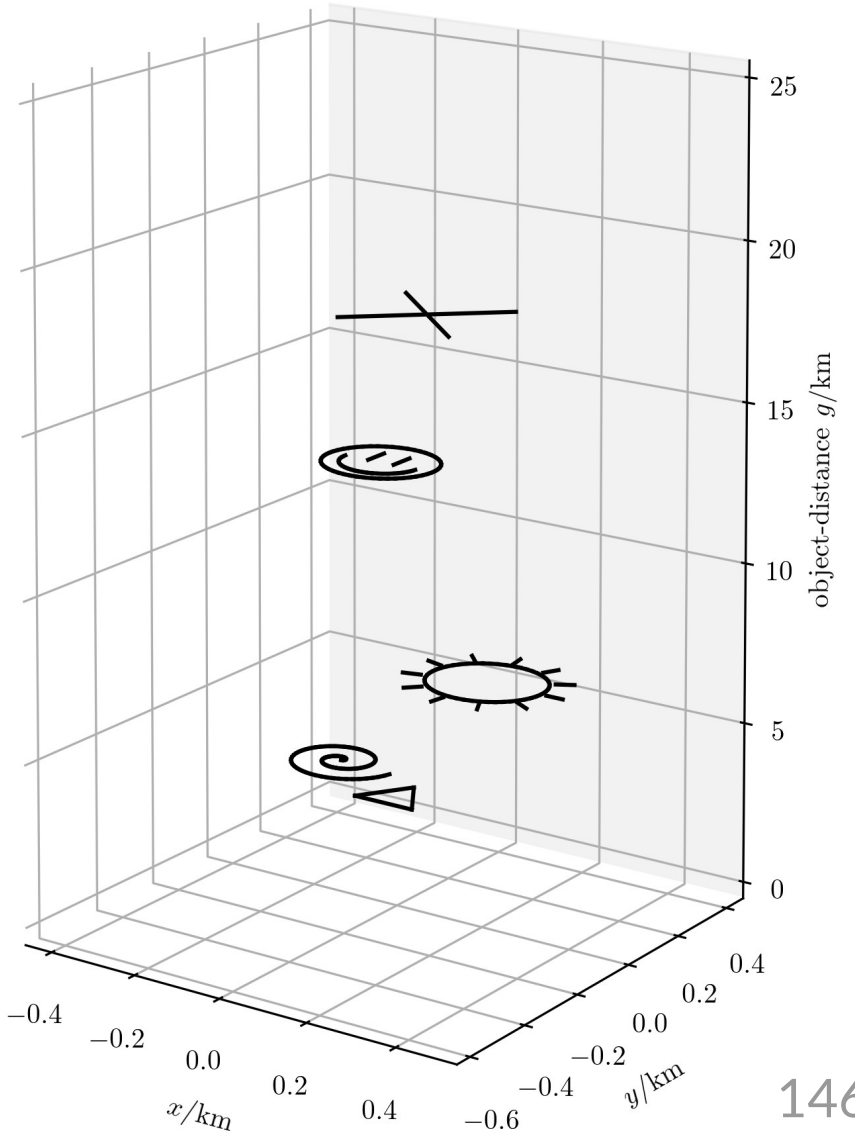
25
20
15
10
5
0
object-distance g/km
−0.4
−0.2
0.0
0.2
0.4
x/km
0.4
0.2
0.0
−0.2
−0.4
−0.6
y/km

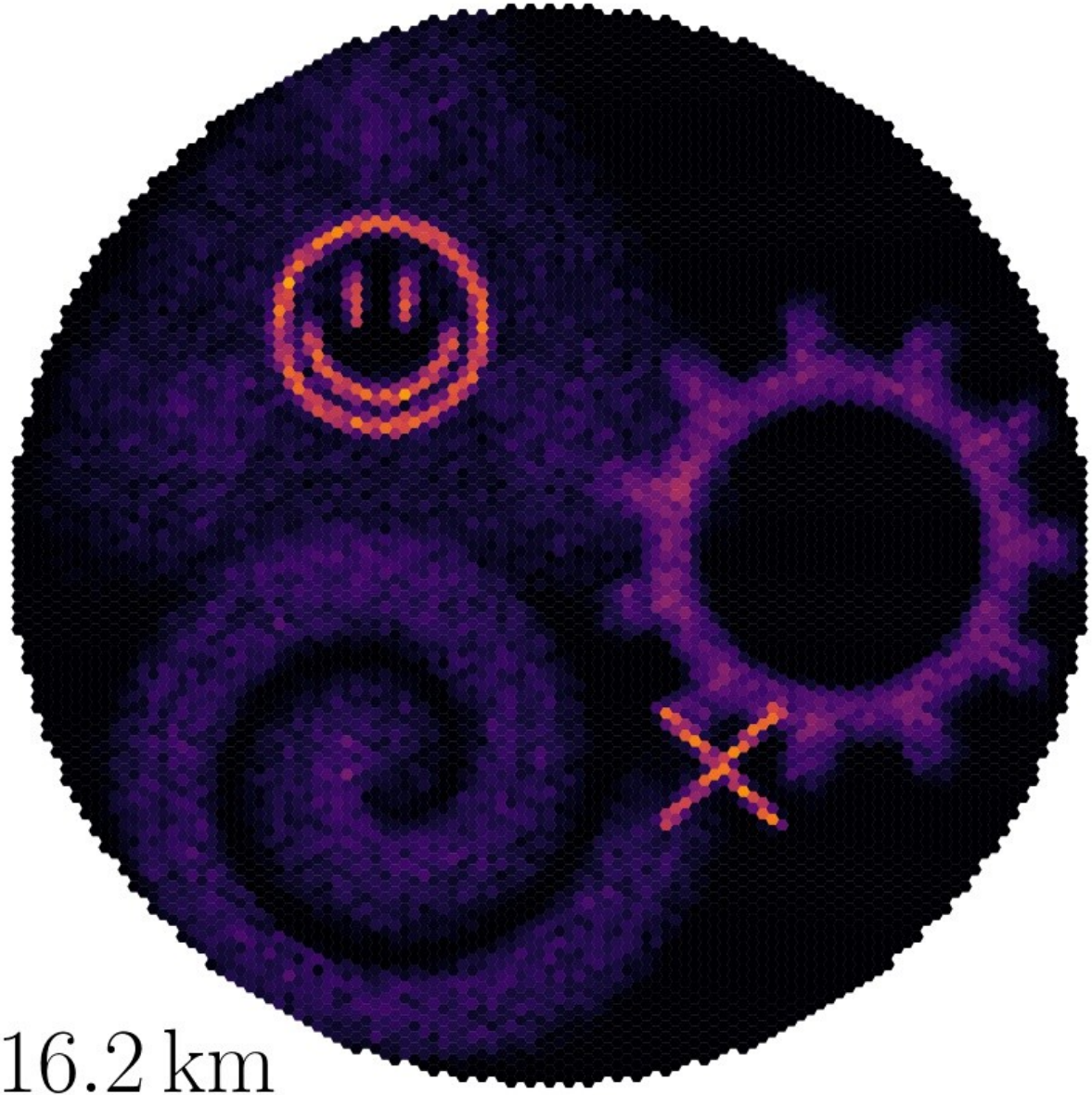

16.2 km

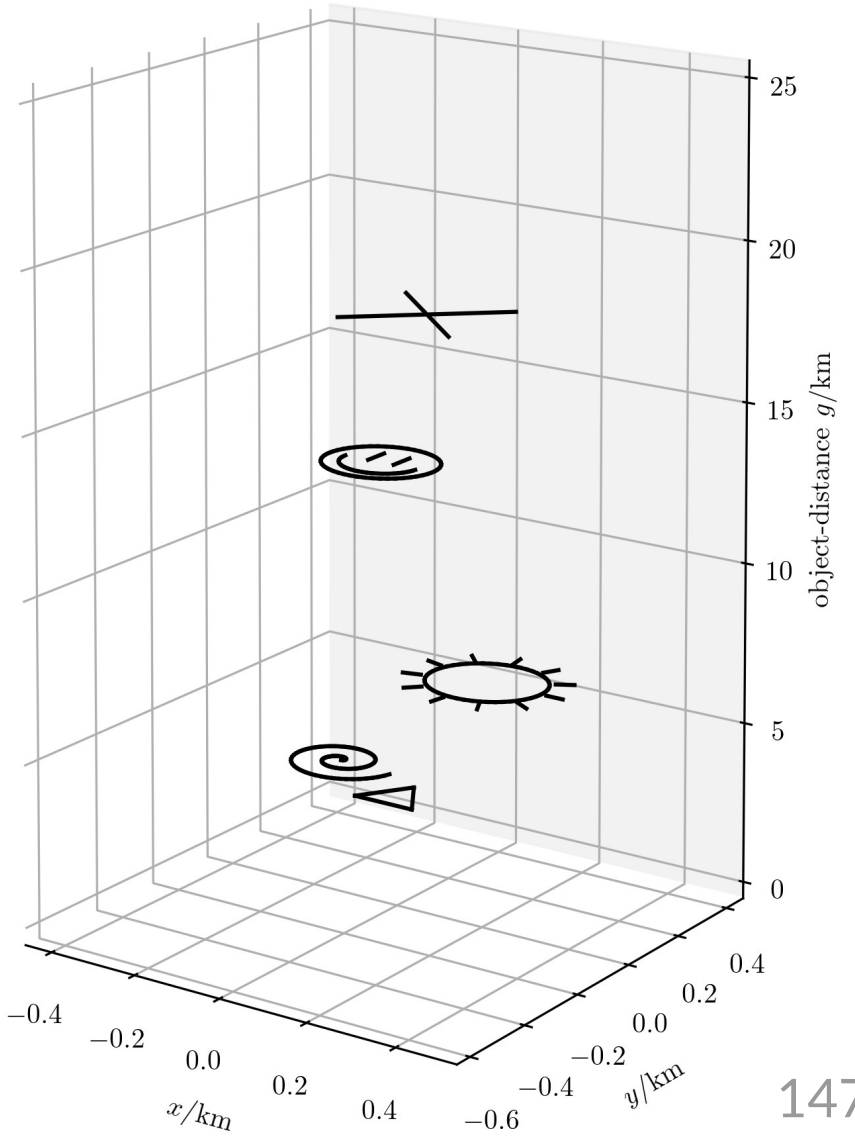
25
20
15
10
5
0
object-distance g/km
−0.4
−0.2
0.0
0.2
0.4
x/km
0.4
0.2
0.0
−0.2
−0.4
−0.6
y/km

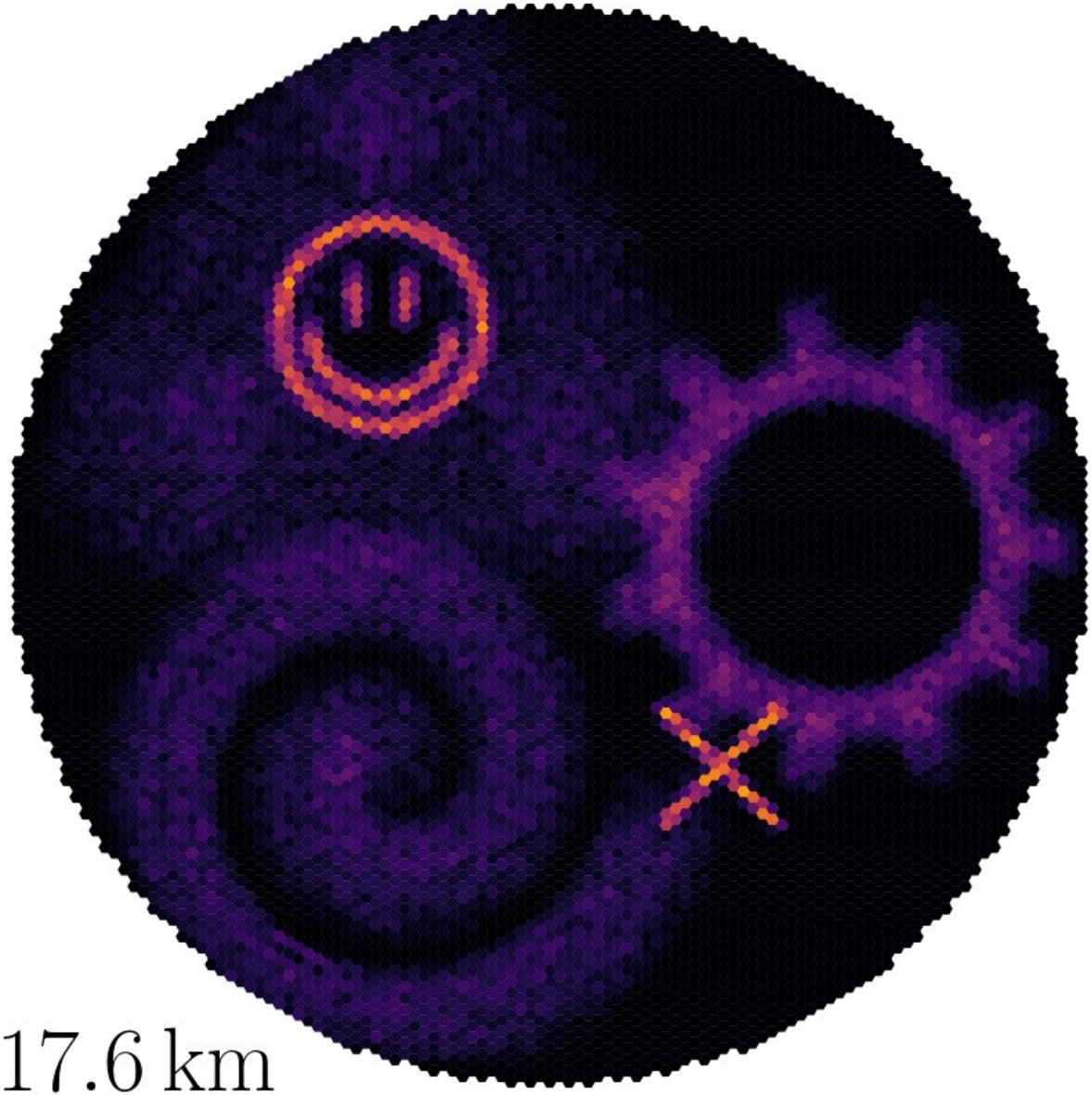

17.6 km

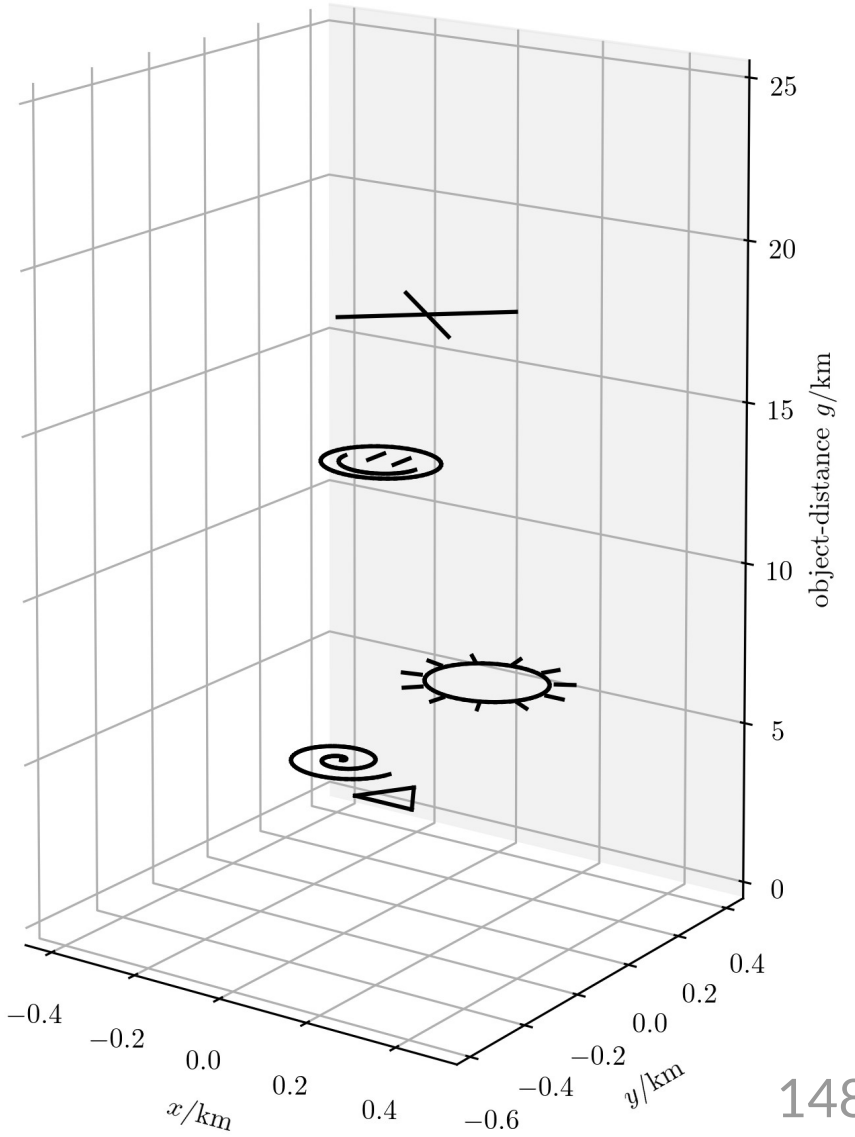
25
20
15
10
5
0
object-distance g/km
0.4
0.2
0.0
−0.2
−0.4
−0.6
y/km
−0.4
−0.2
0.0
0.2
0.4
x/km

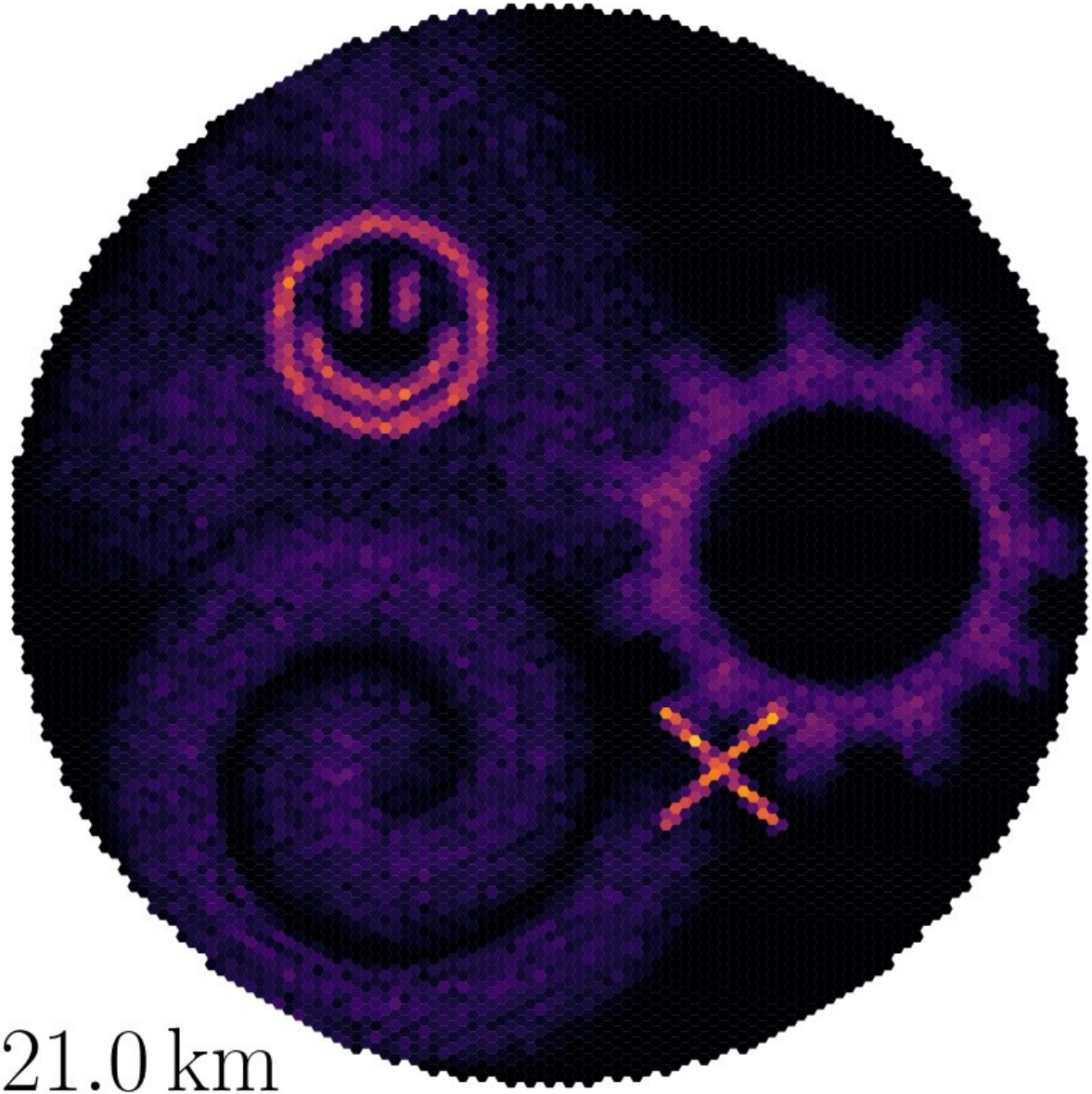

21.0 km

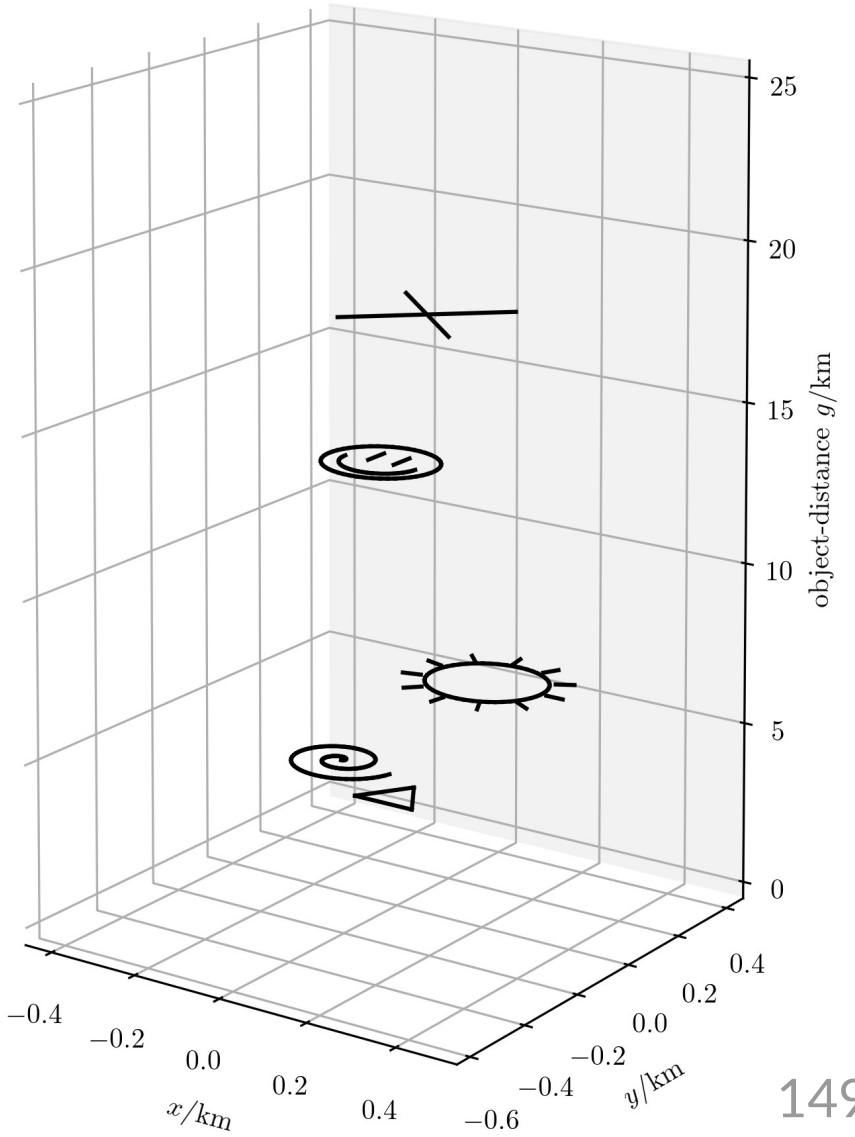
25
20
15
10
5
0
object-distance g/km
−0.4
−0.2
0.0
0.2
0.4
x/km
0.4
0.2
0.0
−0.2
−0.4
−0.6
y/km

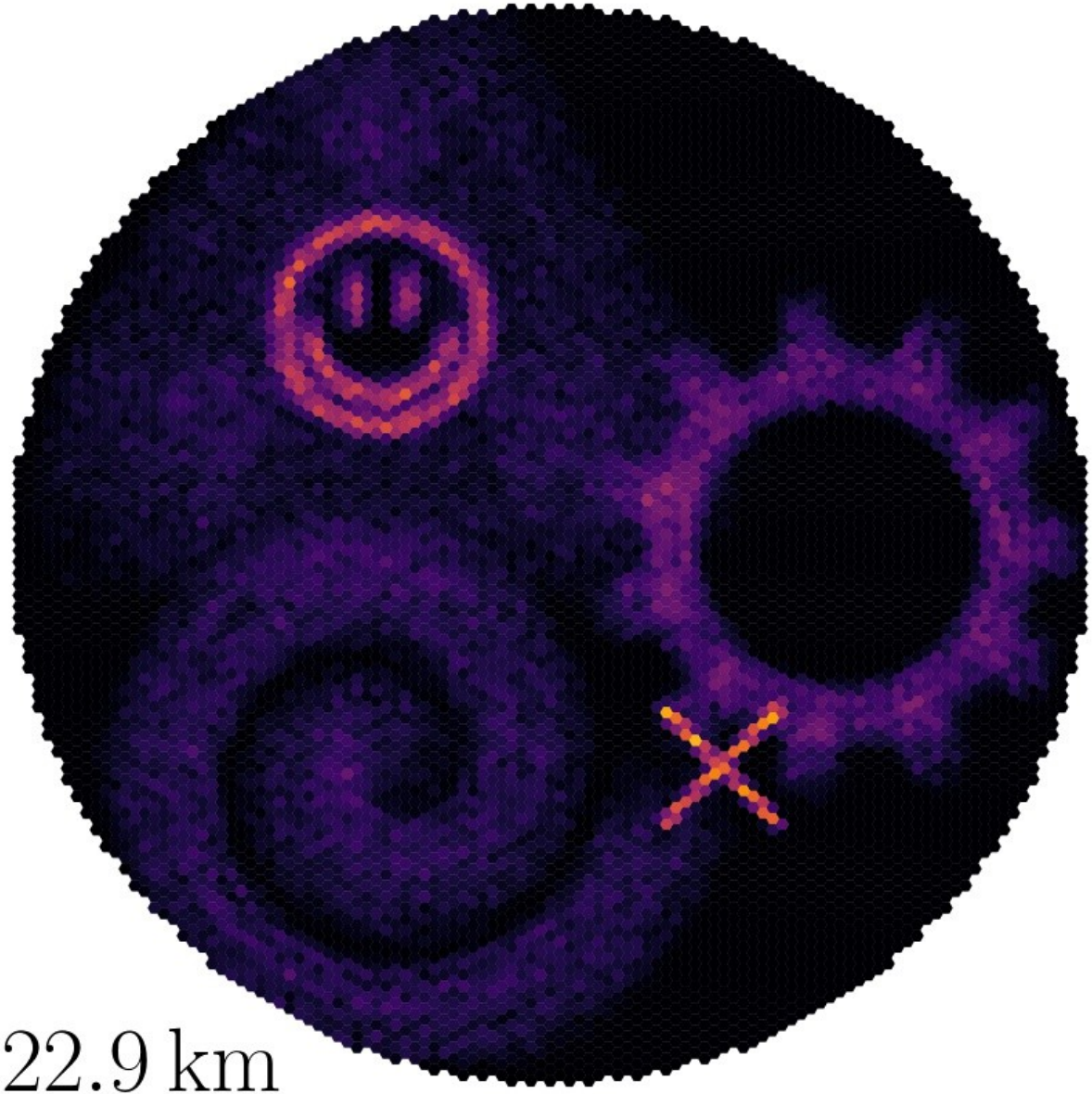

22.9 km

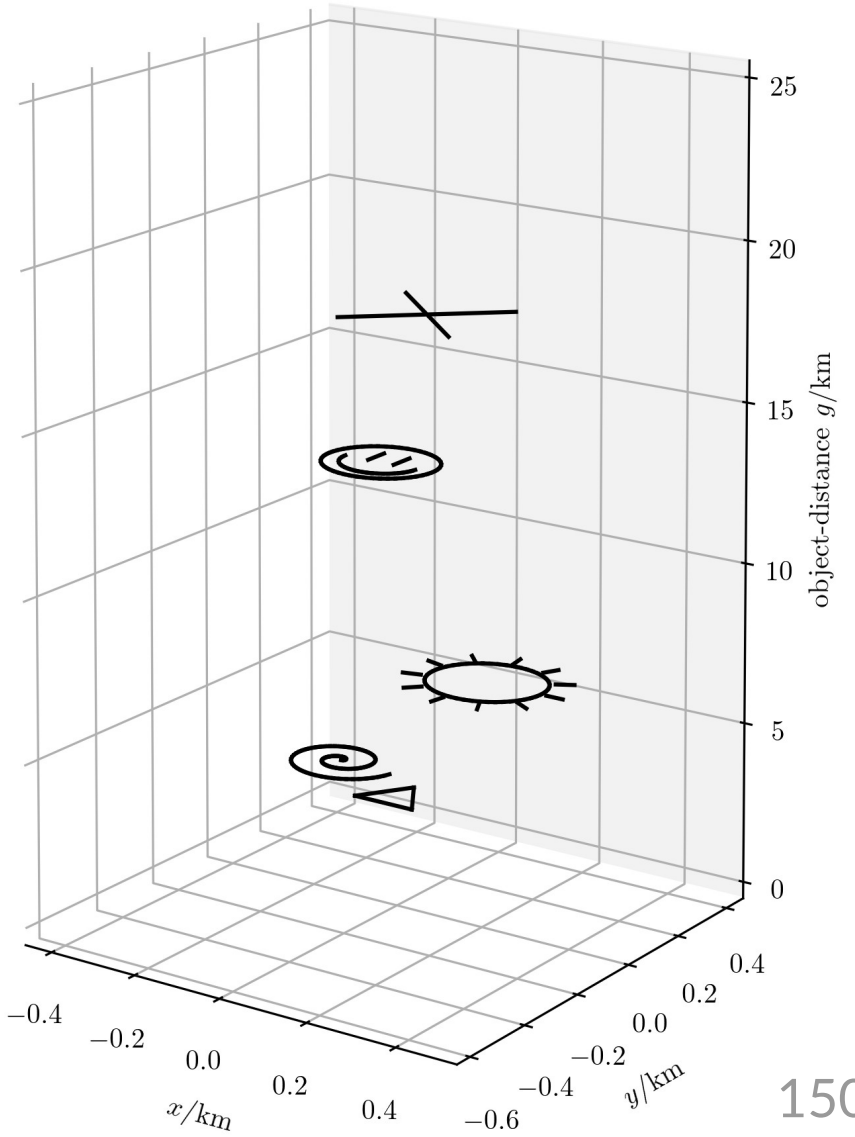
25
20
15
10
5
0
object-distance g/km
0.4
0.2
0.0
−0.2
−0.4
−0.6
y/km
−0.4
−0.2
0.0
0.2
0.4
x/km

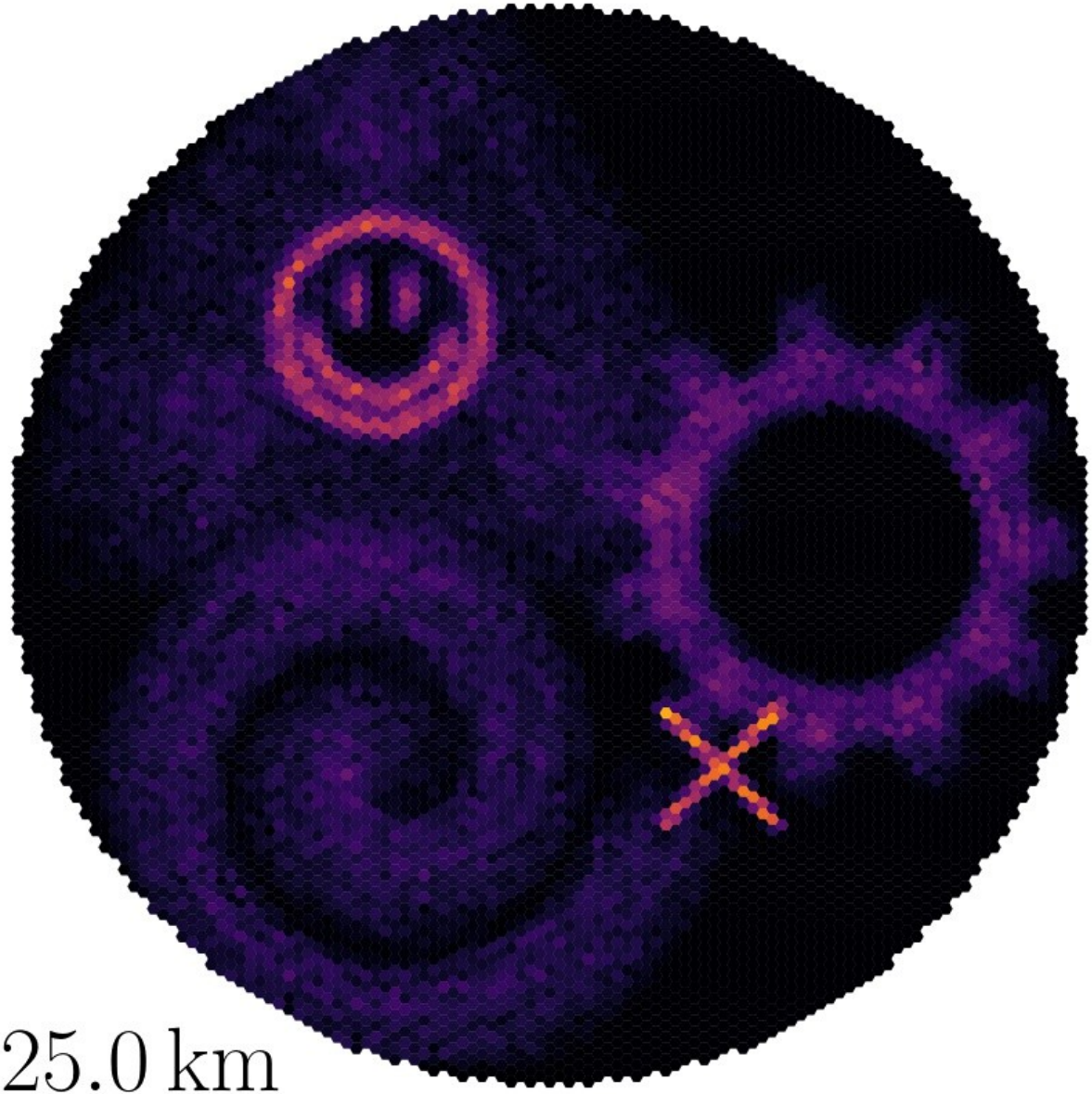
25.0 km

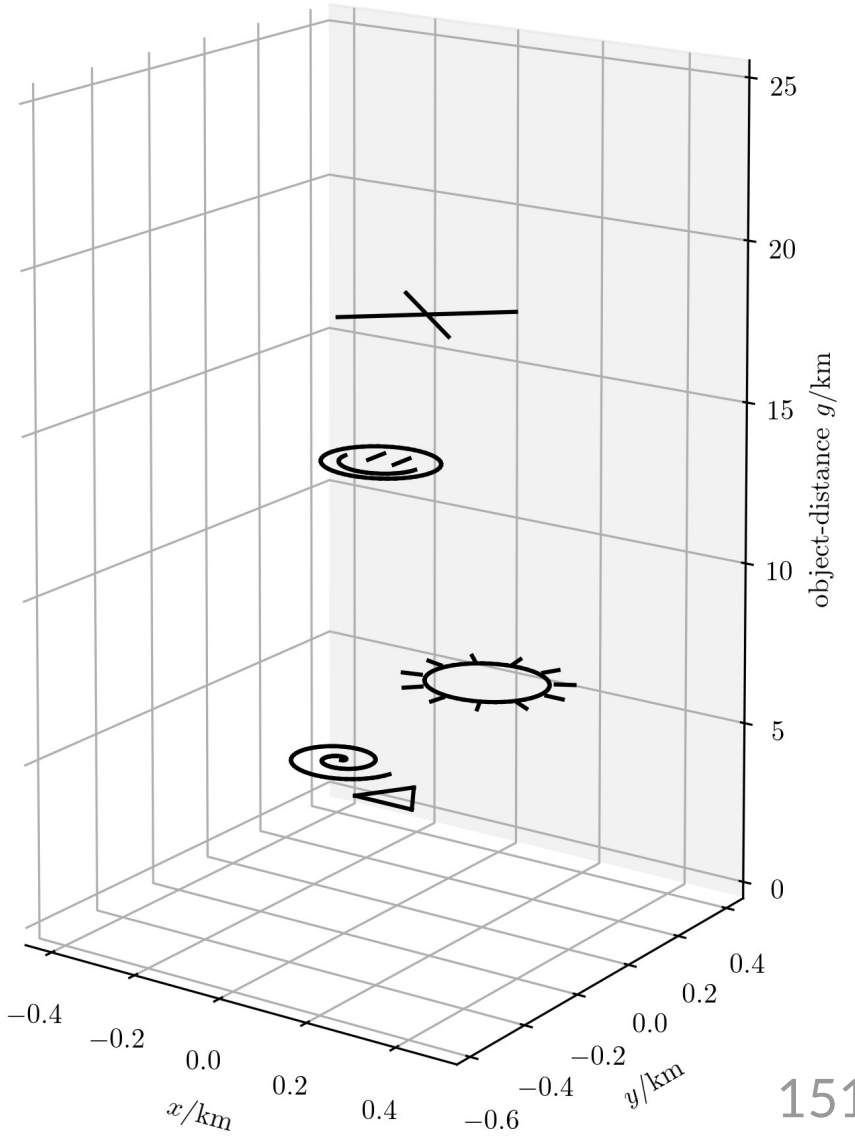
25
20
15
10
5
0
object-distance g/km
0.4
0.2
0.0
−0.2
−0.4
−0.6
y/km
−0.4
−0.2
0.0
0.2
0.4
x/km

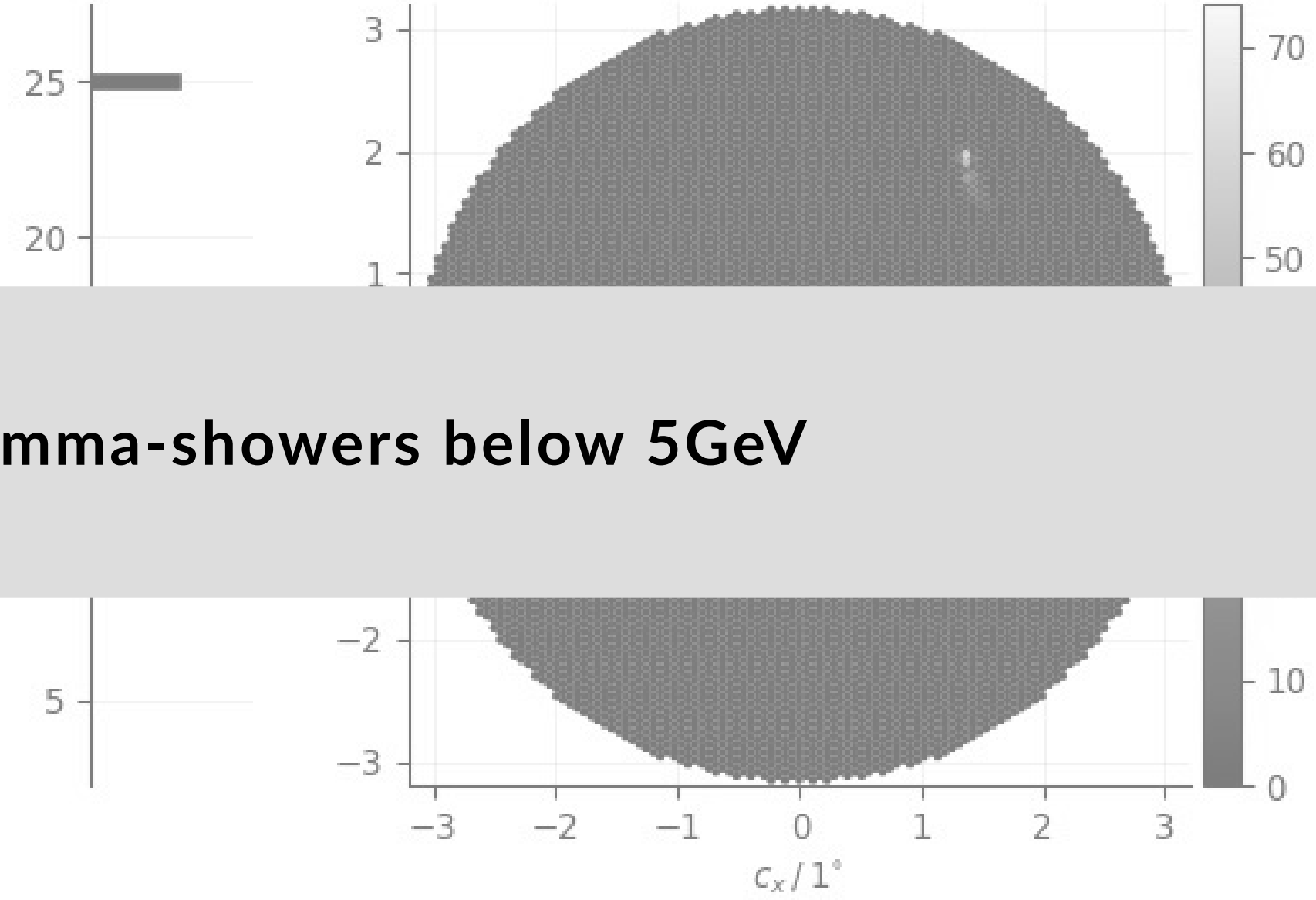

Gamma-showers below 5GeV

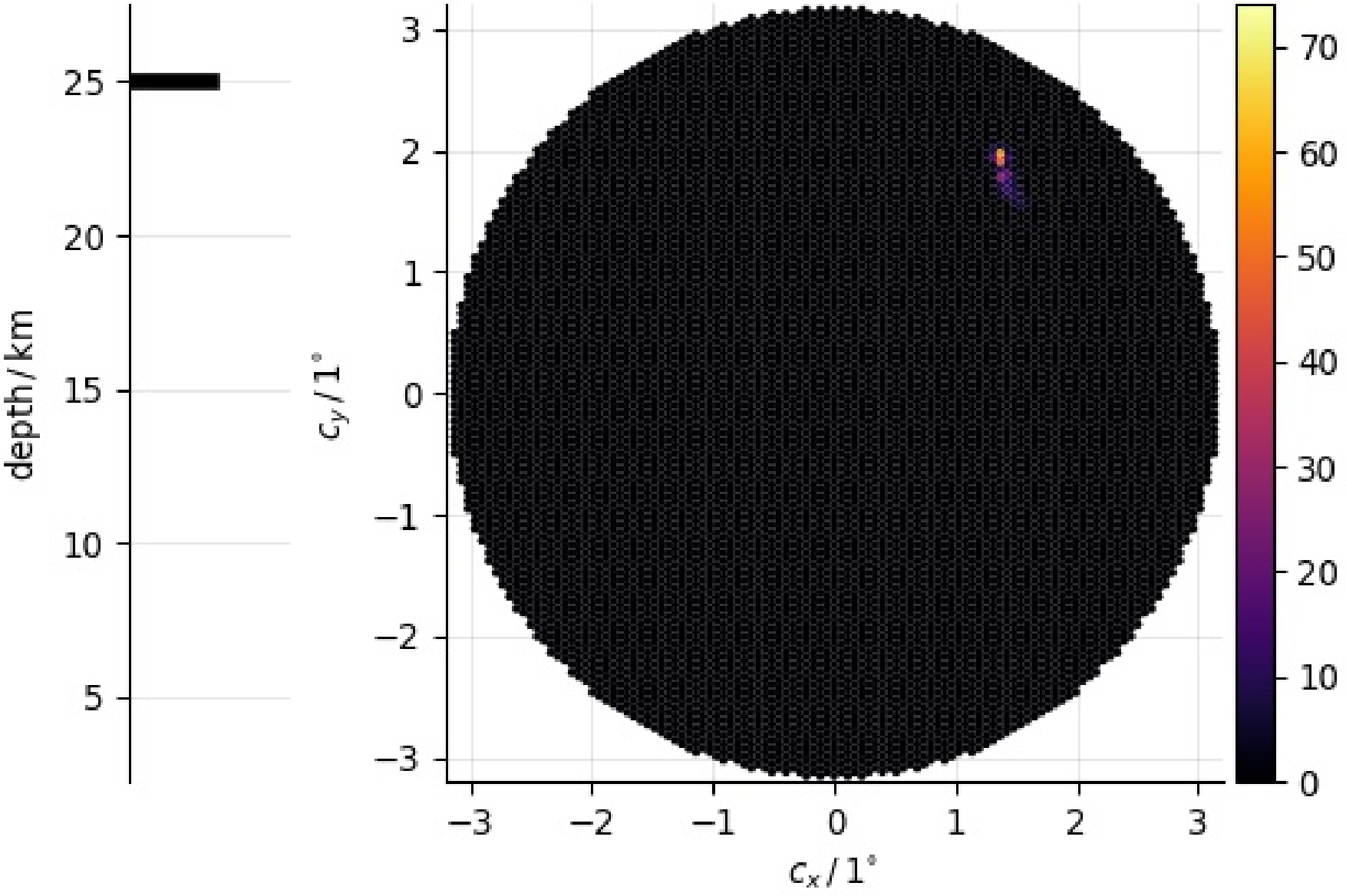
depth / km
25
20
15
10
5
$c_y / 1^\circ$
3
2
1
0
−1
−2
−3
$c_x / 1^\circ$
−3
−2
−1
0
1
2
3
70
60
50
40
30
20
10
0

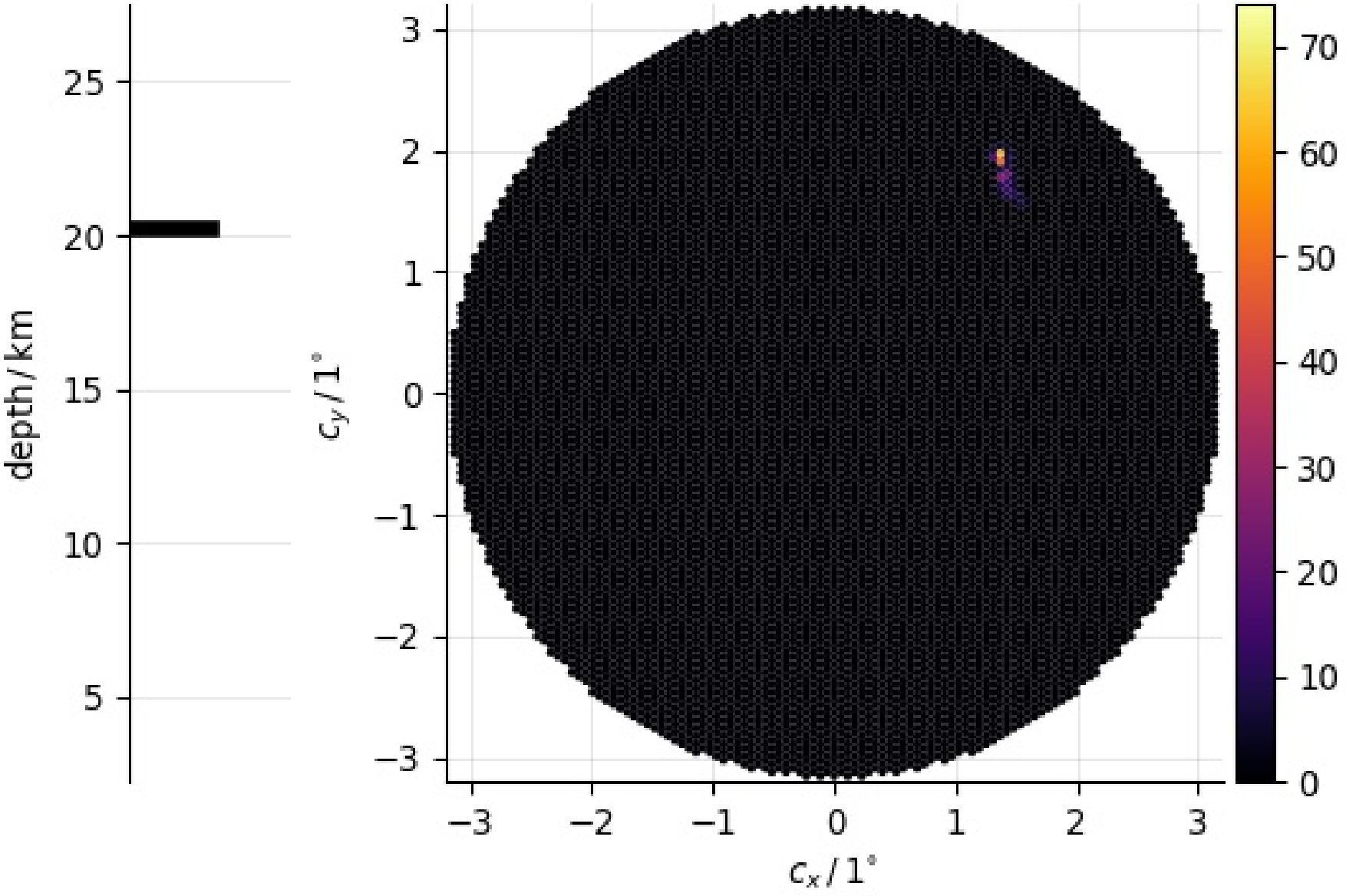
depth / km
25
20
15
10
5
$c_y / 1^\circ$
3
2
1
0
−1
−2
−3
$c_x / 1^\circ$
−3
−2
−1
0
1
2
3
70
60
50
40
30
20
10
0

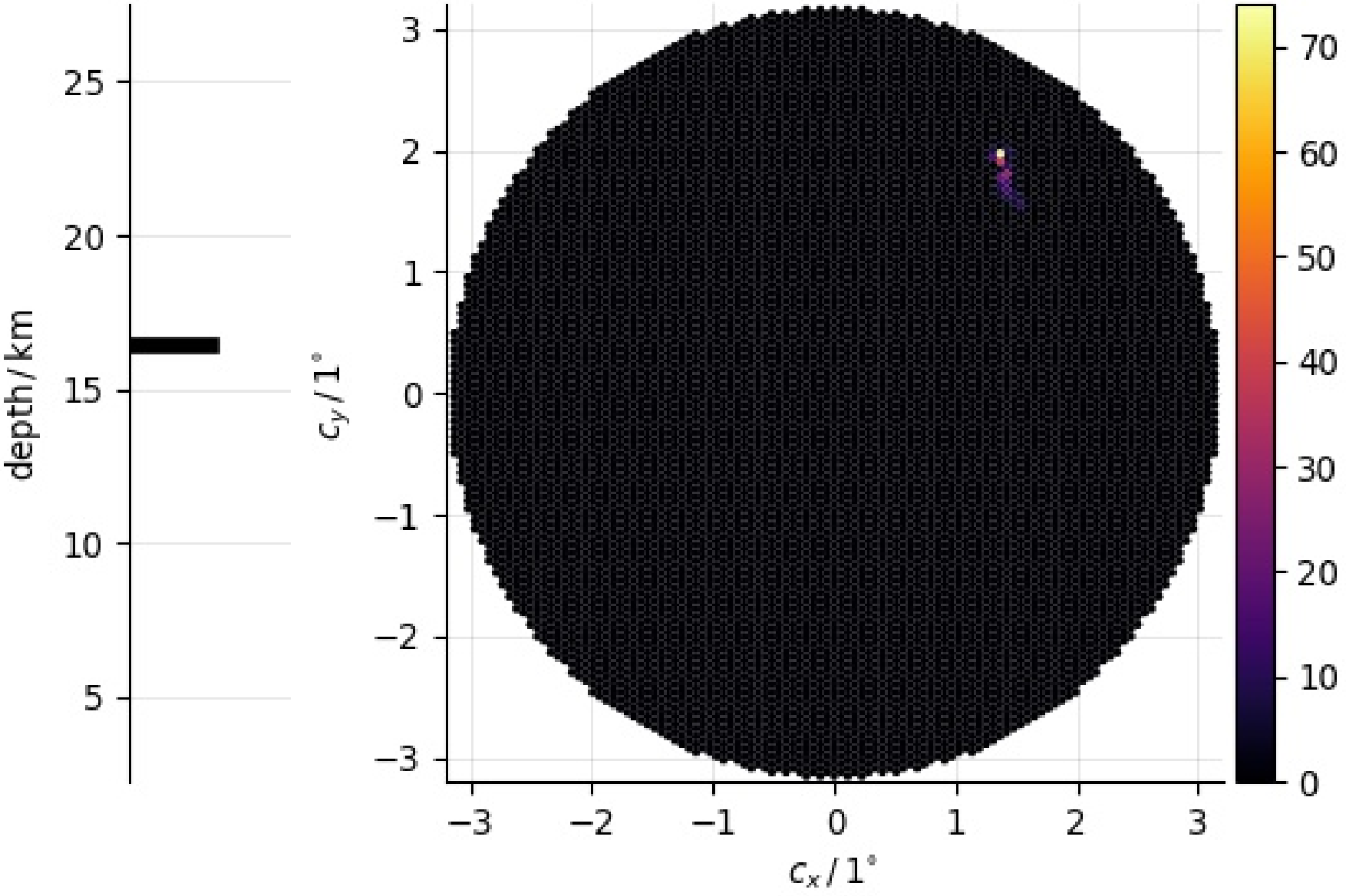
depth / km
25
20
15
10
5
$c_y / 1^\circ$
3
2
1
0
−1
−2
−3
$c_x / 1^\circ$
−3
−2
−1
0
1
2
3
70
60
50
40
30
20
10
0

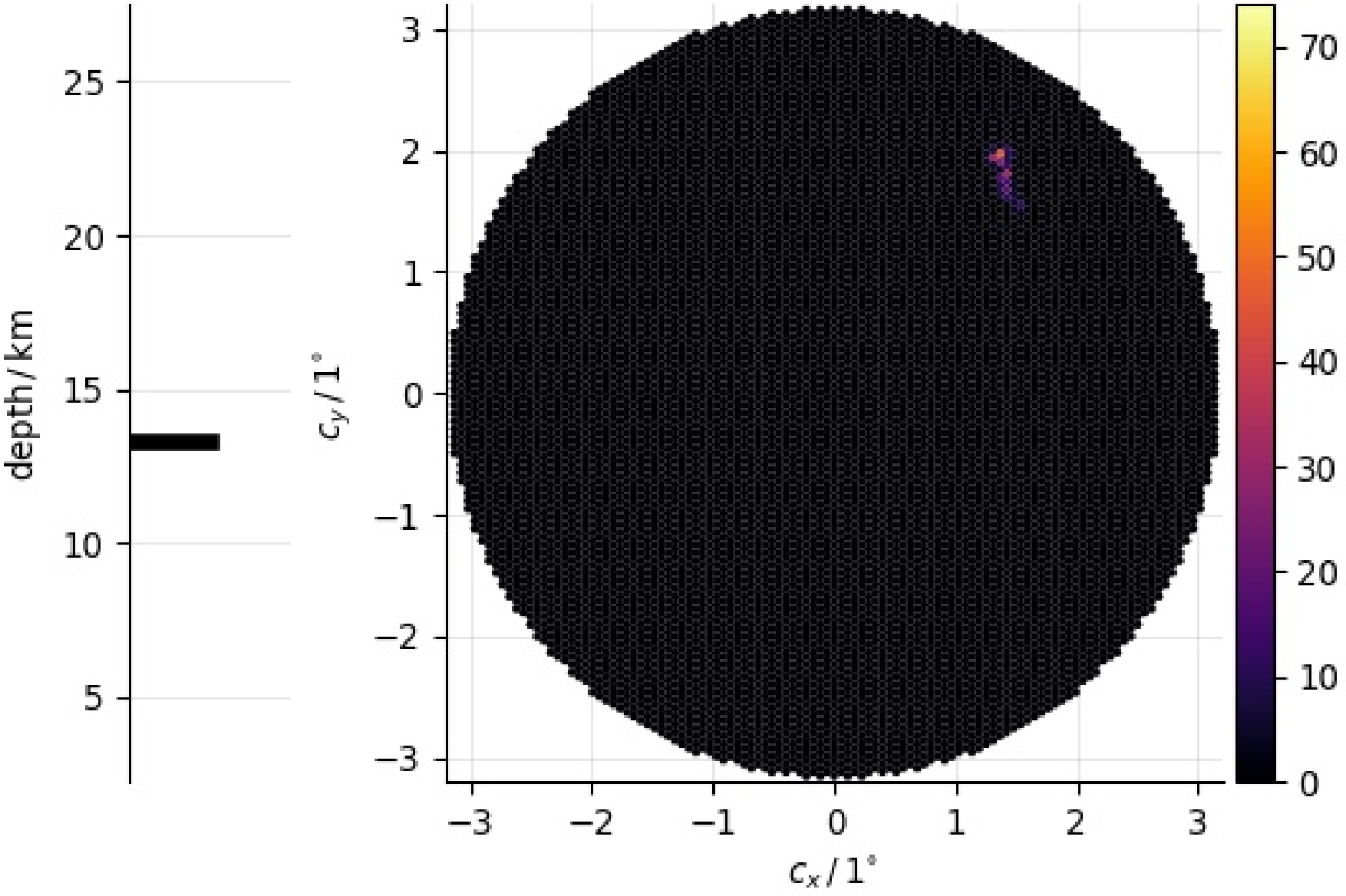
depth / km
25
20
15
10
5
c_y / 1°
3
2
1
0
−1
−2
−3
−3
−2
−1
0
1
2
3
c_x / 1°
70
60
50
40
30
20
10
0

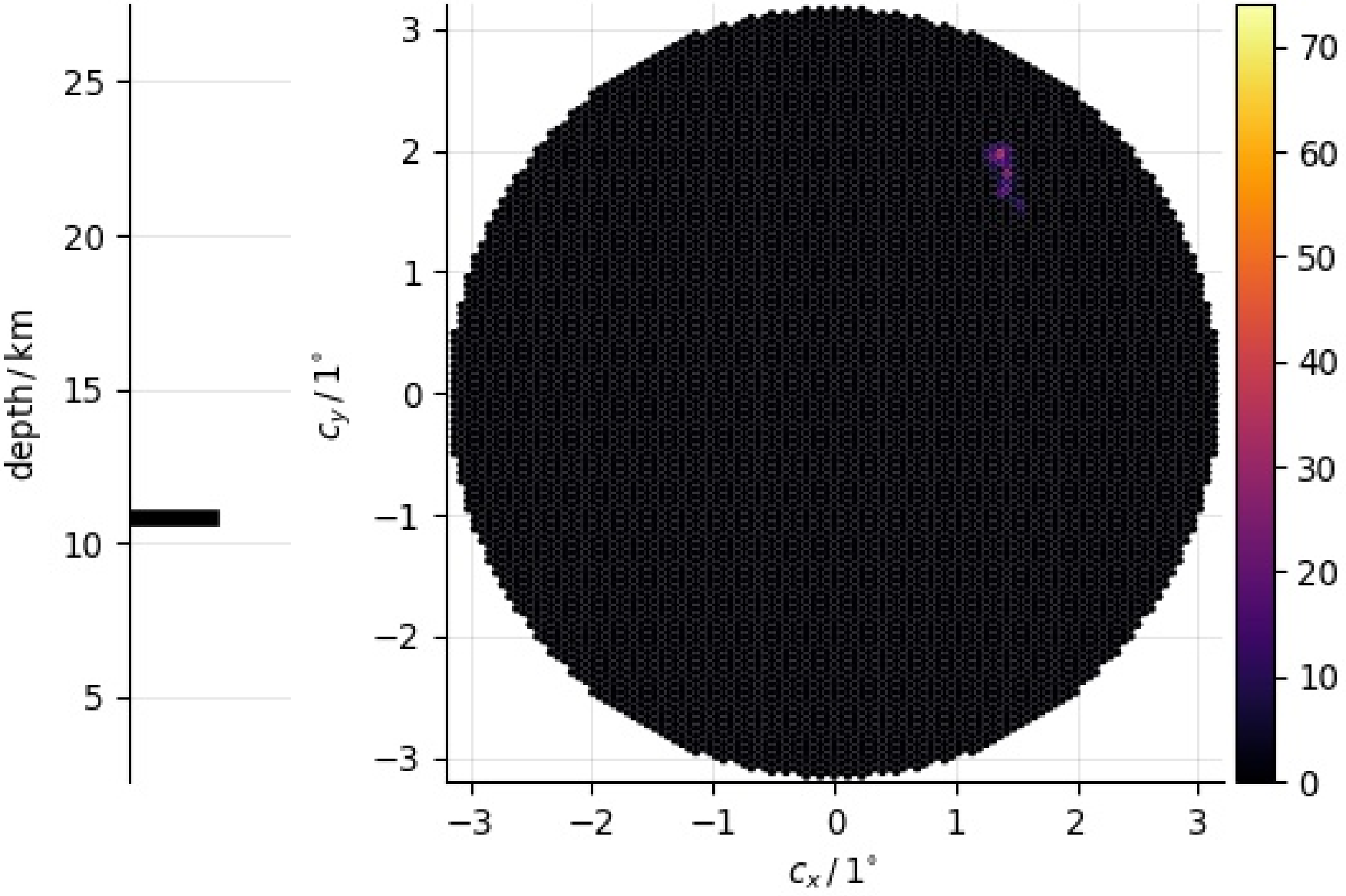
depth / km
25
20
15
10
5
c_y / 1°
3
2
1
0
−1
−2
−3
−3
−2
−1
0
1
2
3
c_x / 1°
70
60
50
40
30
20
10
0

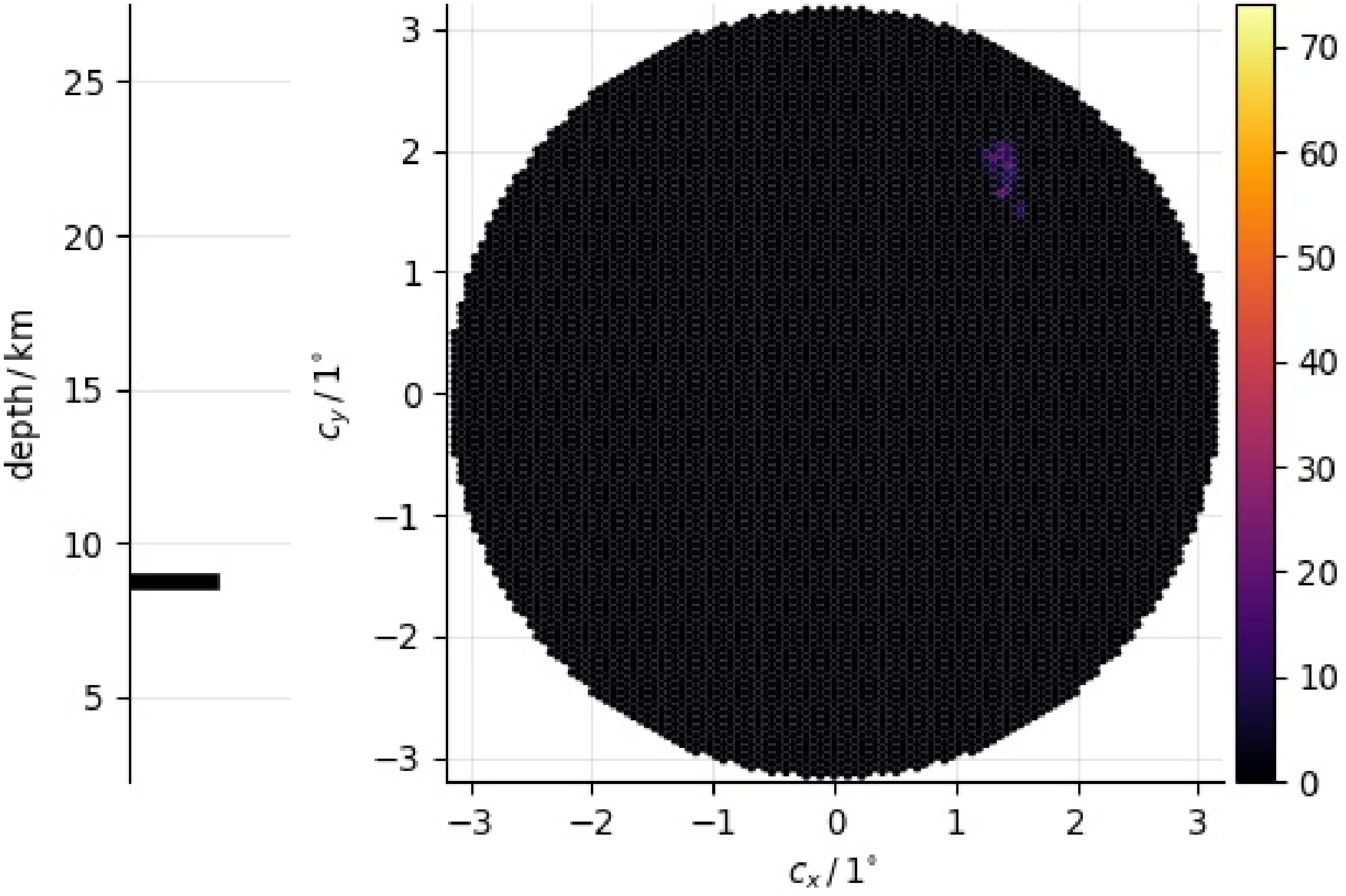
depth / km
25
20
15
10
5
$c_y / 1^\circ$
3
2
1
0
−1
−2
−3
$c_x / 1^\circ$
−3
−2
−1
0
1
2
3
70
60
50
40
30
20
10
0

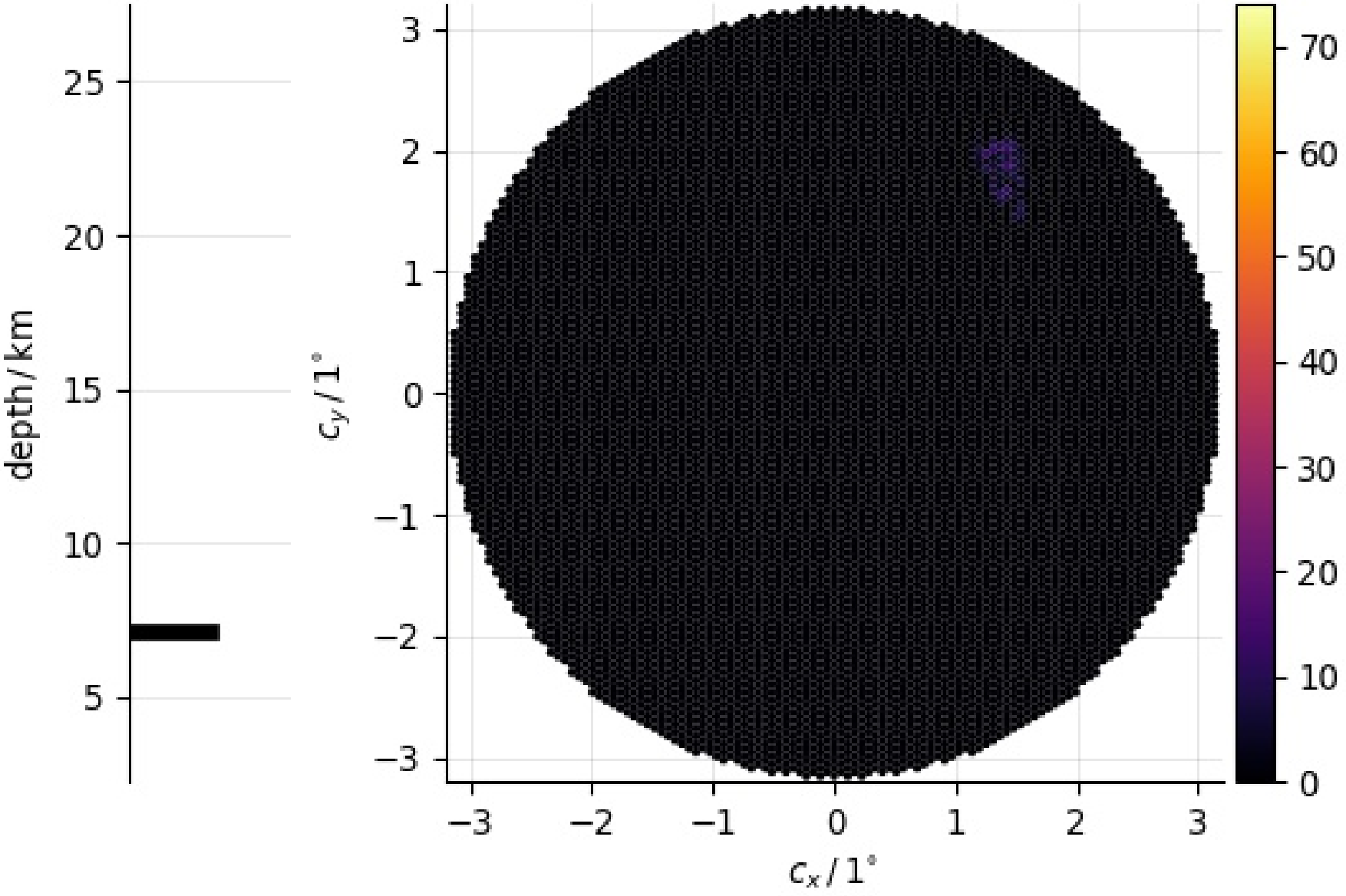
depth / km
25
20
15
10
5
$c_y / 1^\circ$
3
2
1
0
−1
−2
−3
$c_x / 1^\circ$
−3
−2
−1
0
1
2
3
70
60
50
40
30
20
10
0

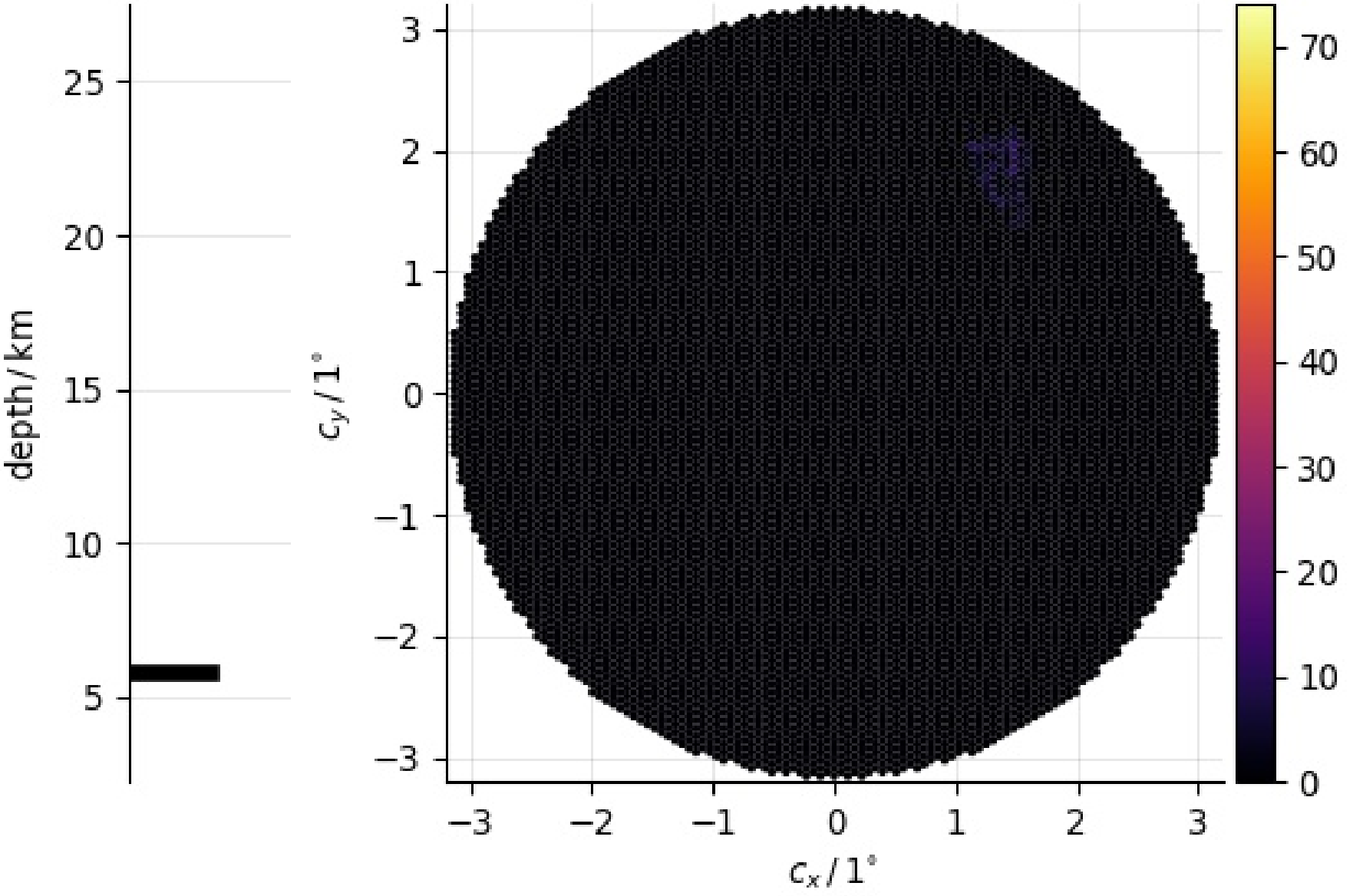
depth / km
25
20
15
10
5
$c_y / 1^\circ$
3
2
1
0
−1
−2
−3
−3
−2
−1
0
1
2
3
$c_x / 1^\circ$
70
60
50
40
30
20
10
0

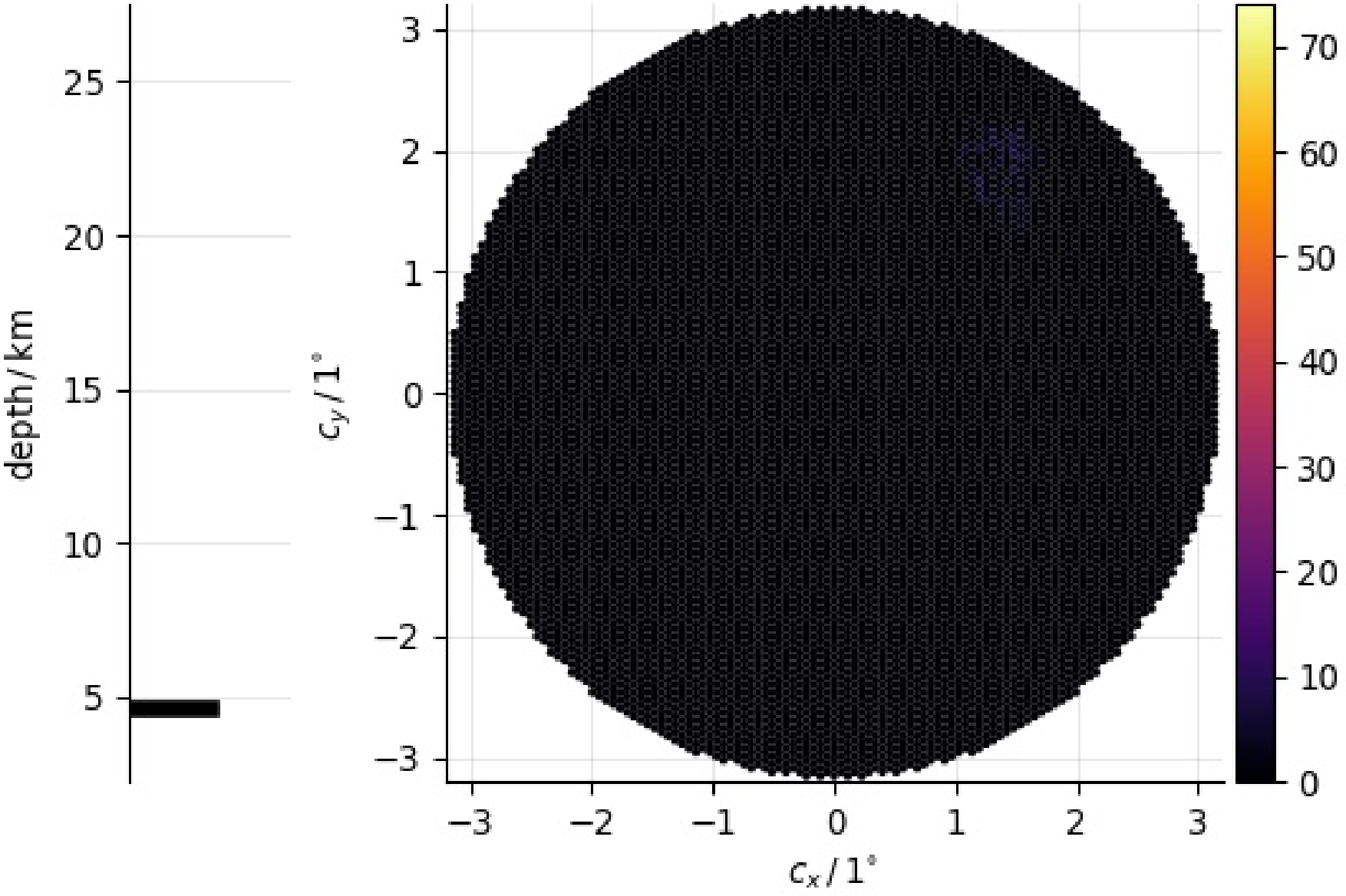
depth / km
25
20
15
10
5
$c_y / 1^\circ$
3
2
1
0
−1
−2
−3
−3
−2
−1
0
1
2
3
$c_x / 1^\circ$
70
60
50
40
30
20
10
0

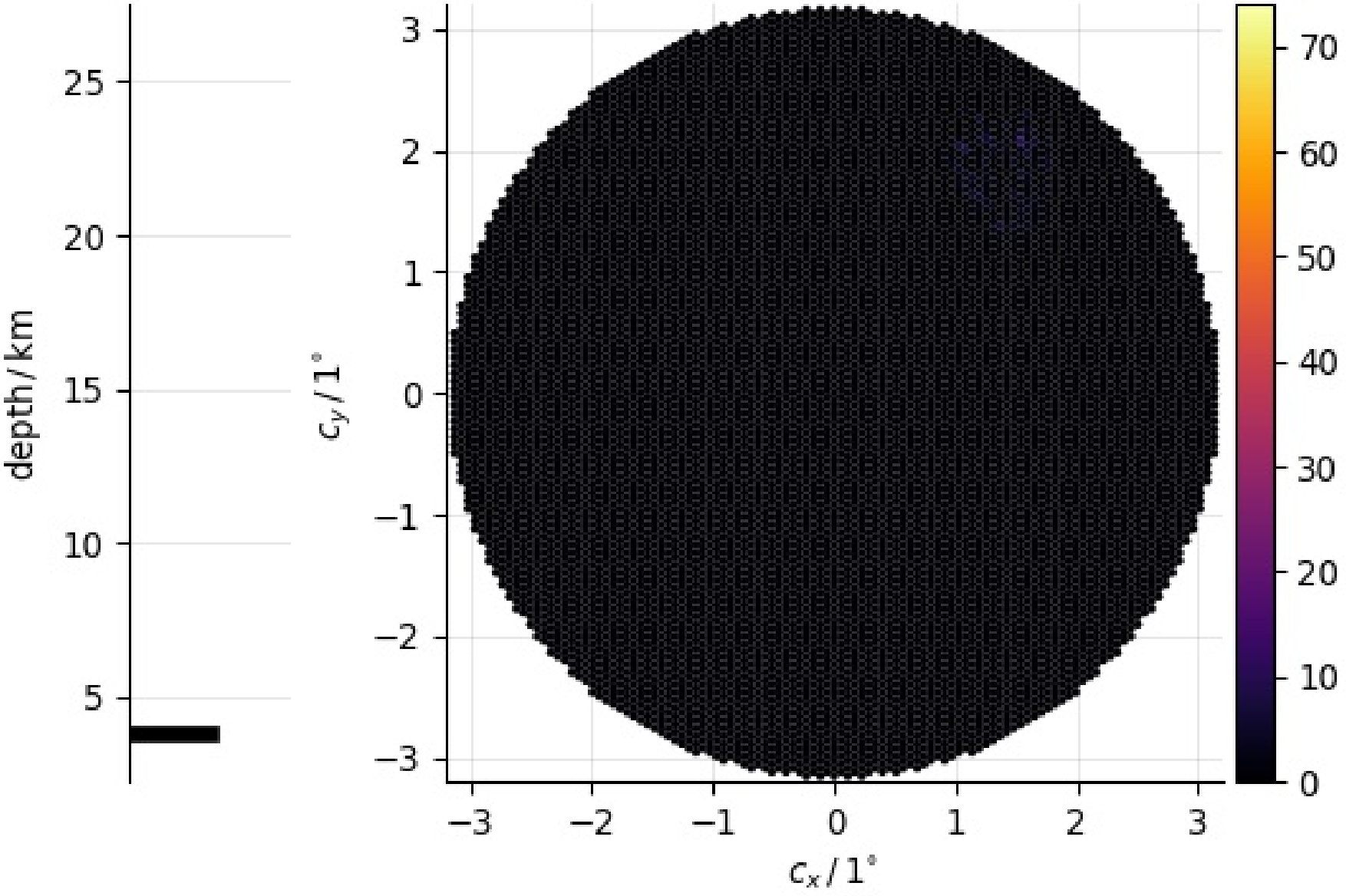
depth / km
25
20
15
10
5
$c_y / 1^\circ$
3
2
1
0
−1
−2
−3
$c_x / 1^\circ$
−3
−2
−1
0
1
2
3
70
60
50
40
30
20
10
0

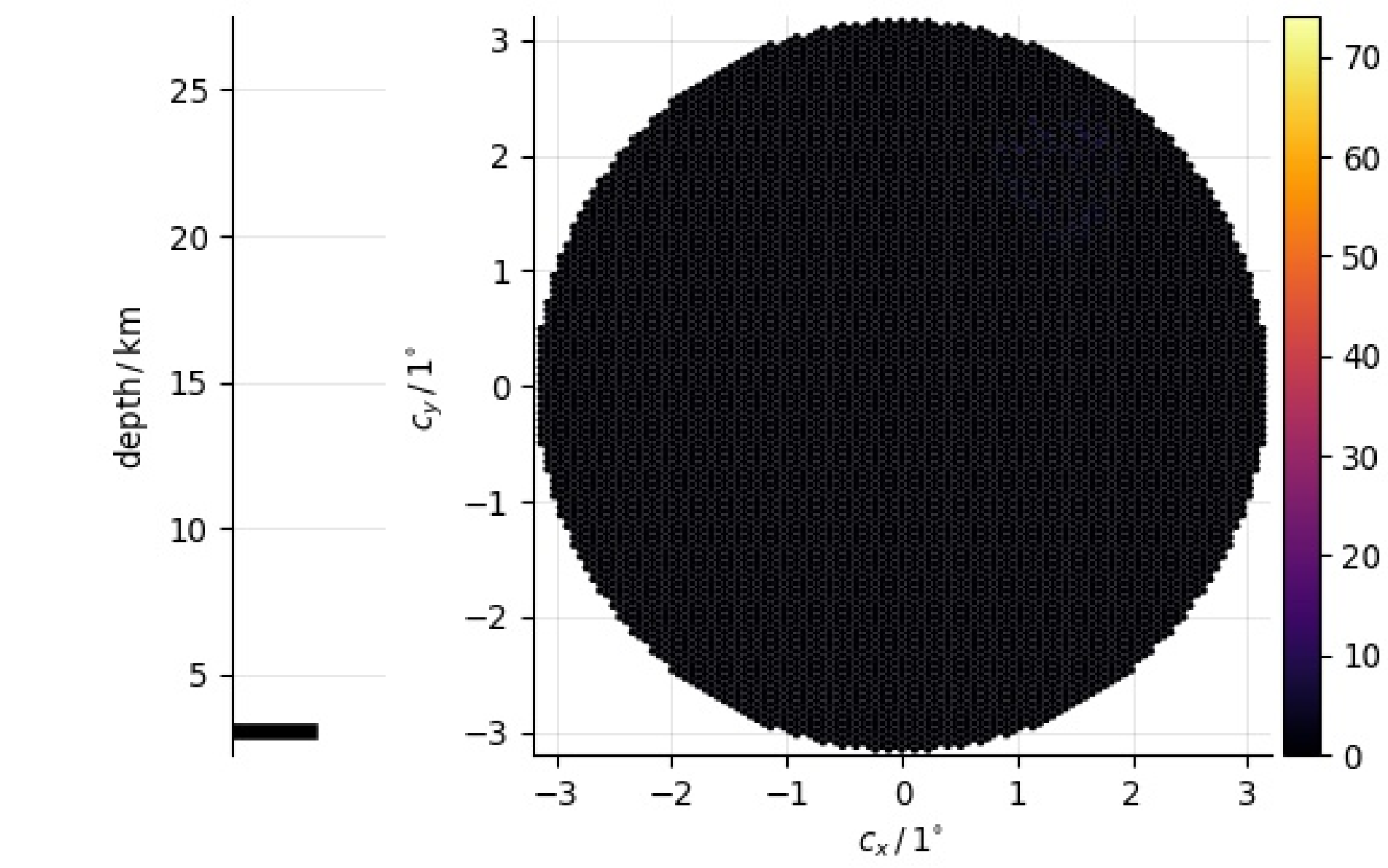
depth / km
25
20
15
10
5
$c_y / 1^\circ$
3
2
1
0
−1
−2
−3
−3
−2
−1
0
1
2
3
$c_x / 1^\circ$
70
60
50
40
30
20
10
0

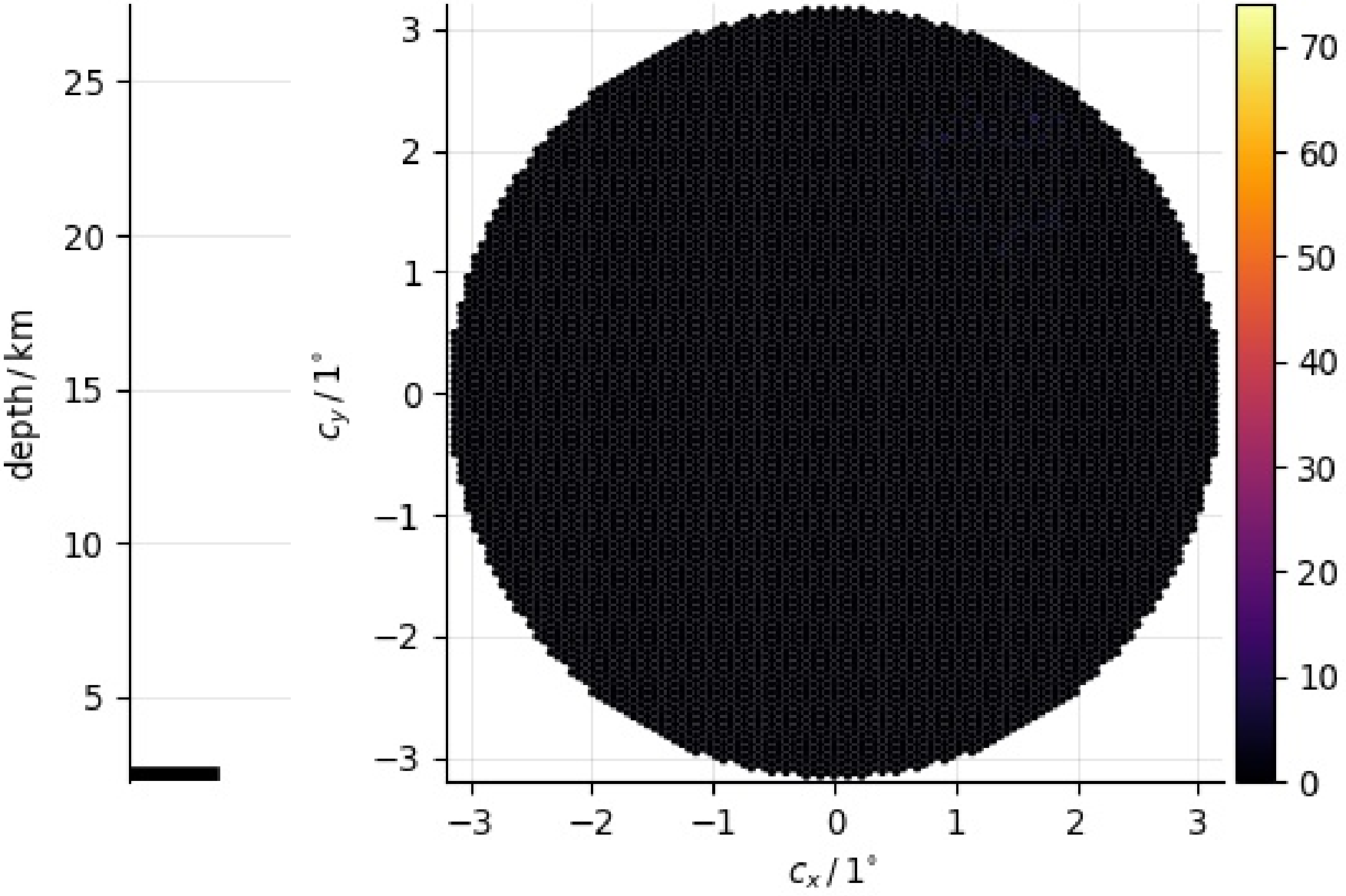
depth / km
25
20
15
10
5
$c_y / 1^\circ$
3
2
1
0
−1
−2
−3
$c_x / 1^\circ$
−3
−2
−1
0
1
2
3
70
60
50
40
30
20
10
0

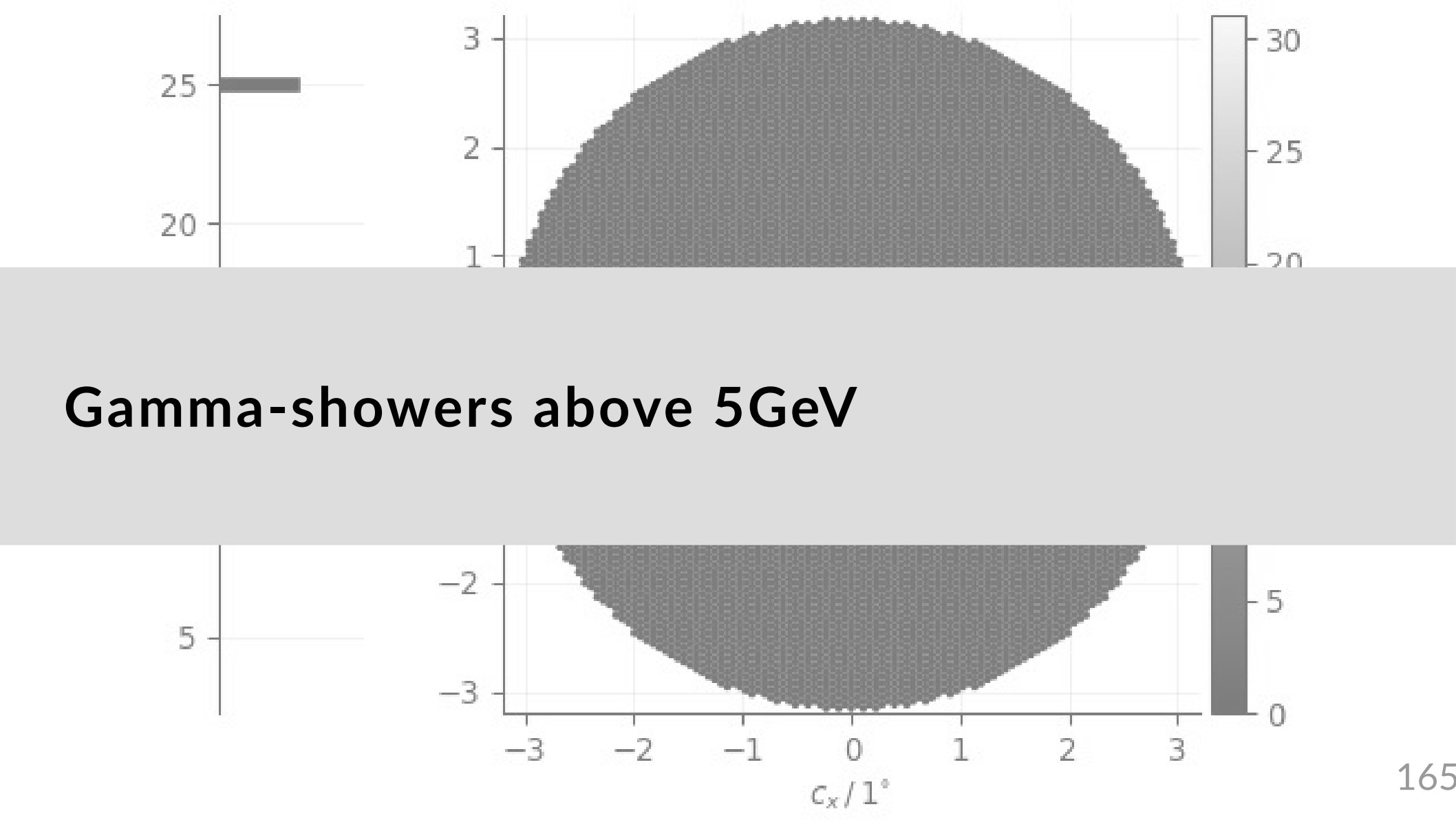

Gamma-showers above 5GeV

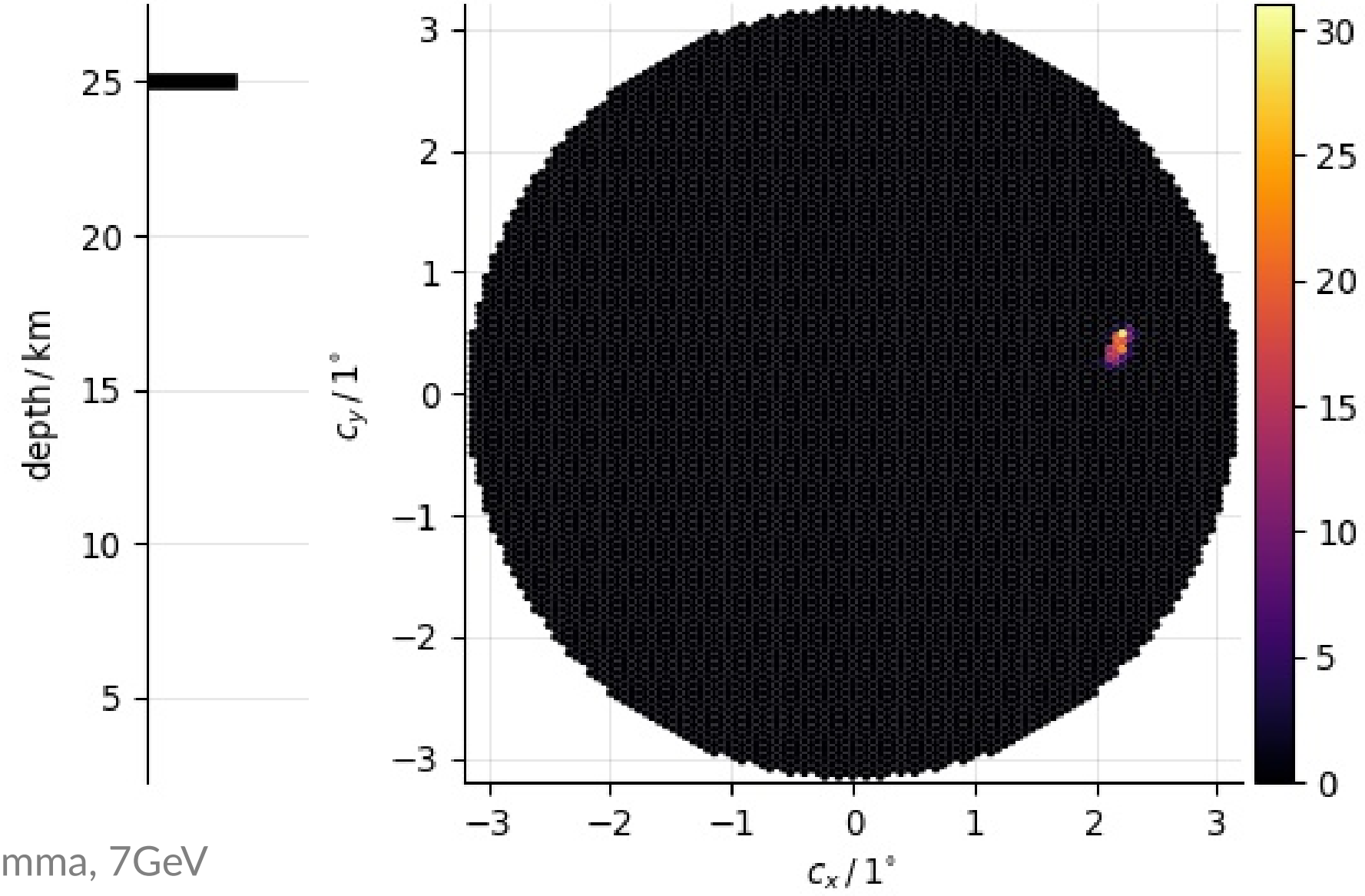
depth / km
25
20
15
10
5
$c_y / 1^\circ$
3
2
1
0
−1
−2
−3
$c_x / 1^\circ$
−3
−2
−1
0
1
2
3
30
25
20
15
10
5
0

Gamma, 7GeV

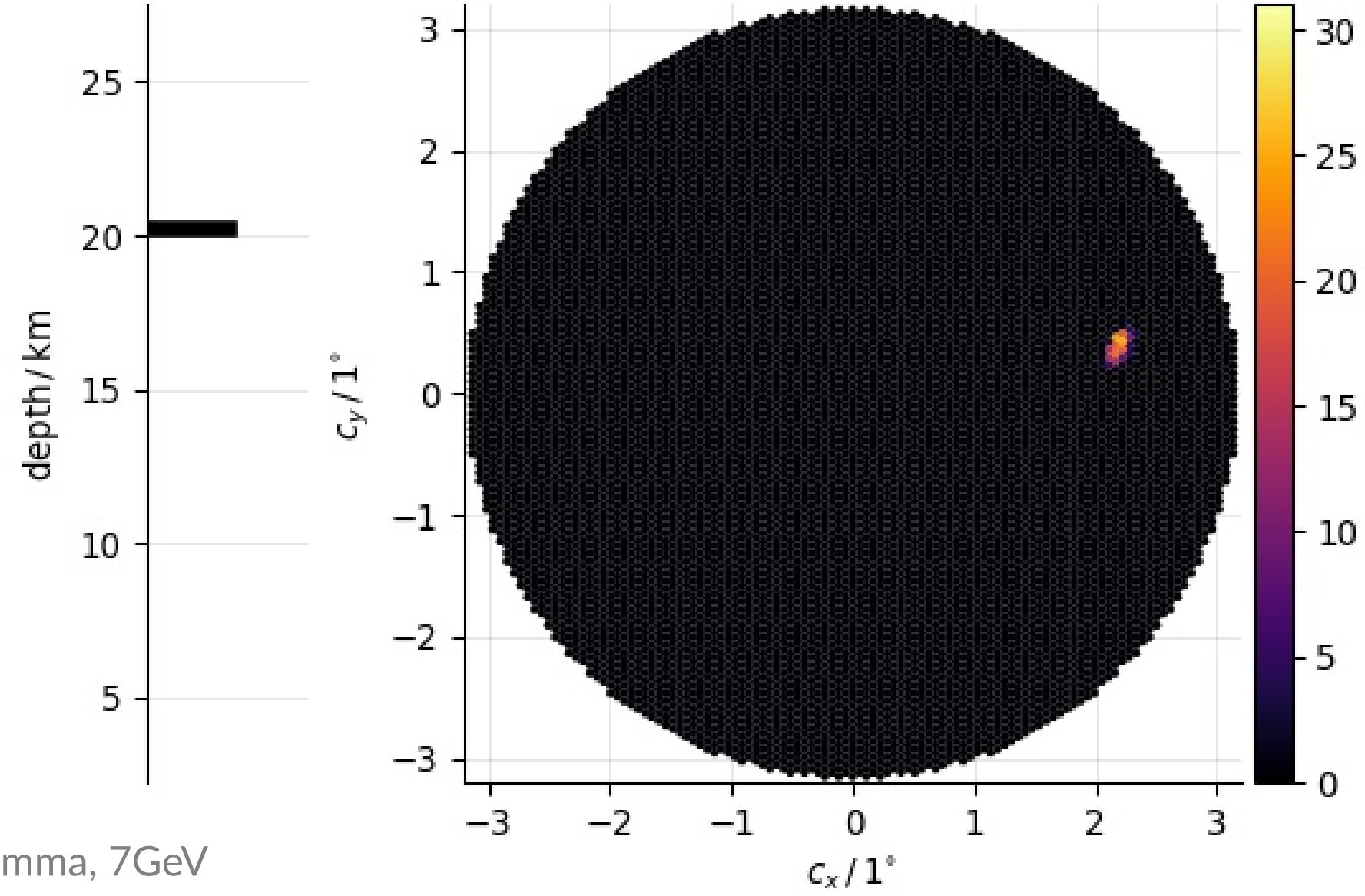
depth / km
25
20
15
10
5
$c_y / 1^\circ$
3
2
1
0
−1
−2
−3
$c_x / 1^\circ$
−3
−2
−1
0
1
2
3
30
25
20
15
10
5
0

Gamma, 7GeV

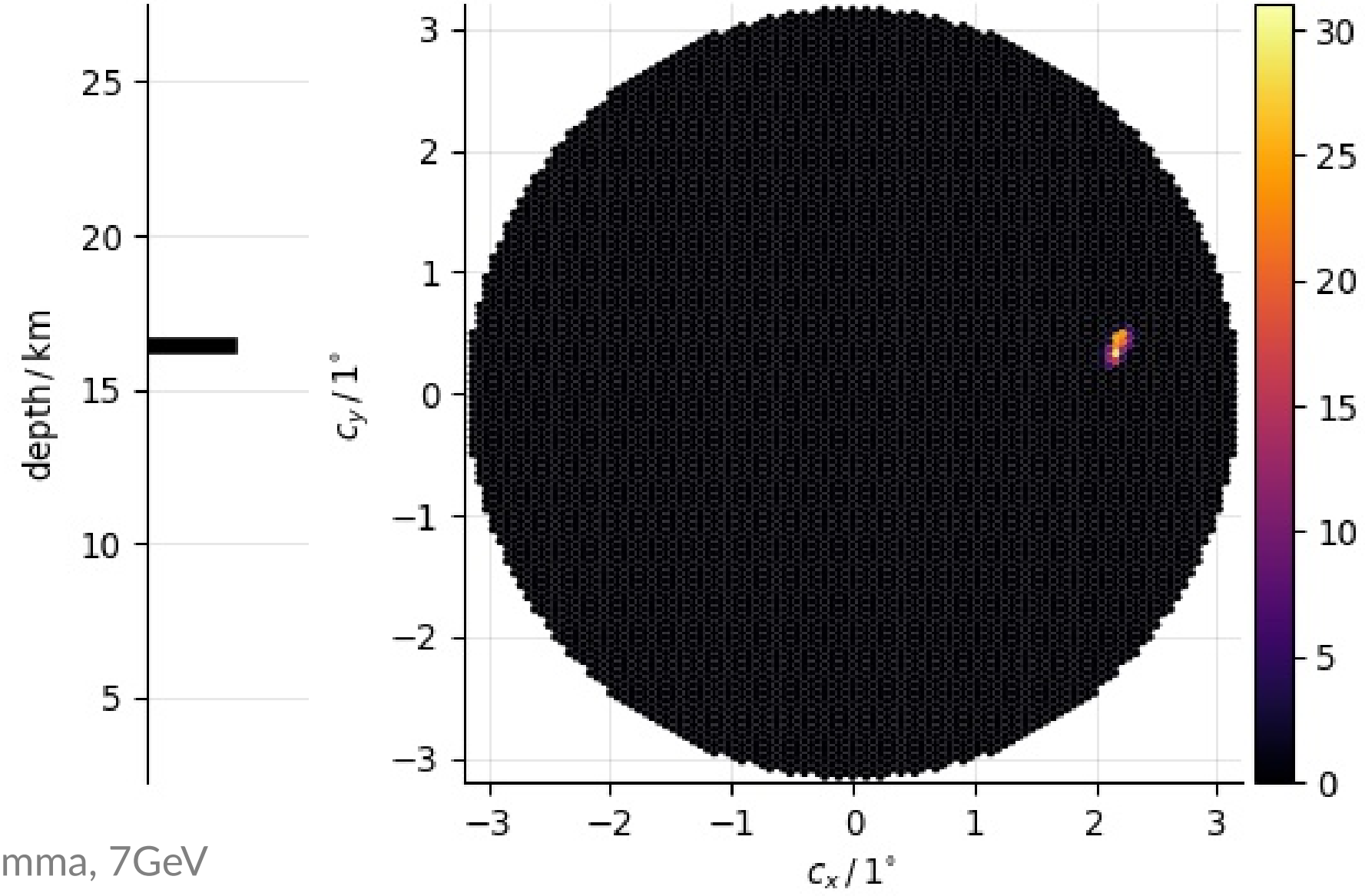
depth / km
25
20
15
10
5
$c_y / 1^\circ$
3
2
1
0
−1
−2
−3
$c_x / 1^\circ$
−3
−2
−1
0
1
2
3
30
25
20
15
10
5
0

Gamma, 7GeV

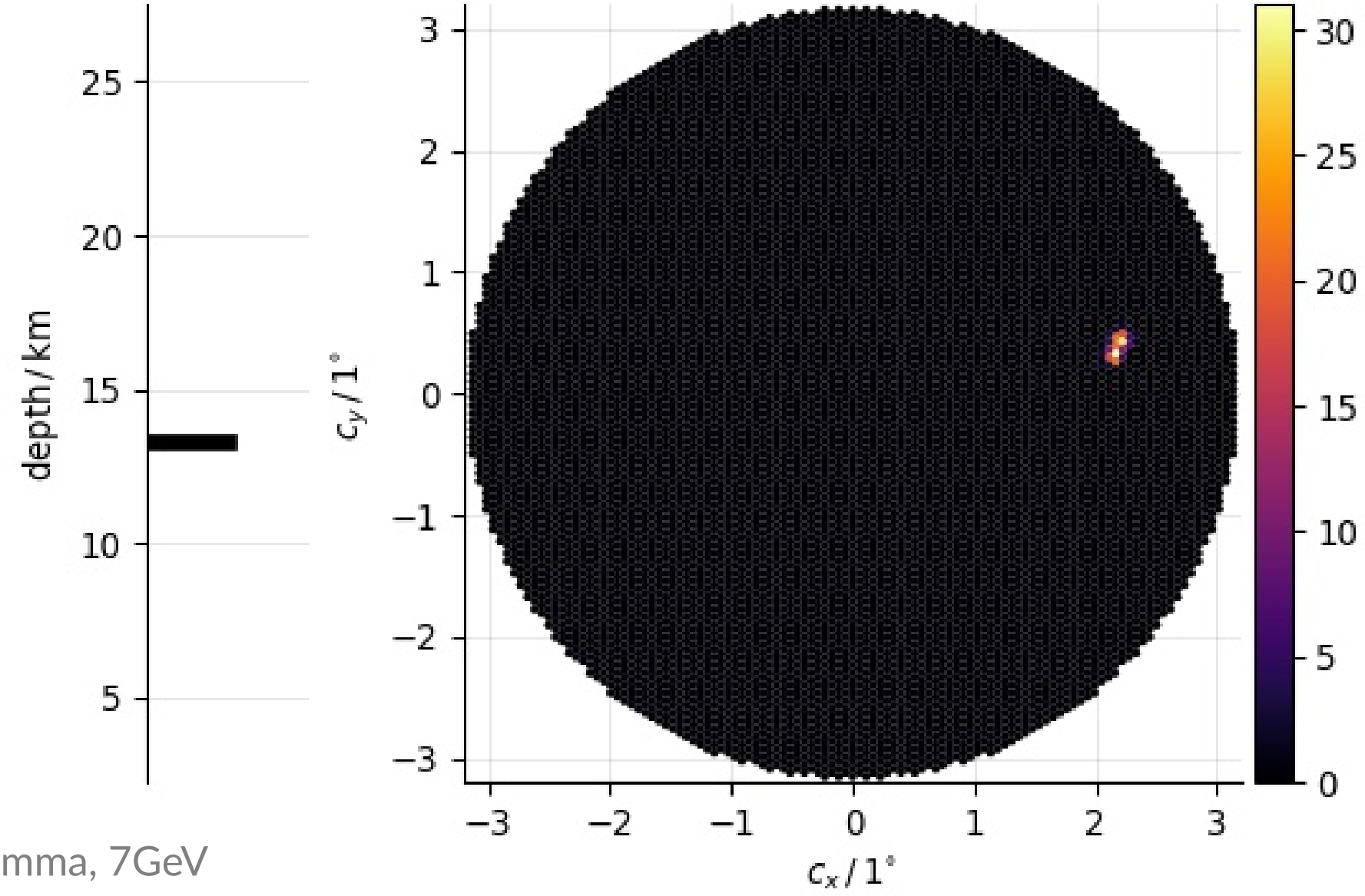

Gamma, 7GeV

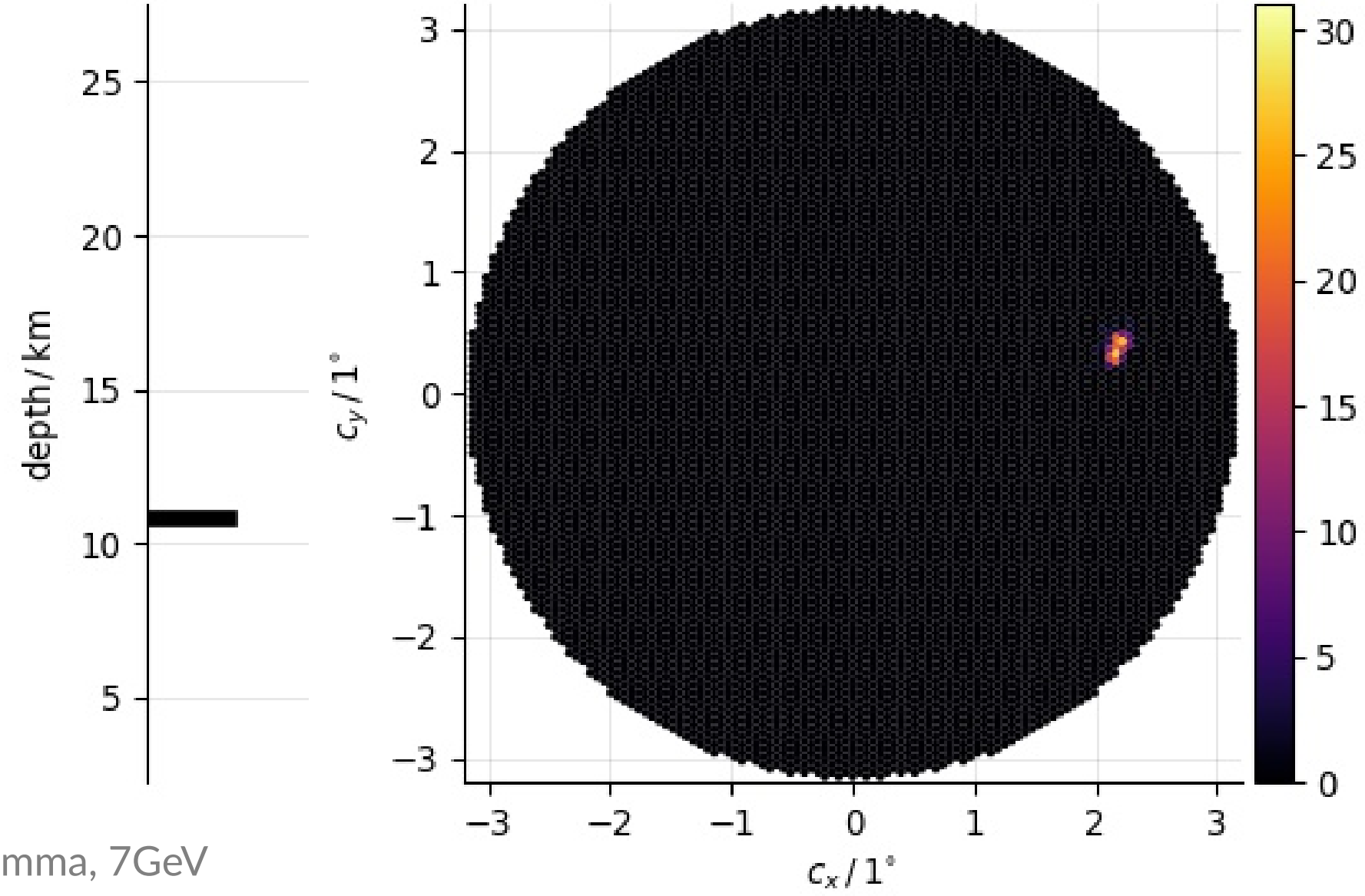
depth / km
25
20
15
10
5
$c_y / 1^\circ$
3
2
1
0
−1
−2
−3
$c_x / 1^\circ$
−3
−2
−1
0
1
2
3
30
25
20
15
10
5
0

Gamma, 7GeV

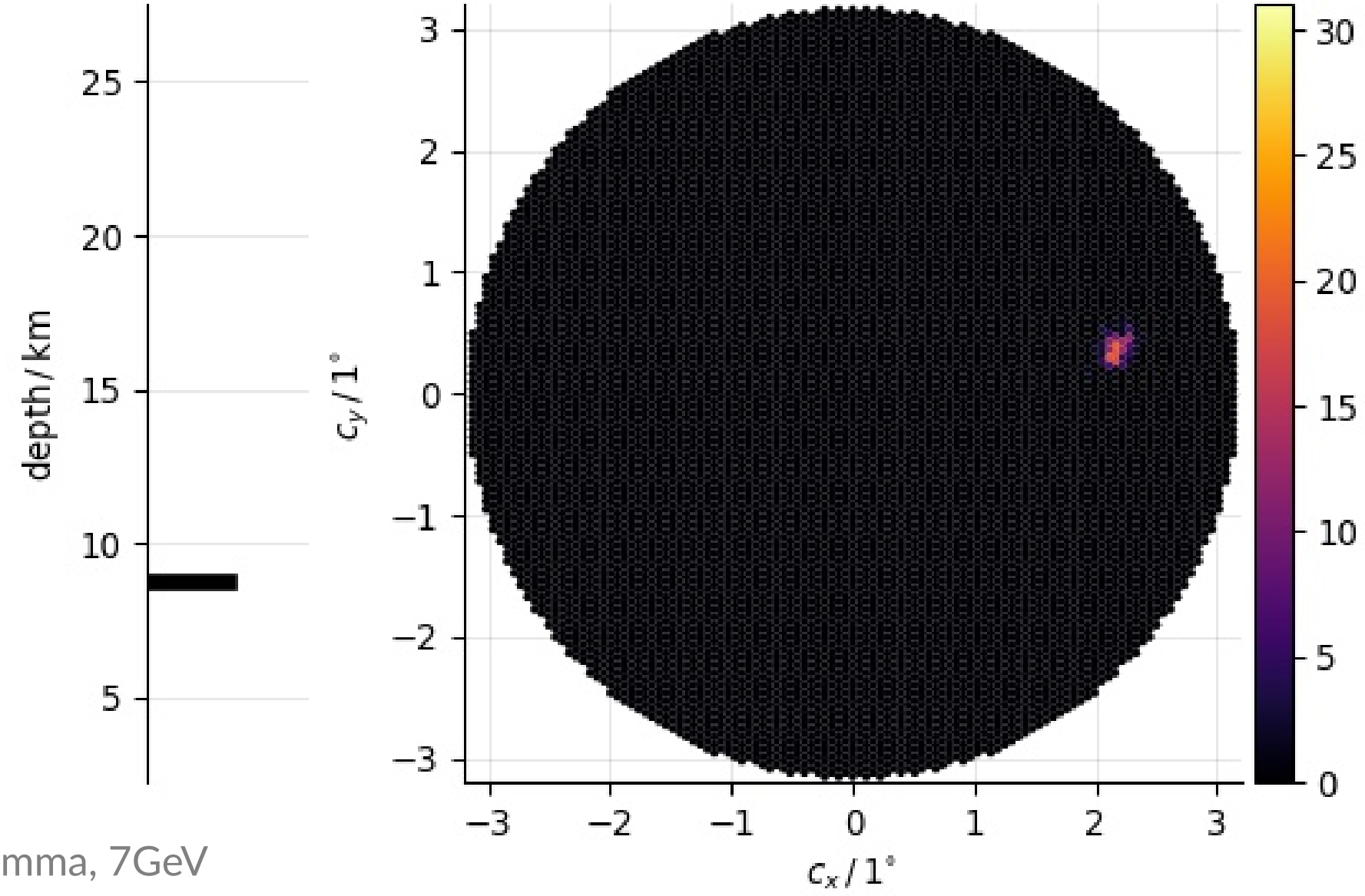

Gamma, 7GeV

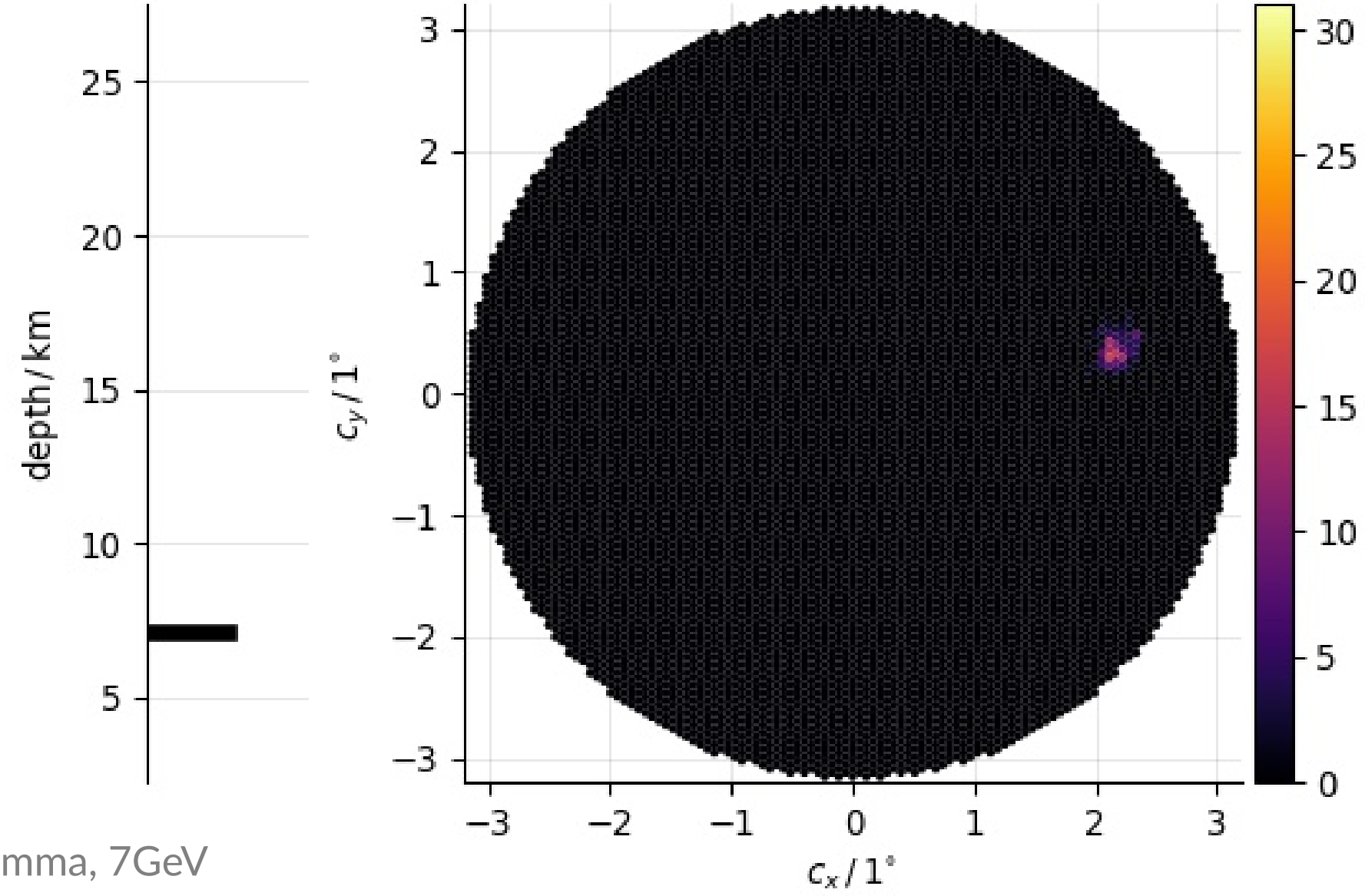
depth / km
25
20
15
10
5
$c_y / 1^\circ$
3
2
1
0
−1
−2
−3
$c_x / 1^\circ$
−3
−2
−1
0
1
2
3
30
25
20
15
10
5
0

Gamma, 7GeV

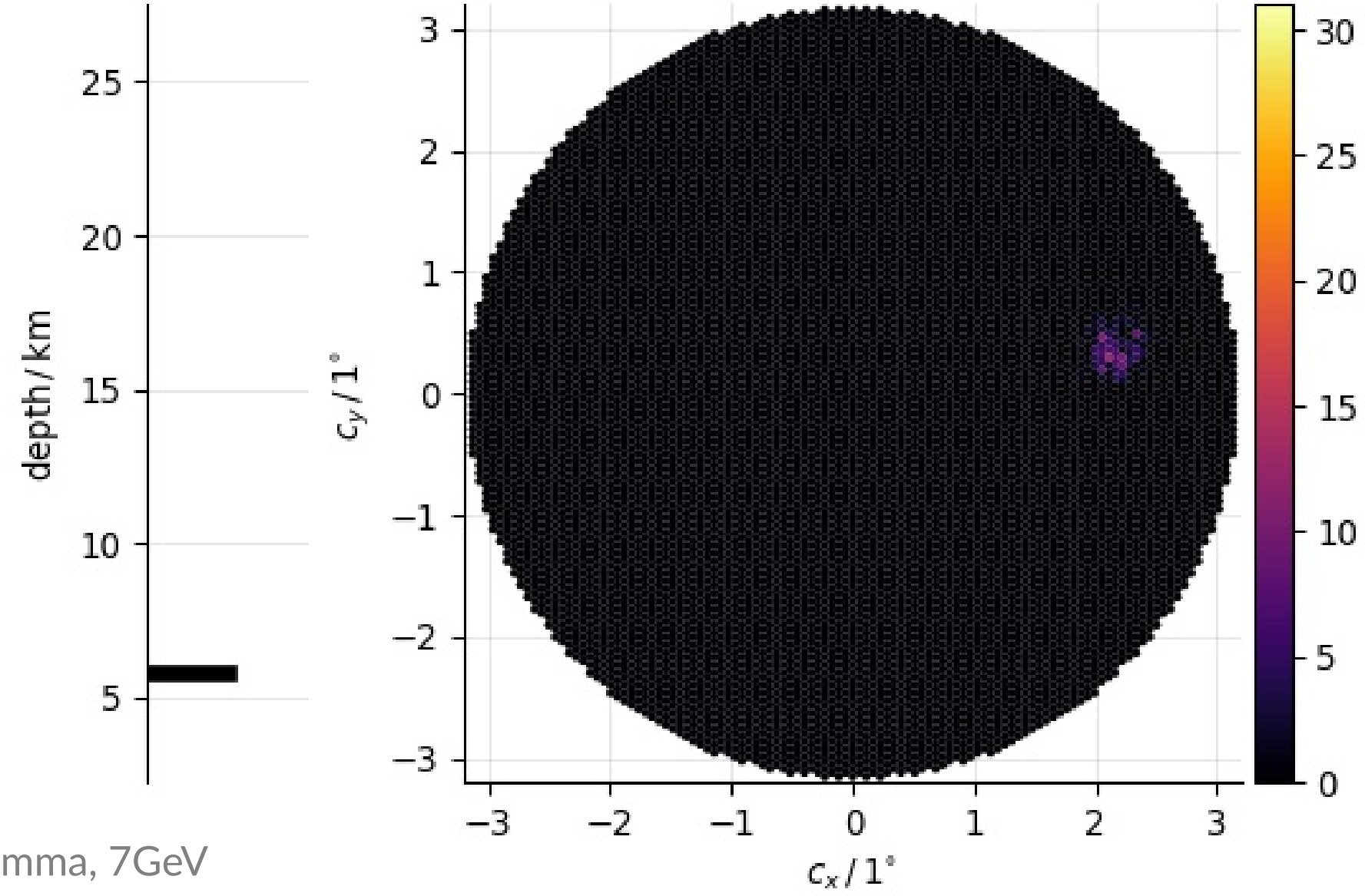
depth / km
25
20
15
10
5
$c_y / 1^\circ$
3
2
1
0
−1
−2
−3
$c_x / 1^\circ$
−3
−2
−1
0
1
2
3
30
25
20
15
10
5
0

Gamma, 7GeV

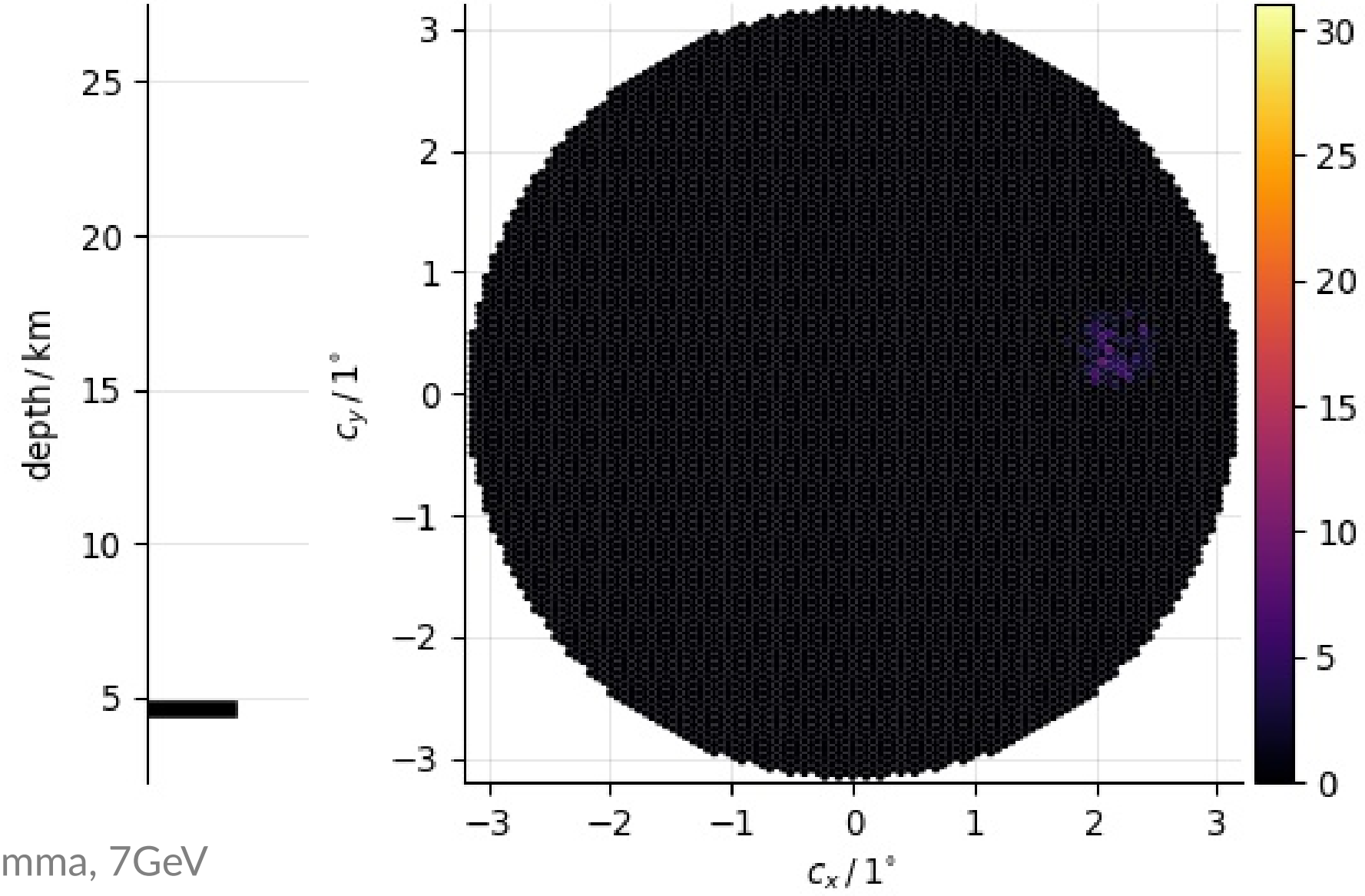
depth / km
25
20
15
10
5
$c_y / 1^\circ$
3
2
1
0
−1
−2
−3
$c_x / 1^\circ$
−3
−2
−1
0
1
2
3
30
25
20
15
10
5
0

Gamma, 7GeV

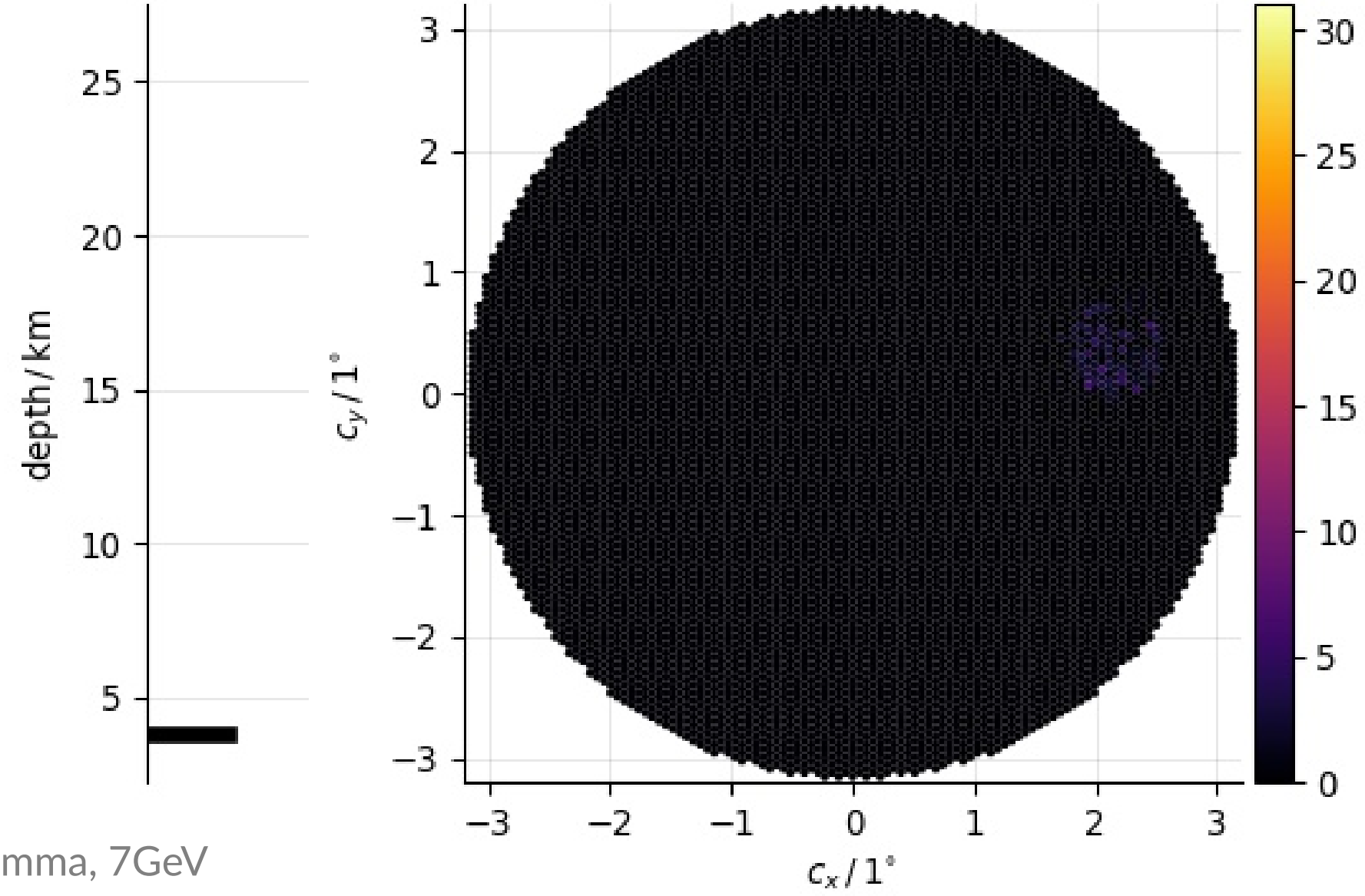
depth / km
25
20
15
10
5
$c_y / 1^\circ$
3
2
1
0
−1
−2
−3
$c_x / 1^\circ$
−3
−2
−1
0
1
2
3
30
25
20
15
10
5
0

Gamma, 7GeV

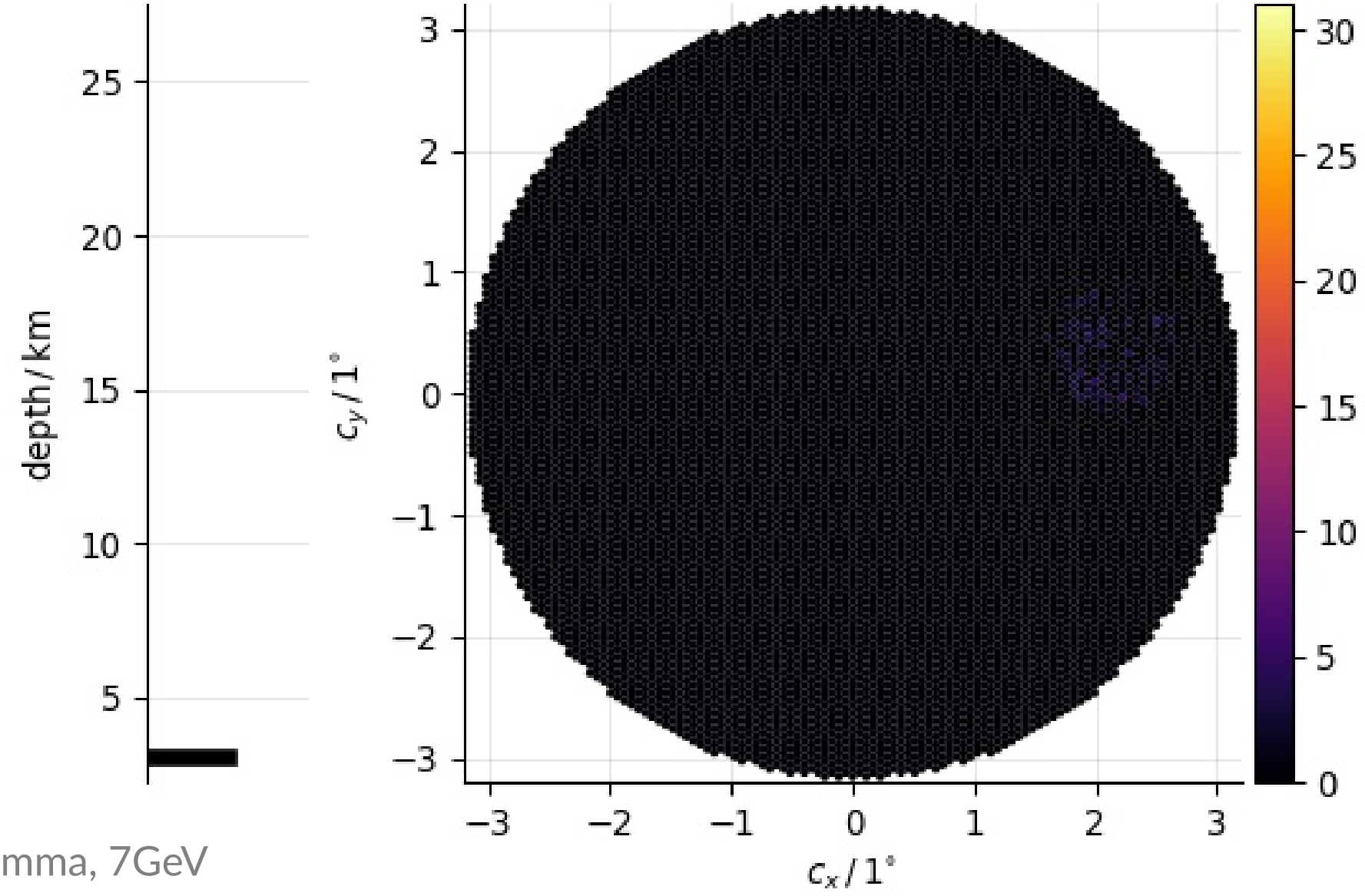
depth / km
25
20
15
10
5
$c_y / 1^\circ$
3
2
1
0
−1
−2
−3
$c_x / 1^\circ$
−3
−2
−1
0
1
2
3
30
25
20
15
10
5
0

Gamma, 7GeV

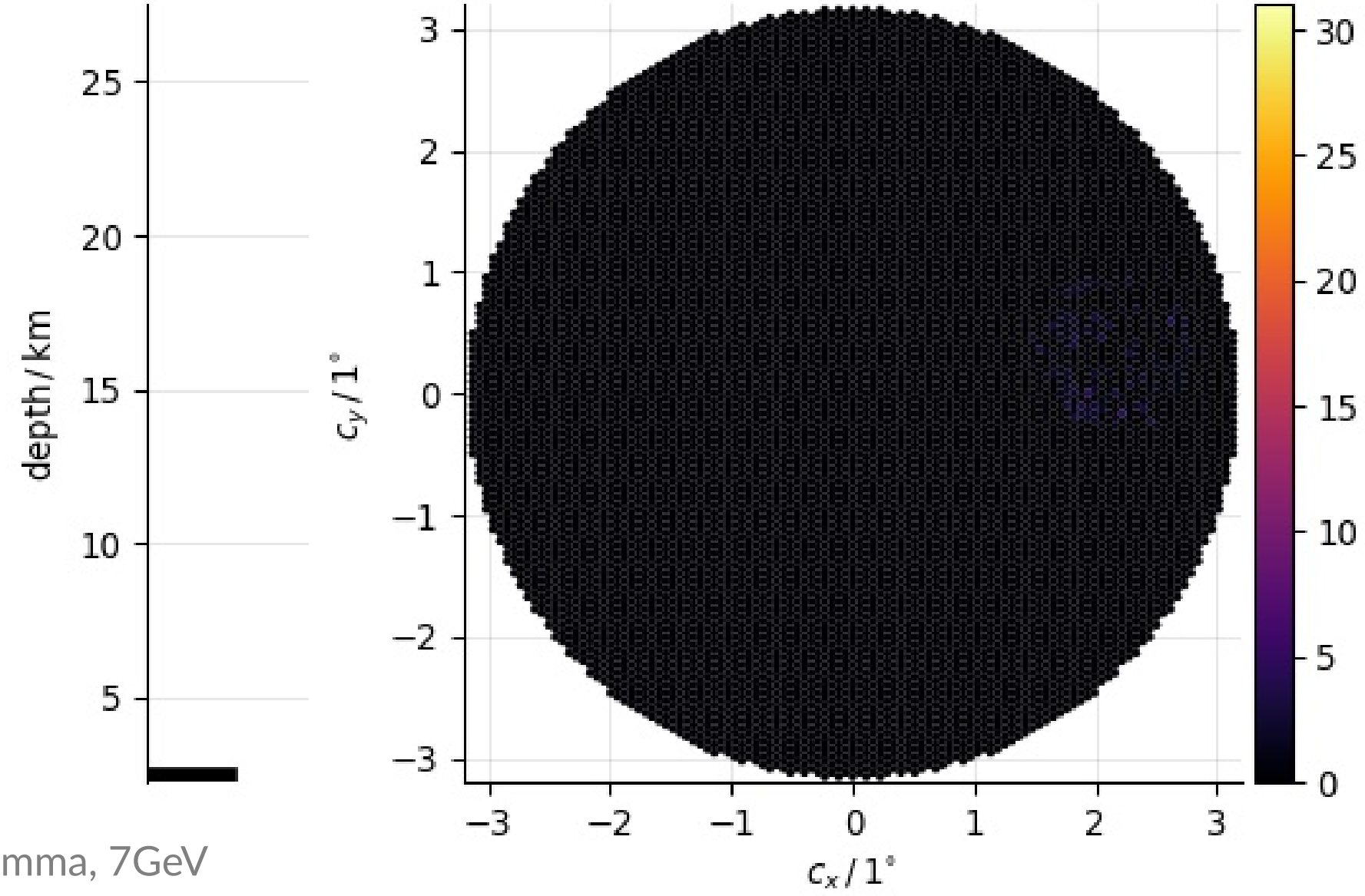

Gamma, 7GeV

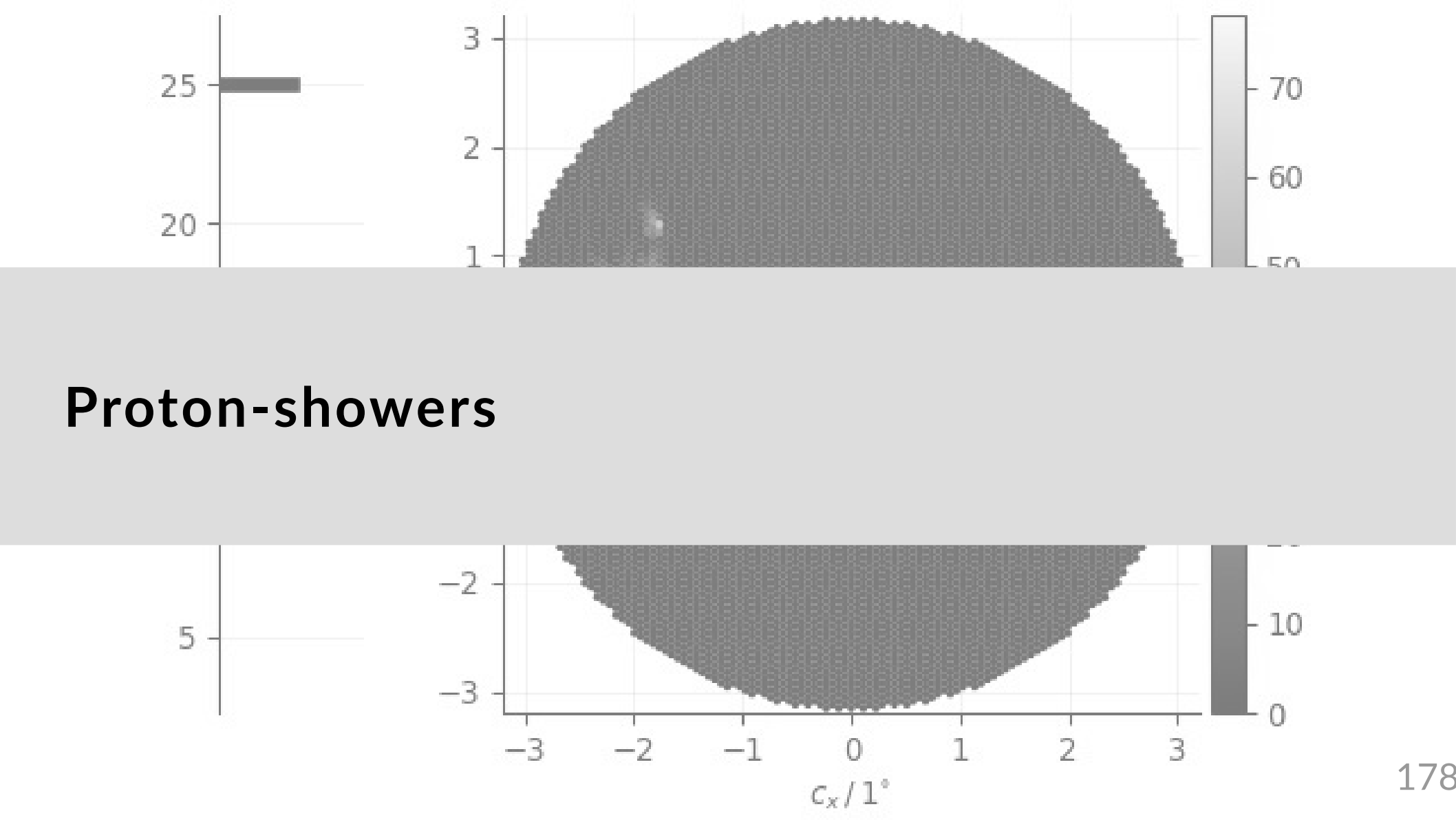

Proton-showers

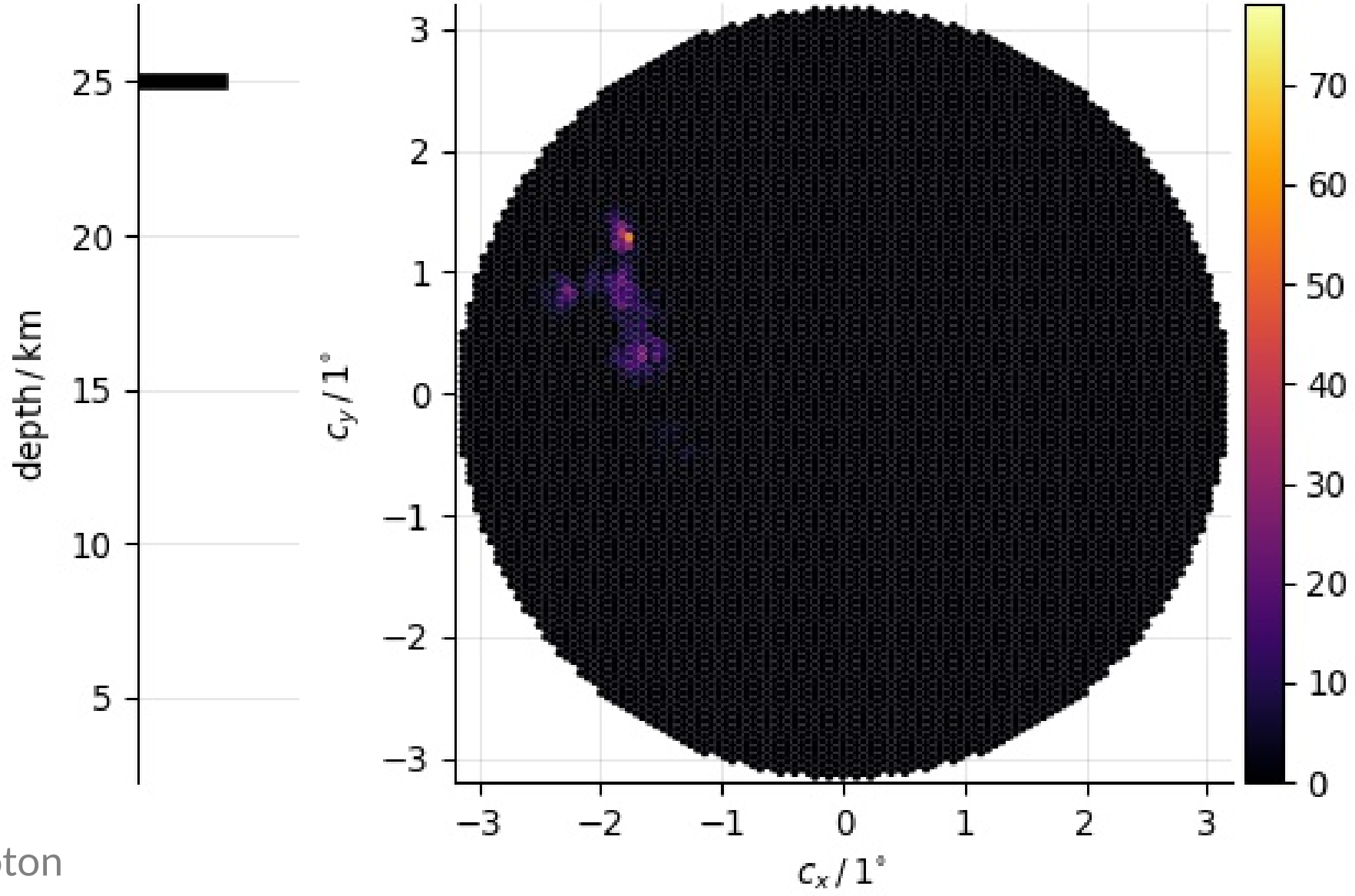
depth / km
25
20
15
10
5
$c_y / 1^\circ$
3
2
1
0
−1
−2
−3
$c_x / 1^\circ$
−3
−2
−1
0
1
2
3
70
60
50
40
30
20
10
0

Proton

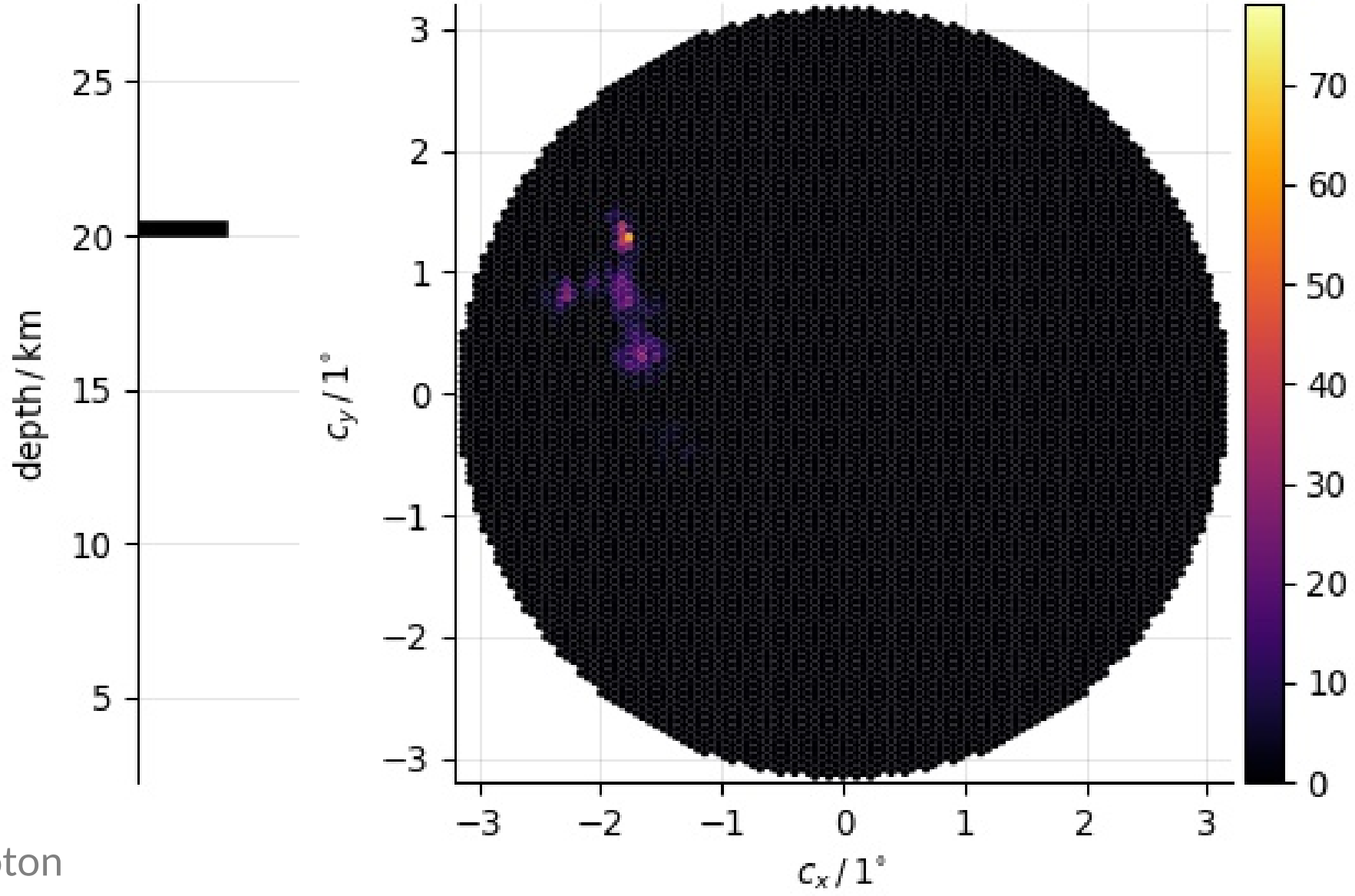
depth / km
25
20
15
10
5
$c_y / 1^\circ$
3
2
1
0
−1
−2
−3
$c_x / 1^\circ$
−3
−2
−1
0
1
2
3
70
60
50
40
30
20
10
0

Proton

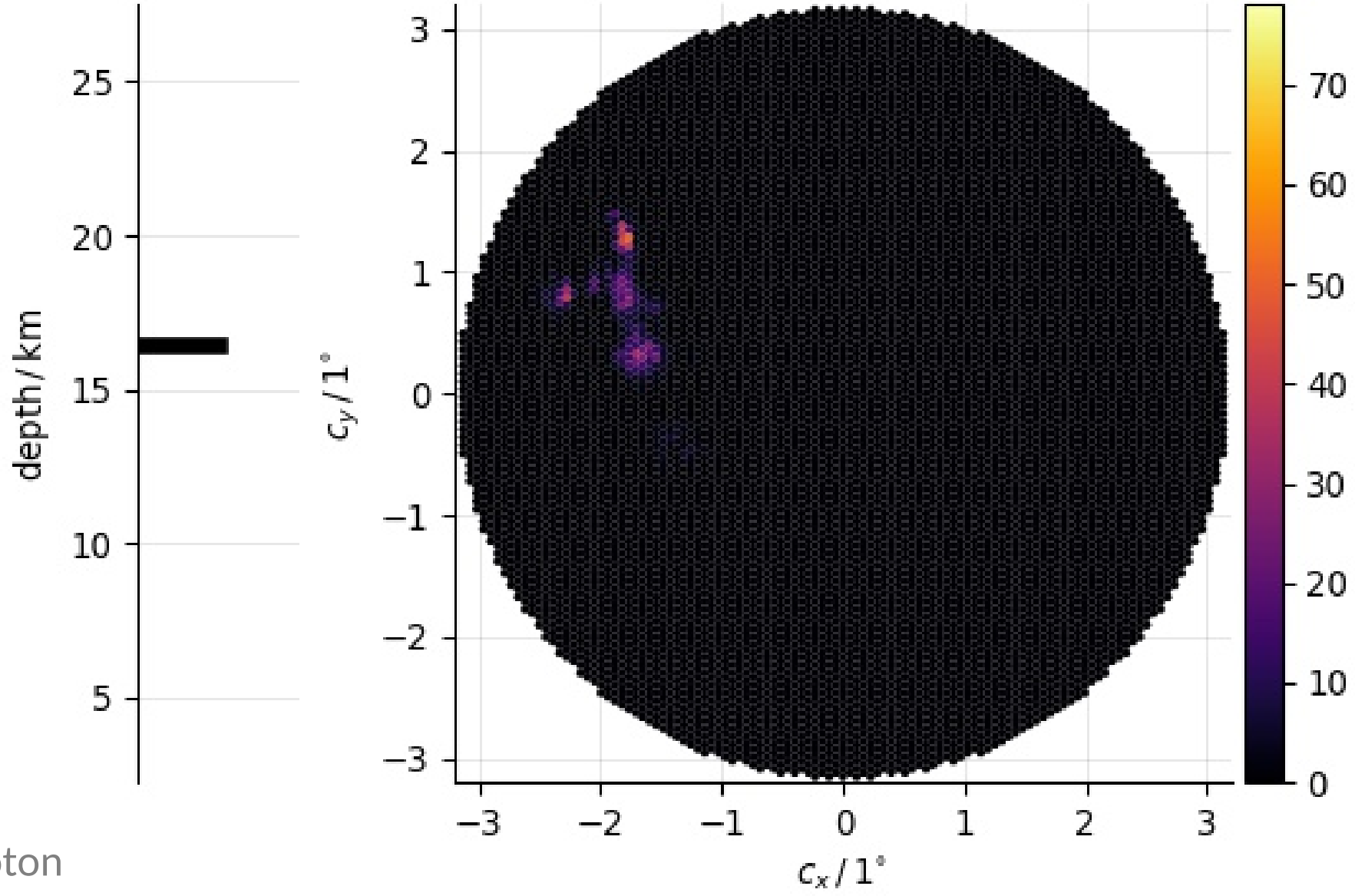
depth / km
25
20
15
10
5
c_y / 1°
3
2
1
0
−1
−2
−3
c_x / 1°
−3
−2
−1
0
1
2
3
70
60
50
40
30
20
10
0

Proton

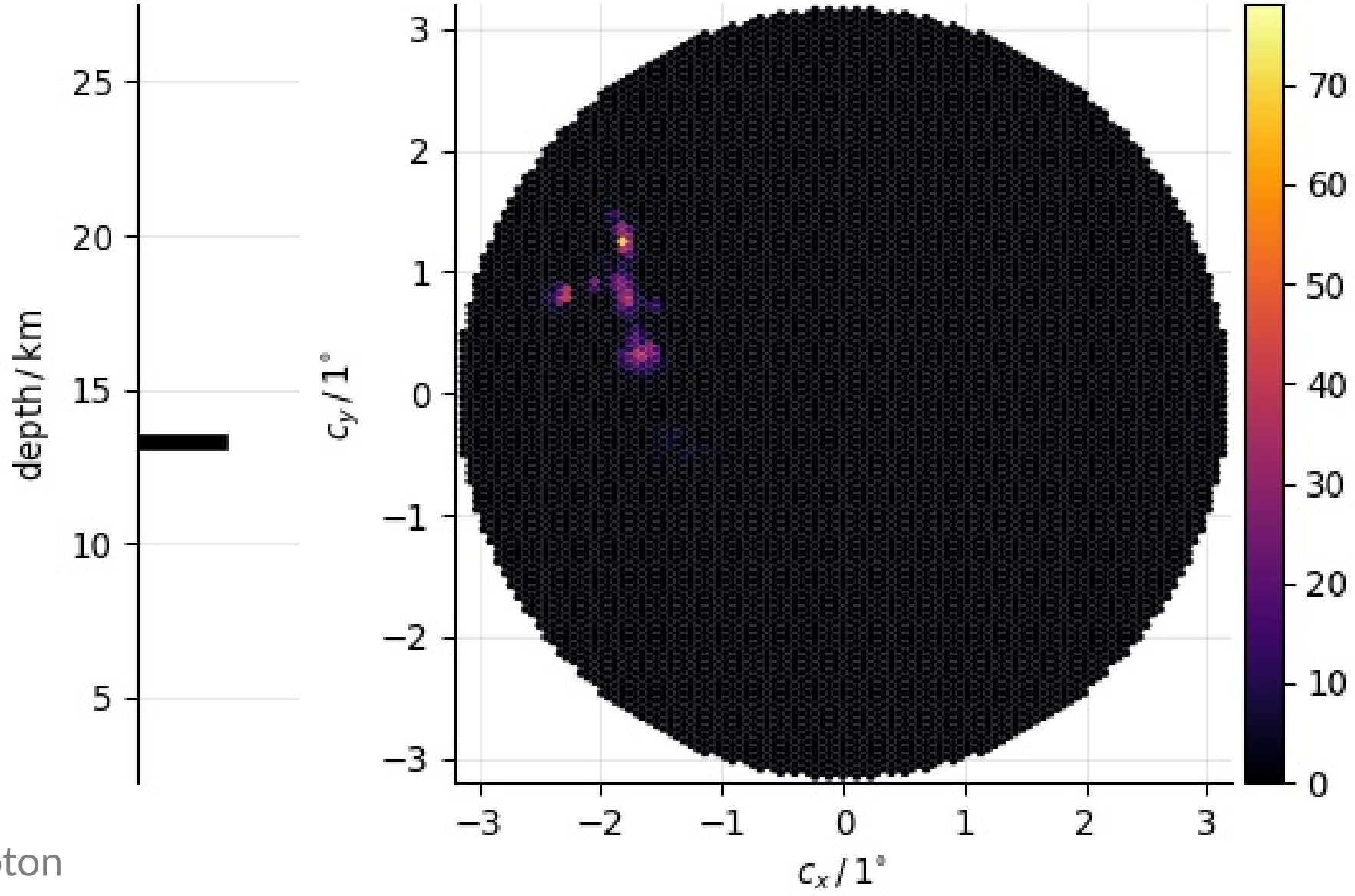
depth / km
25
20
15
10
5
$c_y / 1^\circ$
3
2
1
0
−1
−2
−3
$c_x / 1^\circ$
−3
−2
−1
0
1
2
3
70
60
50
40
30
20
10
0

Proton

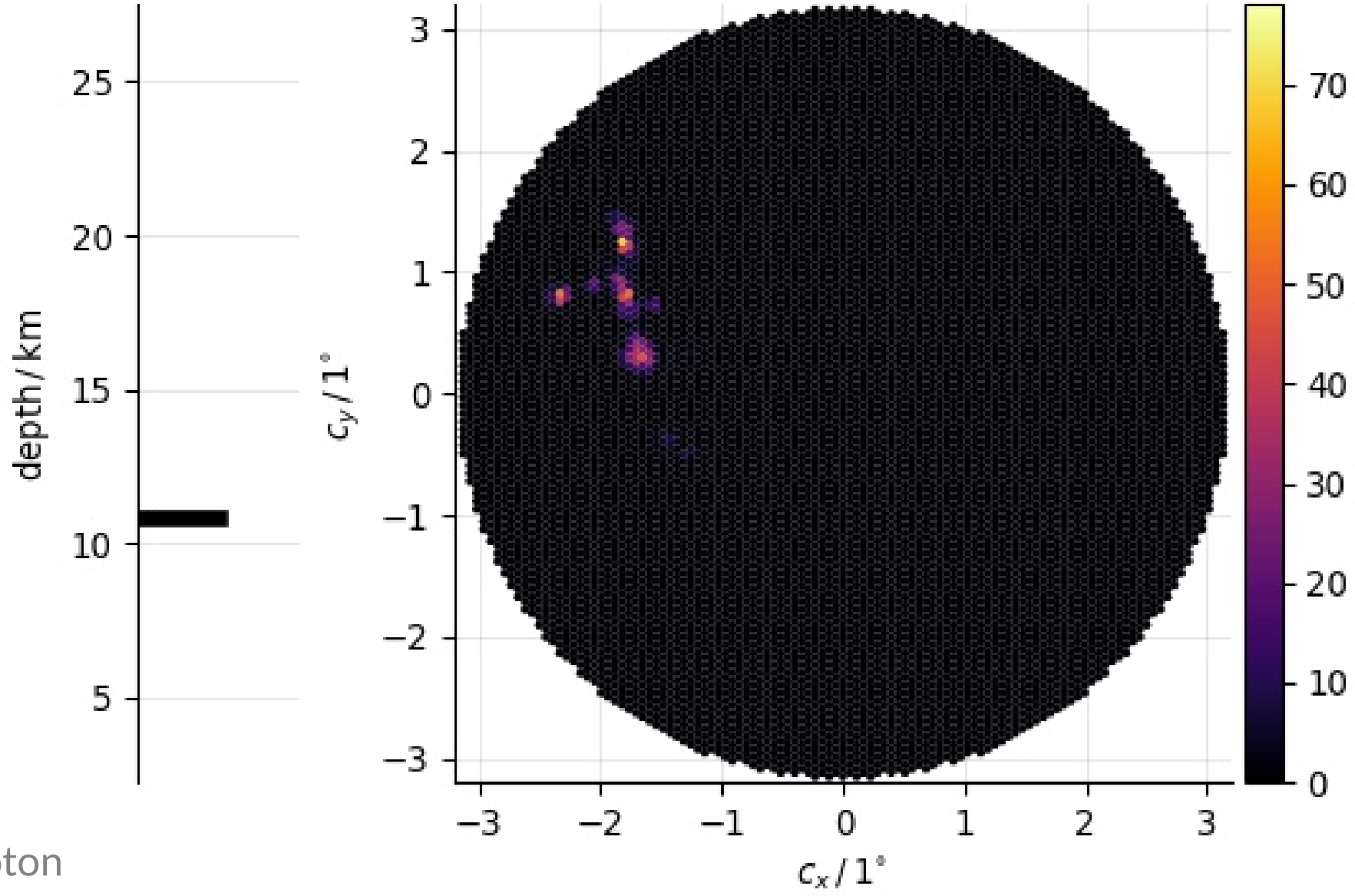
depth / km
25
20
15
10
5
$c_y / 1^\circ$
3
2
1
0
−1
−2
−3
$c_x / 1^\circ$
−3
−2
−1
0
1
2
3
70
60
50
40
30
20
10
0

Proton

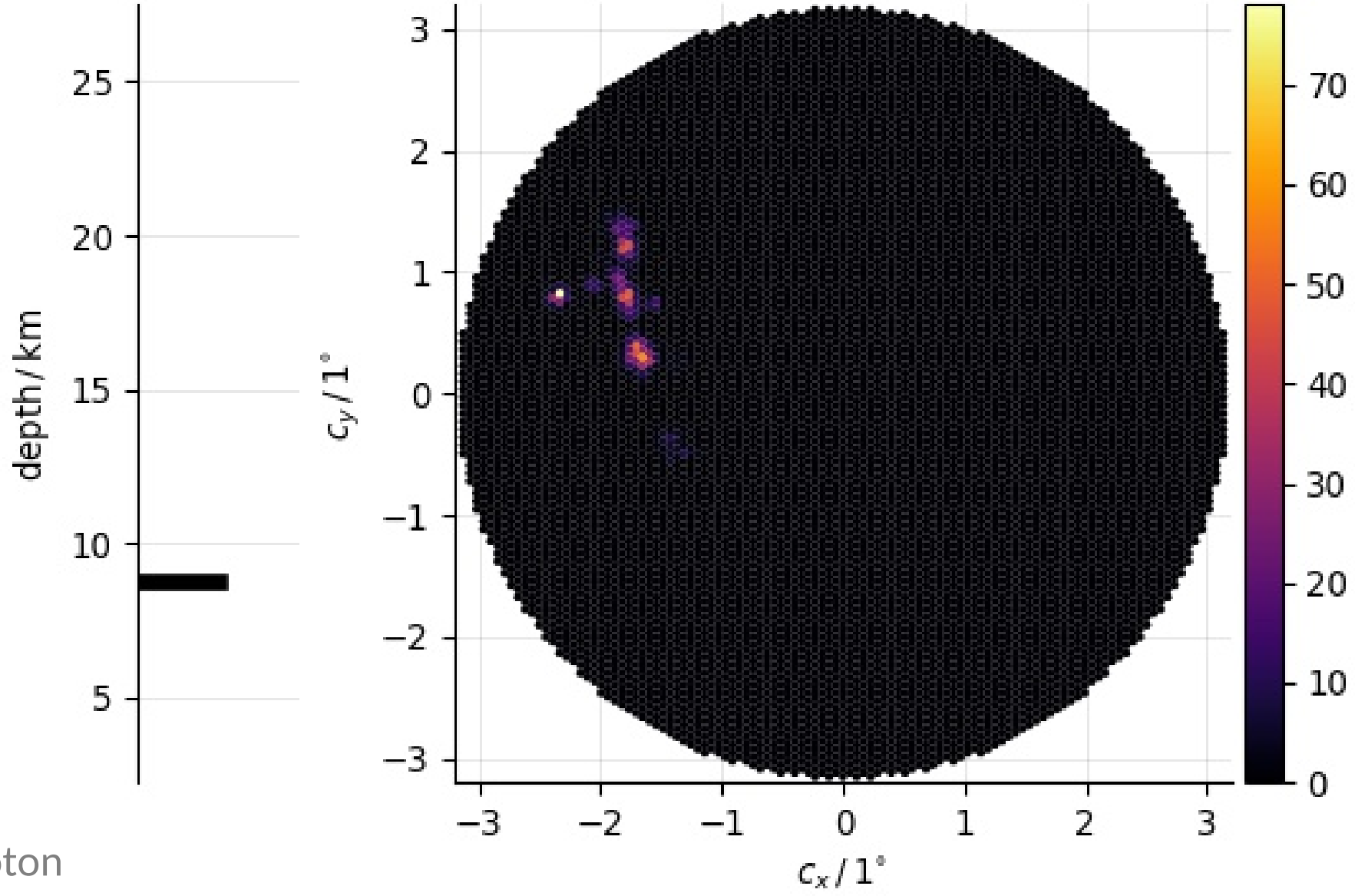
depth / km
25
20
15
10
5
$c_y / 1^\circ$
3
2
1
0
−1
−2
−3
$c_x / 1^\circ$
−3
−2
−1
0
1
2
3
70
60
50
40
30
20
10
0

Proton

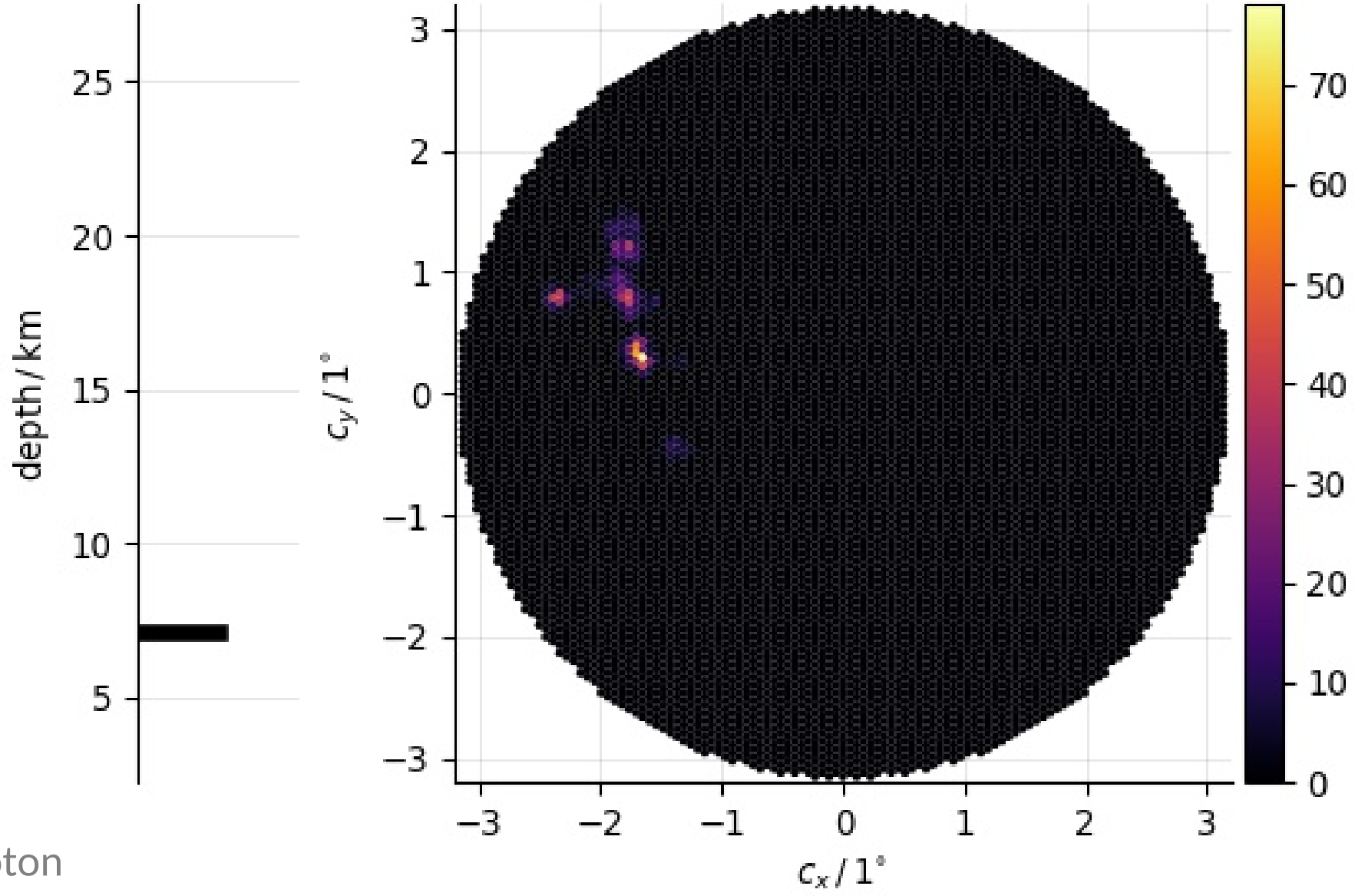
depth / km
25
20
15
10
5
$c_y / 1^\circ$
3
2
1
0
−1
−2
−3
$c_x / 1^\circ$
−3
−2
−1
0
1
2
3
70
60
50
40
30
20
10
0

Proton

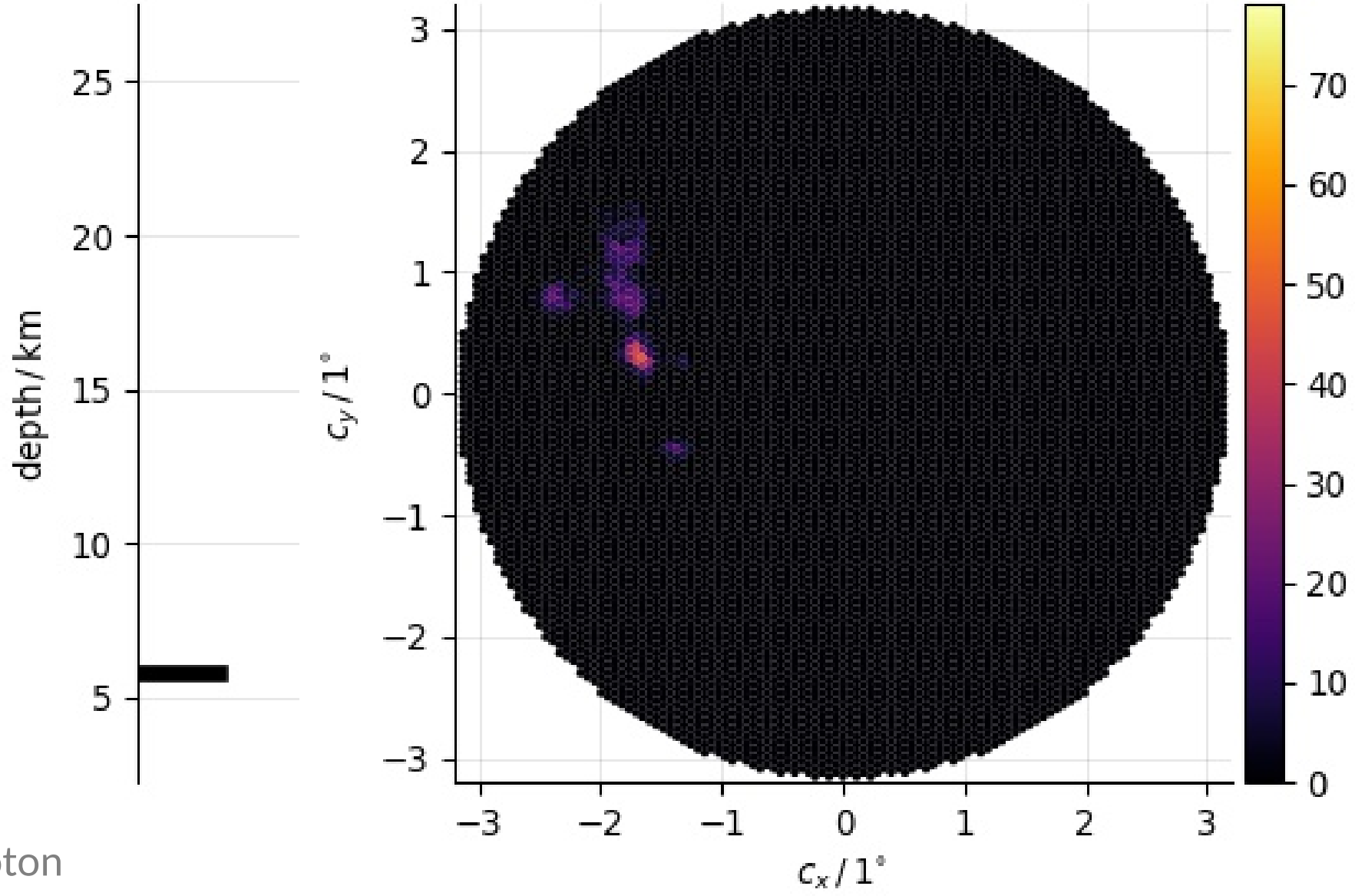
depth / km
25
20
15
10
5
$c_y / 1^\circ$
3
2
1
0
−1
−2
−3
$c_x / 1^\circ$
−3
−2
−1
0
1
2
3
70
60
50
40
30
20
10
0

Proton

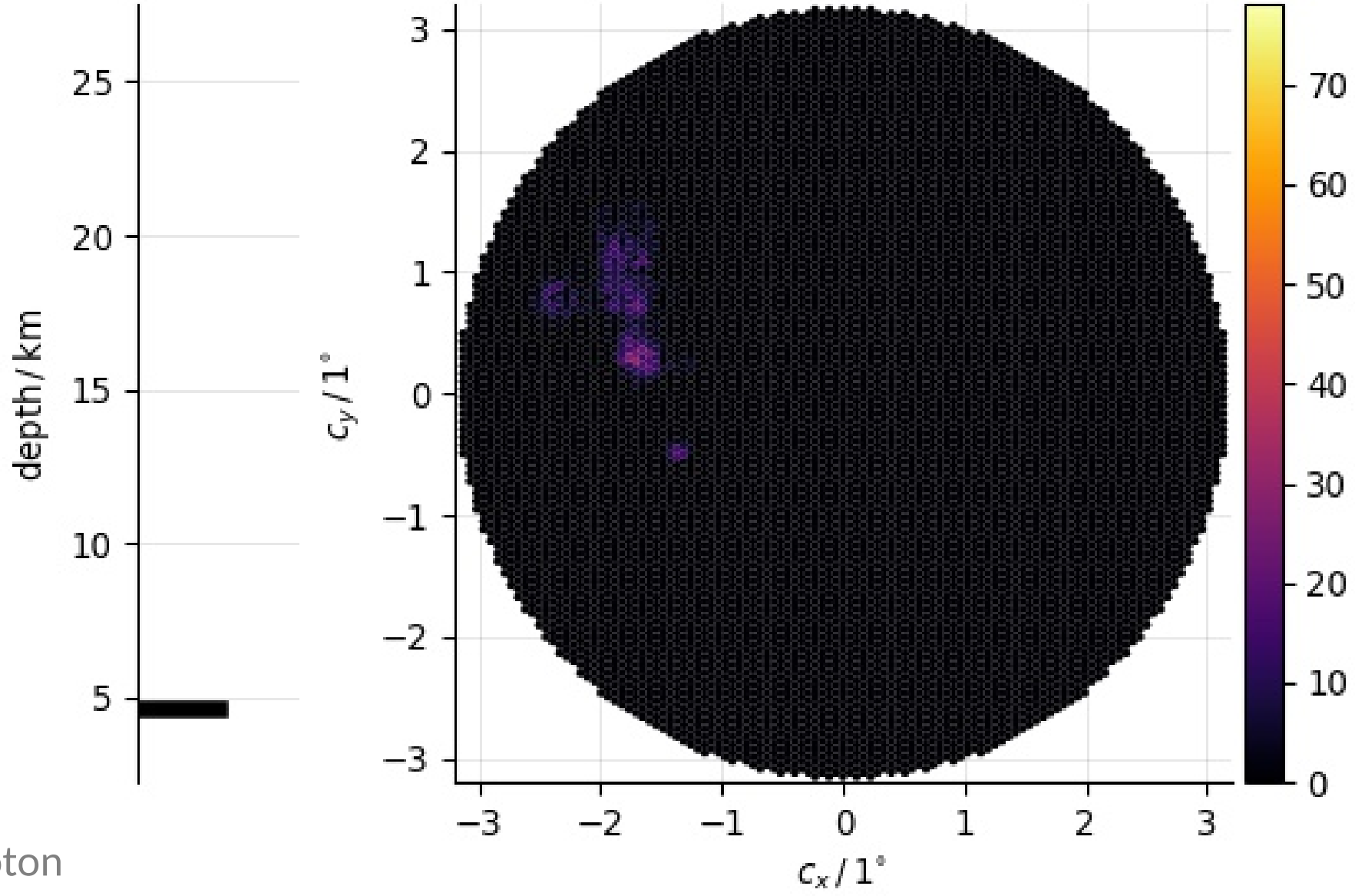
depth / km
25
20
15
10
5
$c_y / 1^\circ$
3
2
1
0
−1
−2
−3
$c_x / 1^\circ$
−3
−2
−1
0
1
2
3
70
60
50
40
30
20
10
0

Proton

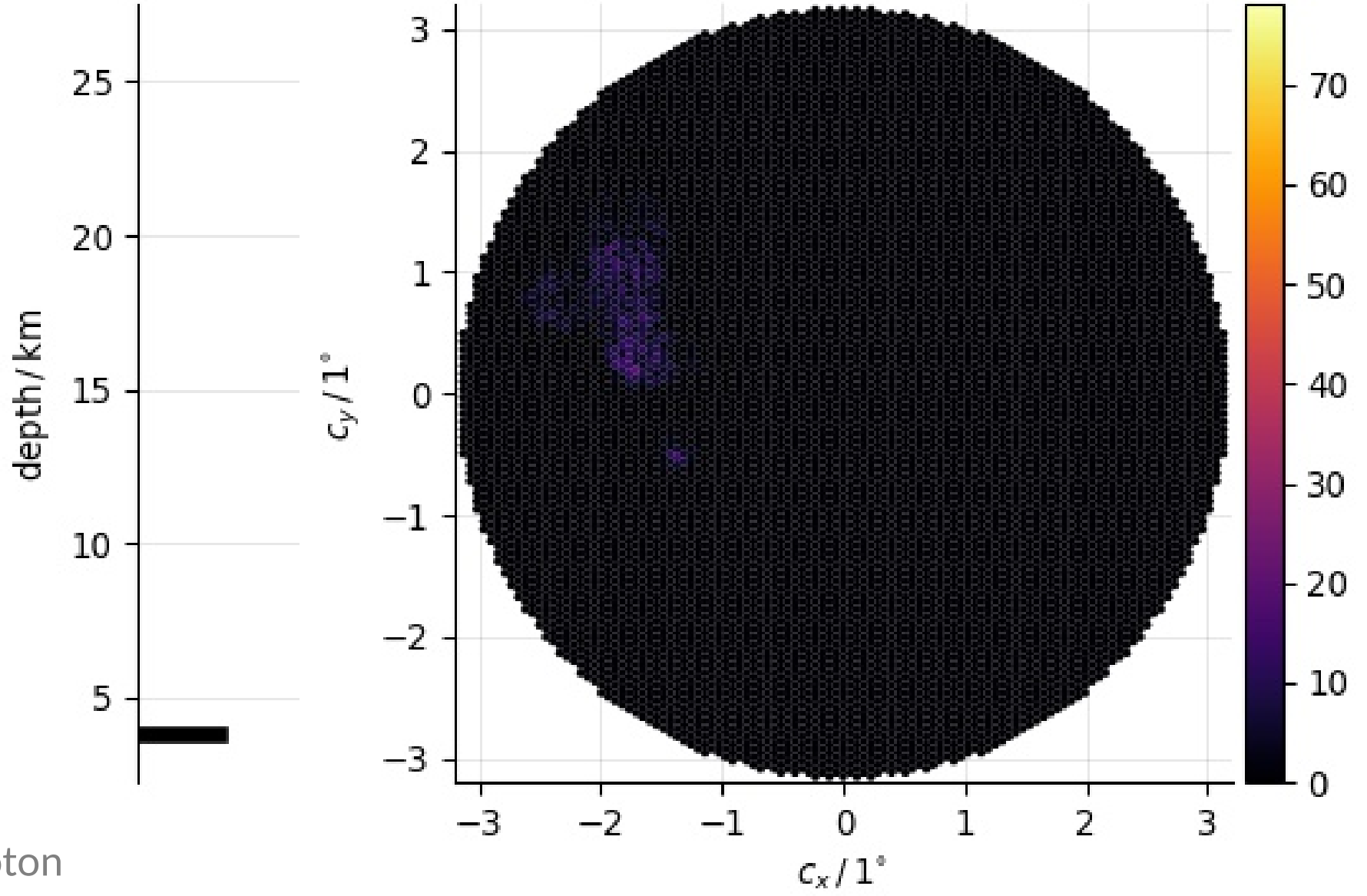
depth / km
25
20
15
10
5
c_y / 1°
3
2
1
0
−1
−2
−3
−3
−2
−1
0
1
2
3
c_x / 1°
70
60
50
40
30
20
10
0

Proton

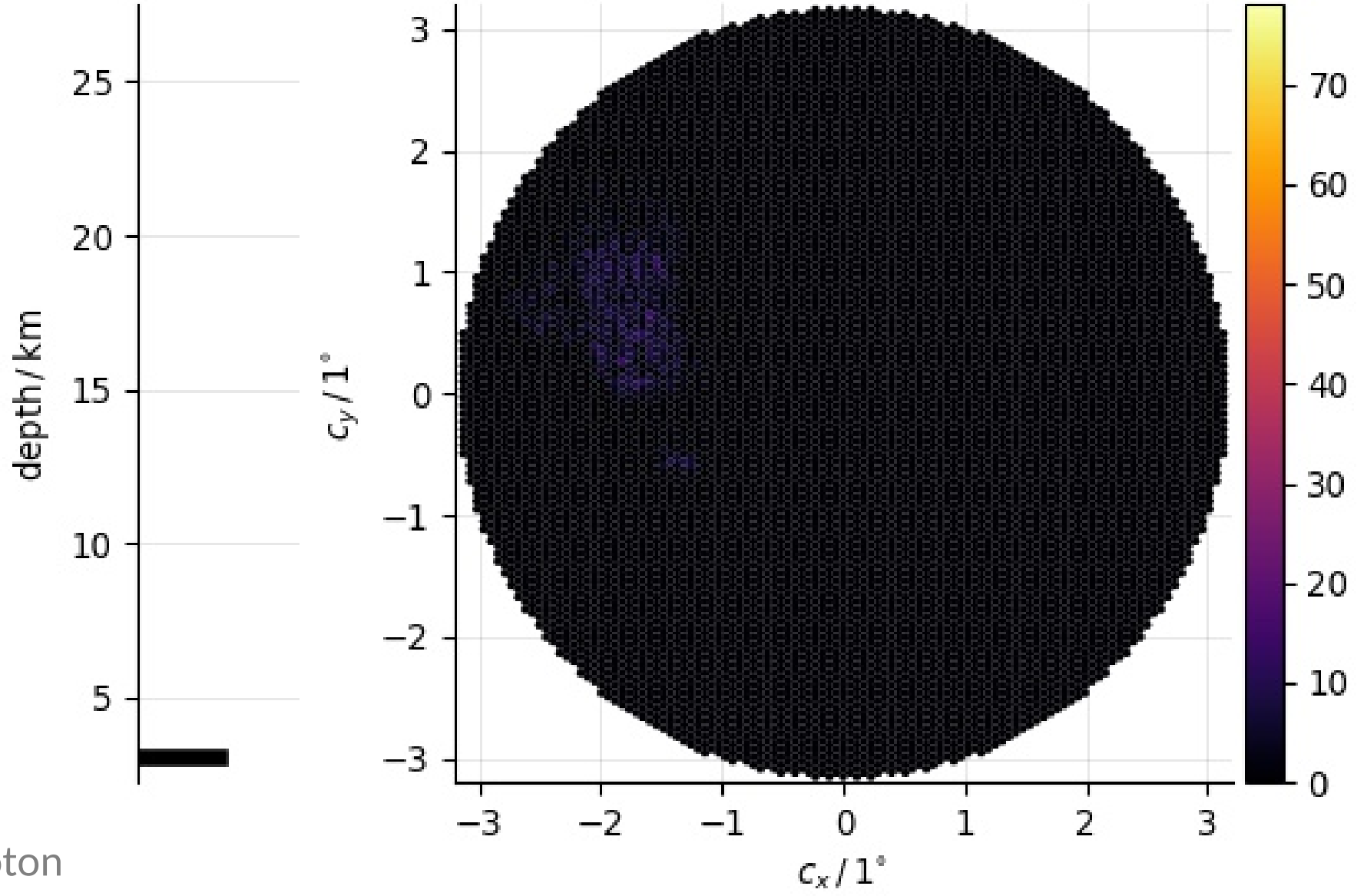
depth / km
25
20
15
10
5
$c_y / 1^\circ$
3
2
1
0
−1
−2
−3
$c_x / 1^\circ$
−3
−2
−1
0
1
2
3
70
60
50
40
30
20
10
0

Proton

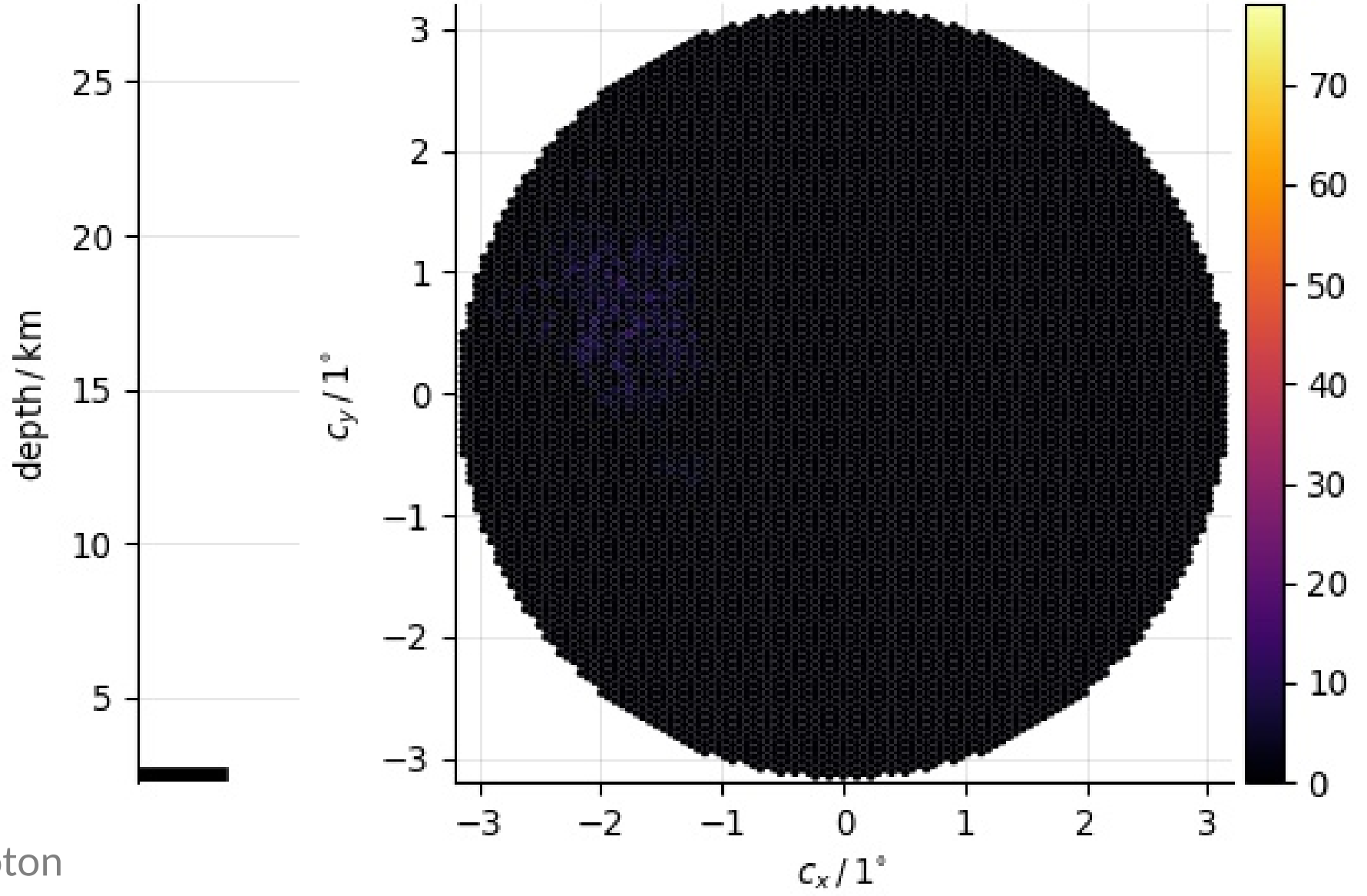
depth / km
25
20
15
10
5
$c_y / 1^\circ$
3
2
1
0
−1
−2
−3
$c_x / 1^\circ$
−3
−2
−1
0
1
2
3
70
60
50
40
30
20
10
0

Proton

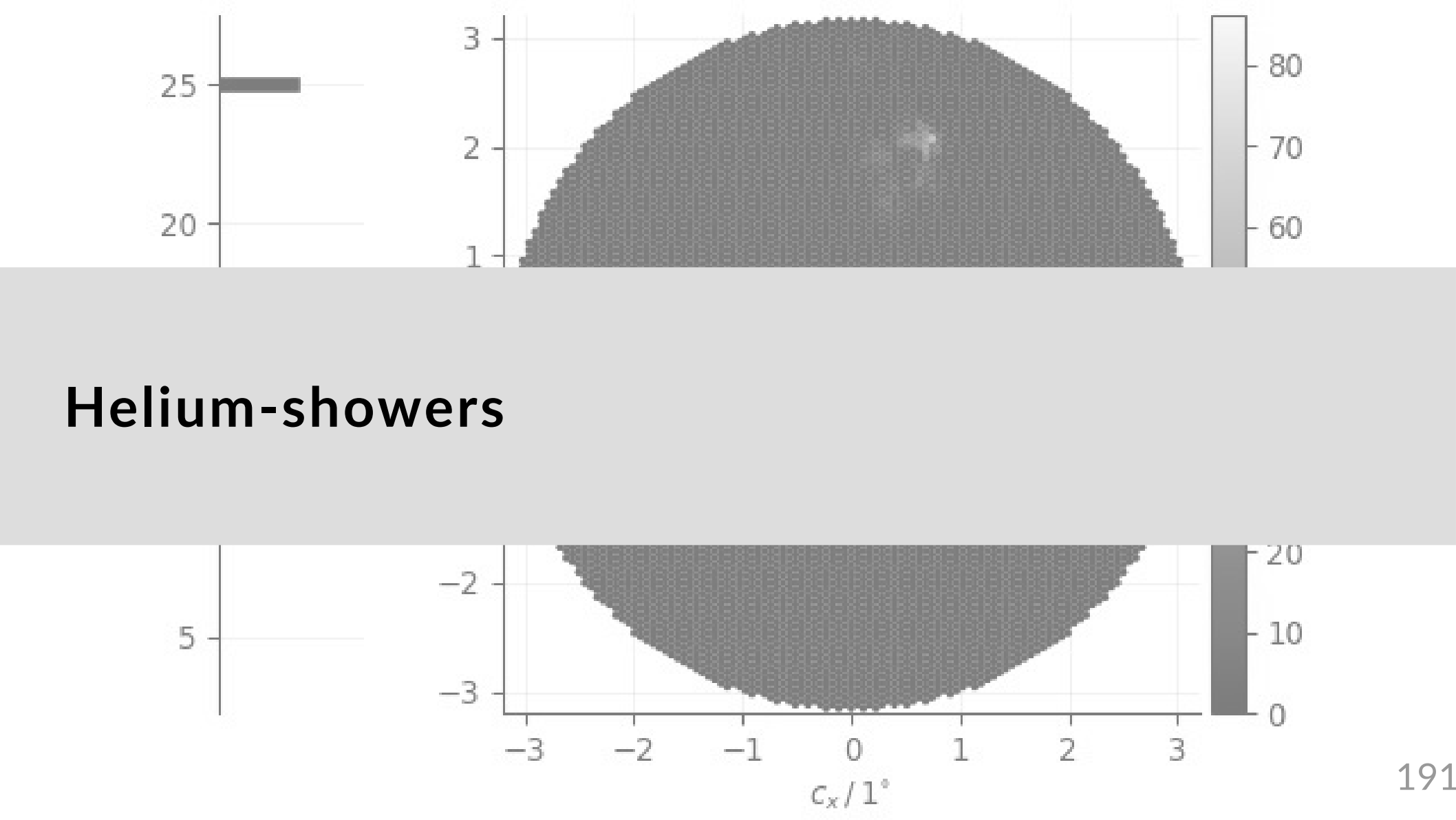

Helium-showers

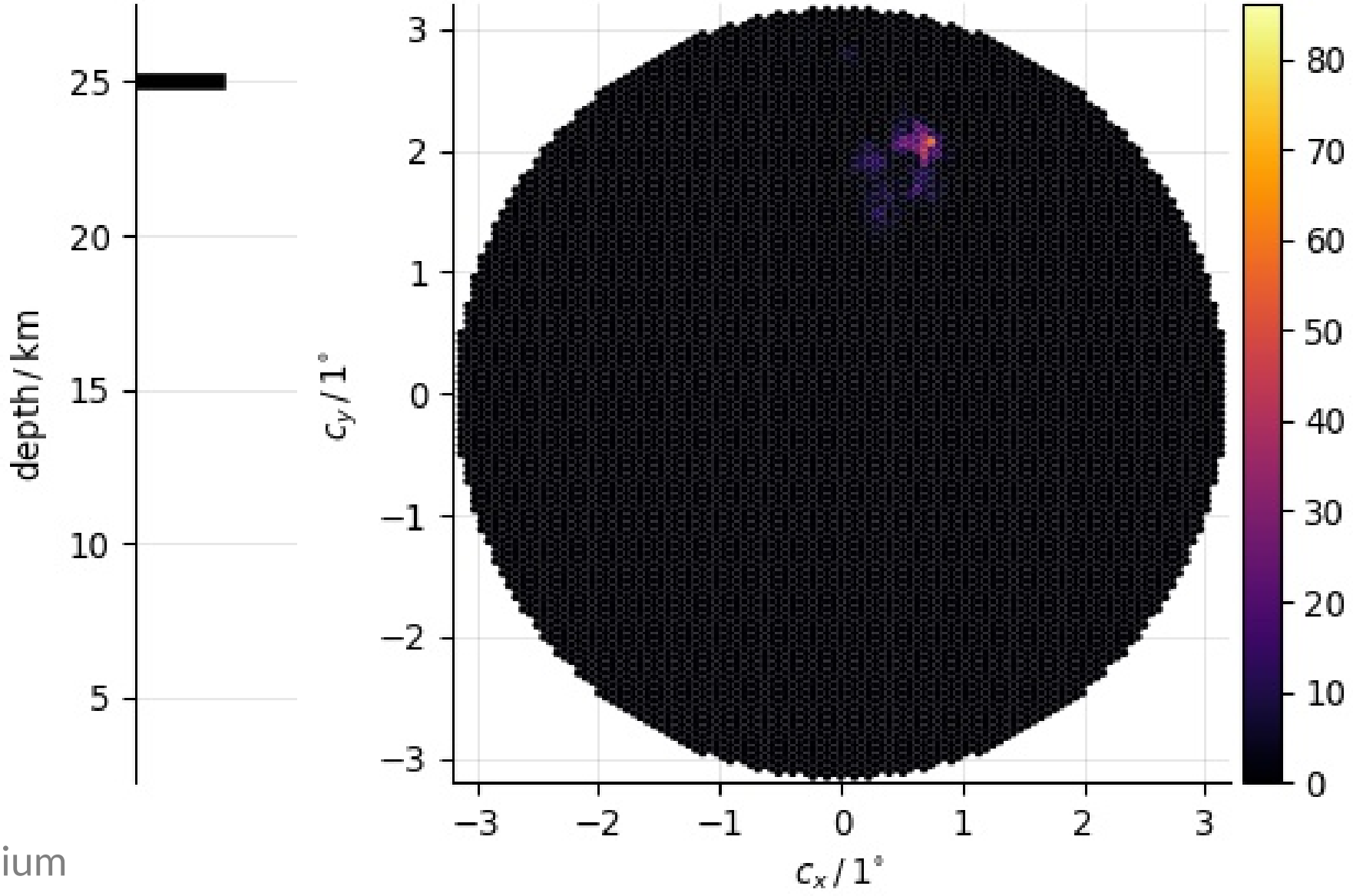
depth / km
25
20
15
10
5
$c_y / 1^\circ$
3
2
1
0
−1
−2
−3
$c_x / 1^\circ$
−3
−2
−1
0
1
2
3
80
70
60
50
40
30
20
10
0

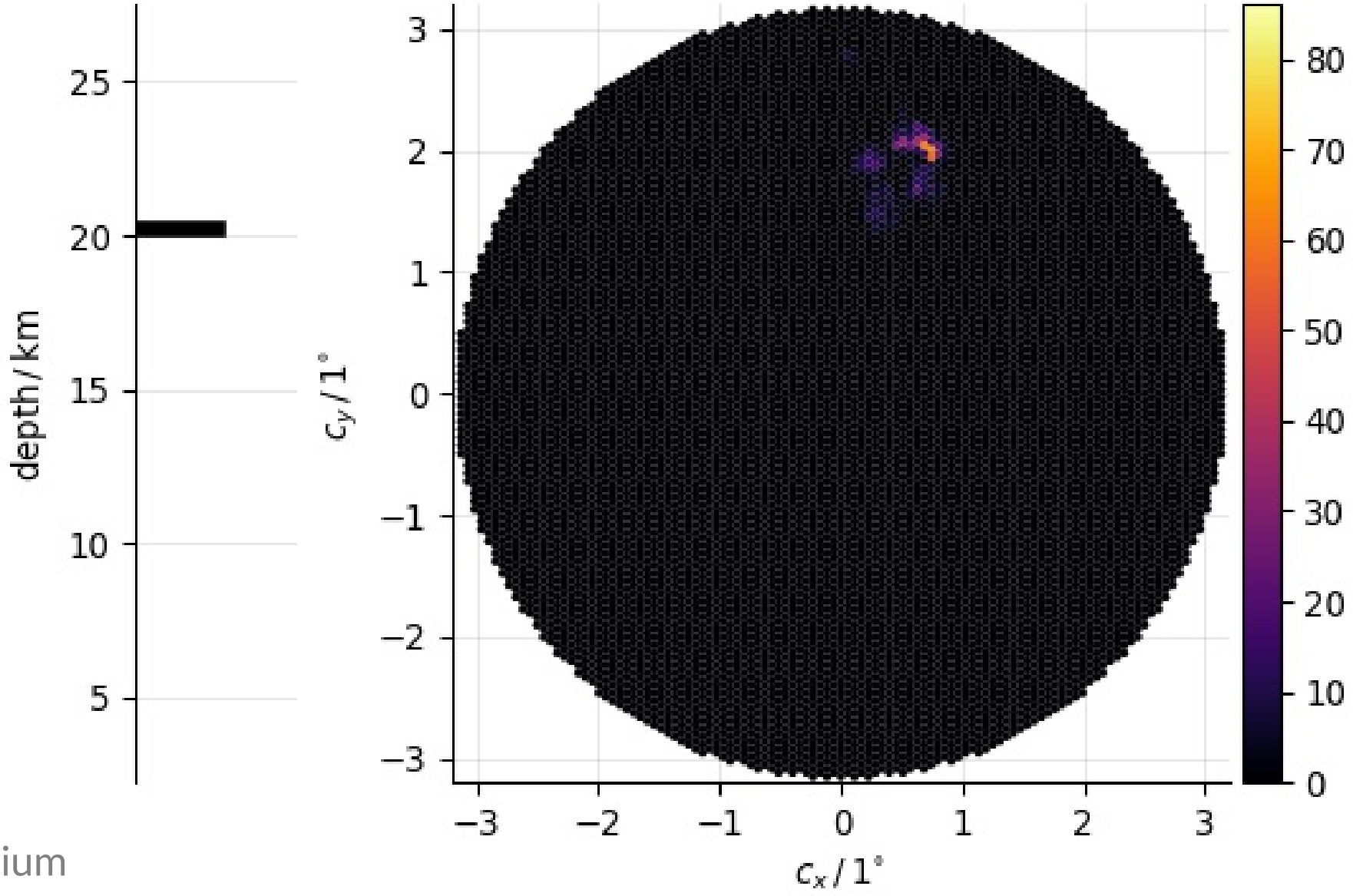
depth / km
25
20
15
10
5
$c_y / 1^\circ$
3
2
1
0
−1
−2
−3
$c_x / 1^\circ$
−3
−2
−1
0
1
2
3
80
70
60
50
40
30
20
10
0

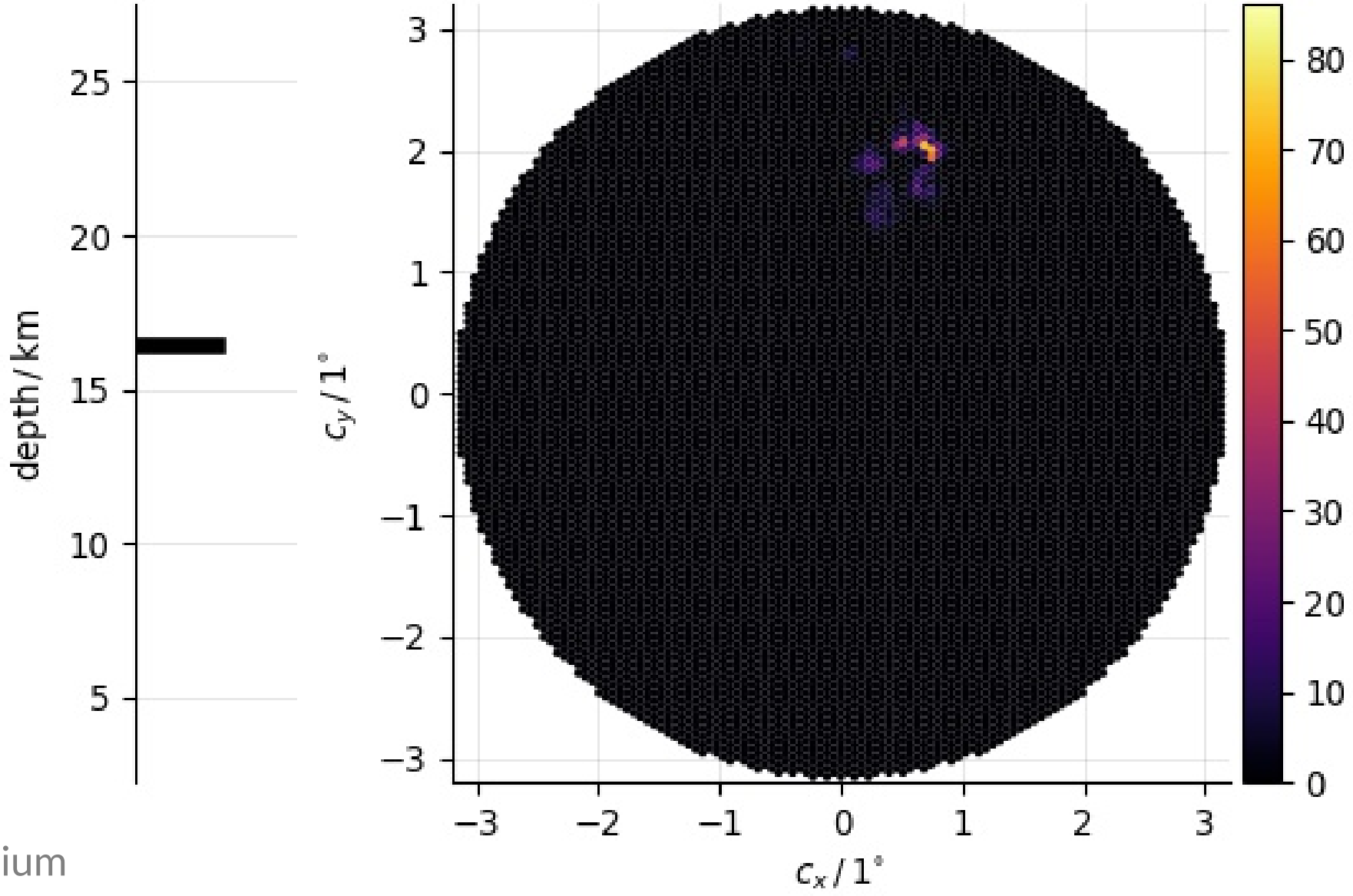
depth / km
25
20
15
10
5
$c_y / 1^\circ$
3
2
1
0
−1
−2
−3
$c_x / 1^\circ$
−3
−2
−1
0
1
2
3
80
70
60
50
40
30
20
10
0

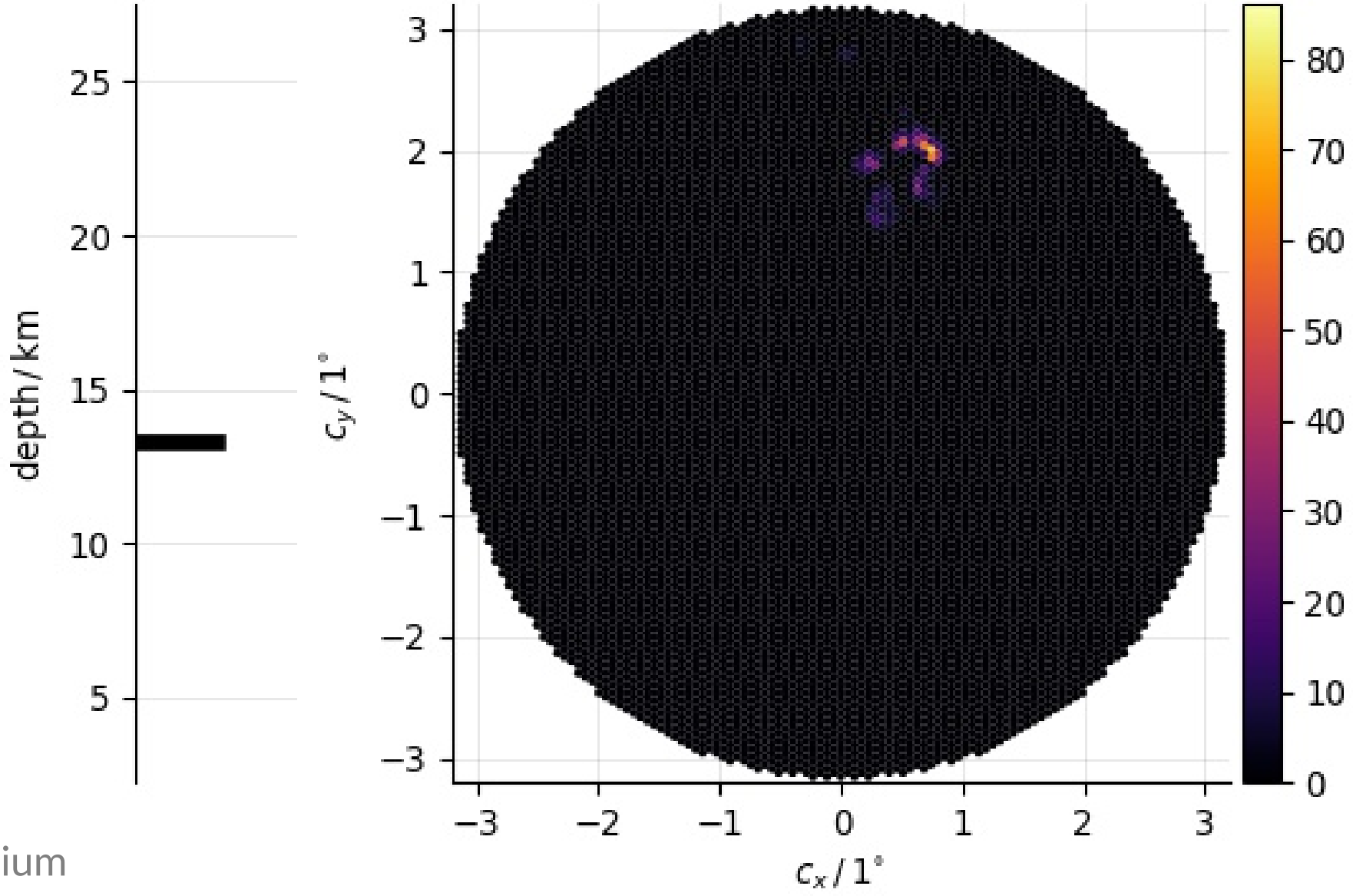
depth / km
25
20
15
10
5
c_y / 1°
3
2
1
0
−1
−2
−3
c_x / 1°
−3
−2
−1
0
1
2
3
80
70
60
50
40
30
20
10
0

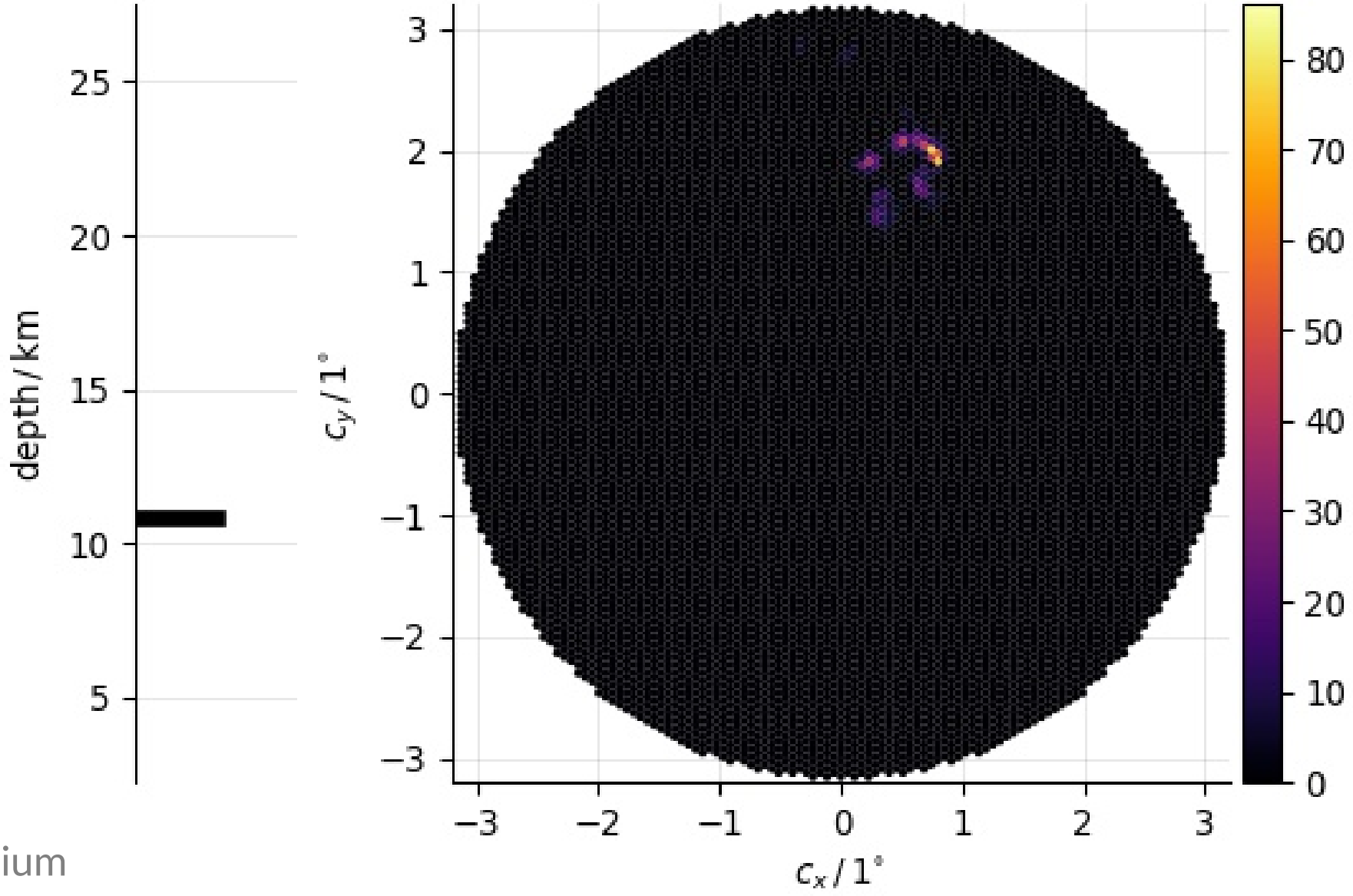
depth / km
25
20
15
10
5
$c_y / 1^\circ$
3
2
1
0
−1
−2
−3
$c_x / 1^\circ$
−3
−2
−1
0
1
2
3
80
70
60
50
40
30
20
10
0

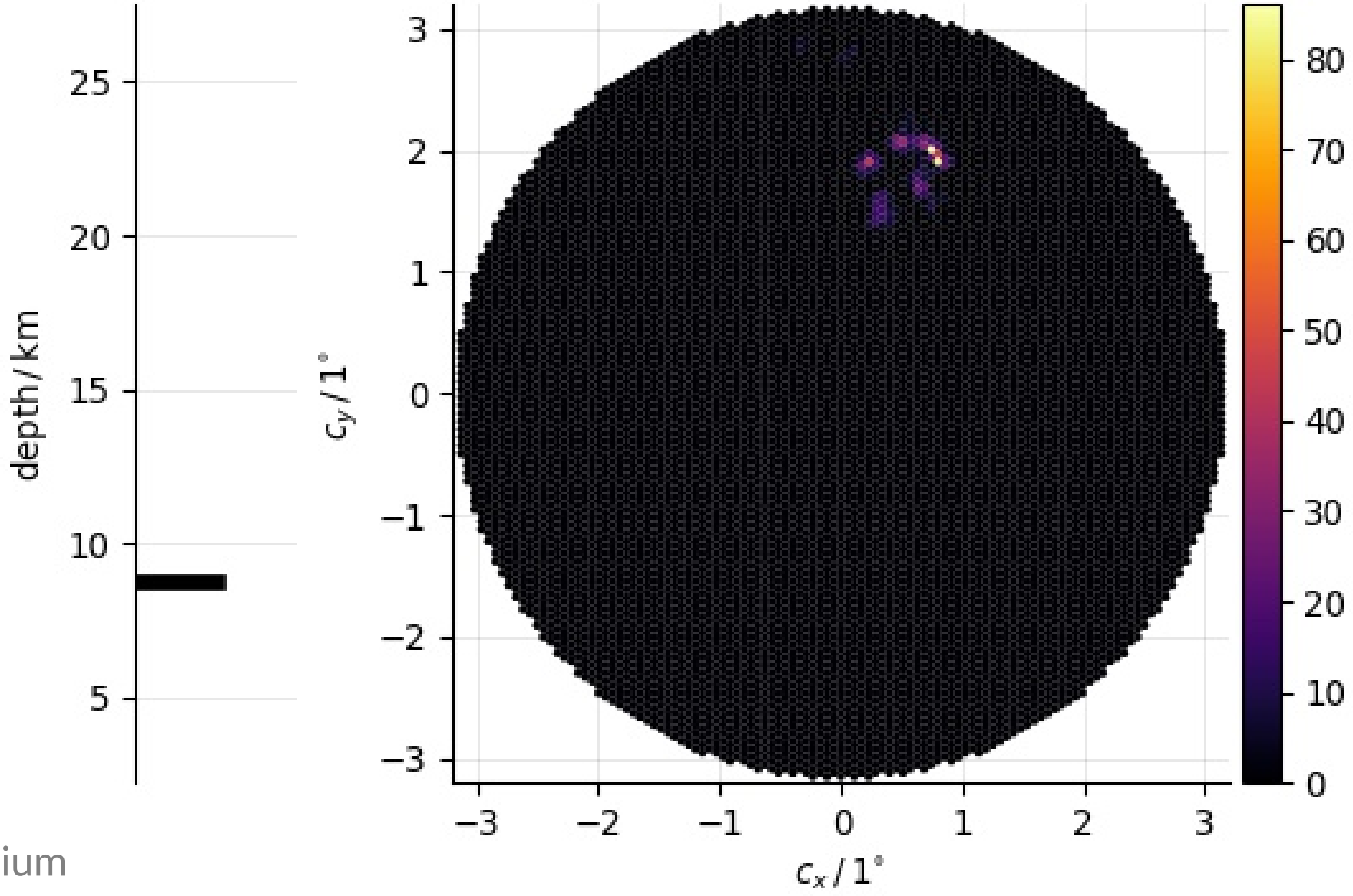
depth / km
25
20
15
10
5
$c_y / 1^\circ$
3
2
1
0
−1
−2
−3
$c_x / 1^\circ$
−3
−2
−1
0
1
2
3
80
70
60
50
40
30
20
10
0

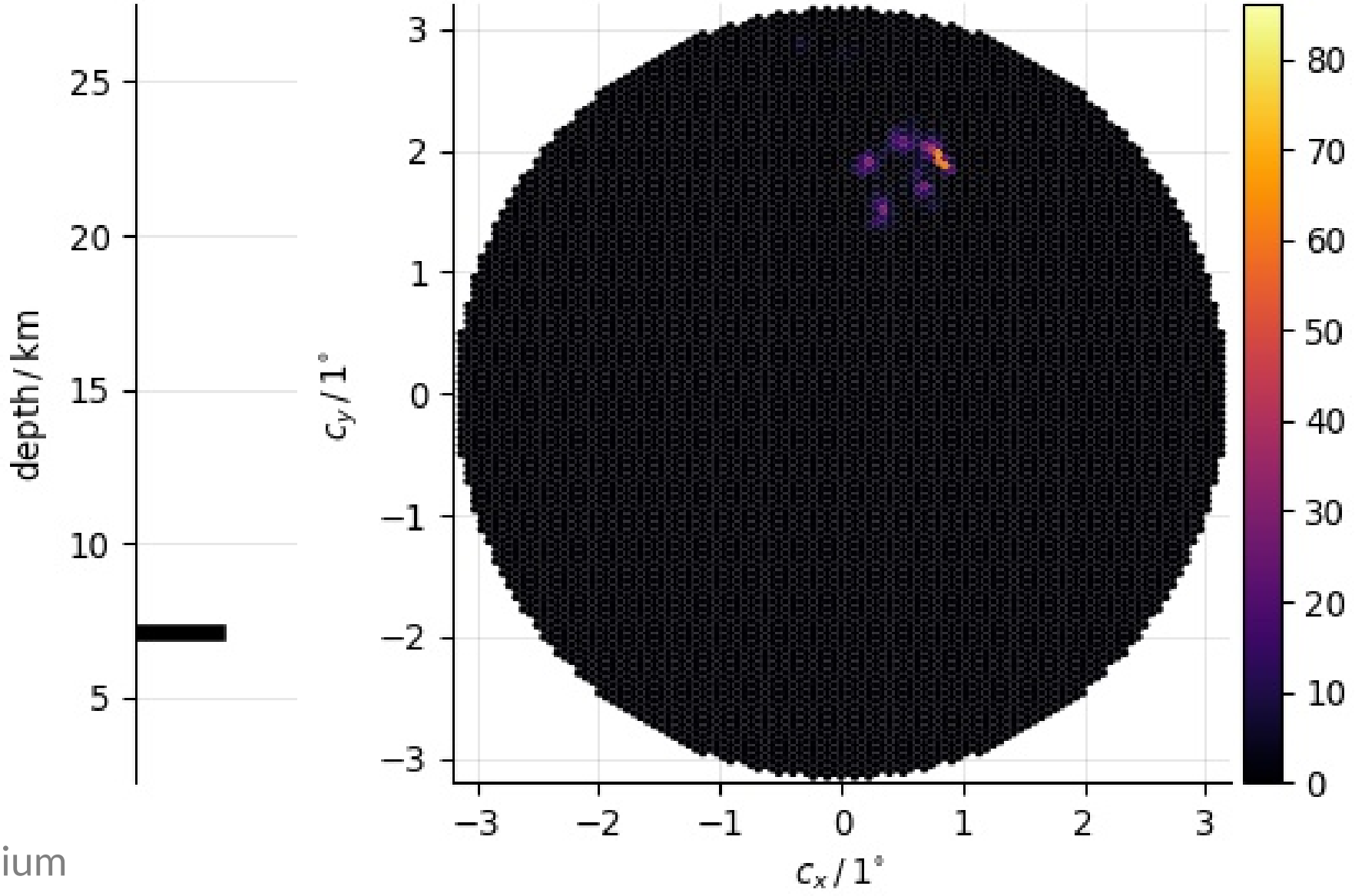
depth / km
25
20
15
10
5
$c_y / 1^\circ$
3
2
1
0
−1
−2
−3
$c_x / 1^\circ$
−3
−2
−1
0
1
2
3
80
70
60
50
40
30
20
10
0

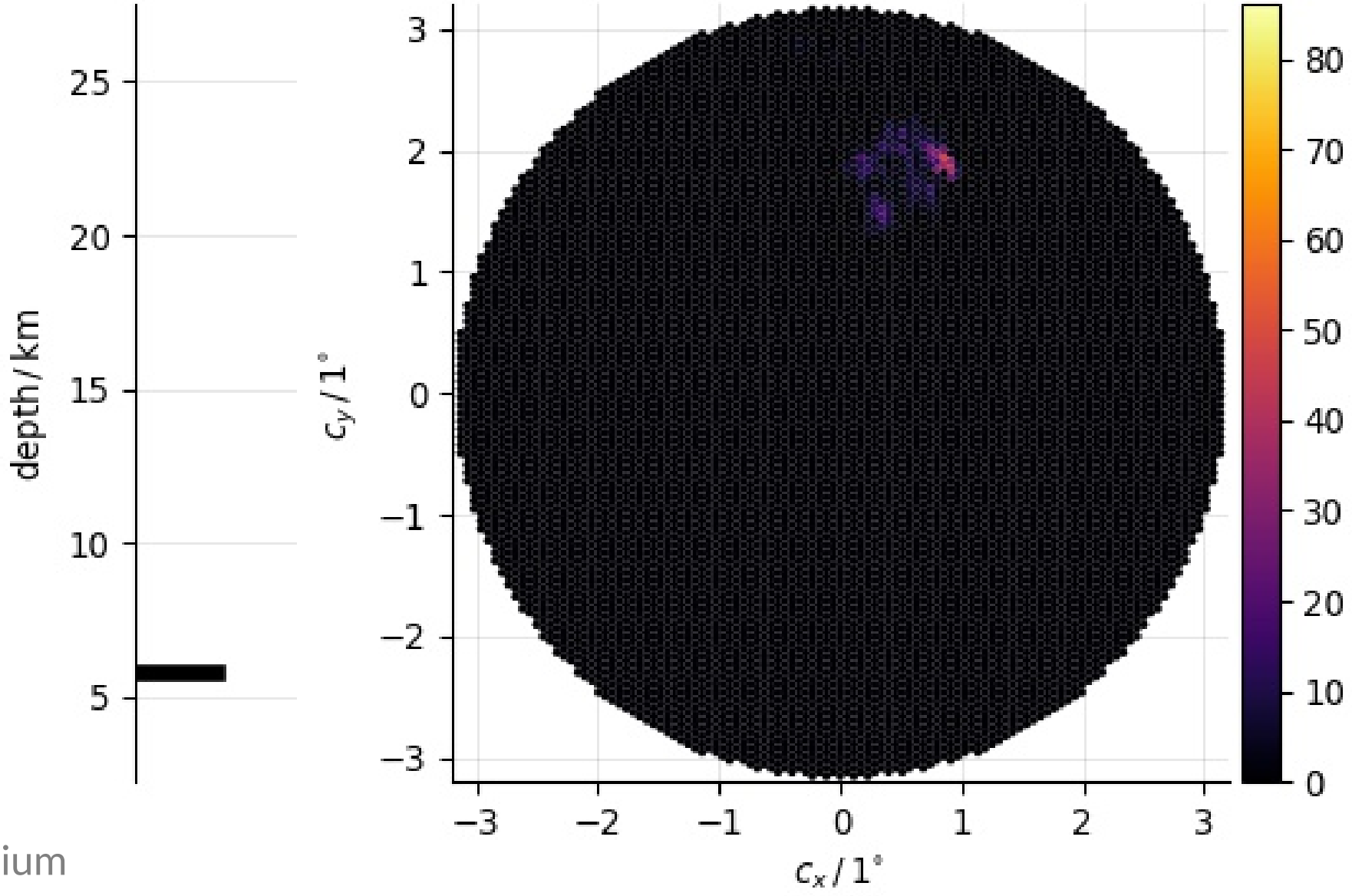
depth / km
25
20
15
10
5
c_y / 1°
3
2
1
0
−1
−2
−3
−3
−2
−1
0
1
2
3
c_x / 1°
80
70
60
50
40
30
20
10
0

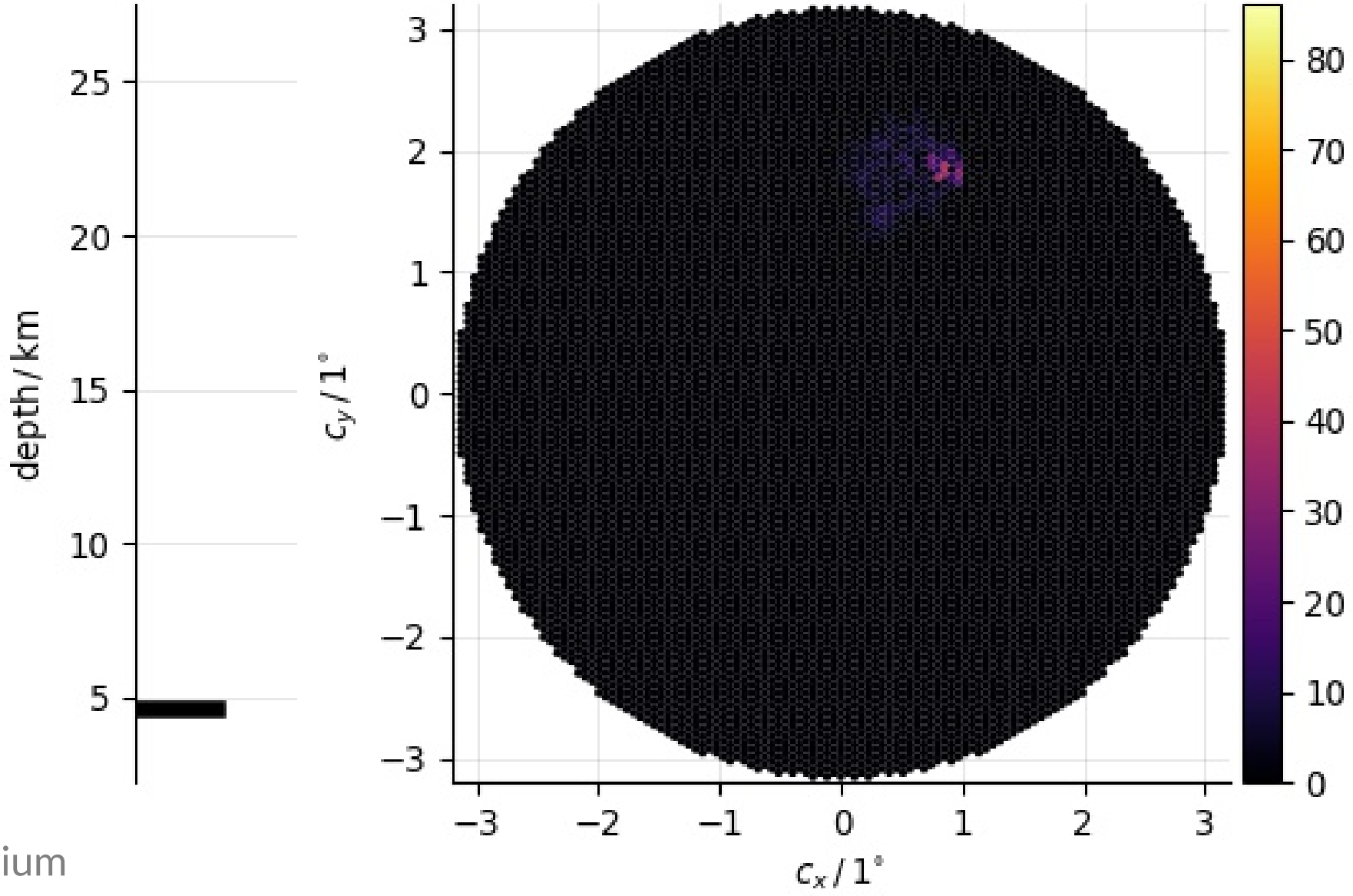
depth / km
25
20
15
10
5
c_y / 1°
3
2
1
0
−1
−2
−3
−3
−2
−1
0
1
2
3
c_x / 1°
80
70
60
50
40
30
20
10
0

Helium

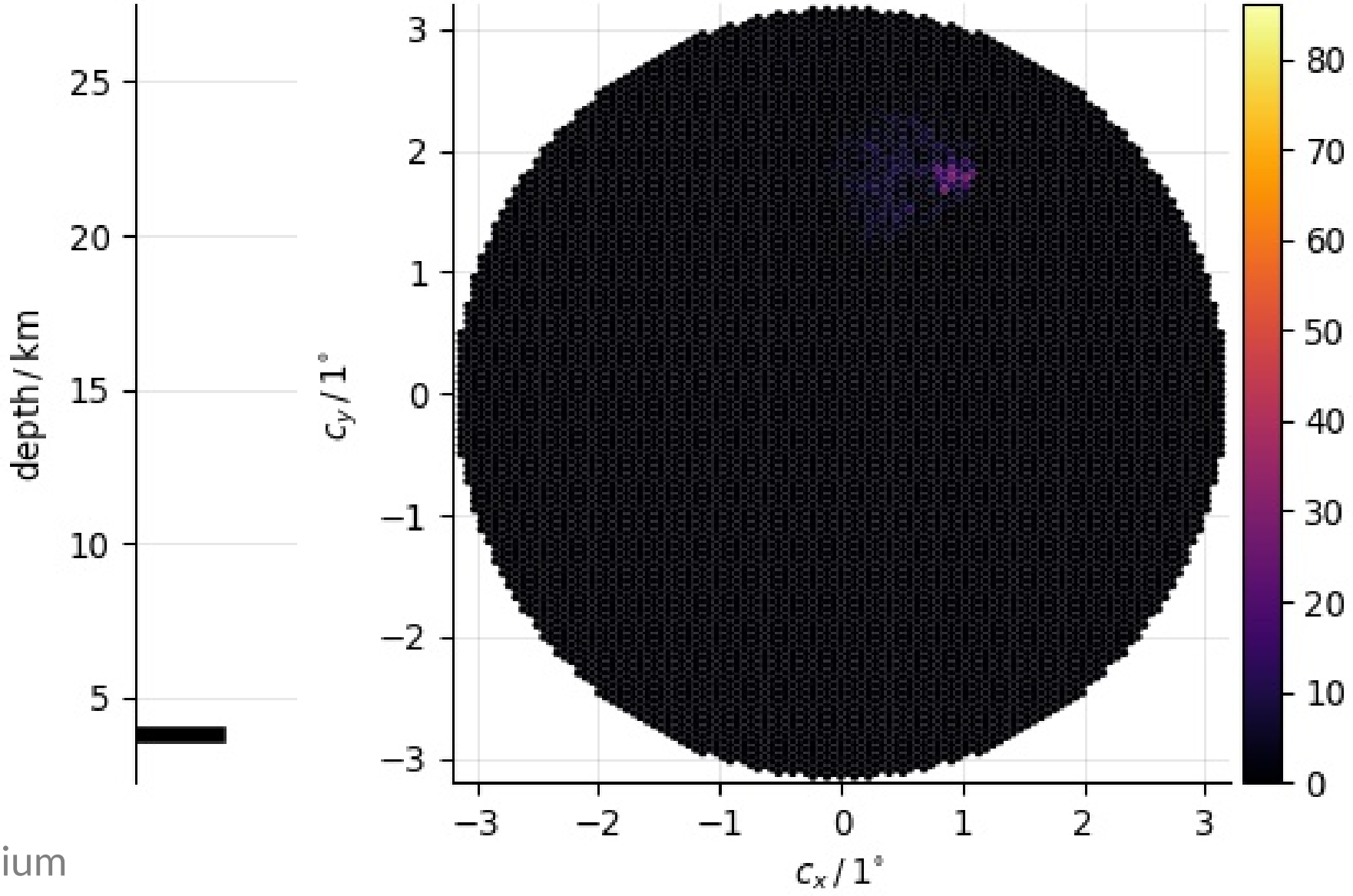
depth / km
25
20
15
10
5
$c_y / 1^\circ$
3
2
1
0
−1
−2
−3
$c_x / 1^\circ$
−3
−2
−1
0
1
2
3
80
70
60
50
40
30
20
10
0

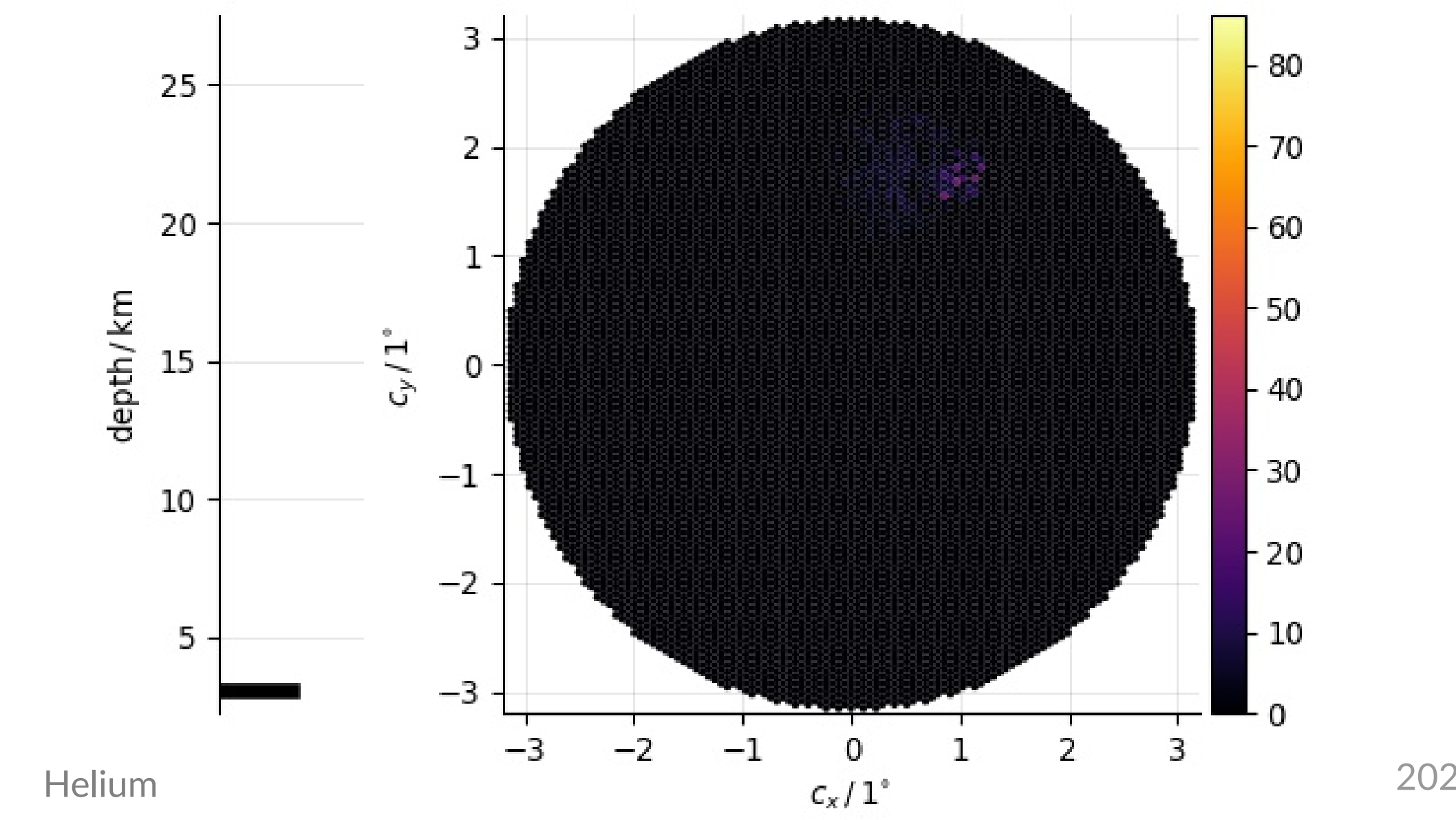
depth / km
25
20
15
10
5
$c_y / 1^\circ$
3
2
1
0
−1
−2
−3
$c_x / 1^\circ$
−3
−2
−1
0
1
2
3
80
70
60
50
40
30
20
10
0

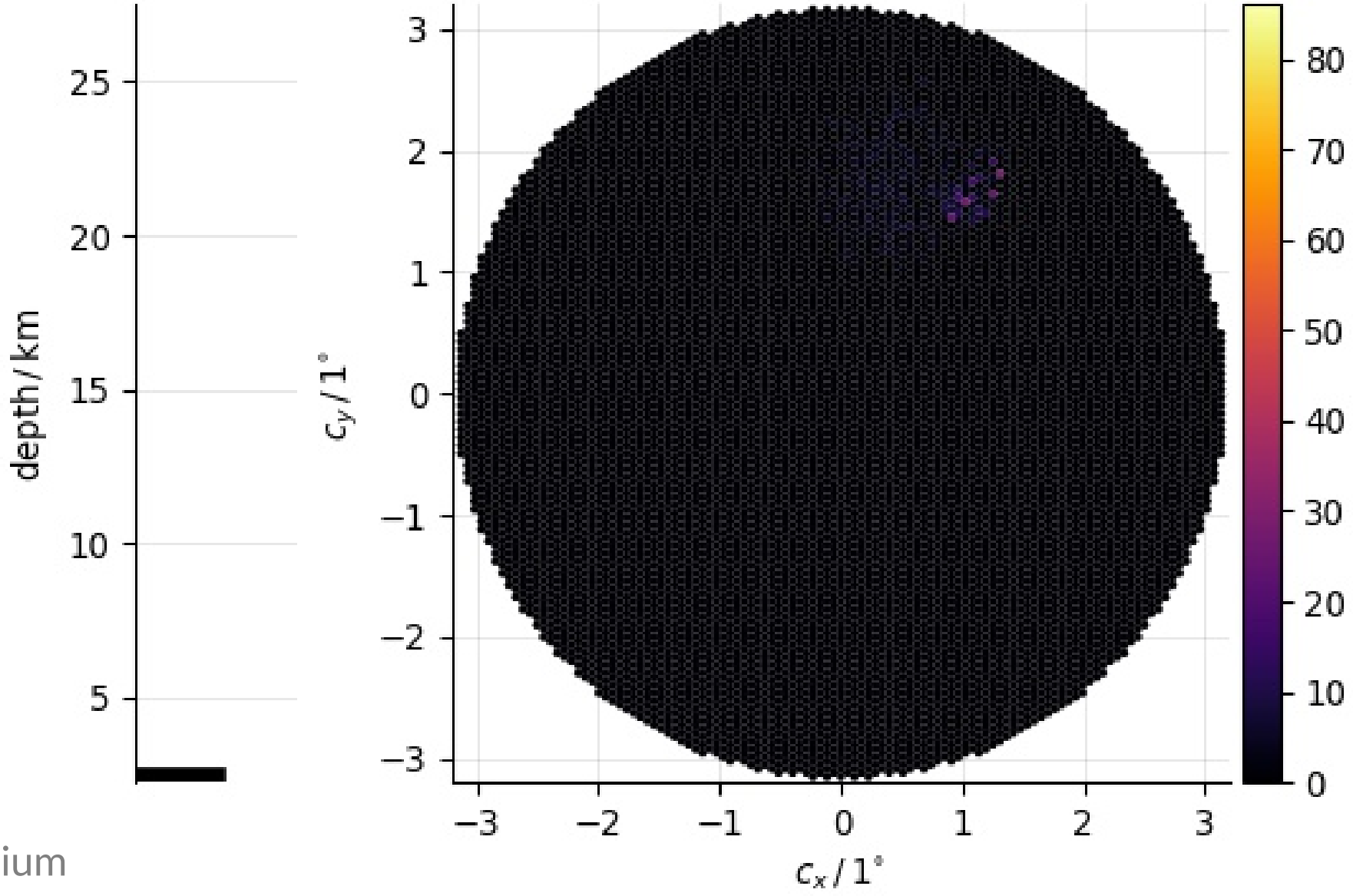
depth / km
25
20
15
10
5
c_y / 1°
3
2
1
0
−1
−2
−3
−3
−2
−1
0
1
2
3
c_x / 1°
80
70
60
50
40
30
20
10
0

Performance (so far)

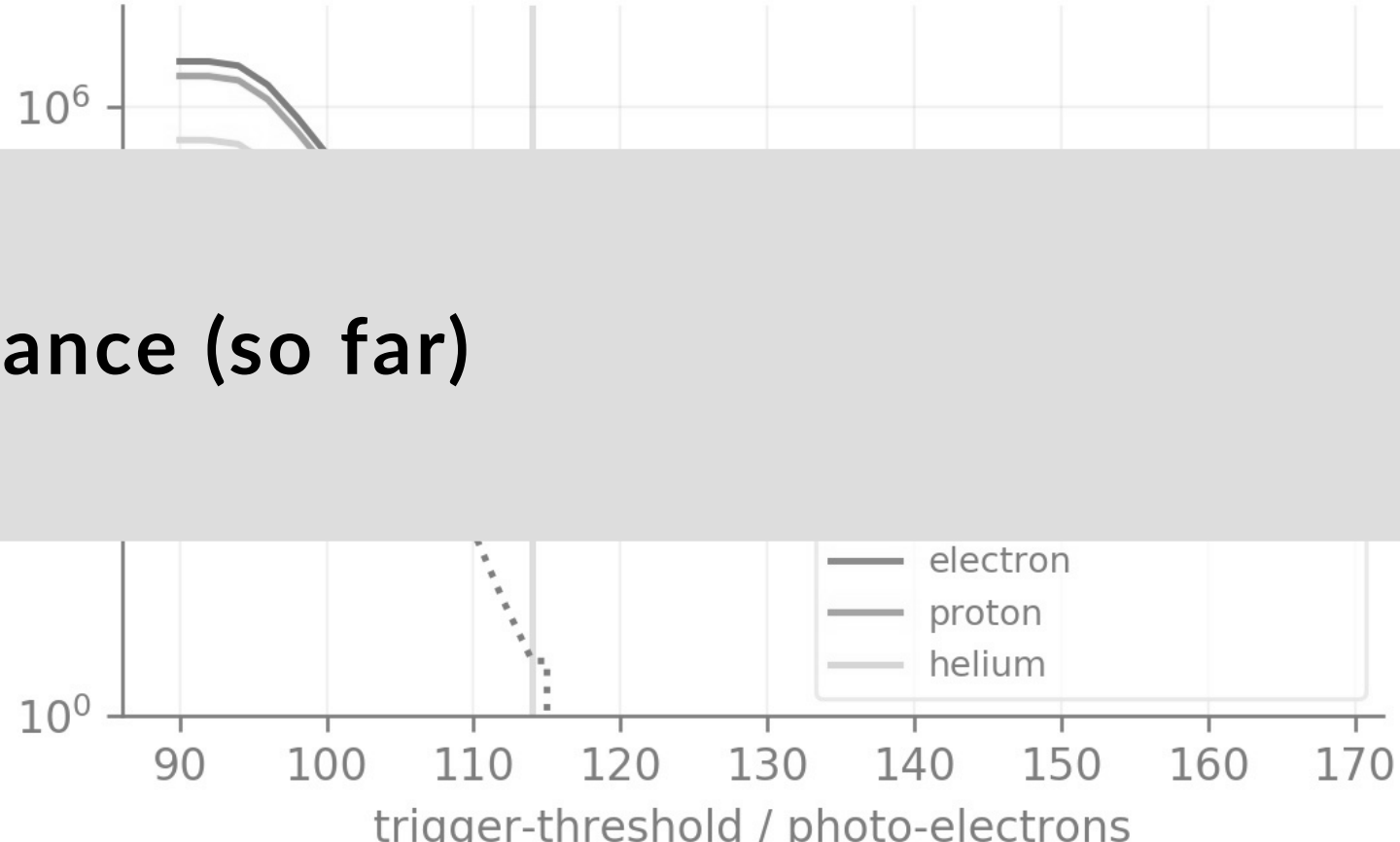

Performance, Rate-Scan

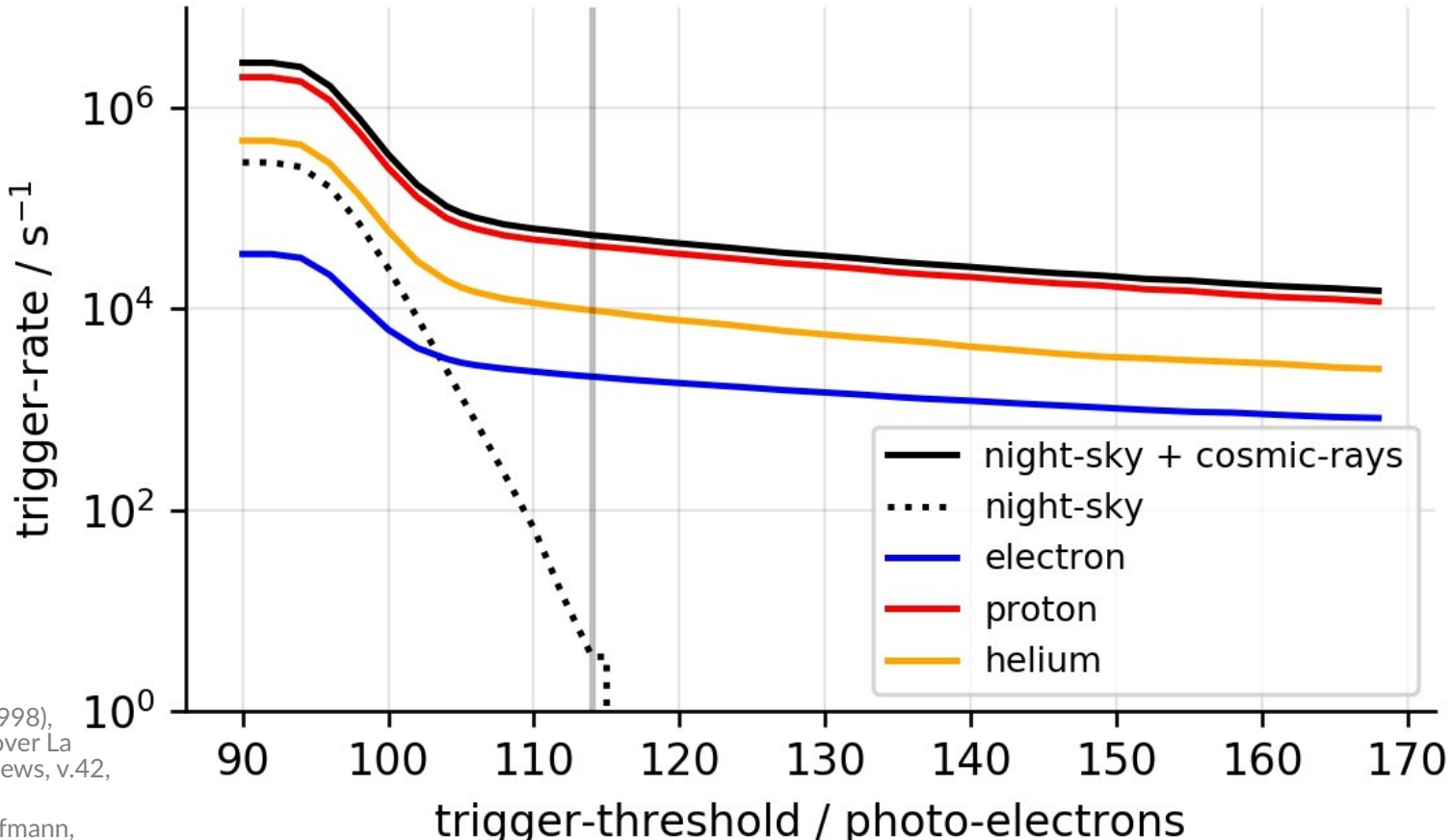

C.R. Benn and S.L .Ellison (1998), Brightness of the night sky over La Palma, New Astronomy Reviews, v.42, n.6-8, p.503-507

S.Preuss, G.Hermann, W.Hofmann, A.Kohnle (2002) Study of ... night sky at La Palma and Namibia..., NIM-A, v.481, p.229-240

Performance, Rates on 3FGL J0534.5+2201

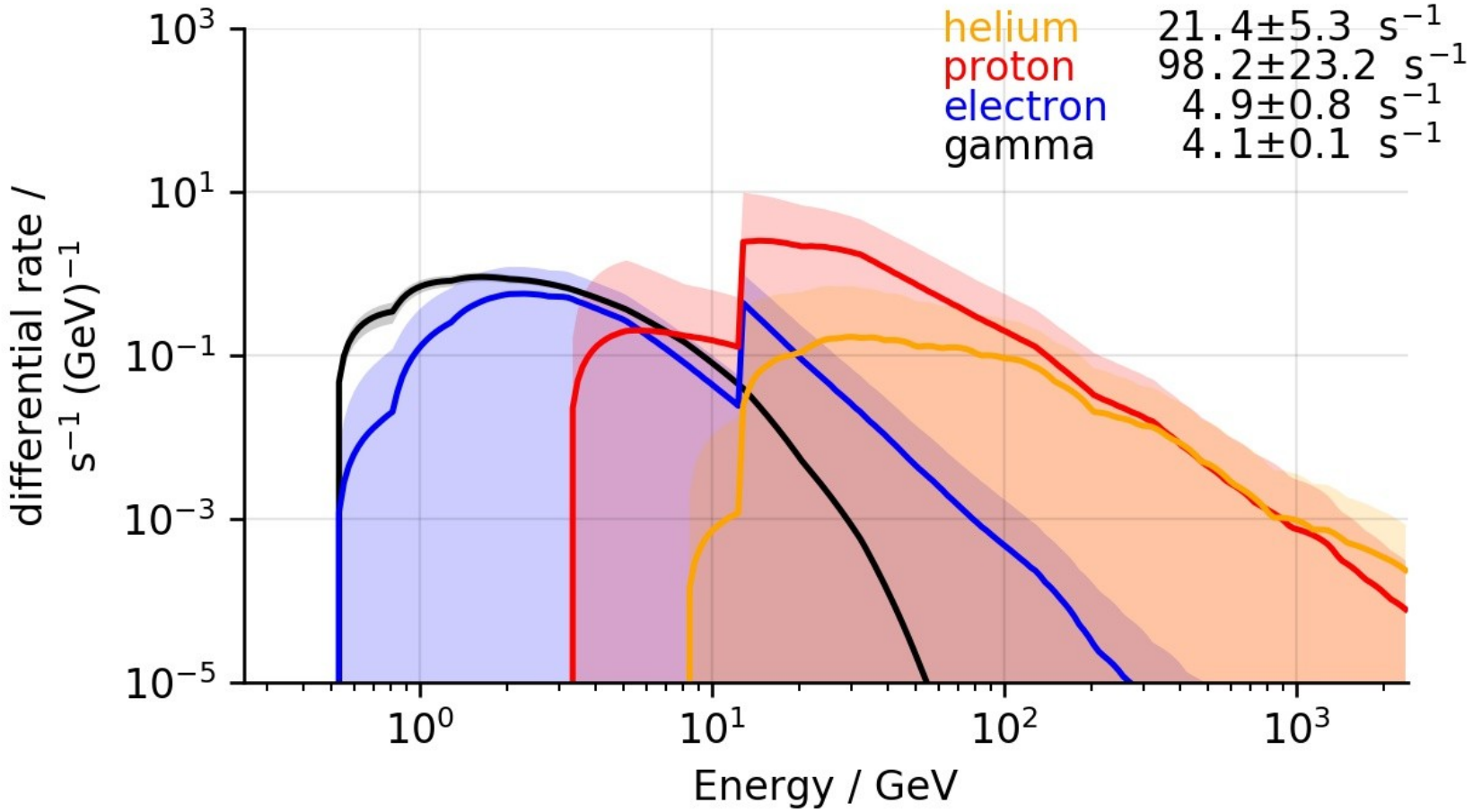

Performance, Gamma-Hadron-Seperation

Not yet.

Performance, Direction

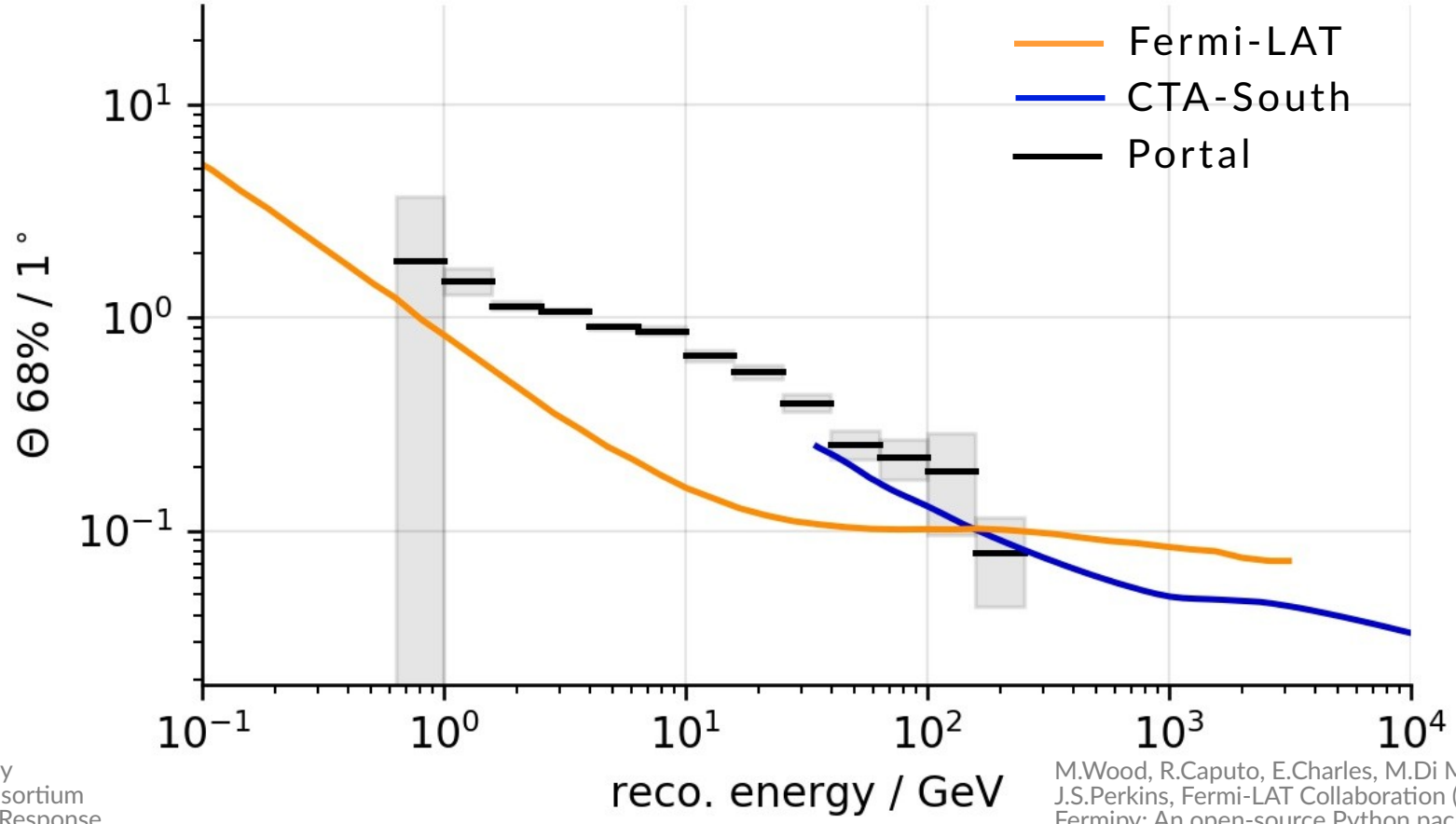

Cherenkov Telescope Array Observatory and CTA Consortium (2021). CTAO Instrument Response Functions - prod5 version v0.1, doi:10.5281/zenodo.5499840

M.Wood, R.Caputo, E.Charles, M.Di Mauro, J.Magill, J.S.Perkins, Fermi-LAT Collaboration (2017), Fermipy: An open-source Python package for analysis of Fermi-LAT Data, Proc. 35th ICRC, PoS(ICRC2017)824, IRF: P8R2_SOURCE_V6

Performance, Energy

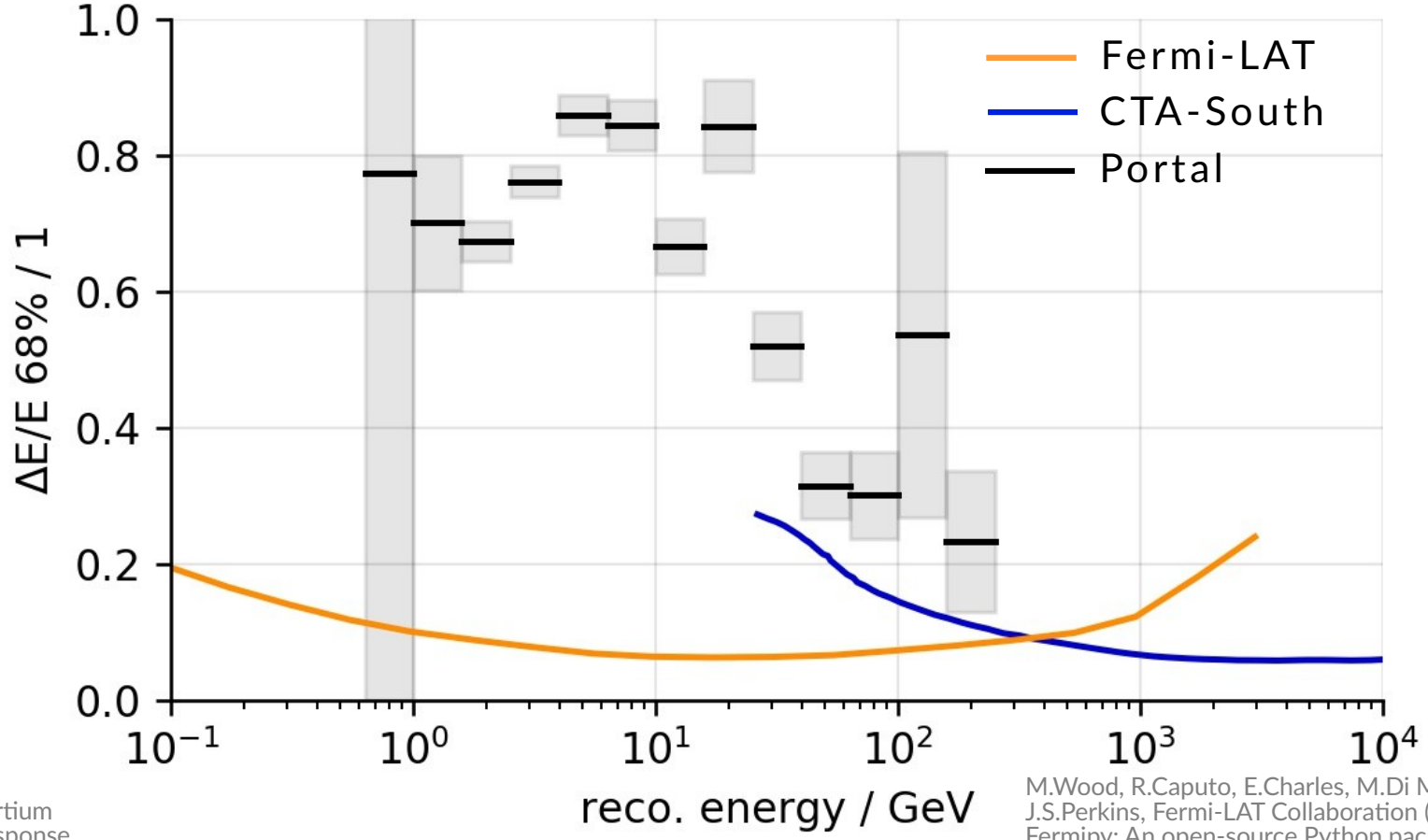

Cherenkov Telescope Array Observatory and CTA Consortium (2021). CTAO Instrument Response Functions - prod5 version v0.1, doi:10.5281/zenodo.5499840

M.Wood, R.Caputo, E.Charles, M.Di Mauro, J.Magill, J.S.Perkins, Fermi-LAT Collaboration (2017), Fermipy: An open-source Python package for analysis of Fermi-LAT Data, Proc. 35th ICRC, PoS(ICRC2017)824, IRF: P8R2_SOURCE_V6

Performance, Sensitivity vs. Energy at 3min

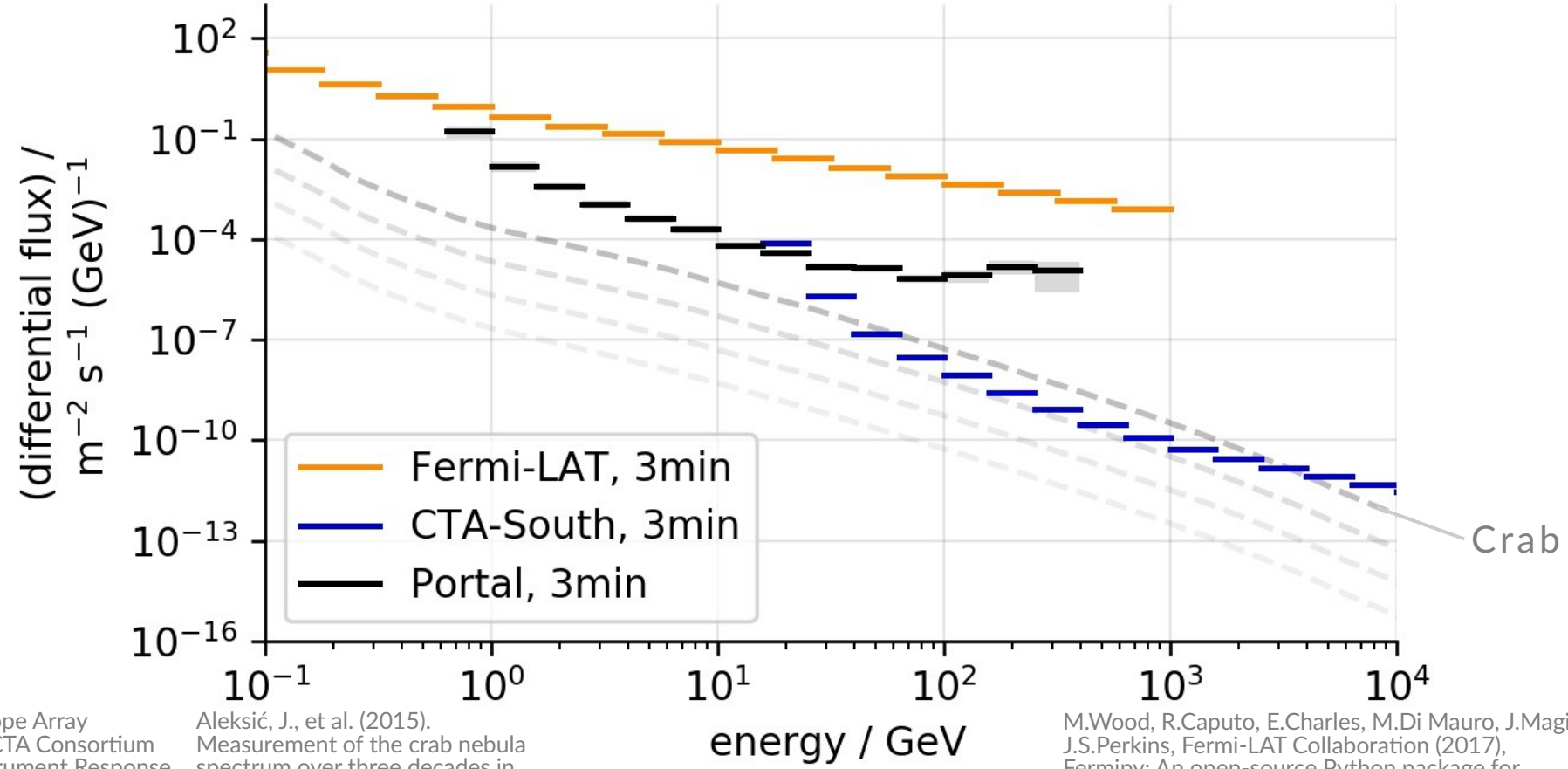

Cherenkov Telescope Array Observatory and CTA Consortium (2021). CTAO Instrument Response Functions - prod5 version v0.1, doi:10.5281/zenodo.5499840

Aleksić, J., et al. (2015). Measurement of the crab nebula spectrum over three decades in energy with the magic telescopes. High Energy Astrophysics, 5:30–38.

M.Wood, R.Caputo, E.Charles, M.Di Mauro, J.Magill, J.S.Perkins, Fermi-LAT Collaboration (2017), Fermipy: An open-source Python package for analysis of Fermi-LAT Data, Proc. 35th ICRC, PoS(ICRC2017)824, IRF: P8R2_SOURCE_V6

Performance, Sensitivity vs. Time at 2.5GeV

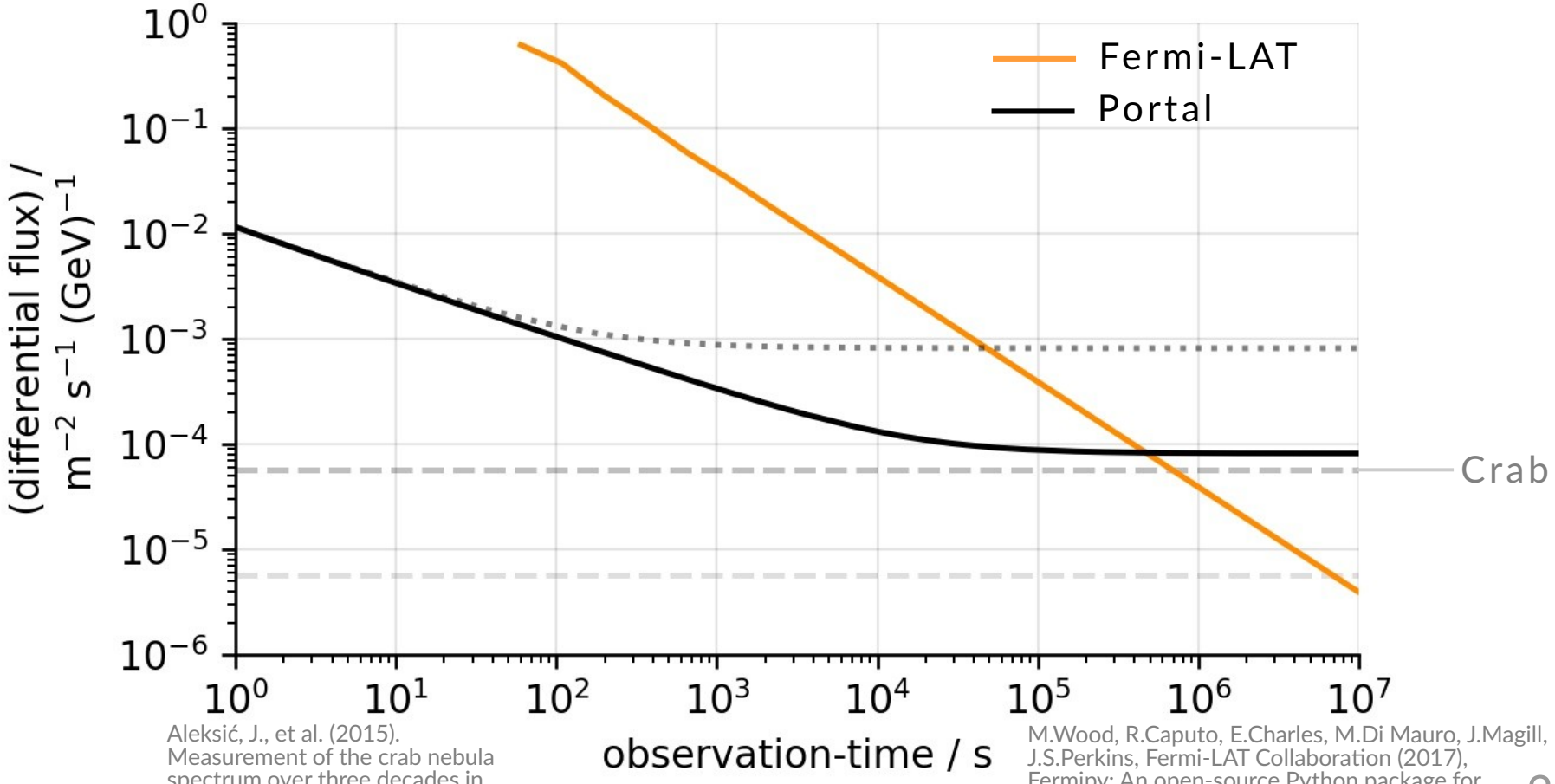

Aleksić, J., et al. (2015). Measurement of the crab nebula spectrum over three decades in energy with the magic telescopes. High Energy Astrophysics, 5:30–38.

M.Wood, R.Caputo, E.Charles, M.Di Mauro, J.Magill, J.S.Perkins, Fermi-LAT Collaboration (2017), Fermipy: An open-source Python package for analysis of Fermi-LAT Data, Proc. 35th ICRC, PoS(ICRC2017)824, IRF: P8R2_SOURCE_V6

Gamma-Ray-Timing-Explorer

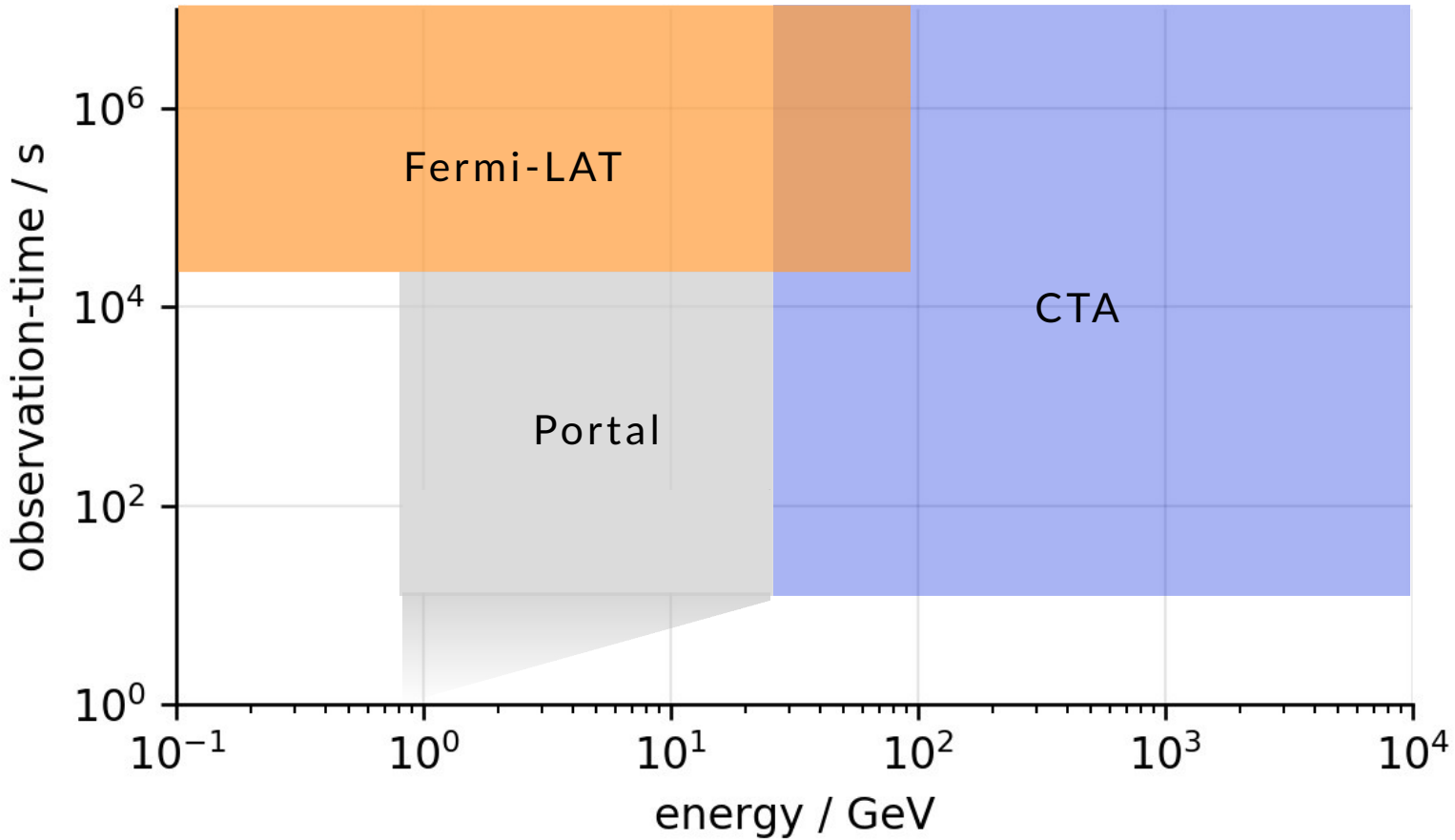

Acknowledgment

MAX-PLANCK-INSTITUT FÜR KERNPHYSIK

Werner Hofmann,
Jim Hinton

ETH zürich

Adrian Biland, Felicitas Pauss,
Max L. Ahnen, Dominik Neise,
Spyridon Daglas, Axel A. Engels,
Eleni Chatzi, Adrian Egger

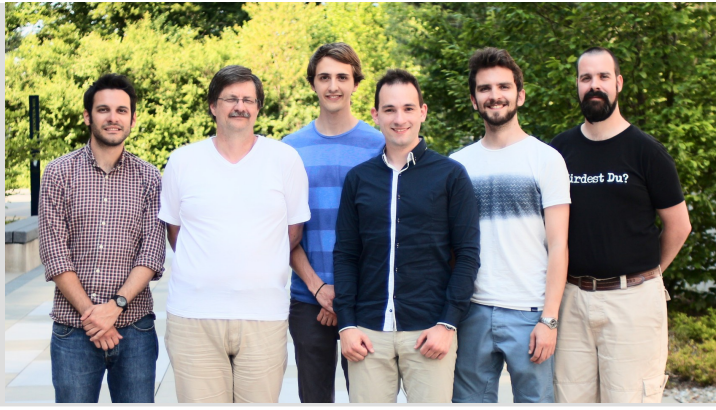

Questions

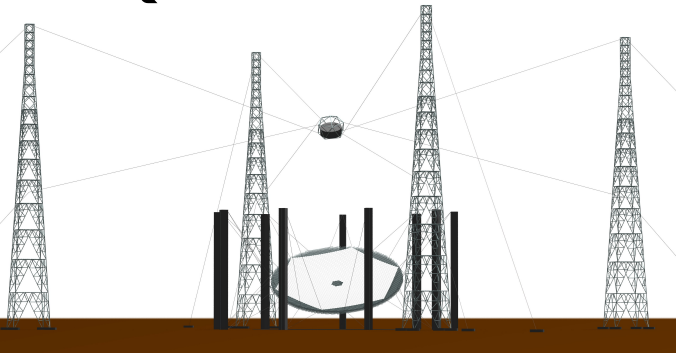

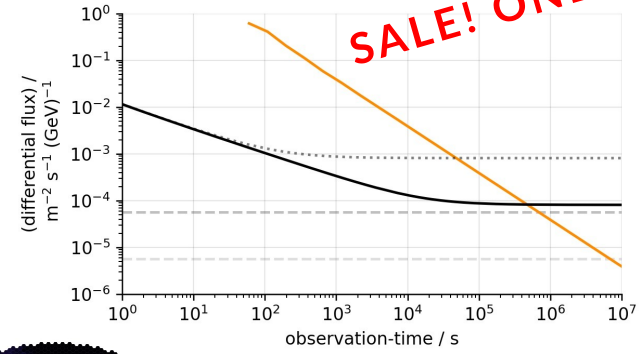

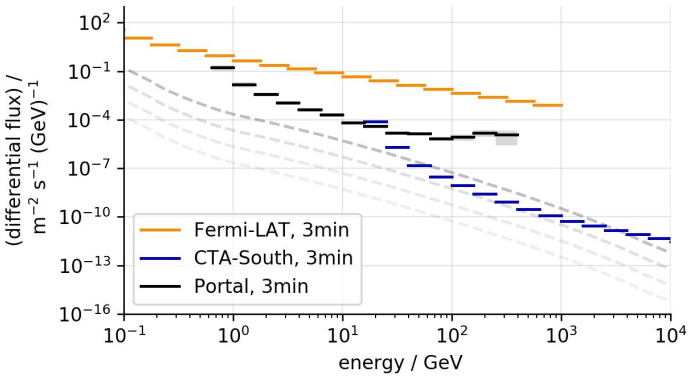

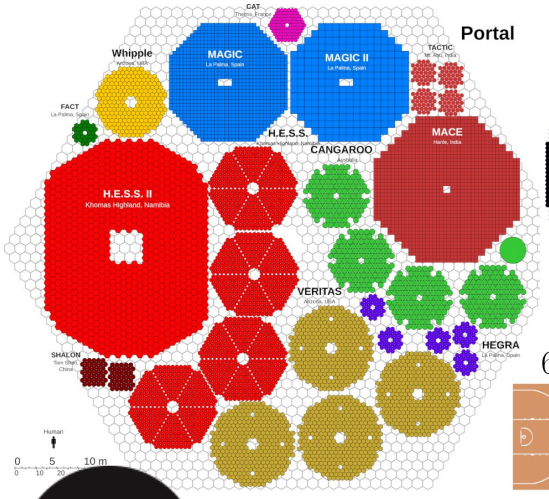

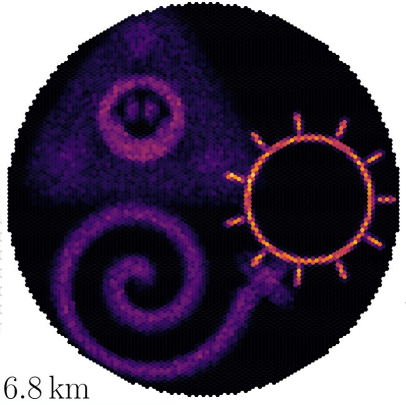

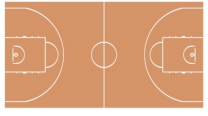

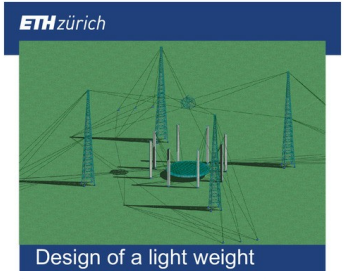

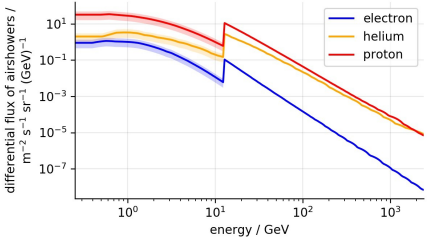

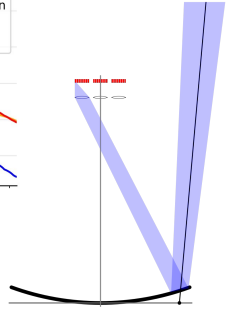

arXiv:1904.13368 (astro-ph)

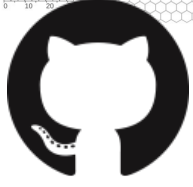

Go visit: https://github.com/cherenkov-plenoscope

Size

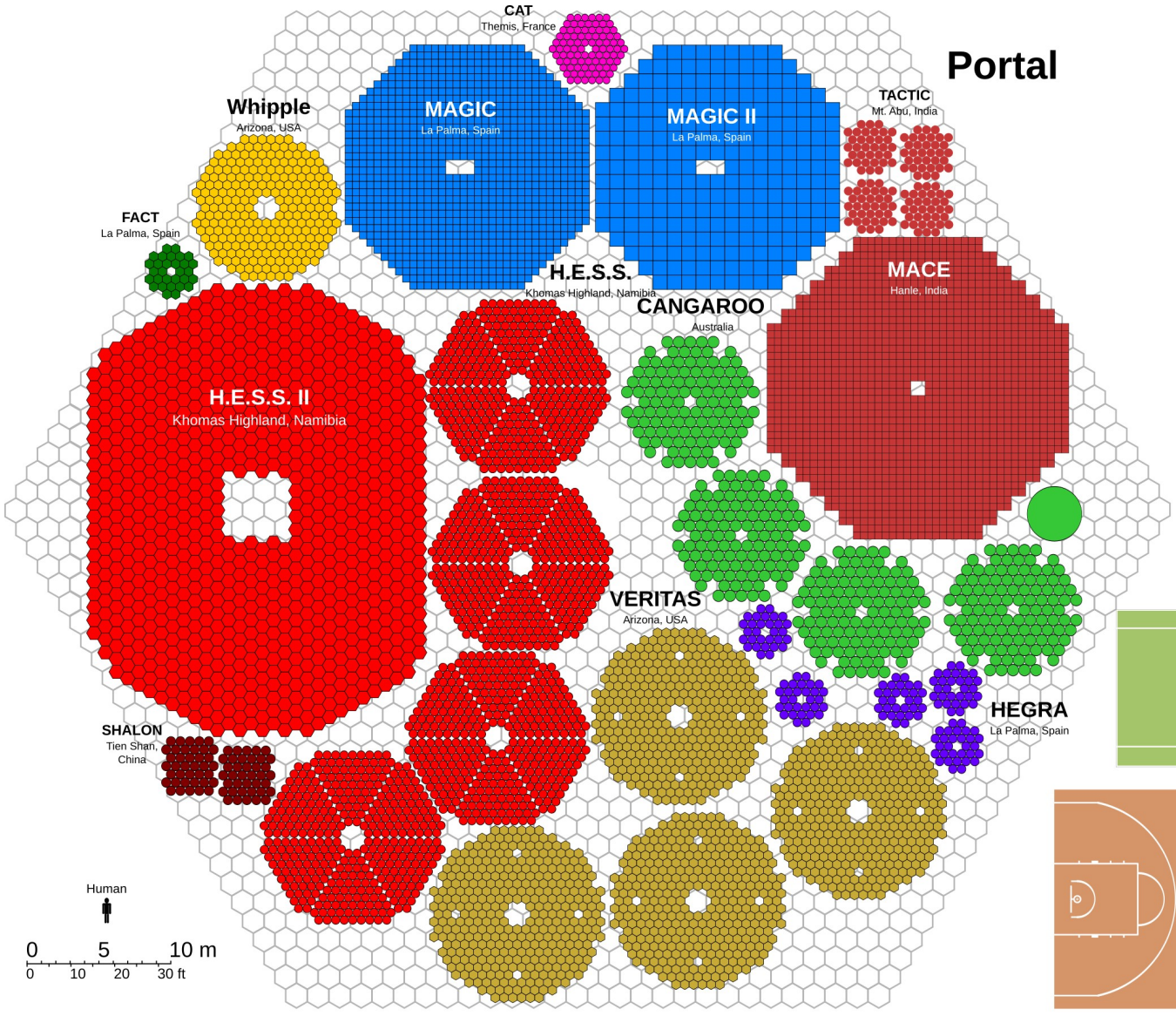
CAT
Themis, France
Portal
Whipple
Arizona, USA
MAGIC
La Palma, Spain
MAGIC II
La Palma, Spain
TACTIC
Mt. Abu, India
FACT
La Palma, Spain
H.E.S.S.
Khomas Highland, Namibia
CANGAROO
Australia
MACE
Hanle, India
H.E.S.S. II
Khomas Highland, Namibia
VERITAS
Arizona, USA
HEGRA
La Palma, Spain
SHALON
Tien Shan, China
Human
0 5 10 m
0 10 20 30 ft

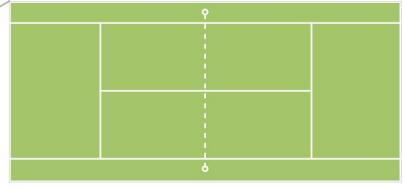

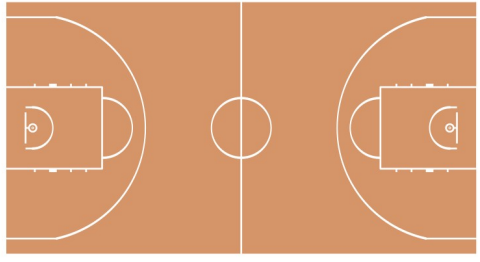

Performance, Sensitivity vs. Energy at 3min

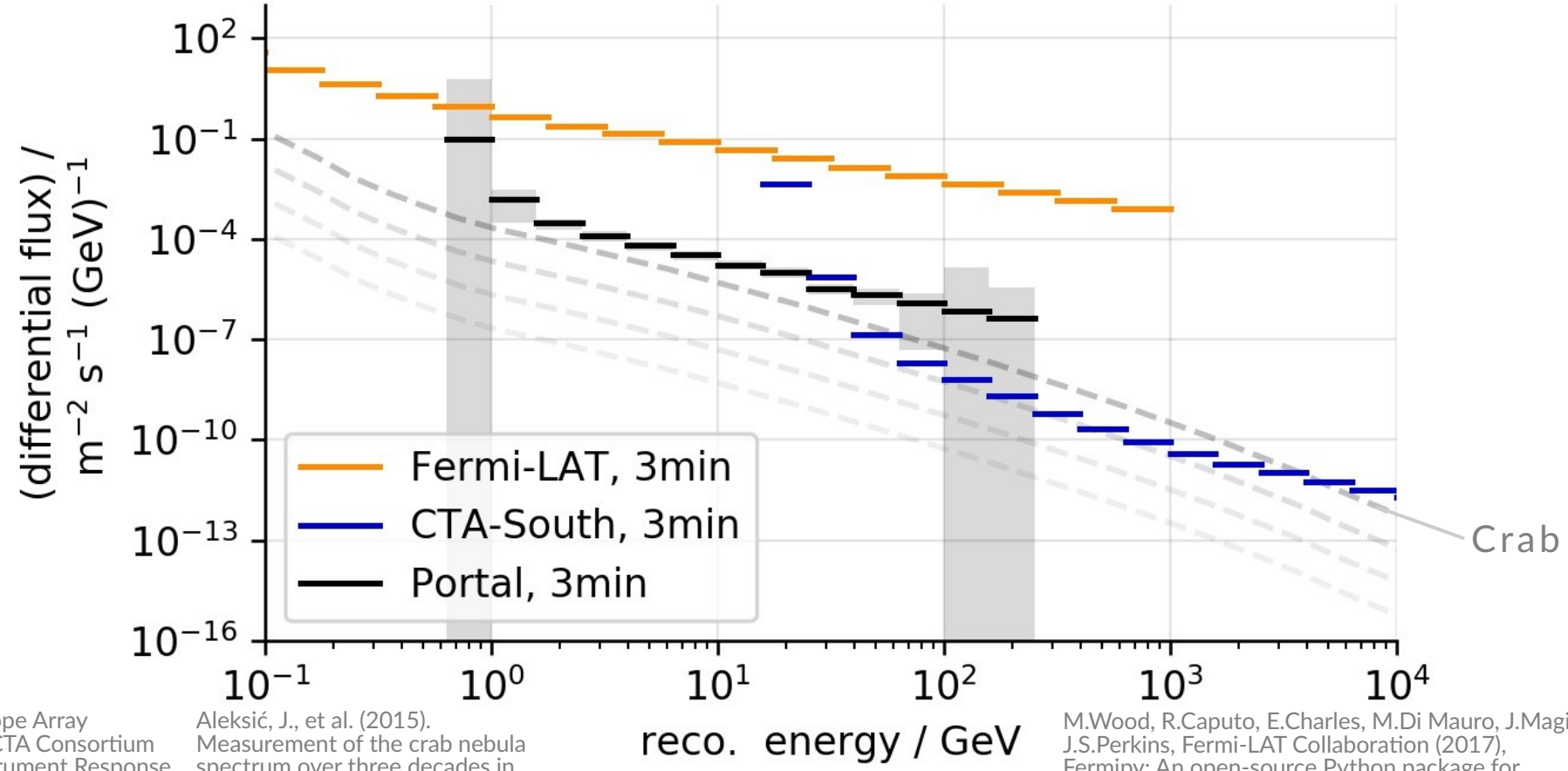

Cherenkov Telescope Array Observatory and CTA Consortium (2021). CTAO Instrument Response Functions - prod5 version v0.1, doi:10.5281/zenodo.5499840

Aleksić, J., et al. (2015). Measurement of the crab nebula spectrum over three decades in energy with the magic telescopes. High Energy Astrophysics, 5:30–38.

M.Wood, R.Caputo, E.Charles, M.Di Mauro, J.Magill, J.S.Perkins, Fermi-LAT Collaboration (2017), Fermipy: An open-source Python package for analysis of Fermi-LAT Data, Proc. 35th ICRC, PoS(ICRC2017)824, IRF: P8R2_SOURCE_V6

Field-of-view

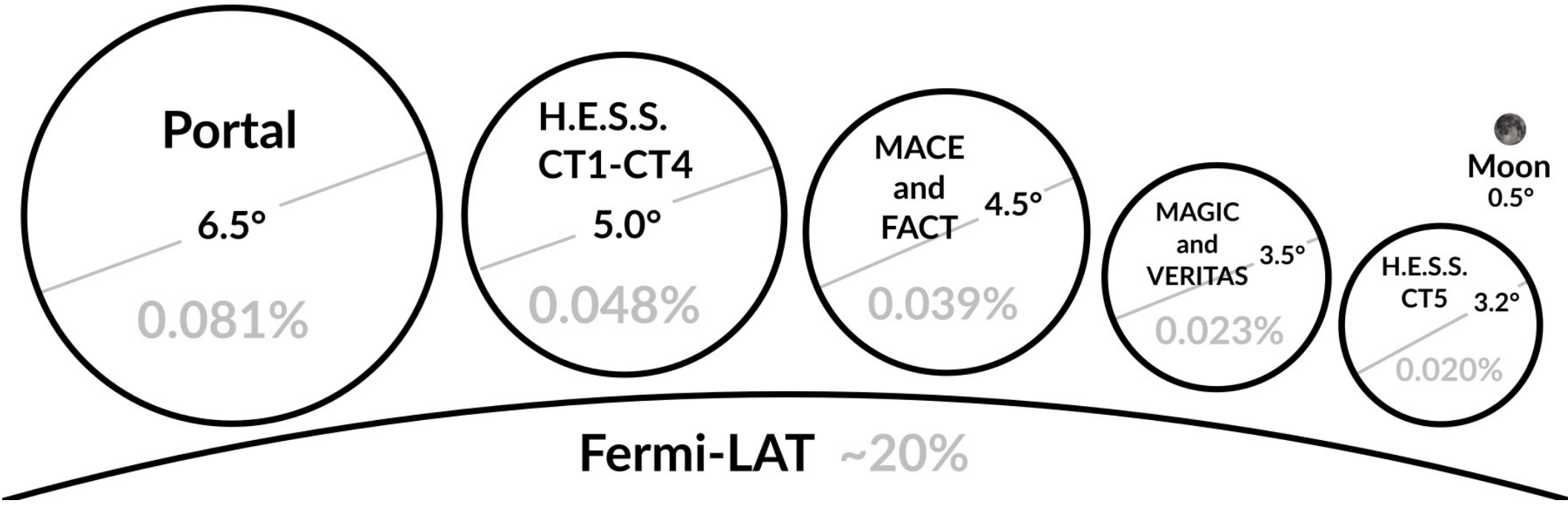

Costs Optics and Electronics

component	unit-costs	demand	cost / 10^6 EUR
Photo-sensors	5×10^5 EUR m^{-2}	115 m^2	57.5
Read-out-electronics	80 EUR $channel^{-1}$	515,023 channels	41.2
Lenses	100 EUR $lens^{-1}$	8,433 lenses	0.9
Mirror-facets	3×10^3 EUR m^{-2}	4174 m^2	12.5
Mirror-facet-actuators	10^3 EUR $facet^{-1}$	2,087 facets	2.1
			114.2

Today: EUR ~ USD ~ CHF

Costs Total

	fraction / %	cost / 10^6 EUR
Optics and electronics	51	114.2
Cable-robot-mount [1]	16	35.8
Central control-system [2]	5	11.2
Project-engineering [2]	5	11.2
Project-management [2]	13	29.1
Site-infrastructure [2]	10	22.4
	100	**223.9**

Today: EUR ~ USD ~ CHF

(1) Civil engineer Spyridon Daglas (2) Adopted from reports by the Eurpean-Southern-Observatory (ESO)